



UNIVERSITY OF NAIROBI

INSTITUTE OF NUCLEAR SCIENCE AND TECHNOLOGY

**EVALUATION OF THE AFRICAN VERY LONG BASELINE INTERFEROMETRY
NETWORK (AVN) FOR ASTRONOMY, GEODESY AND ASTROMETRY.**

ANN NJERI NG'ENDO

S56/78897/2015

**BSc. Astronomy & Astrophysics
(University of Nairobi)**

**A thesis submitted in partial fulfilment for the Degree of Master of Science in Nuclear Science
at the Institute of Nuclear Science and Technology, University of Nairobi.**

August, 2018.

DECLARATION AND APPROVAL

Declaration

This thesis is my original research work. It has not been presented for a degree in any other university.

Name: Ann Njeri Ng'endo

Registration number: S56/78897/2015

Signature:  Date: 24/08/2018

Approval

This thesis has been submitted with our approval as the university supervisors.


1. Mr. David M. Maina,
Institute of Nuclear Science and Technology,
University of Nairobi, Kenya.

} DECEASED.

2. Dr. Aletha de Witt,
Hartebeesthoek Radio Astronomy Observatory,
South Africa.

Signature:  Date: 20/10/2017

3. Prof. Paul Baki,
Technical University of Kenya,
Kenya.

Signature:  Date: 27/8/18

ORIGINALITY DECLARATION

Name of student: Ann Njeri Ng'endo

Registration Number: S56/78897/2015

College: COLLEGE OF ARCHITECTURE AND ENGINEERING


School: INSTITUTE OF NUCLEAR SCIENCE AND TECHNOLOGY

Course Name: MASTER OF SCIENCE IN NUCLEAR SCIENCE

Title of the work: EVALUATION OF THE AFRICAN VERY LONG BASELINE
INTERFEROMETRY NETWORK (AVN) FOR ASTRONOMY, GEODESY AND ASTROMETRY

DECLARATION

1. I understand what Plagiarism is and I am aware of the University's policy in this regard.
2. I declare that this THESIS is my original work and has not been submitted elsewhere for examination, award of a degree or publication. Where other people's work or my own work has been used, this has been properly acknowledged and referenced in accordance with the University of Nairobi's requirements.
3. I have not sought or used the services of any professional agencies to produce this work.
4. I have not allowed, and shall not allow anyone to copy my work with intention of passing it off as his/her own work.
5. I understand that any false claim in respect to this work shall result in disciplinary action, in accordance with University Plagiarism Policy.

Signature: 

Date: 24/08/2018

In loving memory of D. M. Maina.

DEDICATION

I wish to dedicate this work to the AVN dream...

So many of our dreams at first seem impossible, then they seem improbable, and then, when we summon the will, they soon become inevitable. ~ Christopher Reeves

ACKNOWLEDGEMENT

I wish to express utmost sincere gratitude to my supervisors: my school supervisor and the Director of the Institute, the late Mr. D.M Maina for allowing me to follow my dreams. To Prof. Paul Baki, for the continued support throughout the years. My special thanks goes to my project supervisor, a mentor and a friend, Dr. Aletha de Witt. Her professional guidance, valuable and constructive suggestions and help with the research project for the past two years is deeply appreciated.

I acknowledge the contribution of Dr. Leonid Petrov with the weather data on AVN sites, Mr. David Mayer for always being at my disposal and his assistance with the VieVS software and Dr. Gordon MacLeod for his opinions, suggestions ideas and immense assistance with the project. Thanks are also due to Dr. Khadija El Bouchfry for always making me feel at home while at HartRAO.

I also wish to thank the Kenya Nuclear Electricity Board (KNEB) for the MSc scholarship, one Kenyan life has changed for the better as a result and the Institute of Nuclear Science and Technology (INST) fraternity and in particular, Mrs. Mary Karuiruh for her immense help with administrative issues.

Lastly, I wish to thank the HartRAO NRF/DARA Newton Fund Collaboration for funding the AVN project and specifically, this research project.

Ann Njeri,
August, 2018.

ABSTRACT

The African Very Long Baseline Interferometry, VLBI, Network (AVN) will be an African array of radio telescopes across Africa comprising of converted redundant satellite Earth-station antennas and new purpose-build radio antennas. The first one of these antennas, in Ghana, has already been converted into a radio telescope. In this study, the value that these African radio telescopes, and in particular the Kenyan telescope, will add to the AVN as well as to the existing global VLBI networks for astronomy, geodesy and astrometry was reviewed.

The Radio Frequency Interference (RFI) was assessed based on population densities at different radii using the NASA Web Population Estimator and UNDP Population data report (2015), the telephone, mobile and internet subscriptions and the electricity connectivity using the ITU Report, 2015. The weather data was analyzed using NASA's GEOSFIT to determine the atmospheric opacity at each AVN site for a period of three years, January 2013 to November 2015. The SCHED software was used to create U-V coverage plots of the AVN antennas plus the European VLBI Network (EVN) and the Australian Long Baseline Array (LBA) at different declinations. Earth Orientation parameters (EOPs), baseline length repeatabilities and source position estimates were scheduled, then simulated and analyzed through simulated geodetic and astrometric VLBI observations using the Vienna VLBI Software (VieVS). The AVN antennas were added to the International VLBI Service (IVS) geodetic session R1675 scheduled and then simulated to observe changes in the EOPs and Baseline length repeatabilities. The AVN antennas in the south of the equator (AVN1) were added to the IVS Celestial Reference for Deep South (CRDS) session to observe changes in the source positions.

The population densities around the Kenyan site is 70, 78 and 175 people/km² at 5, 10 and 20 km radii while for Ghana is 1175, 981 and 1560 people/km² at the same radii. This is compared to population densities of 24, 25 and 79 people/km² at the same radii at the South African site. The mean atmospheric opacity for the Kenyan site is 0.36, 0.12 and 0.32 at 22, 43 and 100 GHz, whereas for the Ghanian site is 0.50, 0.21 and 0.67 at the same frequencies. HartRAO has values of 0.28, 0.10 and 0.20 at the same frequencies. At x-band, the AVN antennas improve the u-v coverage of the LBA from 7% to 23% at the declination of -10° and from 12% to 36% at a declination of -90°, while improving the u-v coverage for the EVN from 6.47% to 28.76% at declination of 0° and from 47.23% to 73.29% at 80° along the short baselines. For the EOPS, the error in polar motion was reduced from 51.35 μas in R1675 to 24.81 μas in R1675+AVN. As for the source position estimates, the Kenyan antenna adds the most to the CRDS by reducing the errors in the right ascension from 0.345 to 0.240 ms and in declination from 0.557 to 0.351 mas.

The AVN will greatly impact the global VLBI networks by improving the u-v coverage, increasing the accuracy of the EOPs and source positions, have favorable atmospheric conditions for high frequencies observations although measures must be put into place earlier to mitigate RFI.

TABLE OF CONTENTS

DECLARATION AND APPROVAL	Error! Bookmark not defined.
ORIGINALITY DECLARATION	iii
DEDICATION	v
ACKNOWLEDGEMENT	vi
ABSTRACT	vii
TABLE OF CONTENTS	viii
ABBREVIATIONS AND ACRONYMS	x
LIST OF FIGURES	xii
LIST OF TABLES	xiii
CHAPTER ONE	1
INTRODUCTION	1
1.1 Background.....	1
1.2 Problem statement.....	4
1.3 Objectives	4
1.4 Justification and significance of the study	4
1.5 Scope of study.....	5
1.6 Thesis Organization	5
CHAPTER TWO	7
LITERATURE REVIEW	7
2.1 Radio Astronomy and VLBI.....	7
2.1.1 Radio Astronomy	8
2.1.2 Single Dish Radio Astronomy	11
2.1.3 Very Long Baseline Interferometry	12
2.1.4 Radio Astronomical VLBI.....	14
2.1.5 Geodetic and Astrometric VLBI.....	15
2.2 Global VLBI Networks.....	16
2.2.1 VLBI Networks for Radio Astronomy.....	16
2.2.2 VLBI Networks for Geodesy and Astrometry	20
2.2.3 Network Coverage	21
2.3 VLBI Activities in the African Continent.....	23
2.3.1 The African VLBI Network (AVN).....	25
2.3.2 The Longonot Station in Kenya	27
2.4 Site Selection	27
CHAPTER THREE	32
METHODOLOGY	32

3.1 Study Area	32
3.2 Radio Frequency Interference (RFI) assessment.	33
3.3 Weather Assessment	34
3.4 The U-V Coverage	34
3.5 Geodesy Scheduling.....	36
3.6 Astrometry Scheduling	38
CHAPTER FOUR.....	40
RESULTS AND DISCUSSION	40
4.1 Radio Frequency Interference (RFI) assessment	40
4.1.1 Population Densities	40
4.1.2 Electricity Access, Mobile Telephone and Internet Subscription.	41
4.1.3 Terrain of the AVN Sites	43
4.1.4 Overall RFI Assessment.....	54
4.2. Atmospheric Opacity Weather Data	55
4.3 U-V Coverage Plots	65
4.3.1 U-V Coverage for LBA + AVN antennas at X-Band	65
4.3.2 U-V Coverage for LBA + AVN antennas at K-Band	69
4.3.3 U-V Coverage for EVN + AVN Antennas	72
4.4 Geodetic Products	75
4.4.1 Earth Orientation Parameters	75
4.4.2 Baseline Length Repeatabilities.....	77
4.5 Source Position Estimates	80
CHAPTER FIVE	85
CONCLUSION AND RECOMMENDATION	85
5.1 Conclusion	85
5.2 Recommendations.....	88
REFERENCES.....	89
APPENDIX.....	93

ABBREVIATIONS AND ACRONYMS

AGN	Active Galactic Nuclei
AVN	African VLBI Network
CHI	Ceduna Hobart Interferometer
CMB	Cosmic Microwave Background
CRDS	Celestial Reference Frame for Deep South
CRF	Celestial Reference Frame
DE	Declination
DORIS	Doppler Orbitography and Radiopositioning Integrated by Satellite
EOPs	Earth Orientation Parameters
EVN	European VLBI Network
FAST	The Five hundred meter Aperture Spherical Telescope
GLONASS	Global Navigation Satellite System
HartRAO	Hartebeesthoek Radio Astronomy Observatory
IAG	International Association of Geodesy
IAU	International Astronomical Union
ICRF	International Celestial Reference Frame
ISM	Interstellar Medium
ITRF	International Terrestrial Reference Frame
IVS	International VLBI Service
JIVE	Joint Institute for VLBI for European
LBA	Long Baseline Array
LBO	Long Baseline Observatory

NRAO	National Radio Astronomy Observatory
RA	Right Ascension
RFI	Radio Frequency Interference
SEFD	System Equivalent Flux Density
SKA	Square Kilometre Array
VieVS	Vienna VLBI Software
VLBA	Very Long Baseline Array
VLBI	Very Long Baseline Interferometry
WMRS	Weighted Root Mean Standard

LIST OF FIGURES

Figure 2.1: VLBI measurement principle.	13
Figure 2.2: The global distribution of radio astronomy VLBI networks.	16
Figure 2.3: The European VLBI Network (EVN).	17
Figure 2.4: The Wavelengths Distribution for the EVN.	18
Figure 2.5: The Long Baseline Array (LBA) distribution.	18
Figure 2.6: The VLBA telescopes in the USA.	19
Figure 2.7: Global Distribution of IVS Components.	20
Figure 2.8: The proposed AVN antennas.	25
Figure 2.9: EVN + Ghana antenna VLBI U-V diagram for a source at +20 degrees declination.	26
Figure 2.10: Signal Strength of WiFi, Microwave and Mobile network at HartRAO vs VGOS sites.	28
Figure 2.11: Earth's atmospheric transmittance (opacity).	30
Figure 3.1: The structure of the Vienna VLBI Software, VieVS.	36

LIST OF TABLES

Table 2.1: Common radio bands used in Radio Observations.	9
Table 2.2: A summary of spectral line and continuum radio observations.....	10
Table 2.3: Population densities for several main telescopes around the world.....	29
Table 3.1: The AVN Sites.....	32
Table 4.1: Population densities around the AVN sites.	41
Table 4. 2: Electricity access, mobile telephone and internet subscriptions.	42
Table 4.3: Population estimates of people with electricity access, mobile telephones and internet subscriptions.	42
Table 4.4: Contour maps of the AVN sites accompanied by their Google Earth Satellite Images.....	45
Table 4.5: Atmospheric Opacity values at the AVN sites.	55
Table 4.6: Plots of atmospheric opacity at 22.2, 43 and 100 GHz for each AVN site.....	59
Table 4.7: U-V Coverage for LBA antennas (a) and LBA + Kenyan antenna (b) at X-Band.	66
Table 4.8: Percentages of U-V Coverage at Short baselines for LBA + AVN antennas at X-Band.....	67
Table 4.9: Percentages of U-V Coverage at long baselines for LBA + AVN antennas at X-Band.....	68
Table 4.10: U-V Coverage for LBA antennas (a) and LBA+ Kenyan (b) at K-Band	69
Table 4.11: Percentages of U-V Coverage at short baselines for LBA + AVN antennas at K-Band	70
Table 4.12: Percentages of U-V Coverage at long baselines for LBA + AVN antennas at k_band	71
Table 4.13: U-V Coverage for EVN + AVN antennas.	72
Table 4.14: Percentages of U-V Coverage at short baselines for EVN + AVN antennas at X-Band.....	74
Table 4.15: Percentages of U-V Coverage at long baselines for EVN + AVN antennas at X-Band.....	74
Table 4.16: Earth Orientation Parameters (EOPs).....	76
Table 4.17: The number of scans, total observations and number of sources observed per network.	77
Table 4.18: Baselines Length (km).	77
Table 4.19: Plots of baseline length repeatabilities for R1675 + AVN antennas.....	78
Table 4.20: Mean average values for the Right Ascension, RA (hour) and Declination, DE (degree).	80
Table 4.21: Plots of Right Ascension (RA) and Declination (DE).	81

CHAPTER ONE

INTRODUCTION

1.1 Background

The African Very Long Baseline Interferometry (VLBI) Network (AVN) will be a network of radio telescopes comprising of converted telecommunications and new-build radio telescopes across Africa. It was realized that with the advent of new fibre optic cables down the East and West coasts of Africa, many large (30-m class) antennas at Earth satellite stations had become redundant (Gaylard et al., 2014). With the decision that Africa would host a large part of the Square Kilometer Array (SKA), the South African SKA Project (SKA-SA) and the Hartebeesthoek Radio Astronomy Observatory (HartRAO) searched in the partner countries to identify redundant satellite communication antennas with potential to be converted into radio telescopes (Gaylard et al., 2014). Since then, the AVN has become a pathfinder for the SKA in Africa and a means to facilitate Radio Astronomy technology readiness in the SKA partner countries. The SKA has eight partner countries in Africa namely Botswana, Ghana, Kenya, Madagascar, Mauritius, Mozambique, Namibia and Zambia. Some of these countries have large redundant telecommunication antennas which will be converted into radio telescopes, while new telescopes will have to be built in Botswana, Mauritius, Mozambique and Namibia. Apart from the SKA partner countries, there are also other African countries with large telecommunications antennas that could be converted and added to the AVN. In total there are 29 documented 30-m class telecommunications antennas in 19 African countries, though some have been destroyed.

It is envisaged that each of these AVN sites will operate as an independent single-dish astronomical observatory and also as part of a network of radio telescopes in Africa, that would in future provide VLBI capability to the MeerKAT radio telescope currently being built in South Africa as a precursor to the SKA (Booth et al., 2009). It is also planned that the AVN telescopes be equipped to participate in existing global VLBI networks for high-resolution radio astronomical experiments. It is presently proposed that each of these new AVN telescopes will be equipped with the same receivers as Ghana; a 5-and 6.7-GHz receiver (C-band) and later a 1.4–1.7-GHz (L-band) receiver. While it would be advantageous to develop additional receivers covering more frequency bands, there is no funding currently available for this. For example, telescopes equipped with dual receivers at 2.3 (S-band) + 8.4 GHz (X-band) or single receivers at higher frequencies, such as 22 GHz (K-band), could also participate in international geodetic and astrometric VLBI networks.

Observations using the VLBI technique, where radio telescopes can be separated from a few metres to thousands of kilometers, provide very high angular resolution observations of radio sources. In

astronomy, VLBI observations allow the high resolution mapping of the angular radio brightness distribution of radio sources while the use of differential astrometry provides very precise positions, proper motions, and parallaxes of radio sources. Astronomical objects observed and studied using the VLBI technique are radio-bright objects with small angular size, ranging from masers in star forming regions in the Milky Way galaxy to very distant objects such as the Active Galactic Nuclei (AGN). VLBI also plays a fundamental role in the maintenance of the global reference frames. VLBI is the only technique used in determination of the International Celestial Reference Frame (ICRF), through astrometric observations of positions of extragalactic radio sources. Astrometric VLBI is also used for satellite and spacecraft tracking and orbit determination and is essential for deep space navigation (Ma et al., 2016). Geodetic VLBI on the other hand contributes to the maintenance of the International Terrestrial Reference Frame (ITRF) by providing the positions and velocities of VLBI telescopes on Earth (Glaser et al., 2017). Only Geodetic VLBI provides the link between the ICRF and the ITRF needed to determine the Earth's orientation in inertial space and is the only technique that allows the monitoring of the full set of Earth Orientation Parameters (EOPs). Knowing the Earth's orientation in inertial space and positions of VLBI antennas on Earth allow geoscientists to model phenomena that change Earth orientation (e.g. ocean tides and currents) and station positions (e.g. tectonic plate motions). In addition, astrometric and geodetic VLBI also allow determination of certain geodynamic and astronomical parameters, such as ionosphere models and troposphere parameters and parameters of relativistic and cosmological models.

Almost every continent on Earth has a major VLBI Network. The European VLBI Network (EVN) for example, is an array of telescopes spread throughout Europe and Asia that conducts VLBI observations of radio sources largely for astronomical purposes (Charlot et al., 2001), although some of these telescopes also participate regularly in astrometric and geodetic VLBI observations. Astrometric and geodetic VLBI is facilitated through the International VLBI Service for Geodesy and Astrometry (IVS), using a global network of radio telescopes. However, one of the main issues affecting VLBI is the unequal distribution of sites over the globe, especially in the Southern Hemisphere (Mayer et al., 2014). In addition, the African continent has a very poor VLBI network with only two VLBI-capable radio telescopes located at HartRAO in South Africa (de Witt et al., 2016). The two telescopes at HartRAO operate as part of a number of VLBI networks across the globe and are crucial in providing long baselines to radio telescopes on other continents, such as Europe and Australia (de Witt et al., 2016). Radio telescopes that can fill in the gap between HartRAO and Europe and HartRAO and Australia will significantly improve the network geometry and as a result, improve the image quality for Astronomical VLBI and reduce the errors in Astrometric and Geodetic VLBI products. The AVN is a timely and welcome solution for this challenge. For example, the Ghanaian and Kenyan antennas are roughly located halfway between HartRAO and

Europe, and will thus fill in the gap between radio telescopes in South Africa and Europe, while a radio telescope in Mauritius or Madagascar will fill in some of the gap between HartRAO and Australia.

Although new radio telescopes in Africa would initially work with existing VLBI networks, such as the EVN, they will also eventually operate independently as part of the AVN if more radio telescopes in Africa become available. The 26-m telescope at HartRAO in South Africa has played a key role in the development of VLBI in the Southern Hemisphere since 1971. The 26-m telescope is still actively involved in both single-dish and VLBI observing programs and together with the HartRAO 15-m telescope will become the first element in the AVN. The observatory will also serve as a training centre for SKA partner countries in radio astronomy and will act as an archetypal example from which other potential radio observatories in Africa may be derived. The second element in the AVN will be the recently converted Ghanaian telescope. Ghana became the first partner country of the SKA, with the launch of the Ghana Radio Astronomy Observatory on 24 August 2017, to complete the conversion of the telecommunications antenna into a radio telescope. The next focus will be on the conversion of the telecommunications antenna in either Kenya, Madagascar or Zambia, while Botswana and Namibia are possible sites identified for new-build antennas. The AVN Kenyan site is located at the Longonot Earth Station. The Longonot Earth station has two large (32 and 30 m) telescopes for telecommunication which are now redundant. The 32-m antenna will be the most likely to be converted.

While it is clear that more VLBI capable radio telescopes need to be built in Africa, the AVN is still a relatively new concept and its potential is still understudied (de Witt et al., 2016, Mayer et al., 2014). Since VLBI telescopes are very expensive to build and maintain, new sites have to be chosen with care and evaluation of the importance of existing sites has to be carried out. Only a few studies have been carried out to evaluate the impact of the AVN on global VLBI observations (de Witt et al., 2016) and no study has been carried out extensively focusing on the impact of an individual AVN station. This data gap is hindering the proper evaluation of each potential site for the optimization of the AVN, that is, which antennas to convert first, where to build new stations, what next-generation instruments and receivers they should have and finally winning the support of the individual governments for faster realization of the AVN dream. The aim of this study was to re-visit the scientific justifications for the AVN in an attempt to optimize the AVN for each science case, astronomical, geodetic and astrometric. The study was focused on site evaluation and selection as well as the impact that each potential station will have on existing VLBI networks and on the AVN as a stand-alone.

This study investigated the weather conditions and assessed the potential radio frequency interference (RFI) for each AVN site. Plots of the u-v coverage (the density and distribution of tracks formed by the projection of the various VLBI baselines on the u-v plane, the plane perpendicular to the source direction)

for existing VLBI networks together with existing and potential AVN locations were also presented and the impact that these AVN sites could have on global VLBI observations, specifically the impact on the quality of images for astronomical VLBI is discussed. This study also investigated the impact of the existing and potential AVN antennas on astrometric and geodetic products through simulated VLBI observations. From these results, some recommendations are made in an attempt to optimize the AVN for each science case. Furthermore, the AVN is discussed as a stand-alone, what it can do and where collocation of other geodetic instruments can be implemented. In addition, more focus was placed on the Kenyan site as the most likely antenna to be converted next. Understanding and quantifying the impact of the Kenyan antenna on the AVN and global VLBI networks, will help to improve the knowledge base, to influence and support urgently needed policy solutions aimed at speeding up the conversion of the Kenyan antenna for radio astronomy and other related scientific purposes.

1.2 Problem statement

No studies have been specifically carried out to assess the potential impact of the Kenyan and each AVN radio telescope on the AVN and global VLBI networks. Also, the optimization and evaluation of the AVN has not been carried out extensively. These tasks need to be undertaken to inform the implementation of the AVN project.

1.3 Objectives

Assessment and evaluation of the AVN and the potential impact of the Kenyan telescope on the AVN and the global VLBI networks.

Specific objectives:

1. Assessment of the RFI environment at the Kenyan and other AVN sites.
2. Analysis of the available weather data to determine atmospheric opacity at the AVN sites.
3. Create u-v coverage plots of the LBA and EVN with the AVN antennas at different declinations.
4. Investigate the impact of the AVN on geodetic products: the Earth Orientation Parameters (EOPs) and baseline length repeatabilities through simulated geodetic VLBI observations.
5. Determine the accuracy of source position estimates using the AVN for the southern hemisphere through simulated astrometric VLBI observations.

1.4 Justification and significance of the study

Optical fibre has revolutionized telecommunications across the globe. Many African countries, including Kenya are now connected to the undersea fibre optic cables linking them to the rest of the world. As a result of the new optical fibre connectivity in Africa, many large satellite Earth-station antennas have

become redundant since optical fibre provides 1000 times the bandwidth of satellite links. Therefore, there is the possibility of converting these now redundant antennas into radio telescopes at a cost of roughly one tenth that of a new telescope of similar size. The conversion of the Kenyan antenna into a radio telescope will offer an opportunity for training students, scientific research and employment opportunities.

The HartRAO acts as the point of reference for mapping and navigation in South Africa, whereas Kenya still relies on international coordinates for geo-referencing. Thus, if a Radio Observatory is established at Longonot, the site would act as the point of reference for mapping and navigation in Kenya. This will help in upgrading the mapping and surveying systems in Kenya, which is urgently needed.

The AVN sites are envisaged to have huge economical and scientific impacts. First, the AVN will benefit the EVN, LBA, MeerKat, SKA and the IVS for Astrometry and geodesy. Benefits of conversion to an individual country will be low cost of conversion of the antenna compared to building a whole new telescope from scratch, in-country training in practical astronomy for single dish research and VLBI scientific observations. This will create opportunities in training, research, engineering and technology.

Single dish astronomy would be important for student training and research project purposes. Measuring the brightness of broad-band emission sources (radiometry), measuring emission and absorption line strengths (spectroscopy) and measuring the arrival times of pulses from neutron stars (pulsar timing) are some of the techniques that can be developed using a single dish for radio astronomy purposes. Also, observations of interesting astrophysical variable sources over time can be made.

1.5 Scope of study

This thesis focuses on the AVN and the development of radio astronomy and other science that use the VLBI technique such as geodesy and astrometry across the African continent. The study showed the impact that the AVN could have on the global array of VLBI networks and also assessed the proposed AVN sites in terms of the RFI, weather conditions and physical location. The study was primarily based on modeling.

1.6 Thesis Organization

The first chapter gives a brief introduction to the AVN and the VLBI technique and its application in radio astronomy, geodesy and astrometry. A statement of the problem, justification and significance of this research to Kenya, the AVN, radio astronomy, geodesy and astrometry are presented. The objectives of the research and the scope of the study has been listed.

Chapter two gives a background in literature review of the work that is being carried out in radio astronomy, geodesy and astrometry using the VLBI technique. The chapter presents a brief background into the development of the VLBI technique and its application in radio astronomy, geodesy and astrometry. The chapter also covers some of the global VLBI networks and the science or research being carried out using this technique around the world. It also gives an introduction into the development of radio astronomy and the use of the VLBI technique in the African continent and the criteria for site selection.

Chapter three covers the methodology and the techniques used in this research. It explains all the methods as well as the software used in generating and analyzing the data.

The results and discussions of this research are presented in chapter four.

Chapter five gives the conclusions and recommendations from this research study.

The reference materials are given at the end, followed by an appendix of all the results (plots) that were generated for this work.

CHAPTER TWO

LITERATURE REVIEW

The idea of the AVN started with the South African bid to host the largest and most sensitive radio telescope in the world, the SKA. Ghana is the first SKA-Africa partner country where a telecommunications antenna has been successfully converted for radio astronomy purposes. The AVN will significantly strengthen the capability of existing VLBI networks for radio astronomy, geodesy and astrometry across the globe and help fill in the gaps in the network geometry especially in the Southern Hemisphere. The AVN project will also provide the capacity needed in the partner countries to optimize Africa participation in the technological development and science of the SKA.

The aim of this thesis is to revisit the scientific justification for the AVN in an attempt to ensure that it is fully optimized for astronomy, geodesy and astrometry and to evaluate the contribution it can make to the current VLBI networks and as a stand-alone network. This chapter gives an overview of the theory, practice and current research in this field of study. A basic introduction to the theory of radio astronomy and VLBI is given and the current status of VLBI networks and the AVN are also discussed.

2.1 Radio Astronomy and VLBI

Radio astronomy began in 1932 at the Bell Laboratories in the United States when Karl Jansky detected radio waves coming from the Milky Way (Kraus, 1966). Later in 1937, Grote Reber constructed a parabolic radio telescope, the first parabolic dish to be used for radio astronomy, in his backyard and successfully detected radio waves coming from the galaxy as he continued with Karl Jansky's work. In the 1950's, it was discovered that several radio telescopes can be linked together to make radio astronomical observations simultaneously using radio interferometry for improved angular resolution of the radio sources. In the 1960's it was further discovered that these radio telescopes could be thousands of kilometers apart and thus the beginning of VLBI which achieved even higher angular resolution. The first successful VLBI experiment was carried out in 1967. Today, very high precision VLBI observations to measure positions, in sub-milliarcseconds, of extra-galactic radio sources can be made. The VLBI technique has many applications and continues to make significant contributions to science. As a result, there are several global VLBI networks dedicated to radio astronomy and related sciences, Geodesy and Astrometry. These radio telescopes for VLBI are not evenly distributed across the globe and huge gaps exist especially in the Southern Hemisphere with only the HartRAO telescopes in the African continent.

2.1.1 Radio Astronomy

Radio astronomy is the observation and study of the celestial objects using the radio part of the electromagnetic spectrum. The radio and optical frequencies are the only frequencies that are able to pass through the Earth's atmosphere unimpeded. Thus are the only types of astronomy where celestial objects can be observed from the Earth's surface. The radio window ranges from about 30 MHz to over 300 GHz, which corresponds to wavelengths between 100 km to 1 mm. The low frequency end is limited by signal absorption in the ionosphere and prevents ground based observations at wavelengths higher than ~30 m while the high frequency end suffer from signal reduction caused by water vapor and carbon dioxide in the atmosphere (discussed in detail in section 2.4 on site selection).

An antenna and a receiver form a radio telescope. The telescope is used to receive and to measure these radio waves in radio astronomy. The most familiar type of radio telescope is the parabolic dish that focus the incoming radiation onto a small antenna, referred to as a feed. The feed is typically a waveguide horn and is connected to a sensitive radio receiver. Cryogenically cooled solid-state amplifiers are used to amplify the weak radio signals. Radio dishes used at the highest frequencies (mm and sub-mm wavelengths) are built on the highest mountains to avoid attenuation by the atmosphere. For radio telescopes that operate at microwave frequencies or cm wavelengths (0.1-100 cm), RFI is a serious problem and these dishes are usually built in valleys away from large cities to protect them from man-made interference (see section 2.4 for more details). The most common radio bands used by large radio telescopes and interferometers operating at microwave frequencies (such as the proposed AVN telescopes), and their corresponding wavelengths/frequencies, are listed in Table 2.1. At the lower frequencies ($\sim >1$ m), dipole arrays are used instead of parabolic dishes, as these work more efficient at low frequencies and are more cost effective.

The sensitivity of a radio telescope, or its ability to measure weak sources of radio emission, depends on the area and efficiency of the dish, the sensitivity of the amplifier used to amplify and detect the signals, the duration of the observation and the receiver bandwidth. An overall measure of the telescope sensitivity is the System Equivalent Flux Density (SEFD), defined as the flux density of a radio source that doubles the system temperature (system noise). The angular resolution of a radio telescope, or its ability to distinguish fine details on the sky, depends on the wavelength of the observations and the diameter of the dish and is given by the equation $\theta = 1.22 \frac{\lambda}{D}$ in radians, where λ is the wavelength of the observations and D is the diameter of the dish. The resolution of an array of radio telescopes is given by $\theta = \frac{\lambda}{B}$, where B is the maximum distance or baseline between any two telescopes in the array.

Table 2.1 shows the most commonly used radio bands at microwave frequencies and their corresponding wavelengths in cm and frequencies in GHz.

Table 2.1: Common radio bands used in Radio Observations.

Designation	Wavelengths and Frequencies
L-band	18 cm 1.4 GHz
S-band	13 cm 2.3 GHz
C-band	6.0 cm 5.0 GHz
X-band	3.5 cm 8.4 GHz
Ku-band	2.5 cm 15 GHz
K-band	1.3 cm 22 GHz
Ka-band	0.9 cm 32 GHz
Q-band	0.7 cm 43GHz

Radio emission detected from astronomical sources is either continuum emission that occur over a broad frequency range or spectral line emission that occur over a very narrow frequency range. Continuum radio emission is produced by both thermal and non-thermal emission mechanisms. Thermal emission mostly come from cold and dense gas such as the cold and dark dust clouds in the milky way, the warmer redshifted Cosmic Microwave Background Radiation (CMB) regions or warm dust from galaxies at high redshifts. Thermal radio emissions are also detected from hot and ionized regions (HII regions) produced by bremsstrahlung emissions in star forming regions. However, the radio sky is dominated by non-thermal emissions at cm and m wavelengths such as synchrotron emission from jets in AGN, pulsars, quasars and supernova remnants.

Continuum emissions are weak and thus require a long period of observation so as to detect any changes in these radio sources and their variability with time. Therefore, a long integration time and a wide bandwidth is needed in order to increase the sensitivity of a radio antenna to this type of emission (Porko et al., 2011).

Spectral line emissions on the other hand only occur at specific discrete frequencies. The most studied spectral line in radio astronomy is the HI line from diffuse neutral hydrogen gas and is observed at 1.420 GHz ($\lambda = 21$ cm). Molecular rotation lines are detected from dense and cold molecular clouds in the interstellar medium (ISM) while hydrogen recombination lines are also detected from ISM regions where hydrogen is mostly ionized such as the HII regions. Masers (Microwave Amplification by Stimulated Emission of Radiation) are intense tightly collimated beams of spectral line emissions that occur in very

many astronomical objects such as galaxies and star forming regions. They are usually associated with rotational transitions in molecules such as OH, H₂O, SiO and CH₃OH. Masers and other hundreds of spectral lines are used to study different molecules in the universe so as to determine parameters such as the velocities and motions of celestial objects (Gilloire and Sizun, 2009).

A summary of both the continuum radio observations and spectral line radio observations is given in the Table 2.2. The table provides a summary of the most common radiation processes in astronomy that produce radio waves and the environments that they occur in.

Table 2.2: A summary of spectral line and continuum radio observations (Mike Garret, 2011).

Wavelength(λ)	Spectral Line	Continuum
Metre, cm and mm	<ul style="list-style-type: none"> -Neutral Hydrogen (H1) 21 cm fine structure line (neutral gas). -Hydrogen recombination lines (ionized gas). -OH, H₂O, SiO Masers (dense and warm molecular gas). -Molecular rotation lines (cold molecular gas). 	<ul style="list-style-type: none"> -Thermal Bremsstrahlung emission (HII regions). -Synchrotron Radiation (jets in radio galaxies, shocks in supervanovae, cosmic ray electrons in the magnetic fields of normal galaxies and planetary systems). -Thermal emission from interstellar dust (cold and dense gas).
Sub-mm	<ul style="list-style-type: none"> -Molecular Rotation Lines (warm, dense gas). Solid State features such as silicates (dust). -Hydrogen recombination lines (Ionised HII regions). 	<ul style="list-style-type: none"> -Thermal emission (warm dust)

Stars, planets, galaxies, nebulae and supernovae among many other celestial objects naturally emit radio waves (Verschuur, 2007). Studying these emitted radio waves gives important information about the celestial object such as its chemical composition, its distance from the Earth and the Sun, and its position in the Universe, velocity, evolution, lifespan and death.

2.1.2 Single Dish Radio Astronomy

Due to the large distance travelled by these radio waves and the interstellar medium, the radio signals received on the earth's surface are very weak and thus requires very sensitive radio antennas to collect. The smallest antennas are meter diameter dishes mounted on satellites while the largest steerable dish is the 100 m Green Bank Telescope and the largest being the 305 m dish at Arecibo in Puerto Rico and the latest one being the 500 m non-steerable Five hundred meter Aperture Spherical Telescope (FAST) dish in China.

A radio telescope can carry out observations as an individual telescope for spectral line, continuum and solar radio observations. Maser line surveys of star forming regions and late type stars are some of radio observations done using single dish antennas (Lee et al., 2011). HI region surveys and studies of high velocity clouds is one of the major research area using single dishes such as Parkes in Australia and Effelsberg in Germany (Wakker, 2004). The search and study of pulsars is a major domain for single dish radio telescopes since pulsars are point sources in the sky and thus are used for pulsar detection and timing of pulses to detect variations which in turn provide information about the inner neutron stars. Single dishes such as Parkes in Australia, Jodrell Bank in the UK and Arecibo in Puerto Rico are used for pulsar detections and studies (Wright, 2004). Single dish observations is the only choice when it comes to accurate measurement of large scale structure in the sky and as well as the measurements of the 3-Kelvin Cosmic Microwave Background (CMB) radiation (Emerson, 2002).

The sun is a rich emission source and emits across the entire electromagnetic spectrum and is thus a good candidate for any type of astronomical observations including radio observations using a single dish. Solar observations by radio astronomy observations involves the study of different radio activities taking place in the sun. This include phenomena such as radio bursts or solar flares and coronal mass ejections (Porko et al., 2011).

Some advantages of using a single dish for radio astronomy observations are: i) the larger the dish the larger the collecting area and thus increased sensitivity (Burke and Graham-Smith, 1997). Thus single dishes are used for initial detection of very faint radio sources. ii) Single dishes are readily available for astronomers to carry out single radio observations and monitoring campaigns. They are also easy to build and maintain, flexible and relatively cheaper as compared to an array of telescopes. iii) Single dishes are easy to use, that is, no planning and coordination of multiple dishes is required, and the data obtained does not require any correlation (Wright, 2004). Lastly, it is easier to find or make a specialized equipment for example a receiver, for a particular single dish.

Despite all the advantages of a single dish as listed above, the major limitation of a single dish is the fact that it cannot achieve very high resolution of extended radio sources (Stierwalt, Peck, Braatz and Bemis, 2017). The angular resolution of a single dish is limited and therefore the use of two or more radio dishes to increase the collecting area and thus increasing the angular resolution of radio sources.

2.1.3 Very Long Baseline Interferometry

The limited angular resolution of a single dish is overcome by the use of radio interferometry and the VLBI techniques. VLBI is a technique that employs the use of two or more single radio telescopes, distributed from a few meters to thousands of kilometers apart, simultaneously observing one radio source in the sky. The distance between any two radio telescopes in such an array is called a baseline, and the resolution that can be achieved is comparable to that obtained with a single dish radio telescope, whose diameter equals the largest baseline of the array. This technique achieves very high angular resolution and provides milliarcseconds (mas) resolution of radio astronomical sources. The baseline projected to the plane orthogonal to the source direction gives the spatial frequency for a given observing frequency. The maximum frequency is given by the two telescopes farthest apart (Kruithof, 2009). The projected distances between telescopes change during experiments due to the rotation of the earth. This gives the possibility of measuring a range of spatial frequencies using a limited number of telescopes. While the angular resolution of VLBI depends on the maximum projected baseline, the sensitivity depends on the number of telescopes and the bandwidth. Sensitivity of radio telescopes is the ability to measure very weak radio emissions from weak radio sources and depends on the size of the antenna and its efficiency. Bandwidth is the range of frequencies of a radio signal that a radio telescope can receive and record.

The VLBI technique works on the principle that there is an observable difference in arrival time of light at two observing stations from a radio source billions of light years away. The incoming rays from the source to all antennas are assumed to be parallel since the source is placed very far away from the receivers. The difference in arrival time is called the time delay (τ), which is the main observable variable of the VLBI technique. The data collected at different radio telescopes is combined and correlated so as to correct for effects such as geometric delays, ionospheric delays, time delays, phase and instrumental delays. These signals are combined into one signal thus producing a high angular resolution image of the radio source observed.

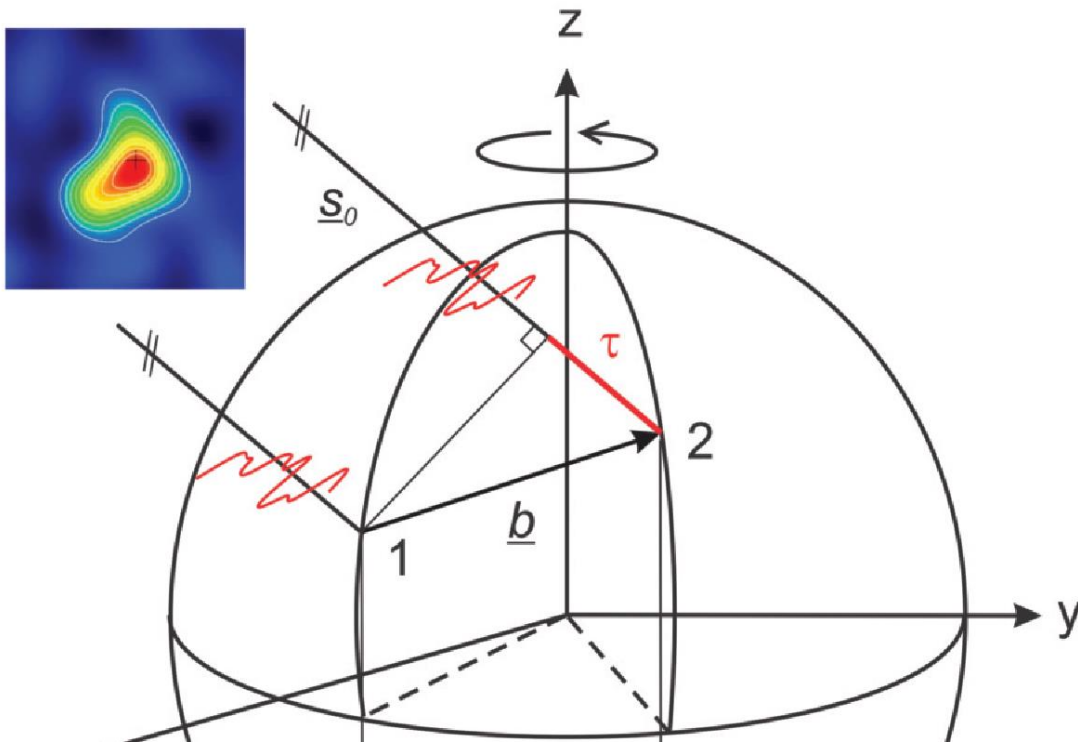


Figure 2.1: VLBI measurement principle (Schuh and Bohm, 2013).

Figure 2.1 demonstrates the VLBI principle. S_0 is the direction of the radio Source, b is the baseline vector, 1&2 are observing stations on the Earth's surface while τ is the time delay between the signal received at the two stations. Time delay τ , represents the elapsed time between recording of the signal at time t_1 on station 1 and time t_2 on station 2 and is given by:

$$\tau = (t_1 - t_2) = -\frac{b \cdot s_0}{c} \dots\dots\dots (1)$$

The VLBI technique has evolved to be the primary tool used in radio astronomy. First, it is used for measuring the photometric magnitudes of the incoming radiation (astronomical VLBI) from sources in space (Lena et al., 2012). Secondly, it is used in the determination of very precise coordinates of extragalactic sources (astrometry VLBI). Thirdly, the technique is used in determination of precise coordinates on the earth's surface as well as monitoring the variations of the earth's orientation and rotation in space (geodetic VLBI) with very high precision (Schuh and Behrend, 2012). VLBI is also used in relativistic studies and cosmological models for describing the universe.

2.1.4 Radio Astronomical VLBI

The use of the VLBI technique in radio astronomy has enabled high resolution imaging of galactic and extra galactic radio sources and imaging of the surfaces of some nearby stars. High resolution radio observations provide information about the AGN such as their accretion discs, their magnetic fields, energetic quasars jets and their absorbing materials. Binary stars, radio stars, supernovae remnants, gravitational lensing are all imaged using this technique. Spectral line VLBI observations makes it possible to study compact maser emitting regions of new star forming regions, galaxies and stellar envelopes as well as tracing their motions and velocities (Middelberg and Bach, 2008).

The VLBI technique is used to study all kinds of stars, from the very young stars to the very old ones, hot to cool ones and from very violent to passive ones. The emission of radio waves from stars depend on the temperature of the star and its magnetic field. VLBI observations give insight into the origin of these radio emissions in these objects and their environments. Cool dwarf stars are the most commonly observed stars since they show occasional flaring and coronal emissions just like the sun. Young stars with radio emissions thought to be due to collision of energetic stellar winds are now well understood before they enter the main sequence phase due to VLBI (Middelberg and Bach, 2008). Binary stars with a compact star such as a neutron star or a black hole with accretion of materials are also well studied using VLBI.

Supermassive black holes are thought to exist in the centers of radio galaxies, quasars and AGNs. Just like the X-ray binaries, these supermassive black holes have extremely energetic jets of materials flowing outwards from the core of the galaxy. These powerful jets interact with the surrounding materials creating complex radio lobes. These radio lobes can be studied in detail about their magnetic field strengths and particle densities using VLBI. If these powerful jets and radio lobes are observed at different times several times, astronomers are able to follow the motions and determine velocities of these celestial objects.

Masers are caused by the excitation of different types of molecules in space and are also sources of radio emissions. Outflows from young star forming regions and circumstellar shells of evolved stars normally trace molecules such as methanol (CH_3OH masers), water (H_2O masers), hydroxyl (OH masers) and silicon oxide (SiO masers). Studying these masers using VLBI gives the information on the condition, motion and velocities of the celestial objects emitting these molecules.

2.1.5 Geodetic and Astrometric VLBI

The VLBI technique is also applied in geodesy and astrometry. Geodesy deals with the measurement of the Earth's movement while astrometry deals with the measurement of position of radio sources in the sky. The difference in arrival time of the radio waves from distant quasars can be used to determine the position of radio telescopes on the earth's surface accurately. Doing this repeatedly can be used to monitor the changes in the distance between any two telescopes over time. These small changes in the position of these telescopes allow scientists to study tectonic plate and earth's crust movements besides determining earth's orientation in space. VLBI technique allows determination of source positions with the highest possible accuracy.

Geodetic VLBI is the only technique that enables full observation of the five Earth orientation parameters (EOPs) which include: two angles of the polar motion (x_{pol} and y_{pol}); two angles of Earth's nutation (n_{utdx} and n_{utdy}); and the Earth rotation angle ($dUt1$). EOPs describe the irregularities of the Earth's rotation in space and link the ICRF to the ITRF. ICRF provides a stable and independent inertial reference frame regardless of the motion of earth in space. The ITRF is important in the areas of modern mapping (cadastral surveying, topographical, geological and hydrological), precise navigation and determination of precise satellite orbits (de Witt, et al., 2016). Accurate EOPs are important for the long-term orbital maintenance of the Global Navigation Satellite System (GNSS) constellations. Accurate measurements of the EOPs relies heavily on long baselines both in the North-South and East-West directions (Dale et al., 2014) and need to be observed continuously for accurate positioning and navigation on Earth and in space.

Geodetic VLBI also gives the orientation of the earth in space through very accurate measurements of the positions of extragalactic radio sources (Schliiter and Behrend, 2007). Extragalactic radio sources are fixed in position and thus create an absolute and fixed reference frame. This has contributed tremendously to the measurements of site positions and lengths of intercontinental baselines with the highest accuracy and monitoring of the Earth's rotation and orientation in space. Geodetic VLBI provides very precise locations for the telescopes which are then transferred to col-located relative position measuring systems such as the global navigation satellite systems GPS and GNSS, laser ranging and DORIS systems used to obtain precise measurements of satellites in orbits.

Astrometric VLBI is used to measure distances to celestial sources and to determine the position of radio sources in the sky. Observation of celestial bodies is a practice that has been in existence since time immemorial. Observation of astrophysical objects and data analysis consists of measuring the positions of heavenly bodies and in dating of events (Lena et al., 2012). The position of these heavenly bodies must

be determined with great accuracy and must be documented. Observing and recording of these positions is a lengthy and complex affair (Perryman, 2012) and dates back to the earliest records of astronomical observations, more than two thousand years ago. The accuracy of these measurements has improved over the years and has made navigation, both on the earth's surface and in space, easy as humans continue to understand the dynamics of motion and structure of the Earth in space and all the other celestial objects.

2.2 Global VLBI Networks

Due to the need for higher angular resolution of celestial objects, several VLBI networks dedicated for either radio astronomy or geodesy and astrometry have been established around the globe.

2.2.1 VLBI Networks for Radio Astronomy

The VLBA, EVN, KVN, LBA and JVN are radio astronomy VLBI networks used in radio astronomical observations across the globe. However, several telescopes from all these radio astronomy VLBI networks can be combined to create a temporary VLBI network for radio astronomical VLBI experiments.

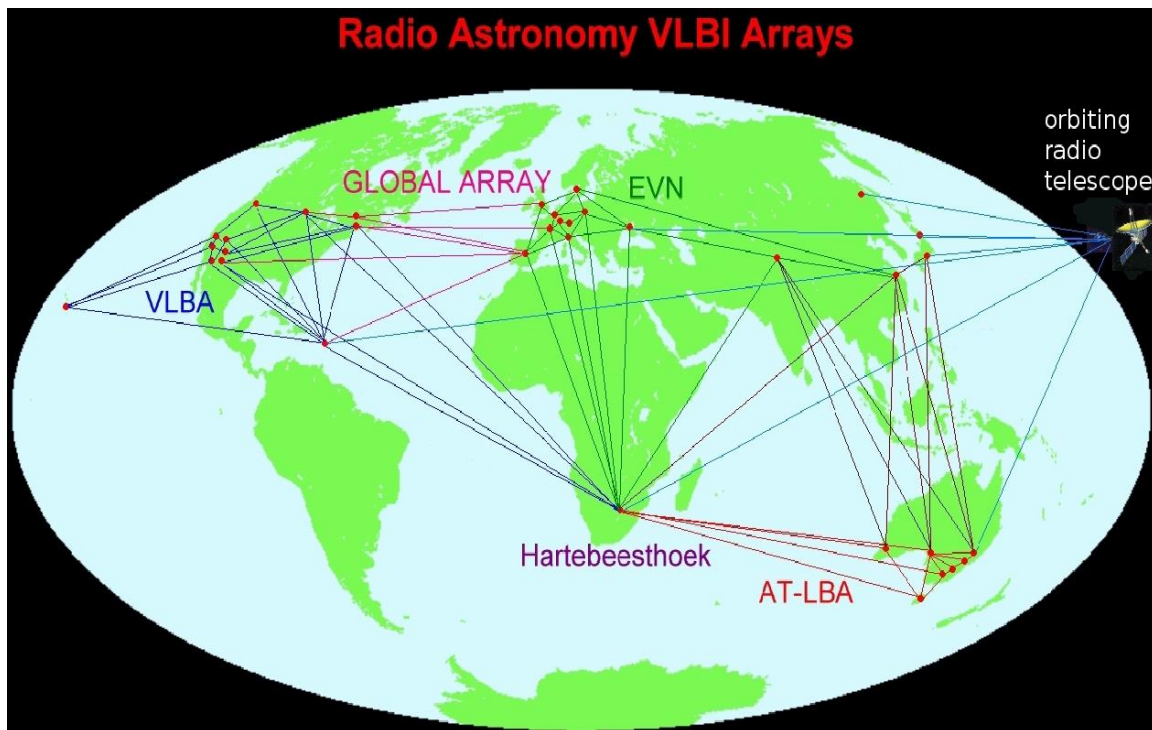


Figure 2.2: The global distribution of radio astronomy VLBI networks (Gaylard et al., 2014).

The figure 2.3 below shows all telescopes that form the EVN. The EVN is centrally managed by the Joint Institute for the VLBI in Europe (JIVE). Some of the VLBI science with the EVN include: radio jets and black hole physics; the evolution of radio sources; masers; starburst galaxies; gravitational lenses; supernovae; gamma-ray bursts; studies of the nature of faint radio source population; H1 absorption studies in AGN; Astrometry and Space Science VLBI (Micheal Lindqvist, 2016).



Figure 2.3: The European VLBI Network (EVN), (Paul Boven, JIVE, 2016).

The EVN operates with the following wavelengths: 90, 18, 6, 5, 3.6, 1.3, 0.7 cm. It operates more at the 21/18 cm as shown in the figure below.

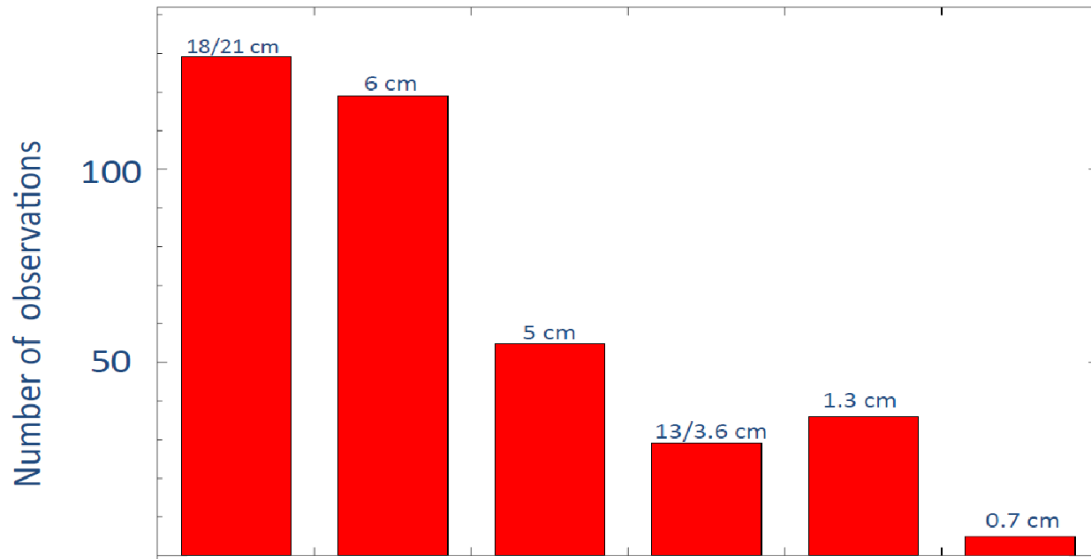


Figure 2.4: The Wavelengths Distribution for the EVN between 2012 and 2016 (Michael Lindvist, 2016).

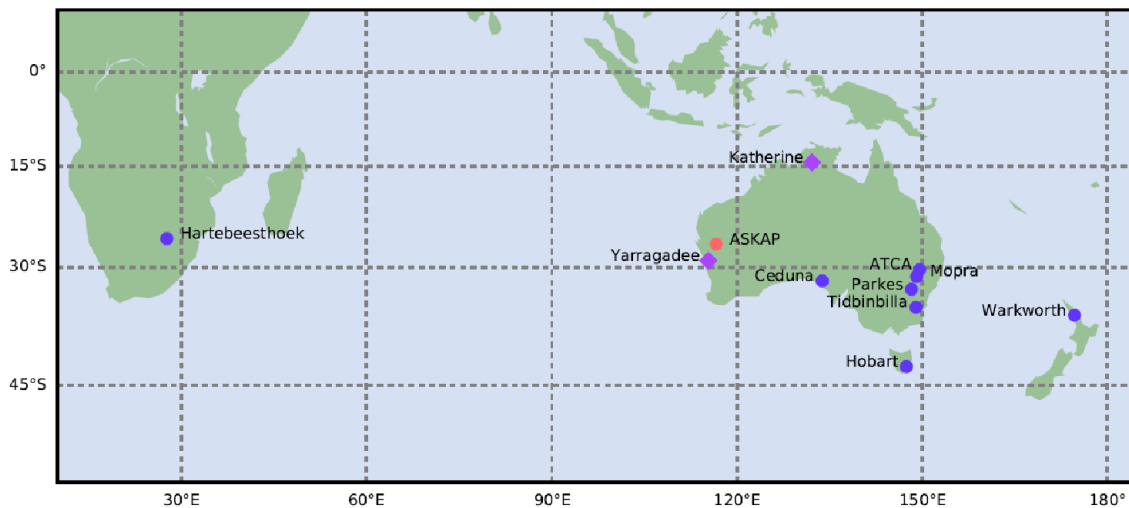


Figure 2.5: The Long Baseline Array (LBA) distribution (www.atnf.csiro.au).

The LBA consists of telescopes in Australia, New Zealand and Hartebeesthoek in South Africa with the correlator based at Pawsey Centre. It covers a radio frequency range from 1 to 100 GHz (C. Reynolds and C. Phillips, 2016). Regular observations are done at the following wavebands: 20, 13, 6, 3 and 1 cm.

Some of the science done with the LBA include: Masers; blazars and jet properties; supernovae; protostars; southern hemisphere calibrators survey (C. Reynolds and C. Phillips, 2016); pulsars; geodesy and astrometry; studying structural changes in the galactic sources and AGNs (P. G. Edwards and C. Phillips, 2015).

Figure 2.6 below shows the distribution of the VLBA telescopes in the USA. The VLBA comprise of ten 25 m dishes with the longest baseline in the array being 8, 611 km. It's operated by the Long Baseline Observatory (LBO). It observes at wavelengths from 28 cm to 3 mm, that is, from 1.2 to 96 GHz (A. Mioduszewski and T. Perreault, 2016) Very Long Baseline Array NRAO Website. The VLBA is the most sensitive VLBI array since it was specifically build to carry out VLBI observations and also has the longest baseline lengths.

The science carried out with the VLBA include: studying of blackholes and cosmology; gamma-ray bursts; the Milky Way galaxy; masers and astrometry; mapping of the universe; monitoring the changing Earth and tracking the near earth asteroids among many other science cases.

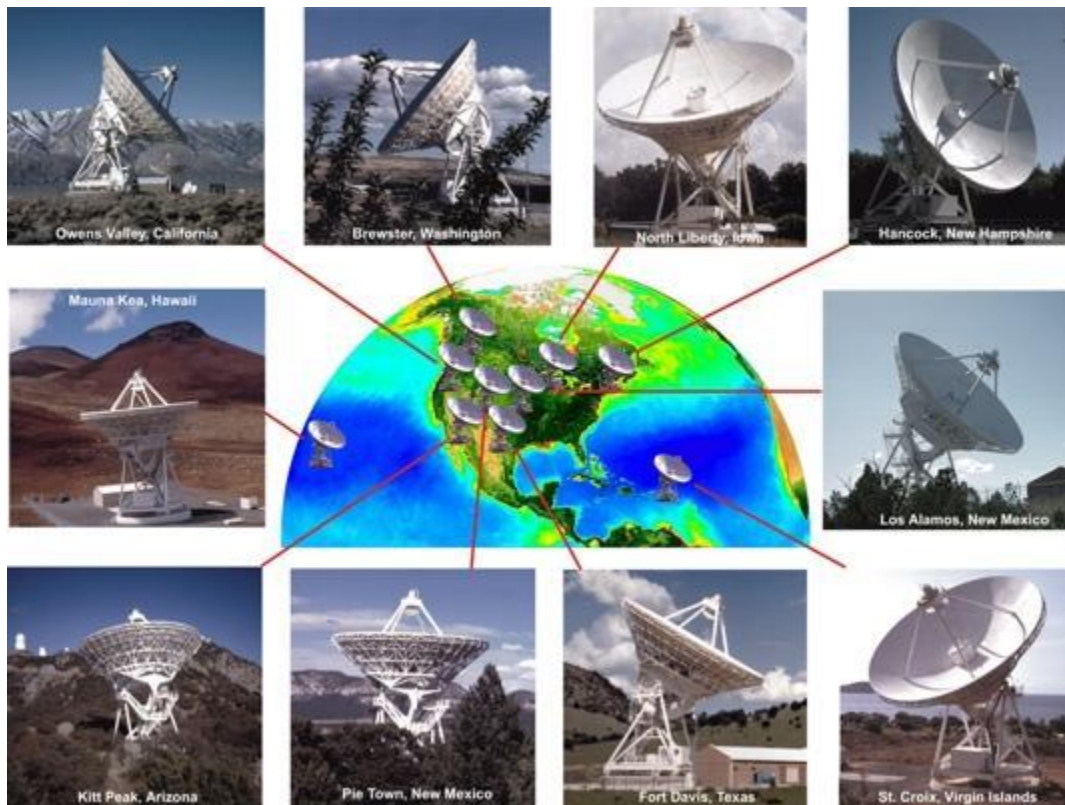


Figure 2.6: The VLBA telescopes in the USA (<http://images.nrao.edu>).

The Korean VLBI Network (KVN), the Chinese VLBI Network and the Japan VLBI Network (VERA) form the Asian VLBI Network. The KVN operates at 22, 43, 86 and 129 GHz and is used to study the maser line survey of the galactic star forming regions, proto stars and late type stars (Lee et al., 2011).

2.2.2 VLBI Networks for Geodesy and Astrometry

The need to produce precise measurements of distances on earth and in space has led to the establishment of several VLBI networks across the globe dedicated for geodesy and astrometry VLBI. Determining exact distances of extragalactic sources in the universe and their composition and distance measurements on the earth's surface require a large number of radio telescope antennas distributed over the globe (Lena, 2012).

The VLBI technique plays an important role in the maintenance of the global reference frames, that is, the celestial and reference frames useful in earth sciences research. These reference frames are required for precise positioning around the globe. All the Geodetic and Astrometric VLBI experiments are coordinated by the IVS. Geodetic VLBI gives the ITRF whereas Astrometric VLBI gives the ICRF. ICRF is based on VLBI observations of compact extragalactic sources using the S-band (2.3 GHz) and X-band (8.4 GHz) (Lanyi et al., 2010). The main task of the IVS as mandated by the International Association of Geodesy (IAG) and the International Astronomical Union (IAU) is to deliver products for the maintenance of the Celestial Reference Frame (CRF) through quasar positions and the maintenance of the Terrestrial reference frame (TRF) like station positions and how this position changes with time (Schluter and Behrend, 2007) and to give the EOPs, nutation parameters and the time difference (UT1-UTC).

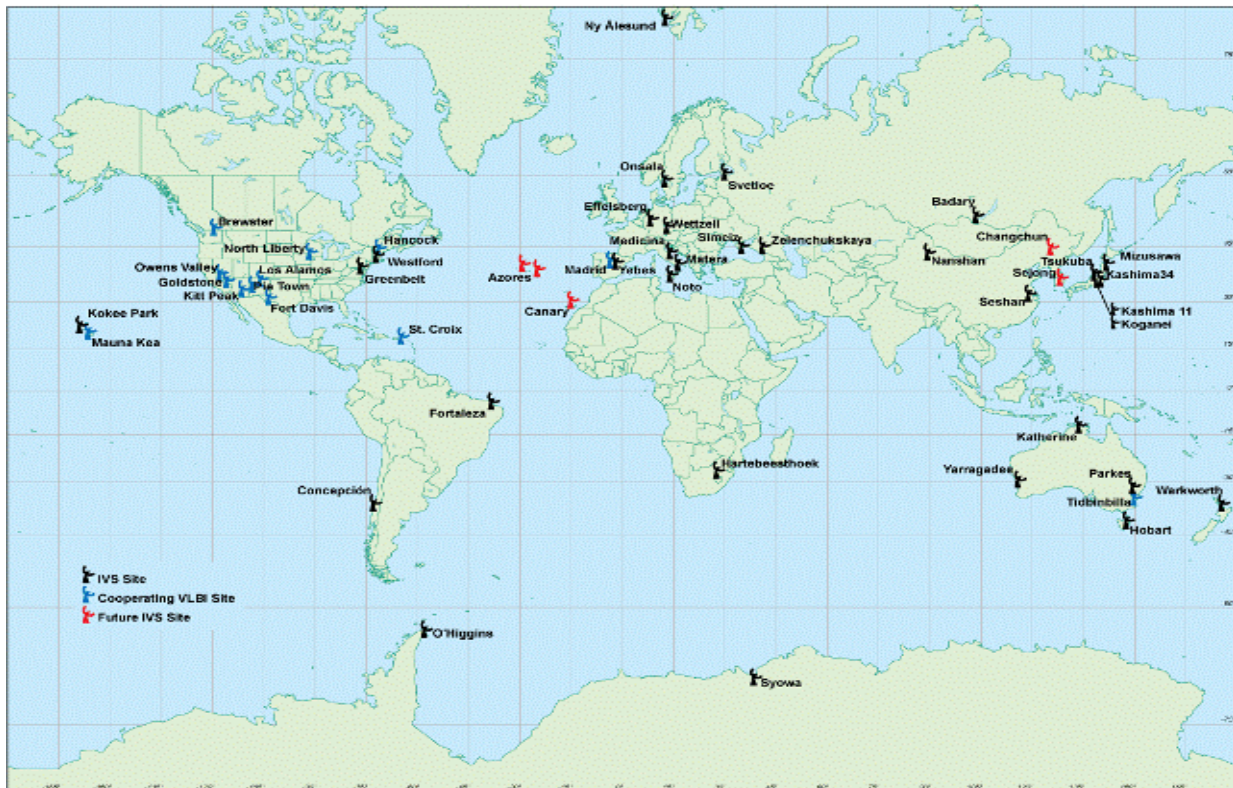


Figure 2.7: Global Distribution of IVS Components (<https://ivscc.gsfc.nasa.gov>)

The same radio antennas in the existing global VLBI networks are still the same used in geodetic and astrometric global experiments. For example, the LBA network is capable of conducting absolute astrometric VLBI surveys with an accuracy better than 5 mas (Petrov et al., 2009).

2.2.3 Network Coverage

Current VLBI networks, for both astronomy and geodesy, consist of a very uneven distribution of radio sites. Due to economic and political reasons, most radio telescopes are located in the Northern Hemisphere (Mayer et al., 2014). As of 2016, the southern hemisphere and the North-South baselines represented only 15% of the total ICRF-3 observations (Ma et al., 2016). There's however hope that more VLBI capable antennas can be established in Africa, South America and generally in the southern hemisphere (Schuh and Behrend, 2012).

Global participation in VLBI observations is required to obtain accurate EOPs (de Witt et al., 2016). Four VLBI telescopes (Wetzell in Germany, HartRAO in South Africa, Tigoconc in Chile and O'Higgins in Antarctica) were used to provide very long baselines in a study reviewing an independent VLBI network for Europe to accurately determine the EOPs. The results were compared against those obtained from a full network session. De Witt et al. (2016), found that excluding some stations from an existing session resulted in a suboptimal schedule that provided less accurate estimates of the EOPs. The results indicated that the EOPs precision decreased when a large number of telescopes were excluded from the analysis. This study concluded that in order to achieve very accurate EOPs, radio telescopes distributed evenly all over the earth, with Africa included, are needed.

Studies done in recent years show that the EVN plays an important role in the maintenance of the terrestrial and celestial reference frames, determination of EOPs with very high precision and provides good u-v coverage for sources in the Northern Hemisphere (de Witt et al., 2016). The EVN and the VLBA has contributed tremendously to radio astronomy, geodesy and astrometry experiments across the globe.

Some telescopes constructed in Australia have achieved centimeter precision in baseline measurements. As a contribution to the global VLBI networks and in a bid to strengthen the Southern Hemisphere Reference radio sources catalogue, Australia constructed and is now operating three 12m telescope dishes for geodetic VLBI in the Australian continent, the AuScope VLBI array, (Lovell et al., 2013). The physical positioning of the three telescopes, Yarragadee, Hobart and Katherine across the Australian continent seeks to optimize the possible improvements to the ICRF and ITRF from the continent and the southern hemisphere at large.

Increasing the number of antennas in the southern hemisphere will improve the long term accuracy of geodetic VLBI. In 2011, first geodetic observations were carried out using two new stations ASKAP-29 and WARK12M in Australia and New Zealand respectively (Petrov, et al., 2011). The results of a successful 7 hour long geodetic VLBI showed that precision of the antenna positions (station coordinates or station position) increased by a factor of two orders of magnitude and reached a millimeter level of accuracy, that is, it provided a 1-3mm accuracy of the tie vector between VLBI and GPS antenna reference points. The WARK12M is in line with the IVS VLBI2010 Strategies for improving the long term accuracy of geodetic VLBI of 1-mm on VLBI baselines (Gulyaev, Natusch and Wilson, 2010). This can only be achieved by increasing the number of antennas globally and especially in the Southern Hemisphere. The AVN antennas, Kenya included can play a very crucial role.

A successful 12-hour 22 GHz VLBI experiment using a heterogeneous network of radio telescopes in the LBA was carried out in 2009 (Petrov, L. et al., 2009). Three VLBI stations that had never participated in geodetic experiments before (Ceduna, Mopra and ATCA-104 antennas) and several stations that regularly participate in geodetic VLBI campaigns were included. In evaluating the possibility of using the LBA antennas for precise geodesy and absolute astrometry, a 1.5-hour long VLBI test and a 12-hour long geodetic VLBI experiment sessions were run. 105 radio sources were observed including 5 objects that had not been previously seen with the existing VLBI networks. The positions of these new sources were determined with an accuracy of 2-5 mas and the positions of the three antennas were determined with a position accuracy of 1-5 cm. This showed that the LBA network was capable of conducting absolute astrometric VLBI surveys with very high accuracy. As a result of these impressive results for geodesy and astrometry, the X-band Calibrator Survey observing campaign for observing and determining positions and images of thousands of objects with declinations below -50 degrees begun (Ojha et al., 2005) with the first session in 2008.

The Ceduna Hobart Interferometer (CHI) in Australia is the only facility that can carry out rapid and high resolution observations of sources about -30 degrees in declination. CHI is a single baseline interferometry formed by the 26 m telescope at Mount Peaseant, Hobart and the 30 m telescope dish at Ceduna, Australia. Both dishes underwent conversion from satellite communication dishes into radio astronomy dishes. The CHI has a baseline of 1,704 km with a resolution of 6.6 mas at 6.7GHz. CHI is a crucial tool in making rapid observations of a radio object when it flares (Blanchard et al., 2009). Its immediate application is to provide rapid radio coverage of AGN flaring at gamma ray frequencies which are then detected by the Fermi Gamma-ray space telescope.

The FAST telescope in Japan can significantly add to the current global VLBI networks. This is due to its large size (collecting area) and the geographical area since it lies at the edge of most VLBI networks. In a study carried out to evaluate the contribution of FAST to global VLBI networks (Jin, C.J. et al., 2008), the u-v coverage of some EVN antennas plus FAST was simulated. The results showed that FAST contributed majorly to the long baselines and increased the baseline sensitivity by an order of a magnitude, yielding more precise position measurement and detection of even more weaker sources.

In the near future, it will be easier to create an ad-hoc global VLBI network on a short notice. In the world's first ever scientific e-VLBI using a global array (Giroletti et al., 2011), the EVN, LBA and the 34m Kashima telescope in Japan were used to study the gamma-ray narrow line PMN J0948+0022 radio-loud galaxy Seyfert 1. The maximum baseline length achieved in the array was 12 458 km. This experiment showed that it would be easy to create temporary global VLBI networks on a short notice and still provide excellent u-v coverage. These ad-hoc arrays would provide long unique base lengths, increased sensitivity due to the more number of telescopes, and thus increased data rate flow.

2.3 VLBI Activities in the African Continent

Very little VLBI activities exist on the African continent. The 15 and 26 m telescopes at HartRAO in South Africa are the only radio telescopes in Africa currently equipped to participate in global VLBI experiments. HartRAO is one of the most important element in the current global VLBI networks. Mayer et al., (2014) carried out a study evaluating the importance of HartRAO for the global VLBI networks. The results proved that remote telescopes, those outside Europe, have high impact on the precision of the EOPs than a single telescope in the EVN. Without HartRAO the number of radio sources observed in the southern hemisphere will be limited and thus maintaining the ICRF will be a challenge. The study concluded that it was important to have telescopes in high and low latitudes for proper estimation of the polar coordinates and long baselines with telescopes at different longitudes for accurate estimations of the earth's nutation (dU_{t1}).

The Karoo Array Telescope (MeerKAT), situated in the Karoo, Northern Cape of South Africa is presently the most sensitive centimeter wavelength instrument in the Southern Hemisphere, and it is the only radio telescope array located in Africa. The MeerKAT provides a high dynamic range of imaging resolution of about 1 arcsec to 1 arcmin at 1420 MHz (Booth et al., 2009). Its array of 80 antennas of 12 m dishes with baselines of a few meters to a maximum of 8 km has an equivalent of an 85 m single dish. This would certainly have a profound effect on the highest resolution measurements made with VLBI. It will also provide increased sensitivity on the longest baselines where visibility amplitude is often low as sources become more resolved. MeerKAT is a precursor to the SKA project.

The MeerKAT increases the u-v coverage in the Southern Hemisphere. In a demonstrated e-VLBI capacity with HartRAO, a big demand for MeerKAT in the VLBI networks was observed, especially with EVN's wide field imaging VLBI of radio sources in the deep fields (Booth et al., 2009). This would produce interesting finer details on galaxies, especially the AGN, in the early universe. Together with high-energy telescope in the neighboring Namibia, the MeerKAT will enhance the importance of the southern VLBI arrays. These arrays will be useful in studying the radio component of high-energy gamma ray sources and masers. This will contribute to the refining of measurements of distances to the Milky Way galaxy and improve the knowledge about its structure.

The addition of SKA1 for VLBI will not result in large improvements in the ICRF. Improvements in the ICRF will only be achieved if more VLBI capable antennas are added in the Southern Hemisphere, thus the SKA2 will play a very crucial role in the improvement of the accuracy of the ICRF. This is due to its long baselines and high frequencies for correcting for opacity shifts in AGN jets for the ICRF defining sources (Paragi, Fejes and Frey 2010). The number of objects detectable with the current VLBI arrays is not high enough to calibrate Gaia. Gaia is a twin telescope in space observing two regions in the sky simultaneously with the aim of charting a three dimensional map of the Milky Way, launched in 2013. The SKA-VLBI will be needed to accurately measure parallaxes for a significant number of Gaia targets. Thus SKA-VLBI will improve the connection between the ICRF defined in optical and radio bands since the high sensitivity of the SKA-VLBI on long baselines will help in probing of deeper sources in the sky especially in the southern hemisphere. Comparing Gaia and SKA-VLBI positions of the centers of galaxies will be a great tool for finding more astrophysical objects as well. SKA-VLBI will also make imaging of radio sources at (sub)-milliarcsec possible and thus allow for observation of sources below the detection limits of current instruments. The AVN antennas are expected to form the SKA-VLBI, SKA2.

The SKA-VLBI will match or even exceed the current capabilities of a typical e-EVN configuration in probing the early universe. This is so because of its ability and capability to assess the entire southern sky including tracking the galactic centre for many hours (Paragi, Fejes and Frey 2010). Adding FAST to the SKA-VLBI will outperform current global VLBI arrays including the most sensitive telescopes (Paragi et al., 2014). This configuration might achieve a sub-nano-arcsec resolution in some cases and will offer great sensitivity of some very bright pulsars by providing local interferometer and phased array data simultaneously. Flux densities and polarization properties of compact calibrators will be measured using local interferometer data during the VLBI observations which will lead to very accurate flux density and polarization calibration of the VLBI data.

Adding two to four remote antennas in Kenya, Zambia, Ghana and Madagascar (AVN Group 1) would greatly add to the SKA core and give a good u-v coverage. The AVN will provide the VLBI component for the SKA forming the SKA phase 2 (SKA2) for possible realization of SKA-VLBI, with the AVN Group1 being the ideal locations. Adding VLBI capability to the SKA will greatly impact on the science of the SKA since it will provide a distributed configuration of antennas providing baselines of up to thousands of kilometers (Paragi et al., 2014).

2.3.1 The African VLBI Network (AVN)

As discussed in Chapter 1 section 1.0, the AVN will comprise of both converted (Gaylard et al., 2010) formerly satellite communication dishes and new builds. The radio telescopes at HartRAO are expected to be the first element in the AVN followed by the recently first successful converted antenna at Kuntunse, Ghana. The figure below shows the distribution of the proposed AVN1 radio antennas which are part of the SKA African member countries. In this research, more antennas especially in the north of Africa, AVN2, were added in order to provide a uniform network coverage. The AVN antennas are initially expected to be equipped with receivers at 1.2-12 GHz and later equipped with receivers at 22 GHz.

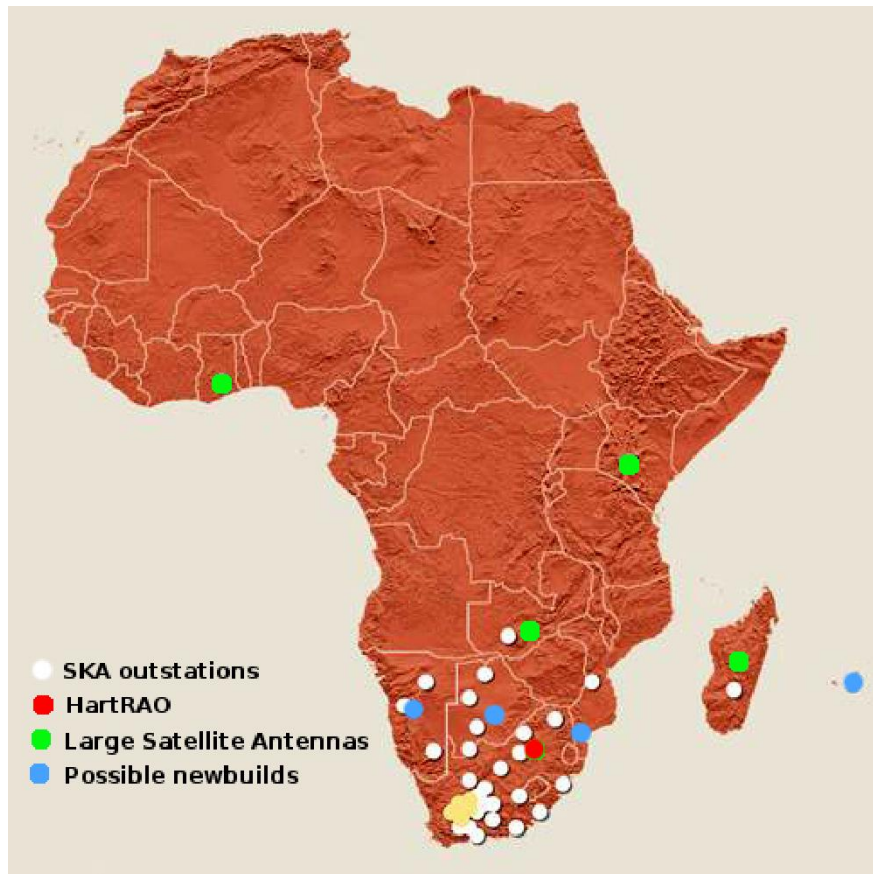


Figure 2.8: The proposed AVN antennas (Mike Gaylard, 2010).

The 32 m dish formerly used for communications at Kuntense in Ghana is the first functioning radio telescope in Africa outside South Africa. The conversion is almost complete and fringe fitting between Kuntense and HartRAO were run recently. The Ghana radio telescope becomes the second radio telescope in the AVN, after HartRAO. The first light science observations included methanol maser detections, pulsars observations and VLBI fringe testing with EVN radio telescopes including HartRAO. The successful methanol detections and pulsar observations means that the dish can carry out research as a single dish (stand-alone) facility and also as part of a VLBI network. Next antennas up for conversion is Madagascar or Kenya, and new builds in Namibia and Botswana.

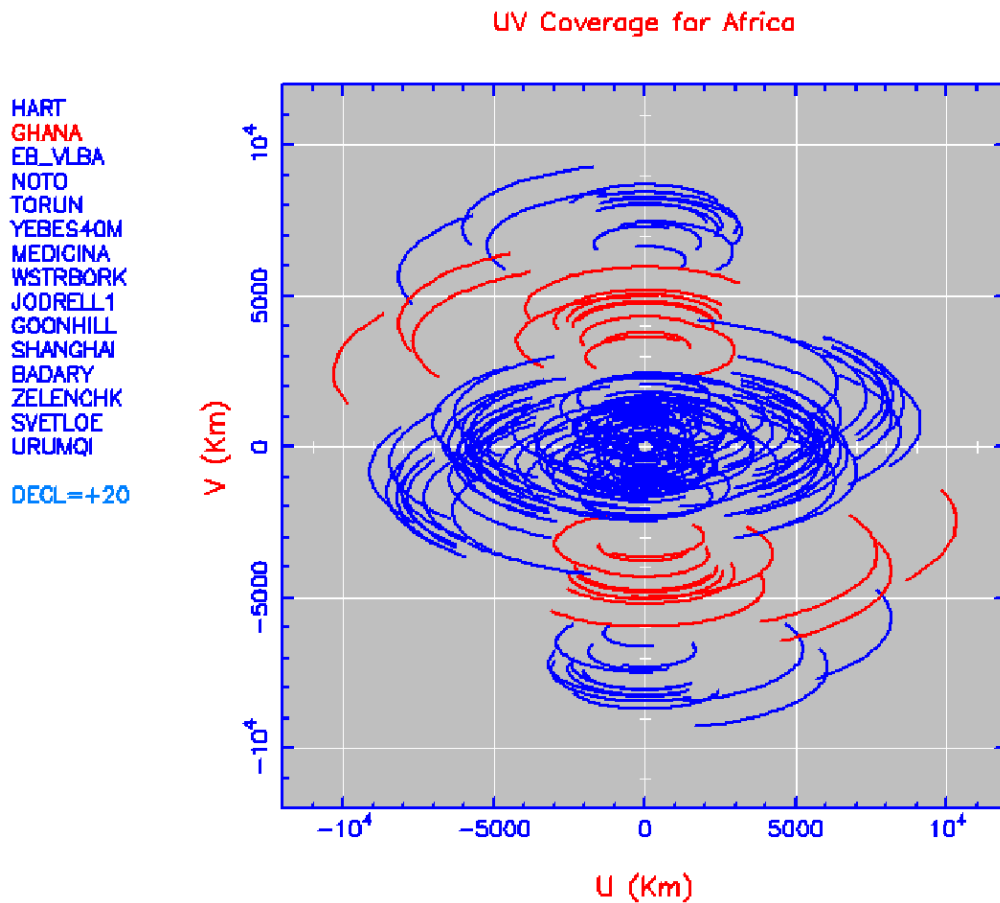


Figure 2.9: EVN + Ghana antenna VLBI u-v diagram for a source at +20 degrees declination.

The red tracks in the above figure 2.9 shows how the Ghanaian antenna will improve the u-v coverage by filling in the gap between Europe and South Africa (Gaylard et al., 2014).

The blue tracks show the u-v coverage already available when using the EVN at that declination.

An African network of VLBI capable radio telescopes will make a significant contribution to current VLBI networks across the globe. Therefore, in-depth studies and research has to be carried out to evaluate the potential contributions that the AVN can make to current global VLBI experiments, as well as what a stand-alone AVN can do. Unfortunately, only a handful of studies have been carried out to evaluate and assess the impact of the AVN and individual telescopes in Africa, on the global VLBI networks and as a stand-alone VLBI network (de Witt et al., 2016; Mayer et al., 2014). The Kenyan telescope can significantly contribute to the EVN as it will fill in the gap in u-v coverage between South Africa and Europe and will substantially increase the image quality (de Witt et al., 2016).

2.3.2 The Longonot Station in Kenya

As a member of the Intelsat, the Longonot Earth Satellite Station with two 30 and 32 m dishes was set up in the 1970 as a telecommunications satellite port. The station served the three East African countries, Kenya, Uganda and Tanzania. The earth station has been redundant for the last 10 years. The SKA-SA and the Kenyan government have plans to convert one of the dishes for radio astronomical purposes soon.

2.4 Site Selection

Most radio astronomical telescopes around the world are located far away from major towns, in areas where the population densities are very low (Ambrosini et al., 2010). These areas are called Radio Quiet Zones (RQZ). These are large tracks of land set aside for radio astronomical observations only, with little to no human activities. More human intrusion means more human generated RFI due to the use of electronics such as mobile phones, radio and television sets and microwaves, businesses and industries, aeronautical and satellites sources which cause RFI and greatly interfere with radio astronomical observations of a telescope. The higher the population density closer to a site, the higher the RFI (Abidin et al., 2013). This means that a site is less suitable for radio astronomical observations and vice versa. Some of the equipment causing RFI are radios, television sets, mobile phones, laptops, wireless internet access, vacuum cleaners and electrical heaters.

HartRAO is located in a RQZ. In an RFI study (Philip May, 2015) for the building of a new VGOS antenna on site, major RFI from mobile phone towers operating at 2100 MHz which is typical for high speed mobile internet was noted. RFI limits the overall productivity of radio astronomy (Ellingson, 2004) and therefore RFI assessments and measurements must be carried out before a new site for radio astronomical observations is selected or set up.

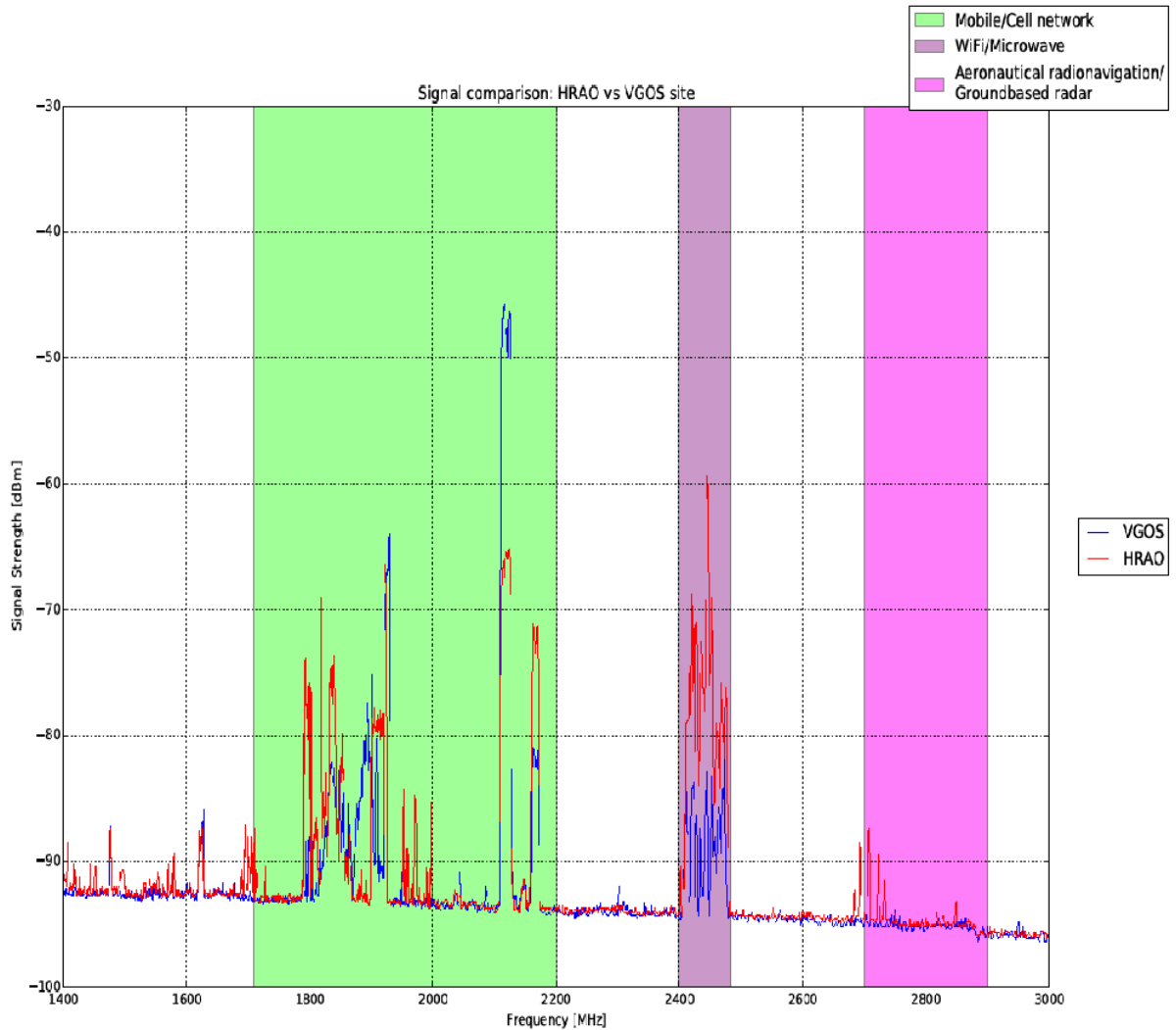


Figure 2.10: Signal Strength of WiFi, Microwave and Mobile network at HartRAO vs VGOS sites (Phillip May, 2015).

One of the criteria for RFI assessment is evaluating the population densities of the area adjacent to the site. Umar et al., (2014), carried out a study in Malaysia evaluating the selection of radio astronomical observatory sites and its dependence on human generated RFI. Eight sites with population densities ranging from 58 – 7089 people/km² were selected and distances of these sites to the nearest towns and cities noted. Actual RFI measurements were taken and the population densities noted. The results indicated that the higher the population density of a site and closer it is to a city or town, the higher the RFI. The study concluded that, to build a radio telescope, a site with population density below 150 people/km² will be ideal while a site with a population density of above 5125 people/km² will be detrimental to any radio astronomy observations.

Many telescopes in the EVN have three RQZ: a radius of 1-3 km is the deeper zone and RFI causing gadgets are totally prohibited; a radius of 20-30 km is the larger zone and only minimum human activities are allowed; and a radius of upto 100 km which is the largest zone where human activities are still controlled (Kucuk et al., 2012). Table 2.3 below shows the population densities around some of the major telescopes in the EVN, LBA, JVN and VLBA among many others (Umar et al., 2012).

Table 2.3: Population densities for several main telescopes around the world (Umar et al. 2012).

Location of Radio telescopes	Diameter (m)	Population Density (people/km²)
Australia, ASKAP	12	0.94
Australia, Mount Pleasant	26	124.8
Australia, Parkes	64	9.12
China, Delingha	13.7	7.48
Finland, Metsahovi	13.7	103
Ukrain, Crimea	22	77
Italy, Medina	32	100
New Zealand, Warkworth	12	29.6
South Africa, MeerKAT	13.5	3.1
United States, VLBA	25	1

Another factor to be considered when selecting a site for radio astronomy due to RFI is the terrain of the area. A hilly or mountainous terrain offers a shield against RFI. A flat land without physical barriers means that the site is open to RFI. A good site for a radio astronomy observatory should have these physical barriers which act as natural shields against RFI. Most radio astronomical observatories around the world are either located in very remote areas, in valleys like HartRAO, or are surrounded by mountains.

The second factor to be considered in site selection is the opacity of the atmosphere. Opacity is the percentage of the electromagnetic radiation that is blocked from reaching the earth's surface by the earth's atmosphere. It is highly affected by the amount of water in the atmosphere (precipitation and temperature). First of all, opacity according to Wikipedia "is the measure of impenetrability of electromagnetic or other kinds of radiation, especially visible light." This case is interested in the opacity

of the radio wave portion of the electromagnetic spectrum where opacity of the atmosphere is the ability of the atmosphere to receive and transmit radio waves. Propagation of electromagnetic radiation within the atmosphere is affected by absorption, emission and scattering processes. In the atmosphere, these processes are affected by the frequencies of the on-coming radio waves. Opacity of oxygen is a major factor of the earth's atmosphere that affects the propagation of electromagnetic waves at millimeter wavelengths (Meeks et al., 1963). An ideal site for radio astronomical observations should have as little precipitation as possible. This is the reason why most radio telescopes are located in very dry areas with very little precipitation. The Atacama Large Millimetre Array telescope located in the Atacama Desert in Chile is a perfect example of a radio astronomy observatory located in a place with very little precipitation in the earth. Not only is it located in the driest place on earth with very little water vapor content in the atmosphere, but also has a very small population density of only about 18 people/km².

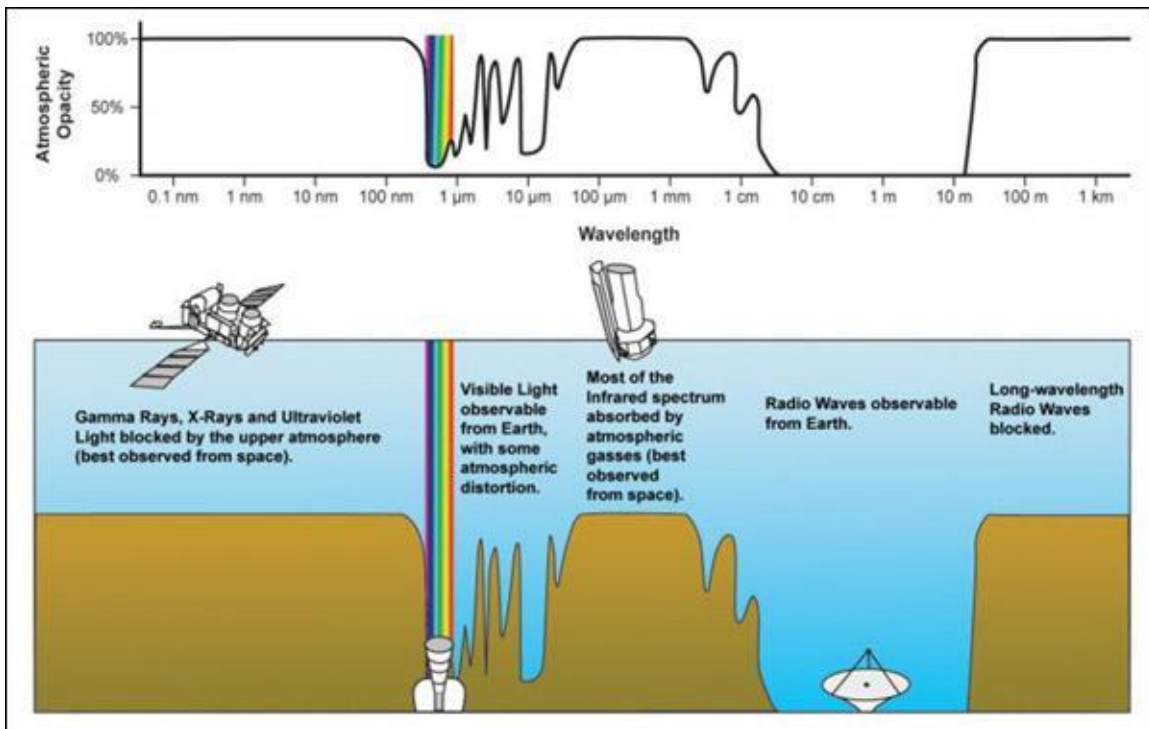


Figure 2.11: Earth's atmospheric transmittance (opacity) at various electromagnetic radiation wavelengths (www.mining-technology.com).

Therefore, before a site is selected for radio astronomical purposes, the atmospheric, meteorological data and the RFI analyses must be done (Kucuk et al., 2012). Besides RFI and weather data measurements and analysis, it is also good to carry out simulations and see what influence a site can have as a stand-alone facility and as part of a VLBI network. Some of simulations that can be performed are the u-v coverage for astronomical VLBI networks, effects on geodetic products, that is the EOPs and show how the antenna will improve the source position estimates using the desired VLBI network combinations.

Most of the proposed AVN antennas are already build in specific locations and thus nothing much can be done about the location of these antennas. But before the conversion of these antennas for astronomy purposes, some criteria for evaluating the suitability of each site and antenna must be put in place. Some of the proposed AVN sites are located in cities or closer to cities and large towns. These cities and towns have high population densities and thus an assessment RFI based on population density at each proposed AVN has to be carried out. This is so because RFI is produced in commercial and dense residential areas (Umar et al., 2014). Another way of accessing RFI is by carrying out actual RFI measurements at the site using a spectrum analyzer and a receiver.

Conversion or new build antenna is a slow and very costly affair. Thus, the above criteria will be used in site selection and antenna conversion in the AVN, so as to see which antennas have a major impact on the network and the best site for setting up a radio astronomy observatory based on the terrain of the site, RFI and atmospheric (ionosphere) conditions.

CHAPTER THREE

METHODOLOGY

Several methods and softwares were used in this study. For the EOP's, eleven different geodetic VLBI schedules were ran and simulated 50 times each so that the average errors and standard deviations were obtained. The astrometric VLBI schedule, simulation and analysis for determining the source positions were also done using VieVS. The u-v coverage plots were created by adding the proposed AVN antennas to existing VLBI networks, the EVN and the LBA. Different u-v coverage plots for different network combinations were created and compared as many times as necessary. The possible RFI was investigated by use of Google-earth maps of the Longonot area (Kenyan case) and all the other proposed AVN sites. The population densities of the nearby towns and the terrain and physical features of the area around the AVN sites were also assessed in this study. This chapter discusses in detail all the different methodologies that were used in achieving this work's results.

3.1 Study Area

The work focused on all the proposed AVN sites as listed in the Table 3.1 below. The country, site location of the dishes with their diameter, location coordinates and the altitude are given.

Table 3.1: The African VLBI Network (AVN) Sites.

Country	Site	Diameter (m)	Coordinates	Altitude (m)
South Africa	HartRAO	26 & 15	25.88° S, 27.68°E	1415
AVN Group1				
Ghana	Kuntunse	32	5.75° N, 0.31° W	70
Kenya	Longonot	32	1.02° S, 36.50°E	1720
Madagascar	Arivonimamo	32	19.02° S, 47.17° E	1450
Mauritius	Cassis	New build	20.17° S, 57.48° E	20
Zambia	Mwembeshi	34	15.33° S, 27.93° E	1125
Namibia	Gemsberg	New build	23.34° S, 16.32° E	1778
AVN Group2				
Egypt	Cairo	32	29.97° N, 31.27° E	40
Ethiopia	Sululta	30	9.14° N, 38.73° E	2725
Morocco	Souk el Arba des Sehoul	30	33.96° N, 6.61° W	90
Nigeria	Kujama	32	10.43° N, 7.64° E	670
Senegal	Gandoul	30	14. 72°N, 17.13° W	50

3.2 Radio Frequency Interference (RFI) assessment.

Several methods were used to help determine and assess the RFI at all the AVN sites. The first method was to assess the population densities around these AVN sites. The satellite images from Google Maps were used to pin point the exact locations of the AVN sites using their coordinates. The NASA Socioeconomic Data and Applications Center (SEDAC) Population Estimator (Gridded Population of the World, GPWv4) was used to estimate the populations enclosed within radii of 5, 10 and 20 km around each site. SEDAC is a Data Center in NASA's Earth Observing System Data and Information System (EOSDIS), which is hosted by Center for International Earth Science Information Network (CIESIN) at Columbia University (<http://www.ciesin.org/>). The Population Estimator is a free web App provided by SEDAC. It estimates population of a user defined region on the Earth's surface. The GPWv4 provides population estimates based on national censuses and population registers of the individual countries, the United Nations DP (UNDP) and the world health organization (WHO). The latest population estimates, 2015 were used for this work. Radii of 5, 10 and 20 km were marked on the GPWv4 map using a circle. The population estimator then provided the estimated population of the enclosed region on the map, together with the area of the region enclosed. The estimated population densities were then calculated.

The second method was to assess the electricity access, telephone or mobile usage and internet subscriptions around these AVN sites. Data from USAID, 2015 for electricity access and data from the International Telecommunication Union (ITU), 2015 for telephone mobile and internet subscriptions for these AVN countries was used. Then the population estimates around these sites at the given radii were used to estimate the number of people that could have electricity access, mobile phones and internet subscriptions around these sites.

The third method was to create contour maps of these AVN sites to determine the terrain of the sites. Contour maps of the proposed AVN sites were created using ArcMap 10.5 from the Environmental Systems Research Institute (ESRI). ESRI is an international supplier of geographic information system (GIS), web GIS and geodatabase management applications (<https://www.esri.com>). ArcMap 10.5 is a software from ESRI that is used to display and explore GIS datasets of a given area to create maps such as contour maps in the case of this study. Raster images of the AVN sites were imported from NASA's USG Earth Explorer website (<https://earthexplorer.usgs.gov>). The raster images were mosaicked in ArcMap 10.5 and contour maps showing the relief and the terrain of each site were created. The contour maps are of 40 by 40 km, roughly a radius of 20 km. Satellite images of these sites were also obtained from Google Earth Maps. The Earth satellite images of the sites were obtained from Google Earth web application.

The fourth and the last method in RFI assessment was to carry out actual RFI measurements at the AVN sites, with emphasis on the Kenyan site. This part of the objective was however not achieved and is hoped to be achieved in subsequent works. This is so because the required spectrum analyzer was not available.

3.3 Weather Assessment

The NASA global numerical weather model, Goddard Earth Observing System Forward Processing for Instrument Teams (GEOS-FPIT, Molod et al., 2012), was used to assess the atmospheric conditions at each of the AVN sites listed in Table 3.1. The GEOS-FPIT assimilates all the available satellite, radiosonde and ground meteorological data to generate an output of 72 vertical layers of 0.652deg x 0.572deg and a 3 hour resolution. The output of this model was then used to derive the state of the atmosphere for each site. Using the state of the atmosphere, the specific opacity at a set of frequencies was computed.

An atmospheric opacity time series, using a step-size of three hours, was generated for each of the AVN sites at a frequency of 22.2, 45 and 100 GHz. This data set covered the period from 1st January 2013 to 8th November 2015. A python script was then used to calculate the minimum and maximum atmospheric opacity at each frequency for each AVN site with their standard deviations. Similarly, a python script was used to get the running mean for each data set for a period of one month. This was done so as to identify any seasonal effects or variations in the atmospheric opacity. Furthermore, the data was binned into where opacity (**a**) value was less than 0.3, $\mathbf{a} < 0.3$, between 0.3 and 0.5, $0.3 > \mathbf{a} < 0.5$ and greater than 0.5, $\mathbf{a} > 0.5$. Where $\mathbf{a} < 0.3$ implies that the site is very dry and thus ideal for radio astronomical observations since the transmissivity of the radio waves is above 70%. Atmospheric opacity value of above 0.5 implies that the transmissivity of the radio waves is below 50%. Histogram plots and percentages of the data points at $\mathbf{a} < 0.3$, $0.3 > \mathbf{a} < 0.5$ and $\mathbf{a} > 0.5$ were calculated. These percentages together with the minimum, maximum and mean values were used to rate each AVN site for suitability to operate at high radio frequencies (> 15 GHz).

3.4 The U-V Coverage

The u-v coverage plots were generated using SCHED. SCHED is a software developed in the US and is used for scheduling radio astronomical VLBI sessions. All the AVN antennas were added to two existing major VLBI networks, the EVN in the Northern Hemisphere at x-band and the LBA in the Southern Hemisphere at both the x and k-bands. These are the global VLBI astronomical networks that would benefit the most from the AVN. The x-band is the most used and k-band is the least used receivers in both networks, they thus give the most and the least number of antennas that can participate in an astronomical

VLBI experiment. In the EVN, declinations of 0, 10, 20, 40, 60 and 80 degrees were considered whereas in the LBA declinations of -10, -30, -50, -70 and -90 degrees were considered.

After the u-v coverage plots were generated using SCHED, the plots were further analyzed using a python script. The u-v coverage percentages at both short and long baselines for each site at each declination was calculated from these plots. Furthermore, histograms showing the initial u-v coverage of the existing network, the backgrounds and the new u-v coverage added by the AVN antennas at all declinations were generated.

Antennas in the EVN include:

1. HartRAO in South Africa
2. Torun in Italy
3. Yebes 40m in Spain
4. Medicina in Italy
5. Westbork in Netherlands
6. Jodrell1 in England
7. Shanghai in Shanghai
8. Noto in Japan
9. Badary in Russia
10. Zelenchok in Russia
11. Sveltoe in Russia
12. Urumqi in China

Antennas considered in the LBA

X-band

1. ATCA in Australia
2. Hobart in Australia
3. Mopra in Australia
4. Ceduna in Australia
5. HartRAO in South Africa
6. Warkworth12 in New Zealand
7. Parkes in New Zealand
8. Katherin in Australia
9. Yarragadee in New Zealand

10. ASKAP in Australia

K-band

1. ATCA
2. Hobart
3. Mopra
4. Ceduna
5. HartRAO
6. Parkes

3.5 Geodesy Scheduling

Geodetic VLBI scheduling, simulations and analysis were done using Vienna VLBI Software (VieVS) to determine the EOPs and the baseline length repeatabilities using the AVN antennas. VieVS is a Matlab based software for VLBI scheduling and data analysis developed by the Institute of Geodesy and Geophysics, Technical University of Vienna. It is used for scheduling, simulating and analyzing geodetic VLBI sessions.

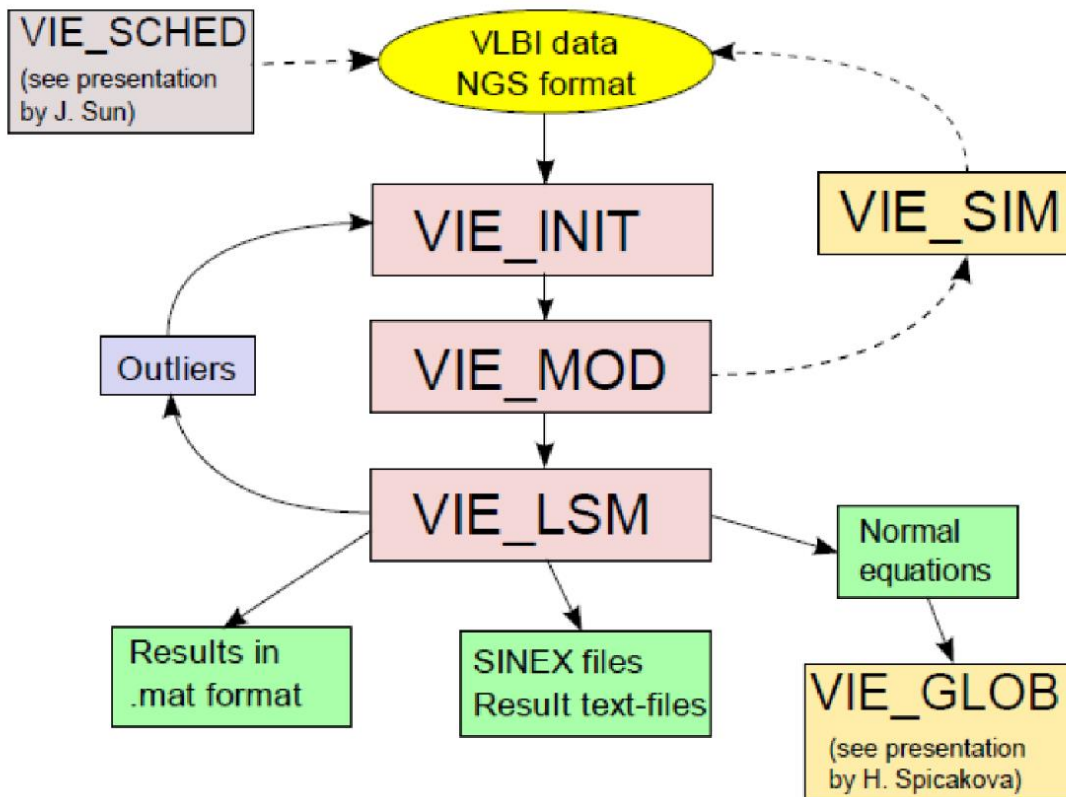


Figure 3.1: The structure of the Vienna VLBI Software, VieVS (Bohm et al., 2014).

Scheduling is the first step preparation in a VLBI observation and VIE_SCHEM is a module in VieVS (see the above figure 3.1) that is used in preparation of VLBI observing schedules automatically. It is normally used for geodetic VLBI sessions. The input in VIE_SCHEM contains information such as the sources and the stations to be scheduled in an experiment. After scheduling the VLBI experiment, initialization of the generated schedule is done by the command VIE_INIT, VIE_MOD stands for modelling of the input information and VIE_LSM stands for Least Square Method which is the preferred data fitting method in VieVS. Finally, VIE_SIM which stands for simulation, is run. All the generated data from VIE_LSM is simulated as many times as one wishes, in this case, 50 times for a 24 hour session. The VIE_GLOB stands for the global solution which in this case was not required.

Eleven different VLBI combination of the R1675 session plus the AVN1 and AVN2 were scheduled, then simulated 50 times and then analyzed. The combinations are shown below. The EOPs were then determined and their errors compared. The average errors in the EOPs and their standard deviations from the 50 simulations for each network configuration were calculated. The VLBI schedules were simulated 50 times so as to reduce the probability of errors in the EOPs estimates.

- 1) R1675
- 2) R1675+AVN
- 3) AVN
- 4) R1675+AVN1
- 5) R1675+AVN2
- 6) AVN1
- 7) AVN2
- 8) R1675+Kenya
- 9) R1675+AVN1-Kenya
- 10) R1675+AVN2+Kenya
- 11) AVN-Kenya

The R1675 session is an IVS geodetic VLBI session that was carried out on 16th February 2015 for determining the EOPs. The R1 session is part of the IVS R1 and R4 sessions which stand for rapid turnaround sessions carried out twice weekly, on Monday (R1) and on Thursdays (R4) for providing EOP results. The spacing between these sessions allows for the periodic monitoring of the Earth tides and nutation. According to the (www.ivscc.gsfc.nasa.gov) the rapid turnaround, R1 and R4, the stations, correlators and analysts must make the recording to final results output time as short as possible, preferably within 15 days. The recorded geodetic VLBI results must reach the correlator (Bonn for

Mondays, R1 and WACO, Washington Correlator, for Thursdays, R4) within the week of the VLBI observations. The R1 and R4 sessions each has a network of 8 stations with a core network for each day plus one or two other stations.

The R1675 session included eight antennas, that is, Hartbeesthoek 15m in South Africa, Warkworth 12m and Yarragadee in New Zealand, Hobart 12m and Katherine 12m in Australia, Matera in Spain, Tsukub32 in Japan, Wetzell in Germany, Onsala 60m in Sweden, Nyaleso 20m in Norway and Raegyeb in Russia. For this work, the R1675 session was rescheduled, simulated 50 times and then the results analyzed. Then each session as shown above adding the AVN antennas was scheduled, simulated 50 times and then analyzed. The results of the EOPs obtained from these sessions were then compared against the rescheduled R1675 session.

The baselines length between all the AVN stations were obtained from VieVS and the baseline length repeatabilities determined and plotted against the standard deviations.

3.6 Astrometry Scheduling

VieVS was used for astrometric scheduling and simulations. The IVS is responsible for scheduling and coordinating astrometric VLBI observations. The Celestial Reference Frame (CRF) sessions are purely astrometric and are intended to improve the present CRF by observing more and new sources. The IVS Celestial Reference Frame for Deep South (CRDS) was used in this work. The CRDS is an astrometric VLBI session that is purely meant for observation of sources in the southern hemisphere which in turn will increase the number of sources in the southern hemisphere and thus improve the CRF. In this work, a CRDS session carried out on 27th-28th of January 2016 and involved antennas in the southern hemisphere only, that is, Hobart 12m and Hobart 26m in Australia, Katherin 12m, Warkworth 12m and Yarragadee 12m all in New Zealand and HartRAO in South Africa, was considered.

Antennas in Kenya, Namibia, Madagascar, Mauritius and Zambia were added to the CRDS antennas and scheduled to observe sources in the southern hemisphere. The results were simulated 50 times and then analyzed using the least square method (LSM) to obtain the errors in right ascension (RA) and declination (DE) of the observed sources.

The sessions were:

1. CRDS
2. CRDS+AVN1
3. CRDS+AVN1-Kenya
4. CRDS+AVN1-Mauritius

5. CRDS+AVN1-Madagascar
6. CRDS+AVN1-Namibia
7. CRDS+AVN1-Zambia
8. CRDS+ Kenya
9. CRDS+ Mauritius
10. CRDS+ Madagascar
11. CRDS+ Namibia
12. CRDS+ Zambia

Plots of the Weighted Root Mean Square (WRMS) of the source positions against errors in RA and DE were generated.

CHAPTER FOUR

RESULTS AND DISCUSSION

This chapter presents the results that were obtained from the site assessments and computer simulations. Section 4.1 gives the results that were obtained from the RFI assessment while section 4.2 gives the weather assessment results for each of the AVN site. Section 4.3 gives the u-v coverage results generated from simulations using the SCHED software. Sections 4.4 and 4.5 give the EOPs results from geodetic VLBI simulations and source position estimates from astrometric VLBI simulations respectively all generated from the Matlab based VieVS software.

4.1 Radio Frequency Interference (RFI) assessment

In this section, the results from various site assessments to determine some indirect measure of the RFI at each AVN site are presented. Evaluation of the RFI environment at all the proposed AVN sites based on population densities, electricity access, mobile telephone subscriptions, internet connectivity and terrain of the sites as presented in sections 4.1.1, 4.1.2 and 4.1.3 respectively. Section 4.1.4 gives the overall assessment of RFI at all AVN sites.

4.1.1 Population Densities

Table 4.1 shows the estimated population densities (people/km²) at a distance of 5, 10 and 20 km around each of the AVN sites, listed by name of the country. The estimated population densities were obtained from the NASA SEDAC GPWv4 online software as discussed in section 3.2.

Based on population density results presented in table 4.1, the Mauritius site has the highest population density of all the AVN1 sites followed by the Ghanaian site. The Namibian site is the least populous of all the AVN1 sites, followed by Kenya. However, the population density for Kenya increases further away from the site and at the 20 km radius the population density compared to Zambia and Madagascar is higher. As for the AVN2, Nigeria has the lowest overall population density while Morocco is the least populated site at the radius of 5 km. Egypt is the most populated site in the AVN2 followed by Ethiopia and Senegal respectively.

Table 4.1: Population densities around the AVN sites.

Sites	Estimated Population densities (people/km ²) at shown radius (km), 2015		
	5 km	10 km	20 km
S. Africa	24.28	25.18	79.02
AVN1			
Ghana	1,175.28	980.54	1,559.92
Kenya	69.91	78.46	175.28
Zambia	111.15	98.41	78.36
Madagascar	203.4	107.97	93.30
Mauritius	2,557.91	1,826.89	1,085.66
Namibia	1.37	0.81	0.41
AVN2			
Egypt	13,660.37	12,813.47	10,768.07
Ethiopia	157.38	1,519.61	2,106.23
Nigeria	100.68	100.19	122.00
Senegal	880.20	799.81	723.55
Morocco	61.68	129.22	852.63

4.1.2 Electricity Access, Mobile Telephone and Internet Subscription.

Table 4.2 lists the percentages of the electricity access as obtained from the USAID 2015 Report, as well as the mobile telephone and internet subscriptions obtained from the ITU Report 2015 as discussed in section 3.2. The given percentages are for the entire country. Table 4.3 shows the population estimates of people with electricity access, mobile telephone and internet subscriptions around each AVN site at 5, 10 and 20 km radius as discussed in section 3.2.

Assessing the RFI based on electricity access, mobile telephone subscription and internet subscriptions, Mauritius leads with all the three factors in the AVN1, Egypt and Morocco leads with 99% electricity access in the AVN2. Madagascar has the least electricity access, mobile telephone subscriptions and very little internet connectivity followed by Zambia and Namibia respectively. Ethiopia has the least electricity access, mobile telephone and internet subscriptions in the AVN2.

Table 4. 2: Electricity access, mobile telephone and internet subscriptions for the entire country.

Sites	Electricity Access (%) USAID, 2015	Mobile Telephone subscription per 100 people,(ITU) 2015	Internet Subscriptions (%) ITU, 2015
South Africa	85	164.51	51.92
AVN1			
Ghana	74	129.74	23.48
Kenya	60	80.68	45.62
Zambia	26	74.47	21.00
Madagascar	15	44.12	4.17
Mautirtius	99	140.58	50.14
Namibia	32	106.58	22.31
AVN2			
Egypt	99	110.99	37.82
Ethiopia	23	42.76	11.60
Nigeria	45	82.19	47.44
Senegal	55	99.95	21.69
Morocco	99	126.87	57.08

Table 4.3: Population estimates of people with electricity access, mobile telephones and internet.

Sites	Estimated Population with Electricity Access at Shown Radius (km), 2015			Estimated Mobile Subscriptions			Estimated Internet Subscription		
	5Km	10Km	20KM	5KM	10Km	20km	5 Km	10Km	20Km
S. Africa	2,064	2,141	6,717	3,994	4,142	12,999	1,260	1,307	4,102
AVN1									
Ghana	69,576	231,465	8,846,394	121,985	405,815	15,509,880	22,076	73,443	2,806,936
Kenya	3,398	15,111	133,140	4,569	20,319	179,029	2,583	11,489	101,231
Zambia	2,341	8,085	25,774.32	6,705	23,159	73,824	1,891	6,531	20,818
Madagascar	2,441	5,166	17,675.10	7,179	15,196	51,988	679	1,436	4,914
Mauritius	141,811	363,533	791,054.5	201,371	516,217	1,123,297	71,822	184,117	400,641
Namibia	36	82	168.32	118	272	561	25	57	117
AVN2									
Egypt	987,235	3,830,970	13,133,597.40	1,106,800	4,294,943	14,724,222	377,144	1,463,508	5,017,300
Ethiopia	2,968	111,494	613,291.5	5,518	207,282	1,140,188	1,497	56,232	309,312
Nigeria	3,624	14,383	68,673.60	6,620	26,270	125,429	3,821	15,163	72,397
Senegal	38,729	139,006	411,480.3	70,381	252,613	747,772	15,273	54,819	162,273
Morocco	5,007	39,914	1,050,062.31	6,417	51,150	1,345,671	2,887	23,013	605,430

A site with less of the above three factors implies less human generated RFI. High electricity access suggests an increase in the use of electronic appliances such as microwaves, radios and television sets which in turn contribute to RFI. Mobile phones, wireless internet connectivity and blue booth devices generate a lot of RFI especially in the lower frequency bands (< 5 GHz).

4.1.3 Terrain of the AVN Sites

Table 4.4 shows the contour maps accompanied by the satellite images of the AVN sites that were generated using ArcMap 10.5 and Google Earth Maps respectively as discussed in section 3.2. The terrain or topographical relief is another very important factor that has to be considered when selecting a site for radio astronomy observatory. A site that is surrounded by mountains or hills provides natural protection from human generated RFI. On the other hand, a site that is on a very flat land without any mountains and hills has no protection against this human generated RFI and thus, extra measures has to be put into place to mitigate the RFI during radio astronomical observations. This is quite expensive and not desirable as one has to either remove the RFI during data analysis, which can be a very tedious job, or filter out some parts of the frequency band which means some part of the desirable signal is also filtered out.

A reliable proxy for RFI measurements can also be determined from visual inspection of each site using Google Earth maps, where little infrastructure suggests little RFI. For new observatories one would choose remote locations away from urban centres and industrial zones and implement radio quiet zones. However, most of the AVN stations will be existing facilities close to cities and will operate in an already established environment. Satellite imagery for each of the AVN sites presented in Table 4.4, cover a 40 X 40 km region around each site at an altitude of 4.2 km. At 4.2 km the types of dwellings can be identified generally as residential, agricultural or industrial. The exact location of the antenna is highlighted by the red Google Maps pointer on the satellite images.

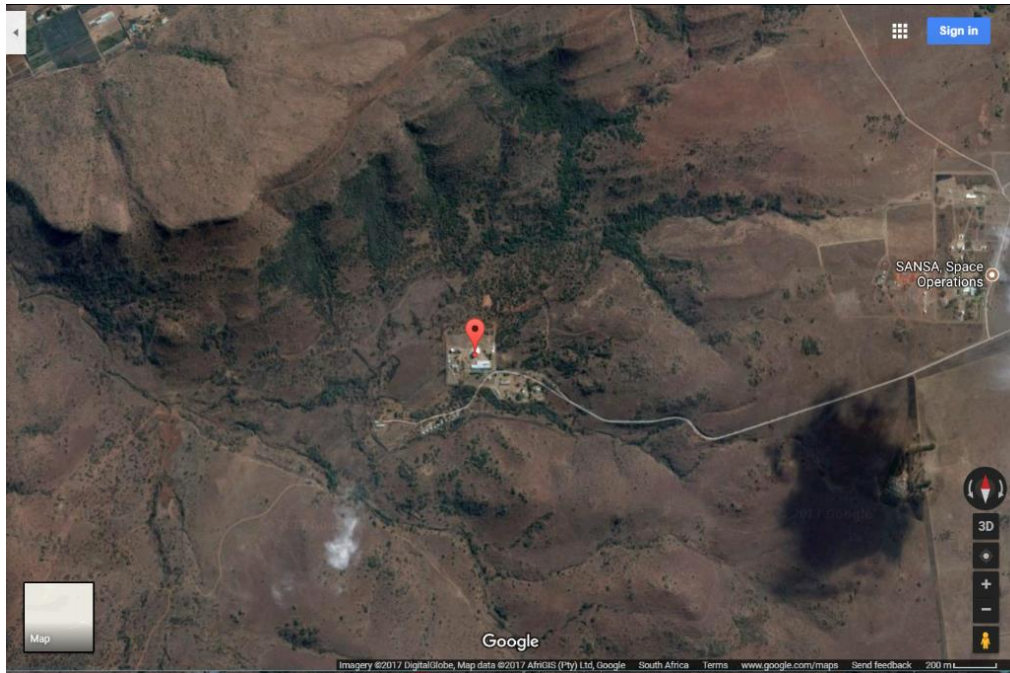
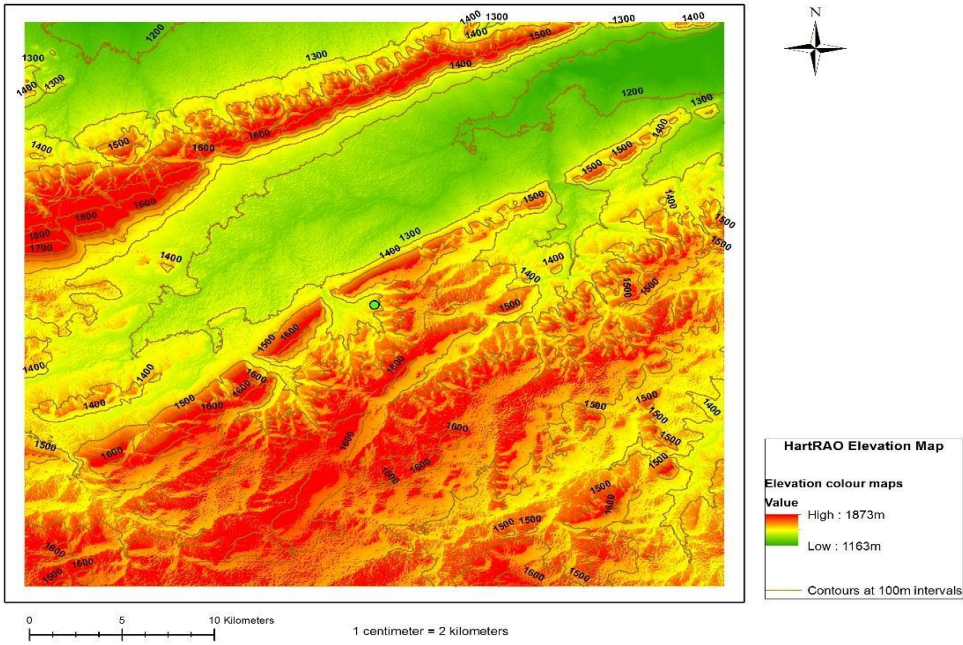
Looking at the contour maps in Table 4.4, the first element in the AVN1, HartRAO is located 1500m above the sea level and is well shielded by hills. The contour map clearly shows that the observatory is located in a valley which is surrounded by hills on all sides and thus is well shielded from human generated RFI. The satellite image also shows that the area surrounding HartRAO has very little human activities implying that the levels of human generated RFI is also very little. The Kenyan and Namibian sites have mountains nearby, Mt. Longonot and Gemsberg Mountains respectively. This mountains will provide a form of natural barrier against RFI from the neighboring towns. The satellite image of the Namibian sites shows no signs of any human activities. This implies that the site has very little human generated RFI. The Kenyan site also has very little human activities at all radii as the satellite imagery shows. The Madagascar site is also shielded by hills as the contour map shows and has little human

activities though the Northern Eastern part of the site shows heavy human settlement as shown on the satellite imagery. The Ghanaian site is only at an altitude of 50m above the sea level and is on a very flat land without any natural physical barriers. The satellite image of the site shows that the site is heavily surrounded by human settlements implying high levels of human generated RFI. The Zambian site is at an altitude of 1100m above the sea level but on a very flat surface, the highest point within the 20km radius being only at 1220m. The site also has very little human activities in its surroundings.

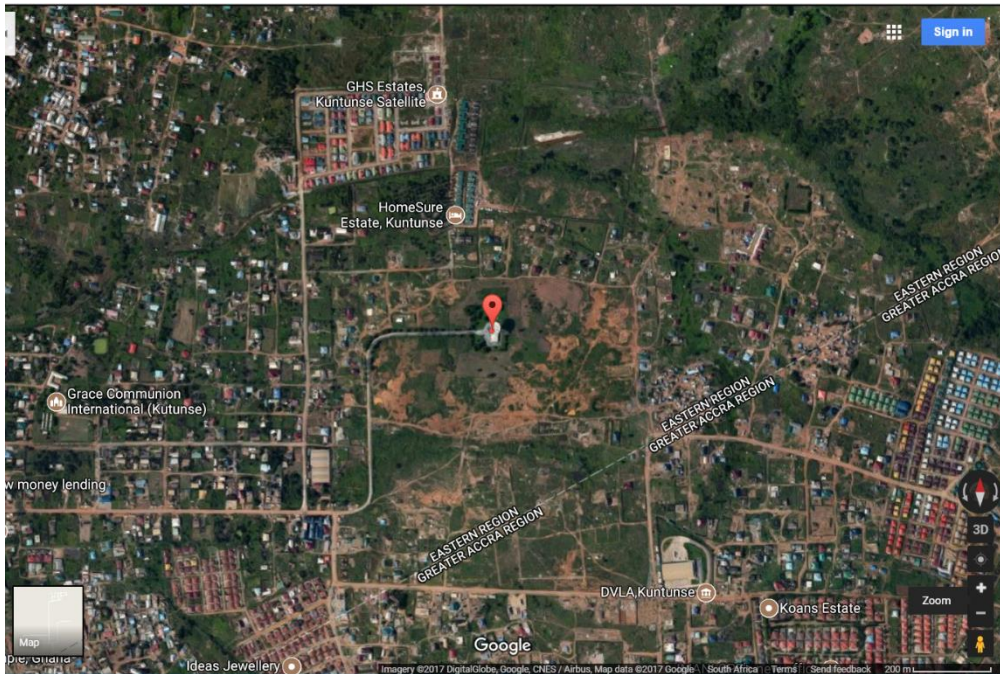
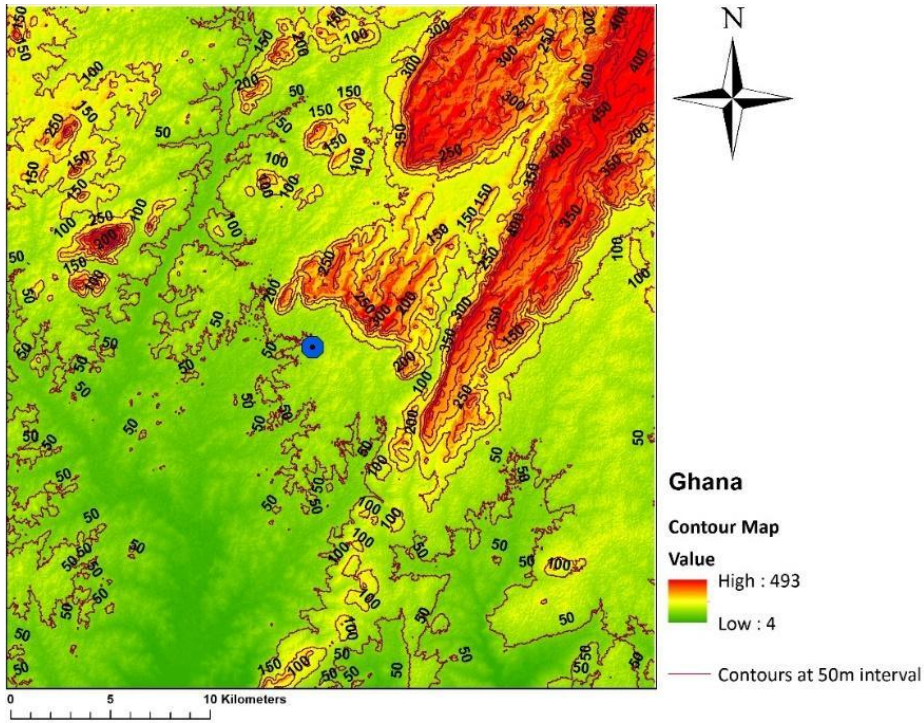
As for the AVN2, the Ethiopian site is located at an altitude of 2700m above the sea level and is surrounded by hills. The satellite image shows heavy settlement especially on the South Eastern side of the site. The Nigerian site is located at an altitude of 700m but on a very flat land surface since the highest point within the 20km radius is only 800m above the sea level. The Senegalese site is near the ocean and has an altitude of only 50m above the sea level and on a very flat surface without any physical barriers. The satellite images of the Nigerian and Senegal sites show very little human activities such as human settlements. The Moroccan and Egyptian sites are located right in the middle of large cities, which implies high levels of human generated RFI. Hence, these sites would be undesirable for radio astronomical observations or setting up of a radio astronomy observatory.

Table 4.4: Contour maps of the AVN sites accompanied by the Google Earth Satellite Images.

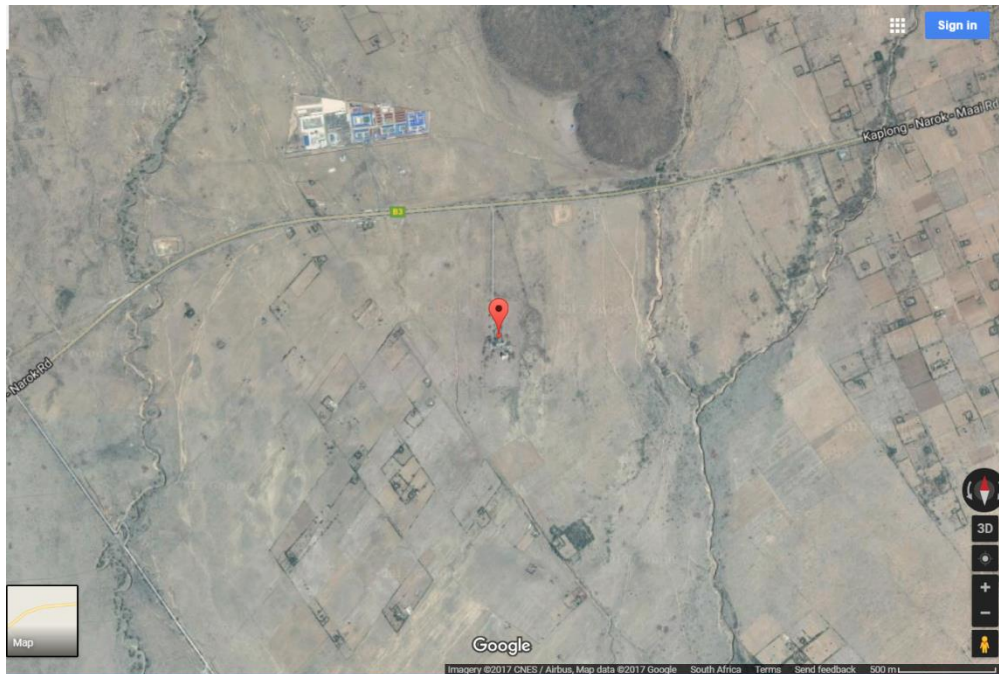
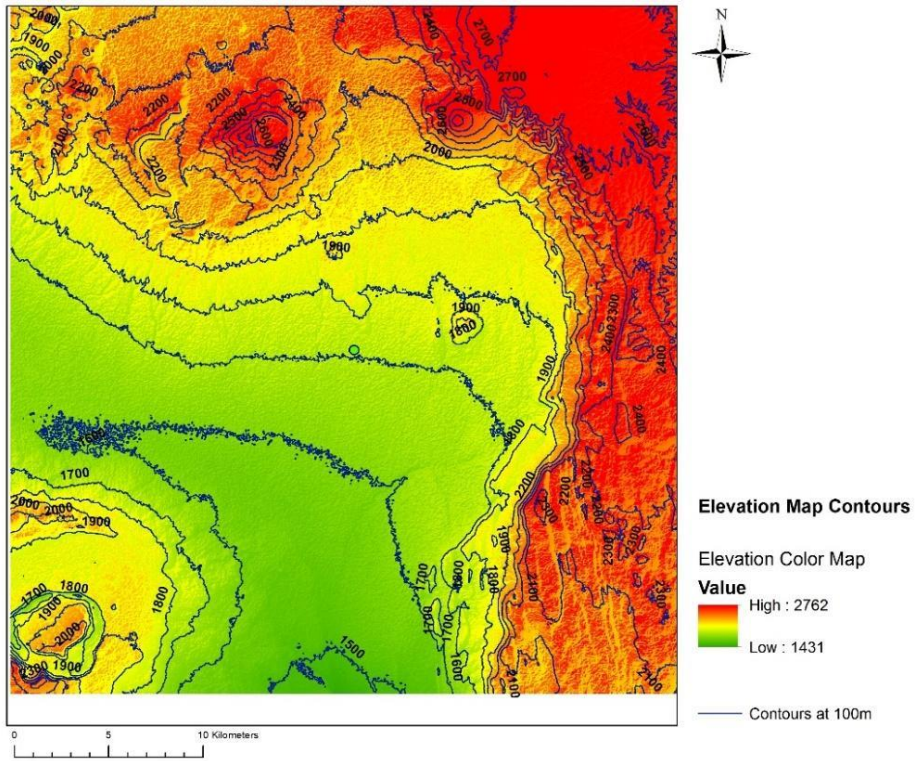
1. HartRAO, South Africa



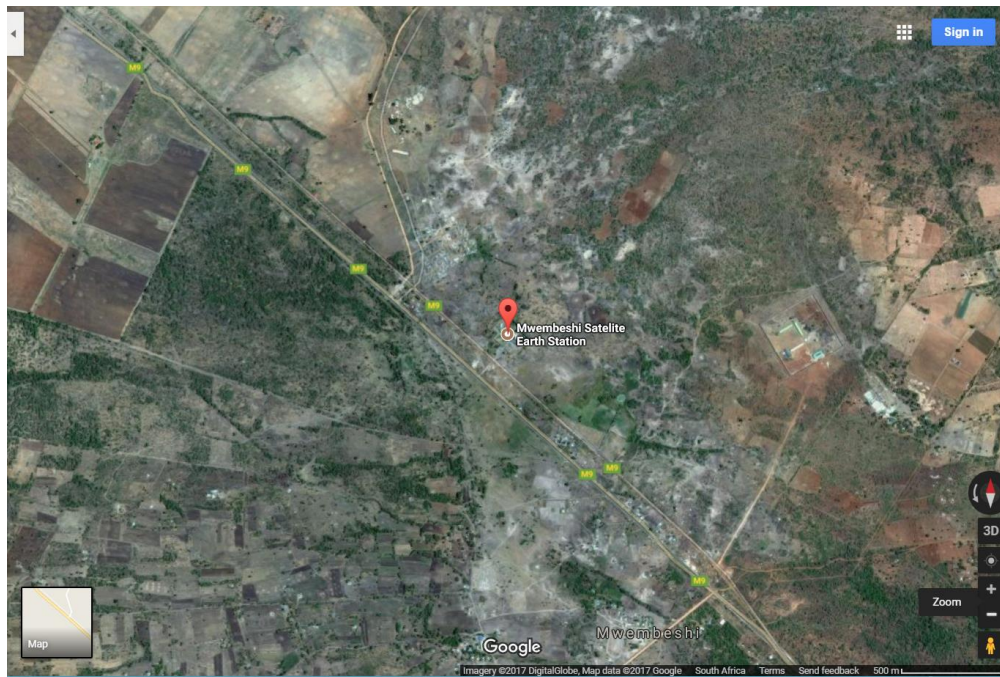
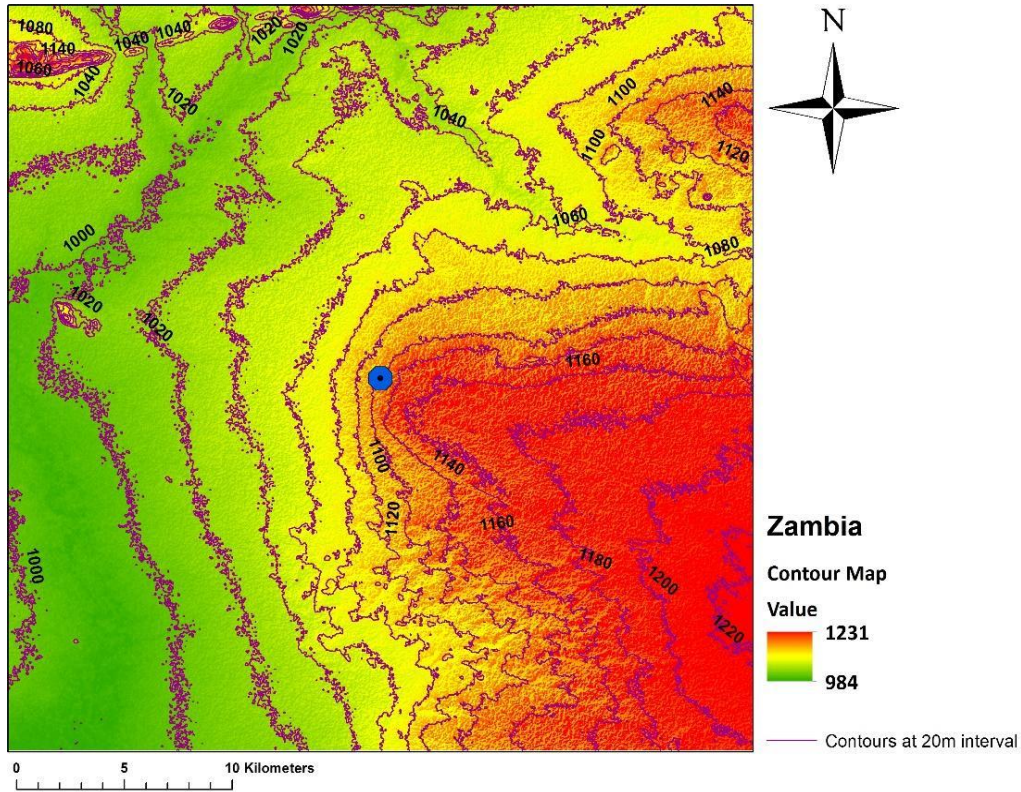
2. Kuntunse, Ghana.



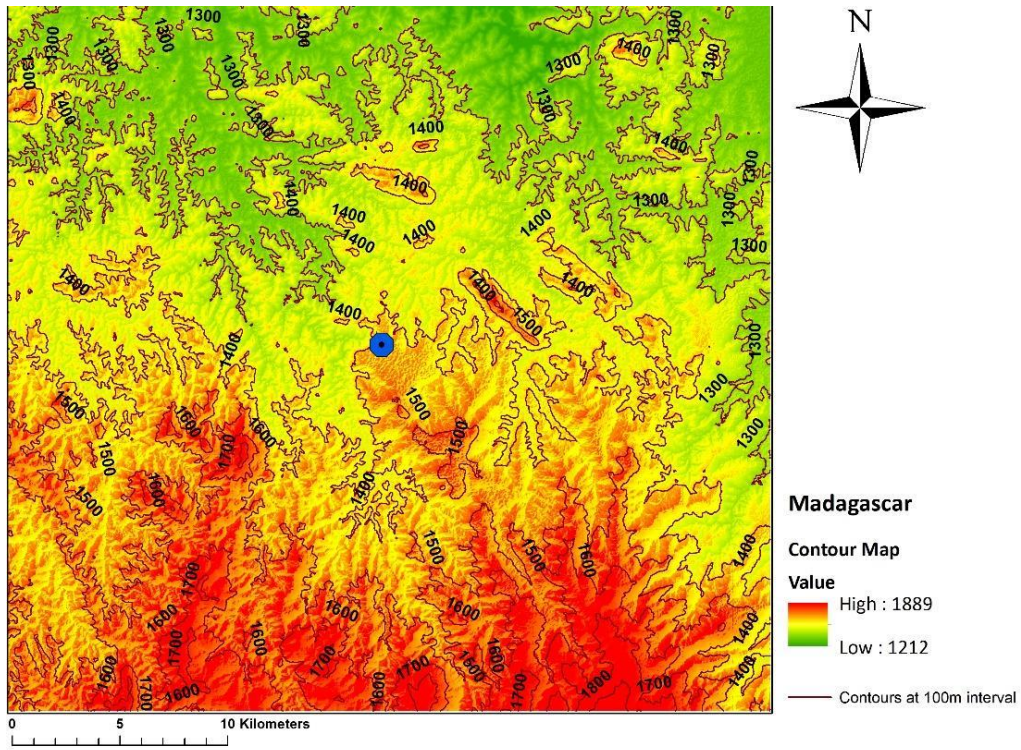
3. Longonot, Kenya.



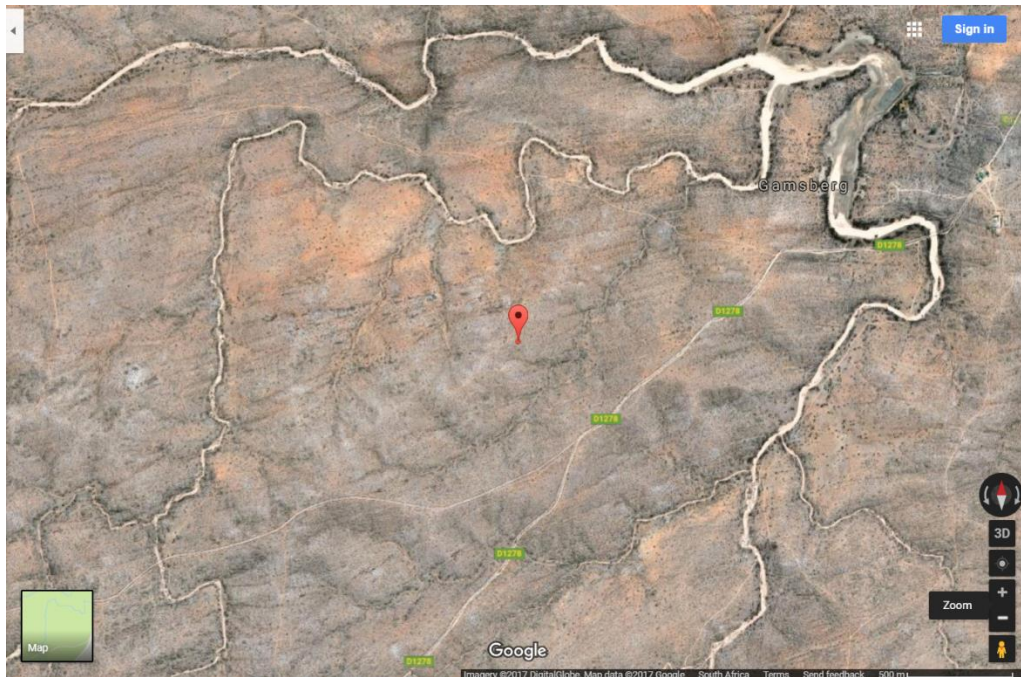
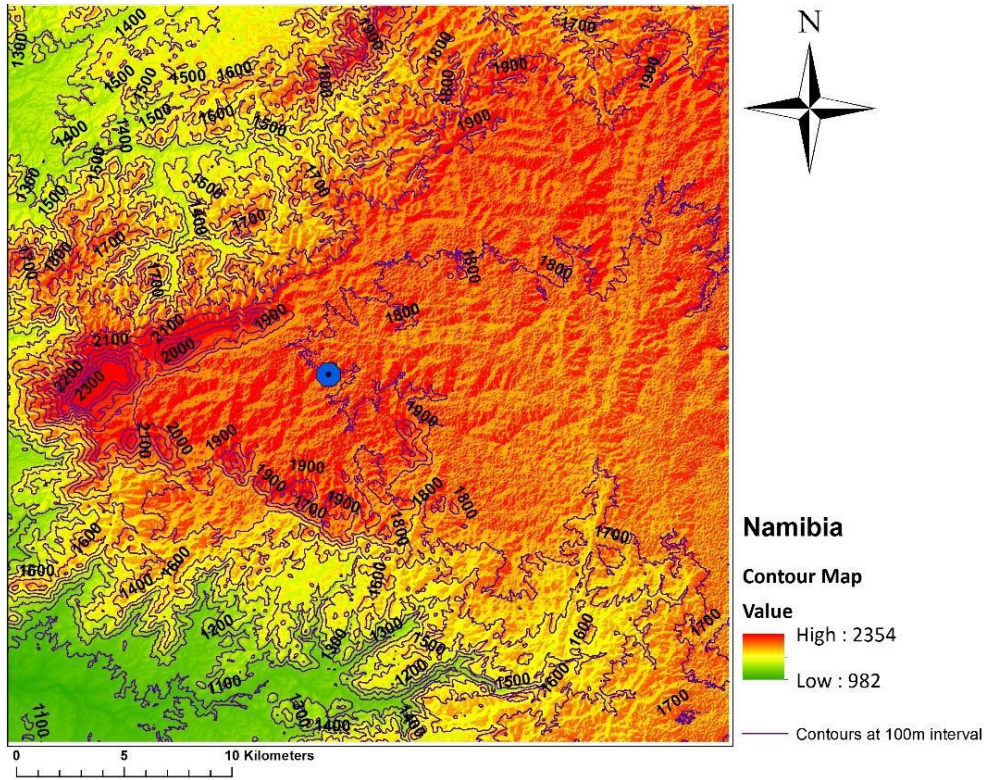
4. Mwembeshi, Zambia.



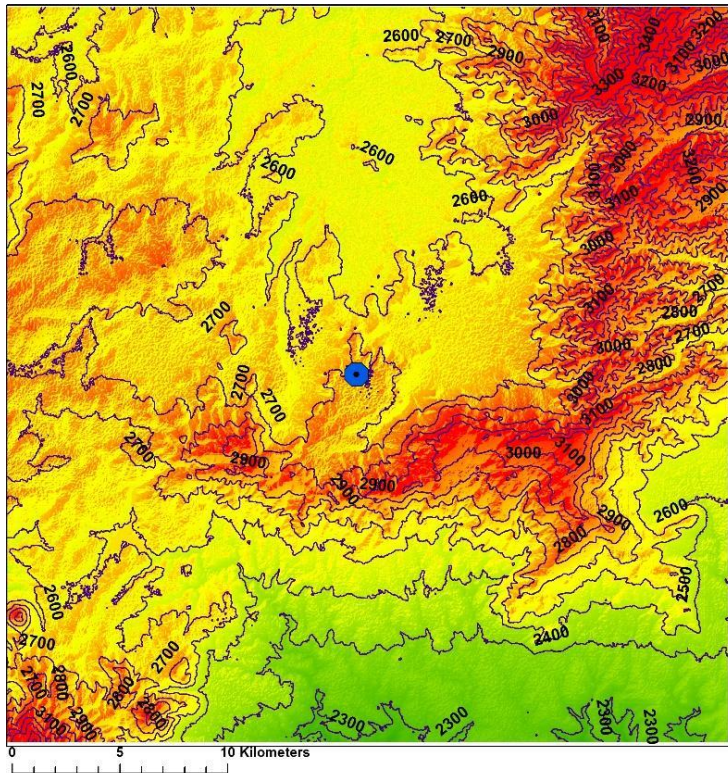
5. Arivonimamo, Madagascar.



6. Gemsberg, Namibia.



7. Sululta, Ethiopia.



Ethiopia

Contour Map

Value

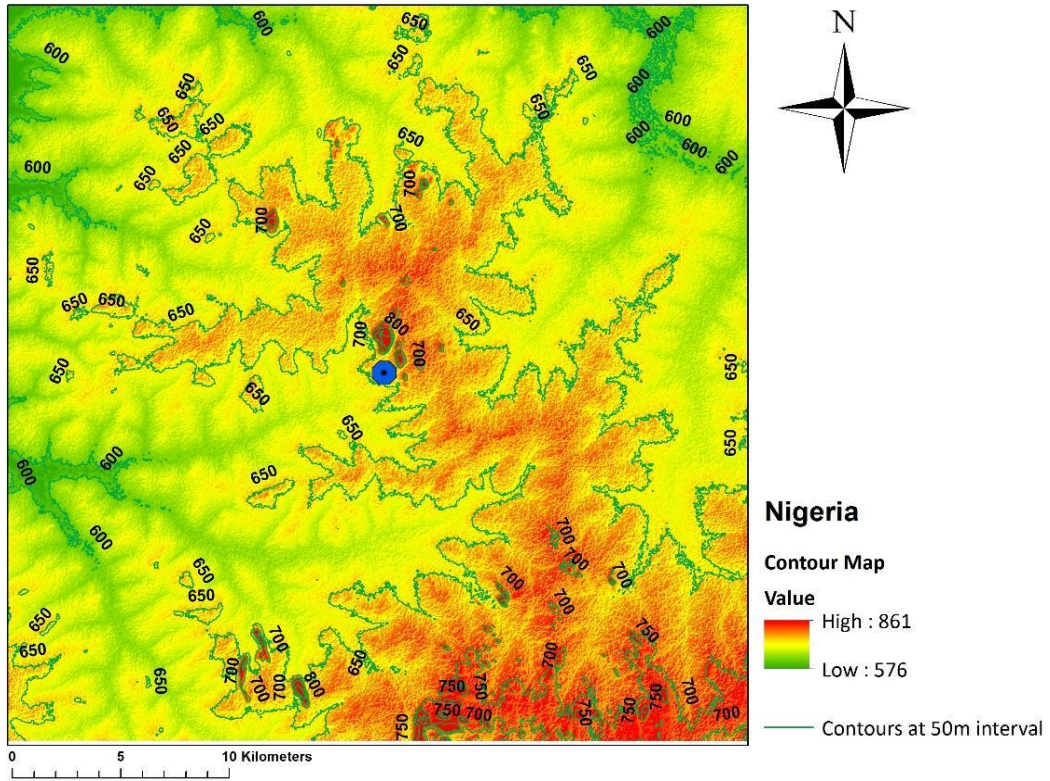
High : 3457

Low : 2217

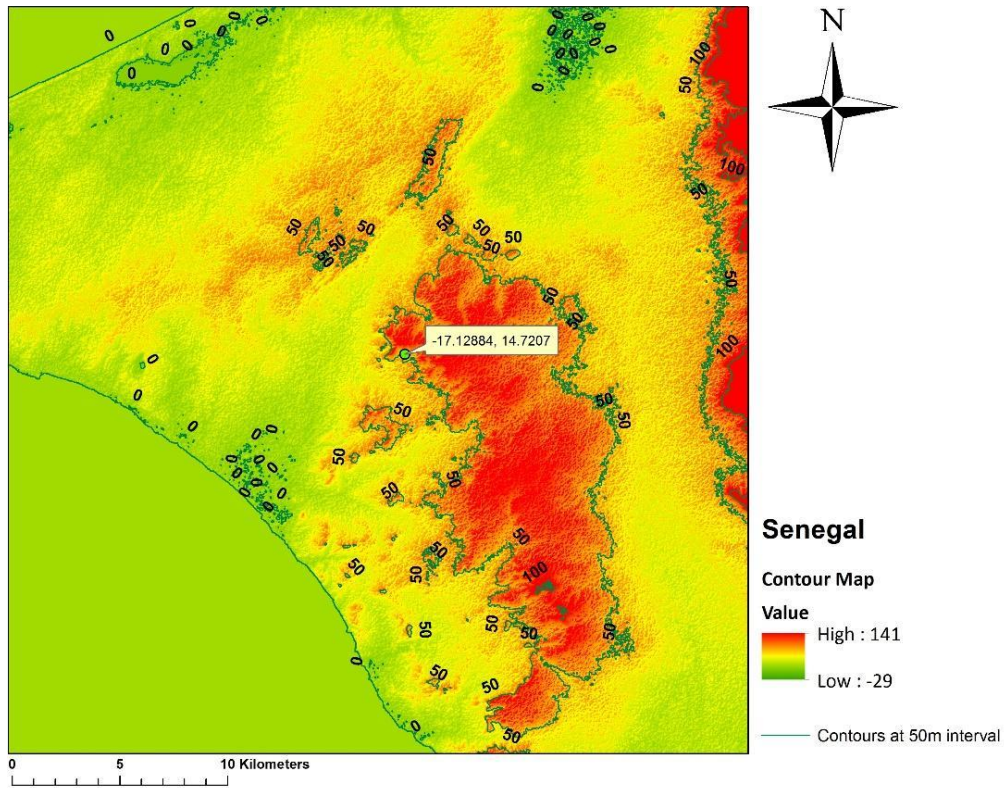
— Contours at 100m interval



8. Kujama, Nigeria



9. Gandoul, Senegal.



4.1.4 Overall RFI Assessment

Considering a general assessment of the RFI at the AVN sites, Namibia has the least population densities at all radii and also has the least number of people with electricity access, mobile telephone and internet subscriptions implying that it has the least human generated RFI. The site is also located on top of a mountain and away from towns. The Kenyan site follows with the least population density at 5 and 10 km radii, followed by Zambia, Madagascar, Ghana and Mauritius respectively. However, the Kenyan site has a higher population with electricity access and internet subscriptions as compared to Zambia and Madagascar, Madagascar has the least followed by Zambia at all radii. The three sites have almost similar mobile telephone subscriptions though the Kenyan site has the least at 5 km and the most at 20 km. The Kenyan site is well shielded from RFI in the North by Mt. Longonot and the nearest town which is about 20 km away is shielded by a small hill from the line of site of the antenna. The Madagascar site is shielded from RFI by mountains on the Southern side but exposed on the Northern side with a highly populated town close by. On the other hand, the Zambian site is at an altitude of 1125 m but on a flat surface meaning that the site is not naturally shielded from any RFI.

Ghana and Mauritius sites have very high population densities of up to 1560 and 1086 people/km² respectively at a radius of 20 km, high electricity access and high mobile telephone and internet subscriptions at all radii as compared to all the other sites. The sites are at very low altitudes of 70 and 20 m above the sea level respectively. Each site is also just a few metres from the ocean and do not have any form of natural barriers.

Considering all the other AVN2 sites, Nigeria has the least population densities overall followed by Morocco at radii 5 and 10 km. The site is located on a flat land with no natural physical barriers. All the other sites in the AVN2 are located either right in the middle of large cities like Cairo or near large cities like Dakar in the case of the site in Senegal.

Based on the values given by Umar et al., (2014), a site with population density below 150 people/km² will be ideal for a radio astronomy observatory while a site with a population density of above 5125 people/km² will be detrimental to radio astronomy observations. Ghana and Mauritius sites in AVN1, have population densities between these two values implying that they may not be very ideal for radio astronomical observations. HartRAO, Kenya, Zambia, Madagascar and Namibia sites are all ideal for radio astronomical observatories. The Egyptian site in the AVN2 has a population density above the 5125 people/km² (Umar et al., 2014) at all radii, meaning that the site will be detrimental to any radio astronomical observations. Ethiopia and Senegal sites have values below 5125 people/km² and Nigeria and Morocco have values below 150 people/km².

4.2. Atmospheric Opacity Weather Data

This section provides the results of the atmospheric opacity calculations and the analysis of the time series data generated for each of the AVN sites as discussed in section 3.3. Table 4.5 shows the Opacity values at different frequencies, while table 4.6 (a) shows the plots of the atmospheric opacity time series for each of the AVN sites at 22, 45 and 100 GHz. Table 4.6 (b) in the Appendix 1, shows the plots of the running mean of the time series (per month) data with the accompanying histograms showing the same.

Table 4.5: Atmospheric Opacity values at the AVN sites.

SITE/FREQUENCY	Opacity (a) %						
	Max	Min	Mean	Stdev	a<0.3	0.3>a<0.5	a>0.5
Kenya							
22GHz	0.50	0.22	0.36	0.04	43.56	56.44	0.00
43GHz	0.15	0.07	0.12	0.01	100.0	0.00	0.00
100GHz	0.50	0.10	0.32	0.06	68.26	31.74	0.00
Ghana							
22GHz	0.63	0.25	0.50	0.05	1.10	86.12	12.78
43GHz	0.26	0.10	0.21	0.02	100.0	0.00	0.00
100GHz	0.93	0.15	0.67	0.09	1.08	6.05	92.87
Madagascar							
22GHz	0.54	0.17	0.32	0.09	64.90	35.10	0.00
43GHz	0.17	0.06	0.11	0.02	100.0	0.00	0.00
100GHz	0.60	0.04	0.28	0.12	69.88	29.73	0.38
Mauritius							
22GHz	0.68	0.24	0.38	0.09	46.88	47.65	5.46
43GHz	0.28	0.12	0.17	0.03	100.0	0.00	0.00
100GHz	1.02	0.21	0.50	0.15	17.70	48.05	34.25
Namibia							
22GHz	0.44	0.16	0.23	0.05	97.51	2.49	0.00
43GHz	0.12	0.05	0.07	0.01	100.0	0.00	0.00
100GHz	0.37	0.03	0.12	0.07	80.41	19.58	0.00

Zambia							
22GHz	0.56	0.18	0.34	0.10	60.50	39.44	0.06
43GHz	0.19	0.07	0.12	0.03	100.0	0.00	0.00
100GHz	0.66	0.06	0.30	0.15	63.17	30.13	6.70
Egypt							
22GHz	0.45	0.18	0.28	0.04	93.96	6.04	0.00
43GHz	0.19	0.09	0.12	0.02	100.0	0.00	0.00
100GHz	0.60	0.07	0.25	0.08	89.80	10.10	0.10
Ethiopia							
22GHz	0.42	0.17	0.29	0.05	85.96	14.04	0.00
43GHz	0.11	0.05	0.08	0.01	99.95	0.05	0.00
100GHz	0.33	0.03	0.18	0.06	99.28	0.82	0.00
Nigeria							
22GHz	0.57	0.20	0.39	0.10	39.16	60.60	0.24
43GHz	0.21	0.08	0.14	0.03	100.0	0.00	0.00
100GHz	0.72	0.07	0.39	0.17	43.45	32.62	23.93
Senegal							
22GHz	0.67	0.19	0.38	0.10	44.30	48.85	6.85
43GHz	0.27	0.09	0.16	0.04	100.0	0.00	0.00
100GHz	1.00	0.07	0.41	0.21	47.80	22.44	29.76
Morocco							
22GHz	0.52	0.19	0.31	0.05	79.66	20.34	0.00
43GHz	0.21	0.09	0.14	0.02	100.0	0.00	0.00
100GHz	0.67	0.09	0.30		72.34	26.49	1.16
HartRAO							
22GHz	0.54	0.17	0.28	0.07	84.00	16.00	0.00
43GHz	0.17	0.06	0.10	0.02	100.0	0.00	0.00
100GHz	0.59	0.04	0.20	0.10	91.23	8.00	0.47

Table 4.5 lists the results of the analysis of the time series data and gives the minimum, maximum, mean and the standard deviation of each time series of the opacity for each AVN site. In addition, it also lists the percentage data points below an opacity of 0.3, between 0.3 and 0.5 and above 0.5 as calculated from the histogram plots (table 4.6 (b), Appendix 1).

Ideal atmospheric opacity is where the opacity values are below 0.3 ($a < 0.3$), the site is good if the values are between 0.3-0.5 ($0.3 > a < 0.5$) but anything above 0.5 ($a > 0.5$) means that the site is not conducive for astronomical VLBI experiments at high frequencies. All AVN sites are ideal for mid frequencies observations around 43GHz since the opacity is always below the 0.3 ($a < 0.3$), that is, opacity is always 100% below 0.3 at all times for all the stations.

For HartRAO, all observations at these frequencies are also below 0.5, majority of opacity being 0.3. However, opacity at this site varies with seasons. From February to July, opacity values for all frequencies are below 0.3. This is during winter months and the site is driest around this time of the year. From August to February, the opacity values rise, this is summer time which is normally accompanied by rainfall. Most of the values are above 0.3. Considering the running mean (Table 4.6 (b), Appendix 1), it is below 0.3 for 100GHz throughout the year, below 0.4 for 22.2GHz and around 0.1 for 43GHz throughout the year.

The Ghanaian site, observations at 43GHz and 100GHz are all above 0.3, most opacity values are between 0.4-0.8. Opacity is fairly constant throughout the year but dips slightly in December and January, probably the driest month in Kuntunse. The running mean (Table 4.6(b), Appendix 1) for 100GHz is around 0.7, 0.5 for 22.2GHz and 0.2 for 43GHz throughout the year.

Maximum values for all the frequencies at the Kenyan site are below 0.5. The atmospheric opacity is fairly constant throughout the year and does not vary much as at the other sites including HartRAO. Apart from around February 2015 where the opacity at 22.2GHz and 100GHz dipped suddenly and jumped back to the normal. The running mean for 100GHz is about 0.33, 0.35 for 22.2GHz and 0.12 for 43GHz throughout the year (Table 4.6(b), Appendix 1).

At the Mauritius site, observations at 22.2GHz, the opacity values are always below throughout the year and for 100GHz are at least below 0.8 throughout the year. The opacity values however vary throughout the year. Between January-April, the opacity values are highest and lowest between May-December. The continuous mean for 100GHz is between 0.5 (highest) to 0.4 (lowest), around 0.4 for 22.2GHz and 0.2 for 43GHz (Table 4.6 (b), Appendix 1).

For the Madagascar site, opacity values are between 0.2-0.5, and 100GHz opacity values are between 0.1-0.6 throughout the year. Opacity values also fluctuate with seasons throughout the year. The opacity values are lowest and below 0.3 between April-July and highest and above 0.3 between August-March. The continuous mean is below 0.4 for 100GHz and 22.2GHz and varies to even lower values throughout the year (Table 4.6(b), Appendix 1).

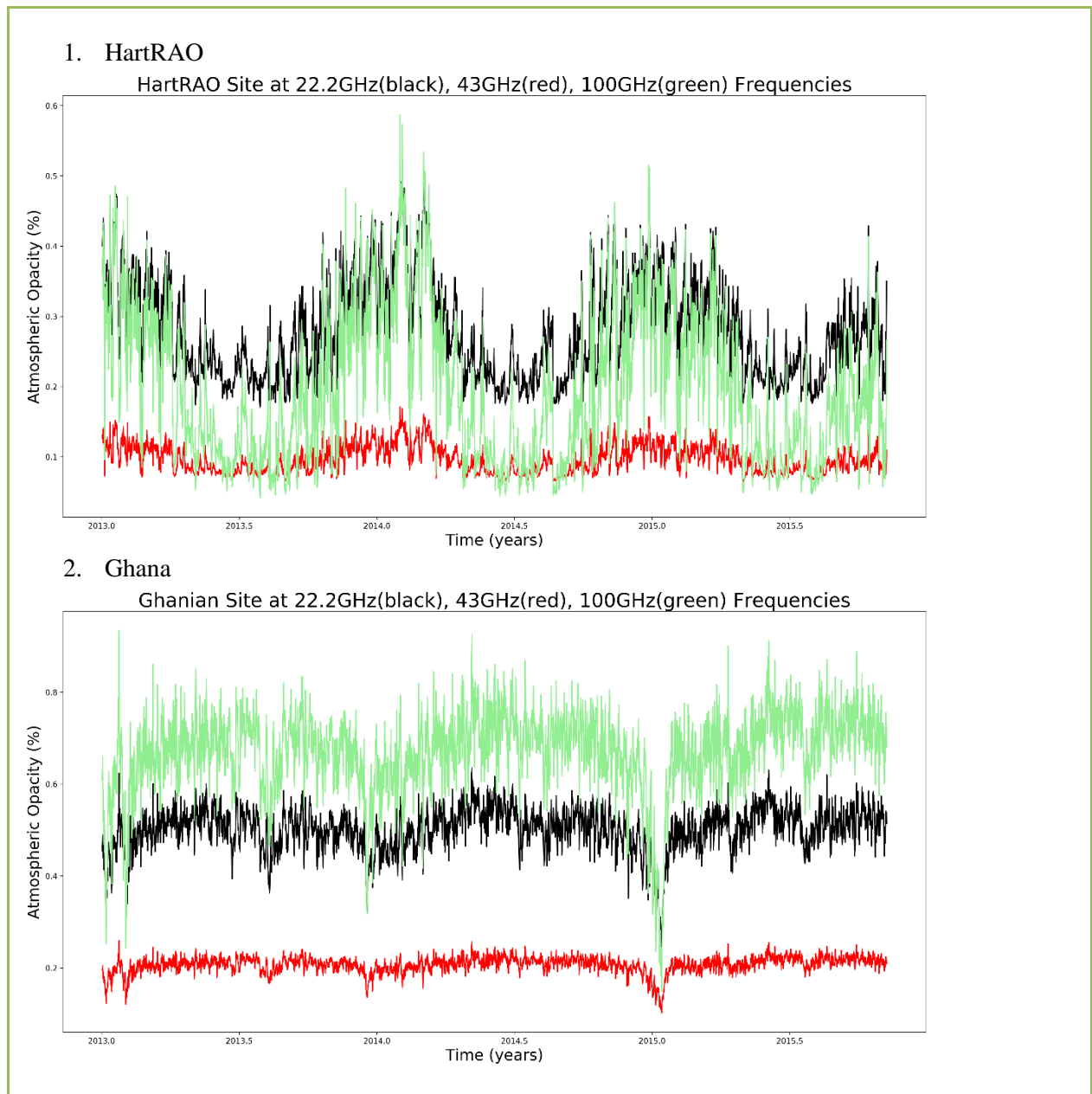
At the Zambian site, opacity values for observations at 22.2GHz varies from 0.2-0.5 throughout the year and for 100GHz, 0.1-0.6 throughout the year. Opacity values are lowest and below 0.3 between March-November and highest around December for the two frequencies. The running mean for 100 GHz and 22.2 GHz is between 0.2-0.5 and 0.15 for 43 GHz respectively (Table 4.6(b), Appendix 1). For the Namibian AVN site, all observations are below 0.4 opacity. The site is ideal for observations at higher frequencies since the opacity values for observations at 100GHz are all below 0.3 throughout the year and most values are below 0.2. The opacity values vary throughout the year as well. April-October opacity values are below 0.1 for 100GHz and 43GHz frequencies, and highest but still below 0.3 are between November-March. The running mean for 100GHz is below 0.2 and below 0.3 for 22.2GHz and below 0.1 for 43GHz (Table 4.6 (b), Appendix 1).

Considering the AVN2 antennas, opacity values at 100GHz are below 0.3 and at 22.2GHz are below 0.4 throughout the year at the Ethiopian site. The opacity fluctuates throughout the year with seasons. The values for opacity are highest during the months April to October and slightly lower during November to March. The site is also ideal for high radio frequency observations. Majority of observations at the Egyptian site, opacity is below 0.4 for 100GHz and below 0.3 for 22.2GHz most of the year. Atmospheric opacity are also constant and do not vary much with seasons throughout the year. Observations at 100GHz slightly pick up increased opacity between May and December. Opacity varies greatly at the Nigerian Site throughout the year. The highest opacity values are recorded during March-August and the lowest opacity values are recorded during the months of September-February where opacity is always 0.3 on average for 22.2GHz and around 0.2 for 100GHz. During March-August, opacity values for 100GHz is around 0.55 on average and around 0.45 for 22.2GHz. High frequency observations can be carried out at the Nigerian site in the months between September-February. Opacity also varies with seasons at the Senegal site, similar to Nigeria. Opacity is fairly constant at the Moroccan site and for 22.2 and 100 GHz.

At 22.2GHz, the Namibian site has the lowest opacity mean value, followed by HartRAO and Egypt sites with the opacity below 0.3 at 97.51%, 93.96% and 84.00% for each site respectively. For the Kenyan site, the opacity mean value is 0.36 with 43.56% below 0.3 and majority of observations are between $0.3 < \alpha < 0.5$ at 56.44% implying that the Kenyan site is fine for observations around 22.2GHz.

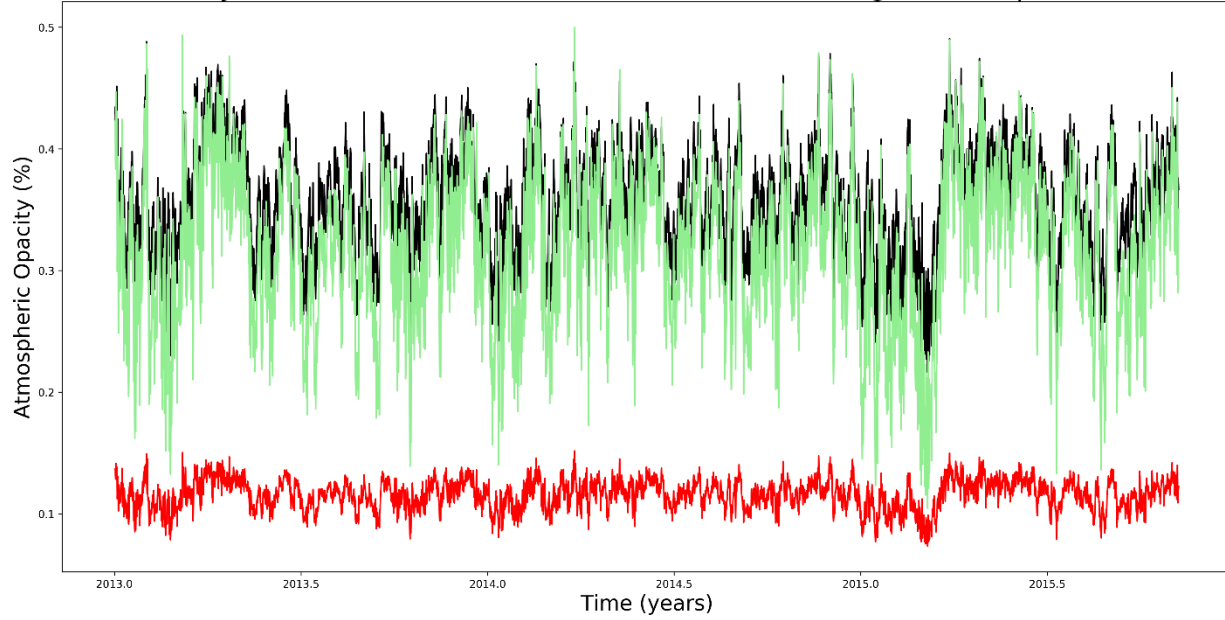
At 100GHz, Namibian site has the lowest mean opacity value of 0.12 and 80.41% of observations are below 0.3. The Ethiopian site follows with a mean opacity of 0.18 and 99.28% of the observations are below 0.3. HartRAO comes in next with a mean of 0.20 and 91.28% of observations are below 0.3. Kenya has a mean of 0.32 and 68.26% of observations are below 0.3 and 31.74% of observations are between 0.3 and 0.5, this implies that Kenyan site can also be used for high frequency observations. The Ghanaian site is the worst site for high frequency observations with a mean of 0.67 and only 1.08% of observations below 0.3 but 92.87% of observations are above 0.5.

Table 4.6: (a) Plots of atmospheric opacity at 22.2, 43 and 100 GHz for each AVN site.



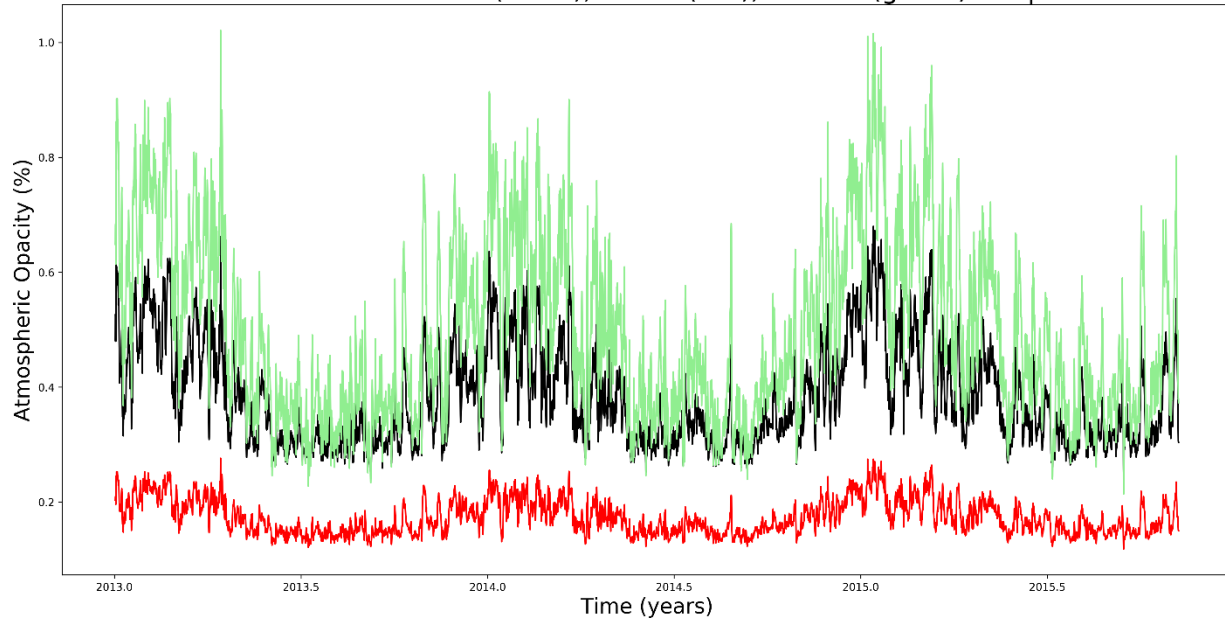
3. Kenya

Kenyan Site at 22.2GHz(black), 43GHz(red), 100GHz(green) Frequencies

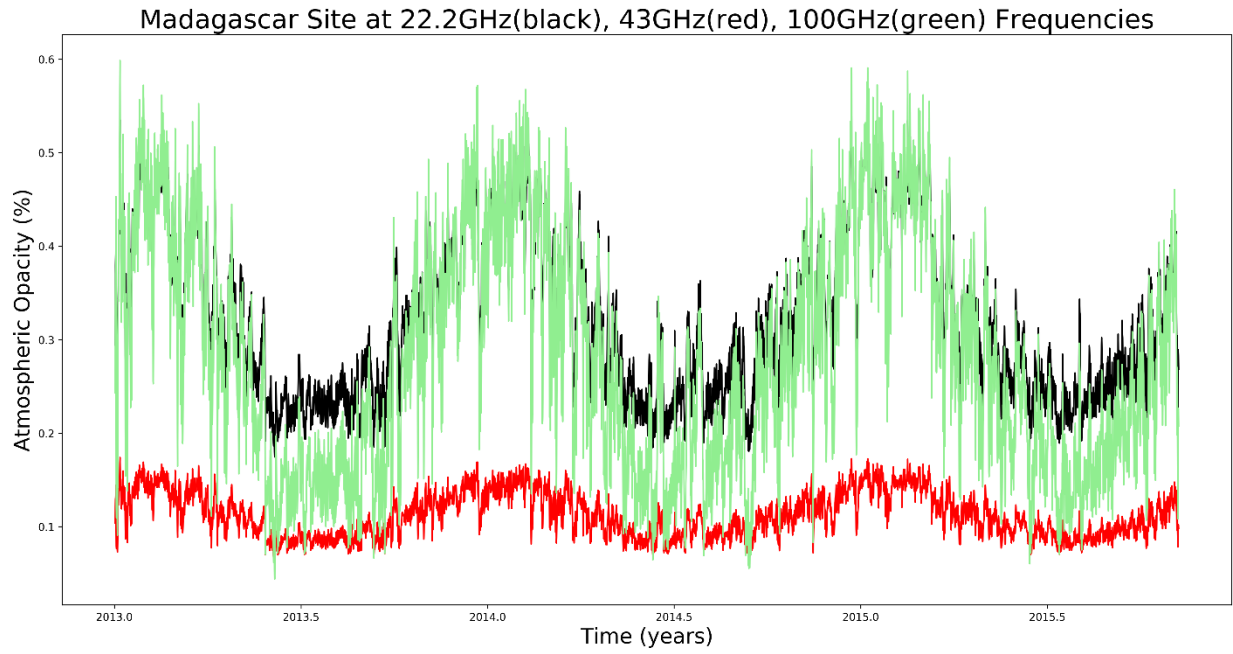


4. Mauritius

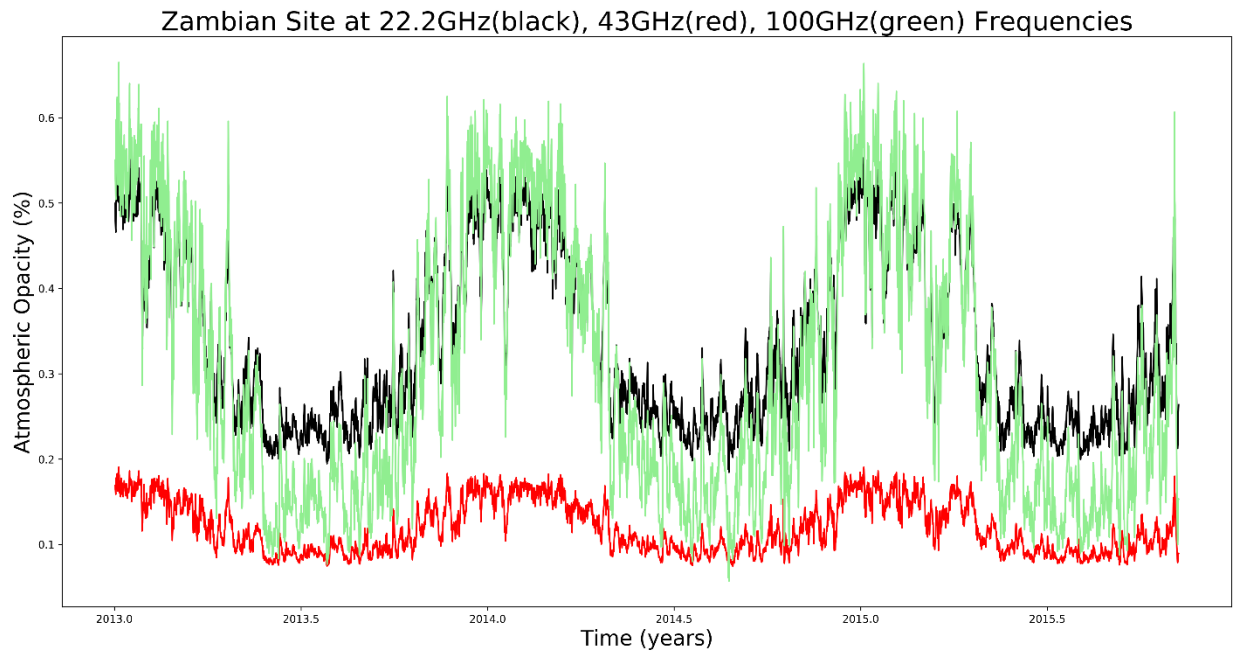
Mauritius Site at 22.2GHz(black), 43GHz(red), 100GHz(green) Frequencies



5. Madagascar

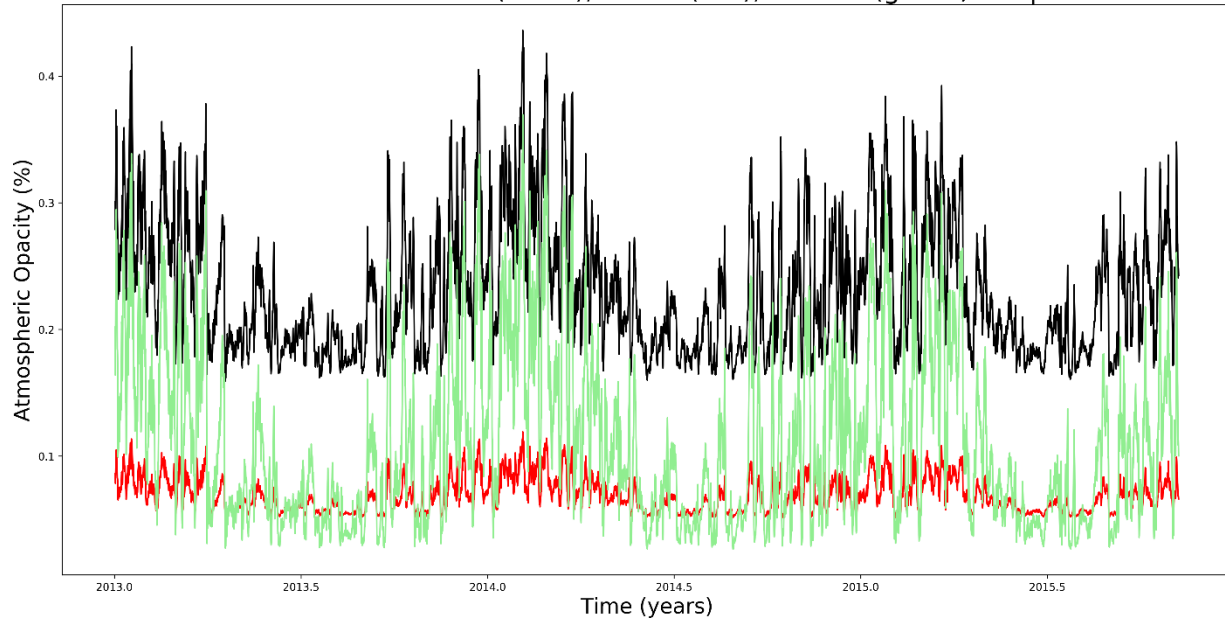


6. Zambia



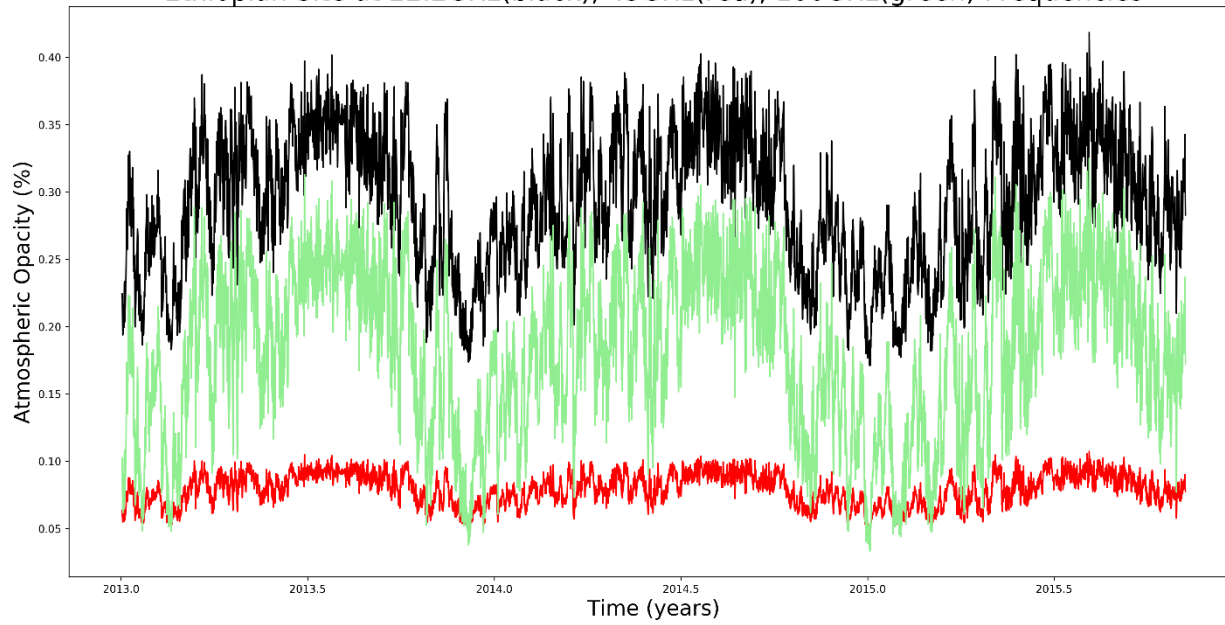
7. Namibia

Namibian Site at 22.2GHz(black), 43GHz(red), 100GHz(green) Frequencies

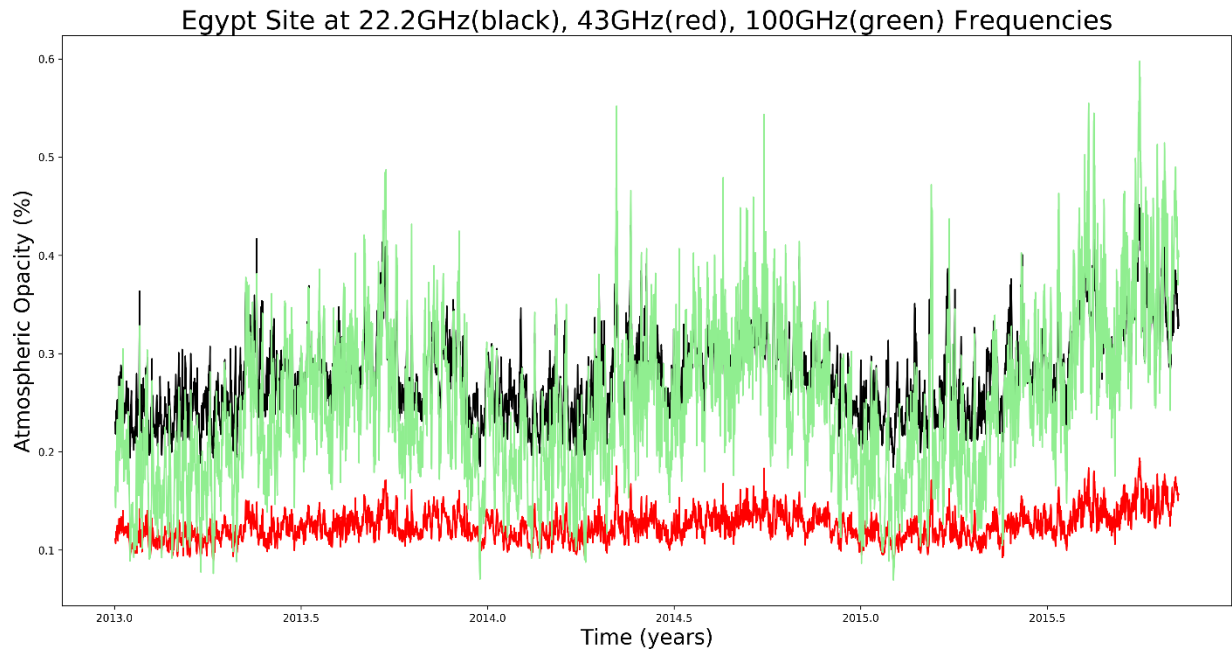


8. Ethiopia

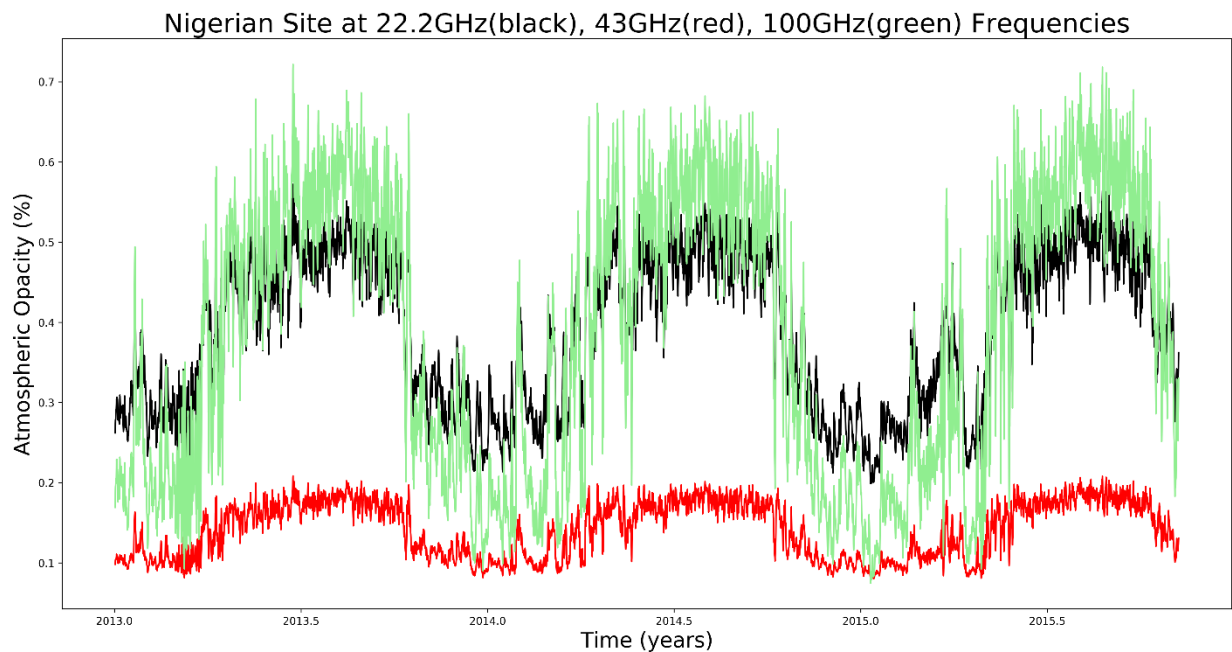
Ethiopian Site at 22.2GHz(black), 43GHz(red), 100GHz(green) Frequencies



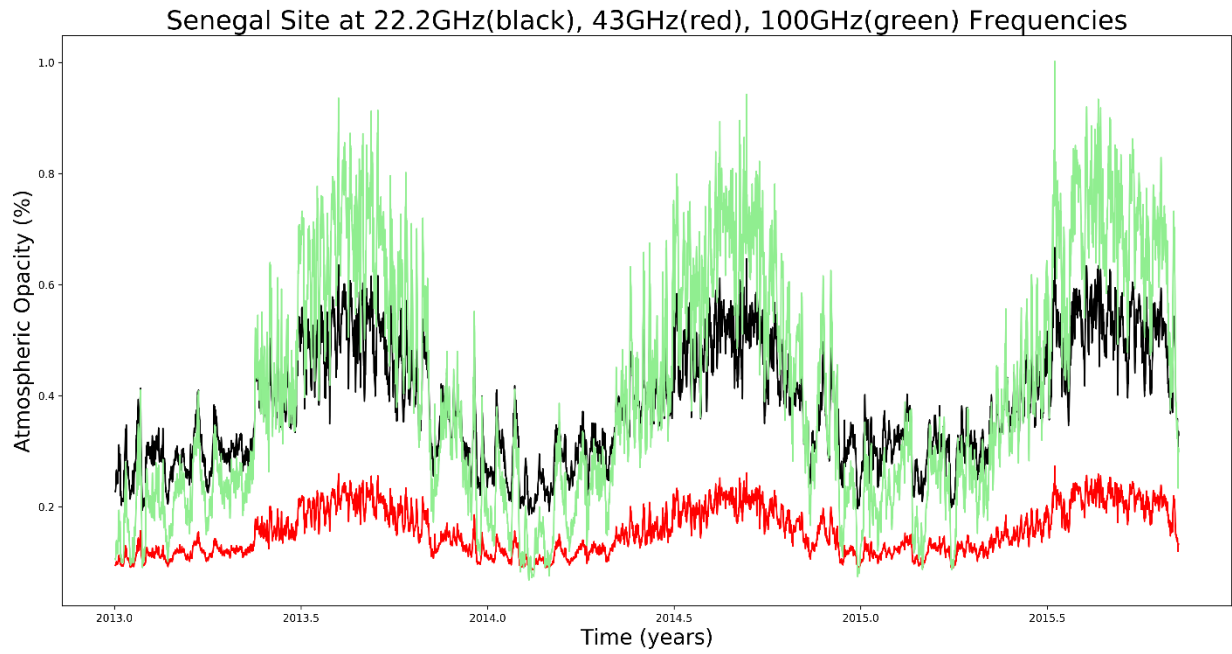
9. Egypt



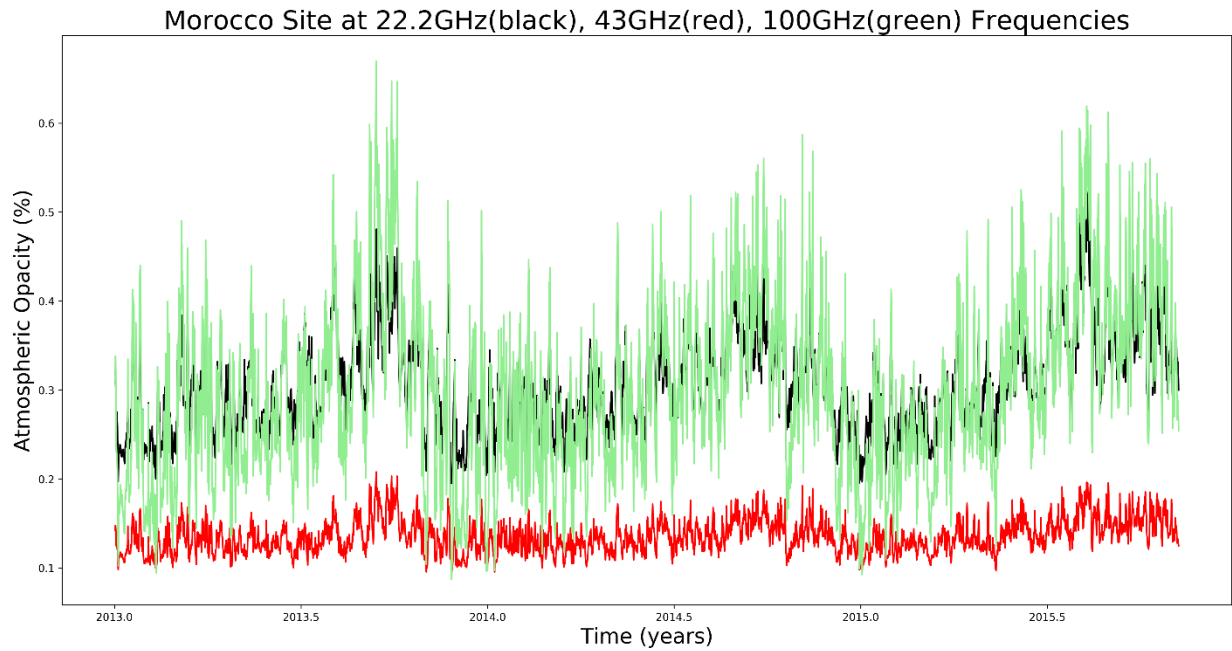
10. Nigeria



11. Senegal



12. Morocco



4.3 U-V Coverage Plots

In this section, the results from different u-v coverage simulations using the SCHED software as discussed in section 3.4 are presented.

4.3.1 U-V Coverage for LBA + AVN antennas at X-Band

Table 4.7 below shows the u-v coverage plots for the LBA antennas only, and the LBA antennas + the Kenyan antenna at x-band at different declinations, all the other plots for the AVN antennas are found in Table 4.7 (continued) Appendix I. Accompanying histograms of these u-v coverage plots are also presented and discussed in the Appendix 1. All the LBA antennas used for x-band are listed in section 3.4.

At a declination of -10° , the LBA in x-band observations can barely see anything. The u-v coverage improves a little bit at -30° and -50° in the East-West direction and at -70° , the u-v coverage for shorter and longer baselines is improved, though at medium baselines East-West and South-North directions, the u-v coverage is almost nil. At -90° declination, the u-v coverage is only for the very short baseline lengths.

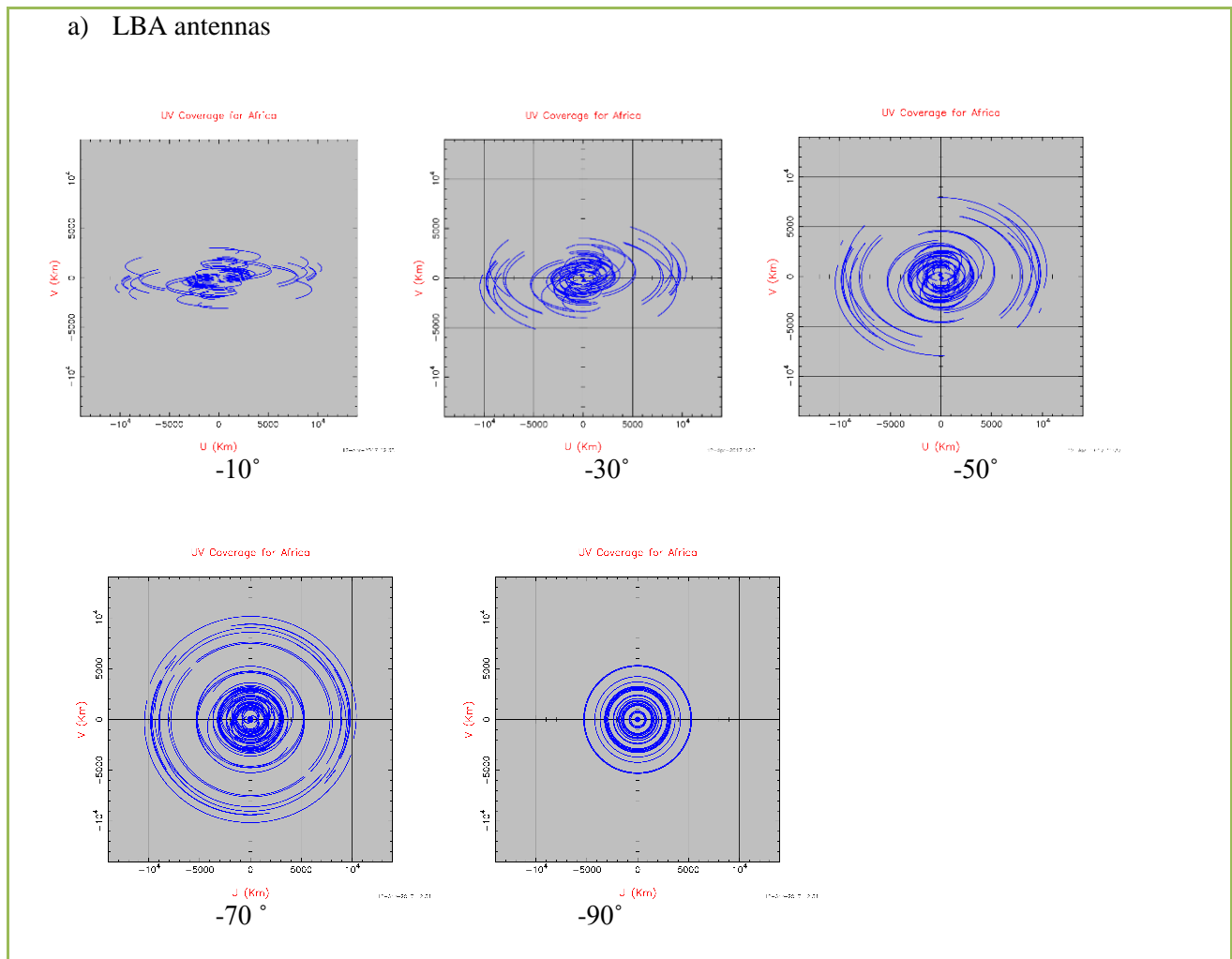
An antenna in Kenya improves the u-v coverage at declination of -70° , both in the East-West and North-South directions at the longer baselines. At -90° , it does not add to the u-v coverage at all. An antenna in Madagascar improves the u-v coverage of the LBA especially in the East-West directions. It nicely fills in the u-v coverage at -70° both in the medium and long baselines. At -90° , it fills in the u-v coverage and provides the medium to long baselines coverage for the LBA. Similarly, an antenna in Mauritius improves the u-v coverage in the East-West direction and fills in the u-v coverage for medium baseline lengths at the declination of -50° and -70° . It provides medium to long baseline lengths u-v coverage for the LBA at -90° .

Zambia also improves the East-West u-v coverage for the LBA (Table 4.7 (a), Appendix 1). It provides medium to long baselines u-v coverage at -70° and provides long baseline u-v coverage for the LBA at -90° . Namibia also improves the East-West u-v coverage for the LBA and provides u-v coverage at long baselines at -70° and -90° . Generally, antennas in the AVN1 fill in u-v coverage in the East-West direction. At declinations of -70° , AVN1 fills in the u-v coverage for LBA for all the baselines, both in the East-West and North-South directions. At -90° , the AVN1 provides long baseline u-v coverage for the LBA.

The AVN2 antennas, Ethiopia, Egypt, Nigeria, Morocco and Senegal, do not add much to the u-v coverage of the LBA. All the AVN antennas combined improve the East-West u-v coverage at the declinations of -10° , -30° and -50° . It fills up the u-v coverage at all baselines in all the directions at -70° and provides long baselines u-v coverage for the LBA at -90° .

Tables 4.8 and 4.9 show the percentages that the AVN and each AVN antenna adds to the u-v coverage to the LBA at x-band both on the long and short baselines respectively. When the AVN is added to the LBA, the u-v coverage is increased by a factor more than three at all declinations at all baselines. The AVN1 antennas, that is, Mauritius, Madagascar, Kenya, Namibia and Zambia significantly increase the u-v coverage respectively at all declinations. However, the Zambian and Namibian antennas stand out at declinations of -70 and -90 at longer baselines.

Table 4.7: U-V Coverage for LBA antennas (a) and LBA + Kenyan antenna (b) at X-Band.



b) LBA + Kenya

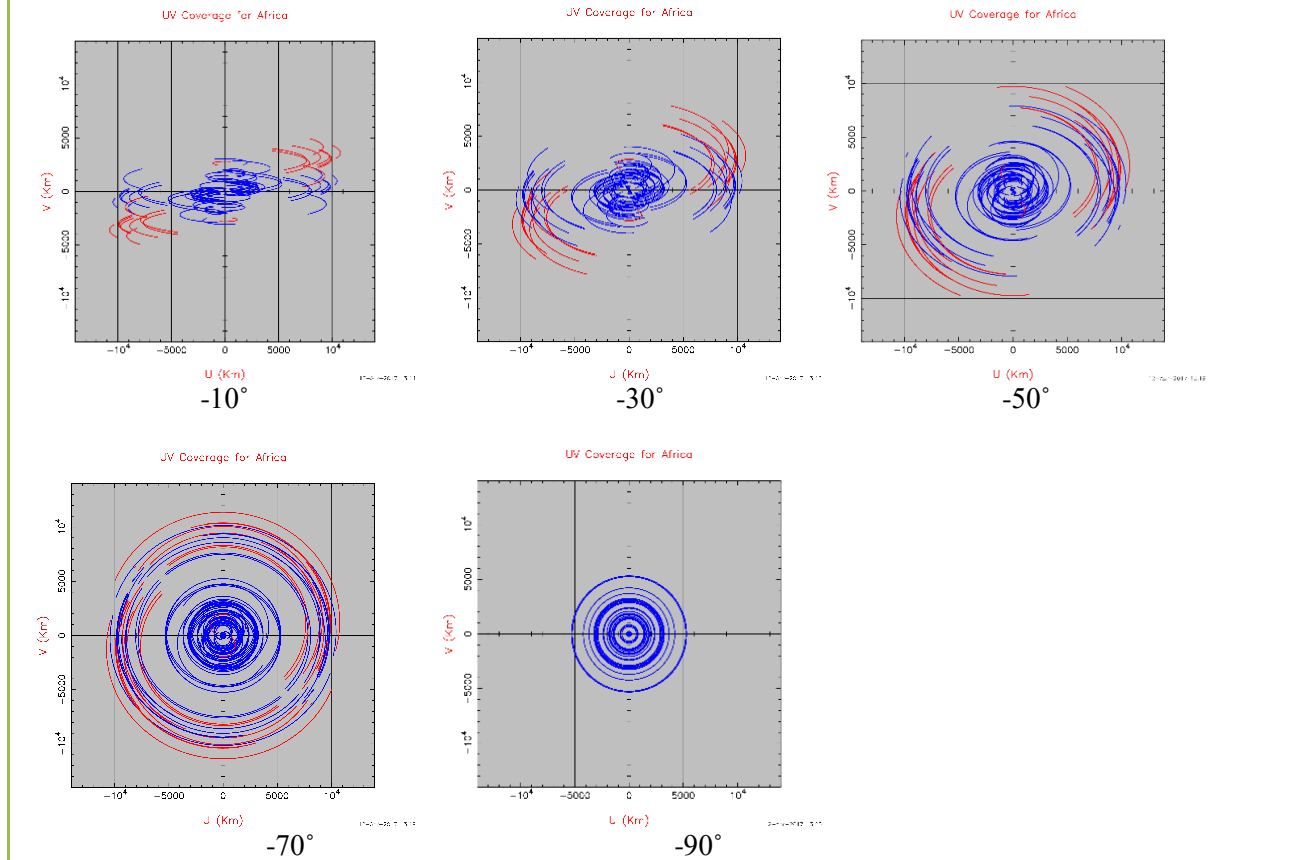


Table 4.8: Percentages of U-V Coverage at Short baselines for LBA + AVN antennas at X-Band

Networks Declinations	U-V Coverage % Short Baselines				
	-10°	-30°	-50°	-70°	-90°
LBA	7.09 ± 0.26	10.63 ± 0.26	14.09 ± 0.25	20.75 ± 0.24	12.15 ± 0.26
LBA+ AVN	23.30 ± 1.02	32.41 ± 1.40	42.40 ± 1.73	56.63 ± 2.01	36.27 ± 0.99
LBA +AVN1	14.63 ± 0.68	23.70 ± 1.06	34.68 ± 1.44	52.88 ± 1.87	36.27 ± 0.99
LBA + Kenya	8.13 ± 0.32	12.42 ± 0.37	16.31 ± 0.41	23.94 ± 0.48	12.15 ± 0.26
LBA+ Ghana	7.33 ± 0.27	11.01 ± 0.29	14.54 ± 0.28	21.12 ± 0.27	12.15 ± 0.26
LBA + Zambia	7.74 ± 0.30	11.95 ± 0.35	16.81 ± 0.45	26.24 ± 0.59	17.00 ± 0.45
LBA + Mauritius	9.16 ± 0.39	14.41 ± 0.52	20.72 ± 0.67	32.77 ± 1.02	22.46 ± 0.59
LBA + Madagascar	8.74 ± 0.36	13.71 ± 0.47	19.43 ± 0.60	30.93 ± 0.89	20.06 ± 0.50
LBA + Namibia	7.40 ± 0.28	$15.58 \pm$	$16.78 \pm$	$27.03 \pm$	15.33 ± 0.36

		0.32	0.43	0.65	
LBA + Ethiopia	8.18 ± 0.13	12.34 ± 0.37	15.88 ± 0.37	22.60 ± 0.37	12.15 ± 0.26
LBA + Egypt	7.87 ± 0.30	11.66 ± 0.32	15.08 ± 0.32	20.75 ± 0.24	12.15 ± 0.26
LBA + Nigeria	7.35 ± 0.27	11.06 ± 0.29	14.55 ± 0.28	21.01 ± 0.27	12.15 ± 0.26
LBA + Senegal	7.39 ± 0.27	10.98 ± 0.29	14.49 ± 0.28	20.99 ± 0.26	12.15 ± 0.26
LBA + Morocco	7.34 ± 0.27	10.89 ± 0.28	14.23 ± 0.26	20.75 ± 0.24	12.15 ± 0.26

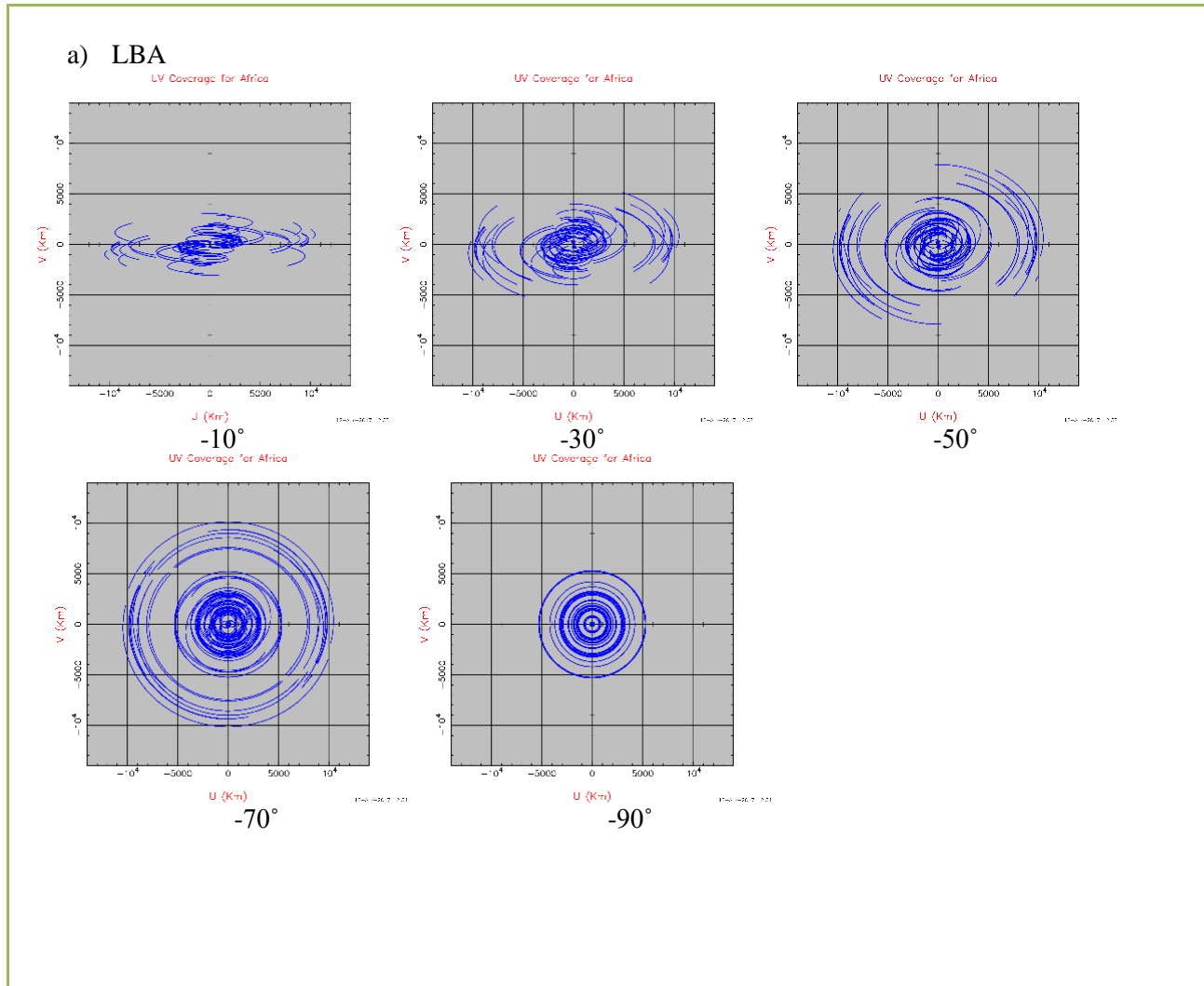
Table 4.9: Percentages of U-V Coverage at long baselines for LBA + AVN antennas at X-Band

Networks Declinations	U-V Coverage % Long Baselines				
	-10°	-30°	-50°	-70°	-90°
LBA	5.40 ± 0.22	7.33 ± 0.22	9.21 ± 0.22	13.39 ± 0.21	7.13 ± 0.22
LBA+ AVN	14.82 ± 0.67	21.64 ± 0.94	30.47 ± 1.27	46.49 ± 1.67	27.45 ± 0.76
LBA +AVN1	10.09 ± 0.48	15.98 ± 0.72	23.73 ± 1.04	40.84 ± 1.51	27.45 ± 0.76
LBA + Kenya	6.24 ± 0.27	8.80 ± 0.32	11.50 ± 0.37	17.47 ± 0.48	7.13 ± 0.22
LBA+ Ghana	5.82 ± 0.24	8.25 ± 0.28	11.09 ± 0.33	17.17 ± 0.44	7.13 ± 0.22
LBA + Zambia	6.07 ± 0.26	8.72 ± 0.32	11.83 ± 0.41	19.43 ± 0.58	13.91 ± 0.45
LBA + Mauritius	6.38 ± 0.28	9.12 ± 0.34	12.27 ± 0.41	19.34 ± 0.59	12.47 ± 0.38
LBA + Madagascar	6.30 ± 0.28	9.02 ± 0.34	12.05 ± 0.41	19.48 ± 0.59	12.51 ± 0.37
LBA + Namibia	5.90 ± 0.25	8.66 ± 0.31	12.06 ± 0.42	21.71 ± 0.72	13.29 ± 0.38
LBA + Ethiopia	6.22 ± 0.26	8.75 ± 0.29	11.30 ± 0.35	16.09 ± 0.39	7.13 ± 0.22
LBA + Egypt	6.06 ± 0.26	8.48 ± 0.29	10.79 ± 0.32	13.39 ± 0.21	7.13 ± 0.22
LBA + Nigeria	5.91 ± 0.25	8.35 ± 0.28	11.12 ± 0.34	16.81 ± 0.44	7.13 ± 0.22
LBA + Senegal	5.68 ± 0.23	7.95 ± 0.26	10.46 ± 0.30	15.24 ± 0.33	7.13 ± 0.22
LBA + Morocco	5.69 ± 0.23	7.79 ± 0.25	9.58 ± 0.24	13.39 ± 0.21	7.13 ± 0.22

4.3.2 U-V Coverage for LBA + AVN antennas at K-Band

Table 4.10 below shows the U-V Coverage plots for the LBA antennas only, and the LBA antennas + the Kenyan antenna at k-band at different declinations, all the other plots for the AVN antennas are found in Table 4.10 (continued) Appendix I with their accompanying histograms. All the LBA antennas used for k-band are listed in section 3.4. Tables 4.11 and 4.12 list the percentages of the u-v coverage for the LBA plus the AVN antennas at k-band at both the long and short baselines. Similar to u-v coverage percentages at x-band (section 4.3.1), the AVN as a whole more than triples the u-v coverage of the LBA while Mauritius, Madagascar, Kenya, Namibia and Zambia add the most to the u-v coverage respectively. However, the Namibian site adds the most u-v coverage at a declination of -70 while Zambia adds the most u-v coverage at a declination of -90 at all baselines. The AVN2 antennas do not stand out in terms of u-v coverage to the LBA since the AVN1 antennas add as much and even more.

Table 4.10: U-V Coverage for LBA antennas (a) and LBA+ Kenyan (b) at K-Band



b) LBA + Kenyan Antenna

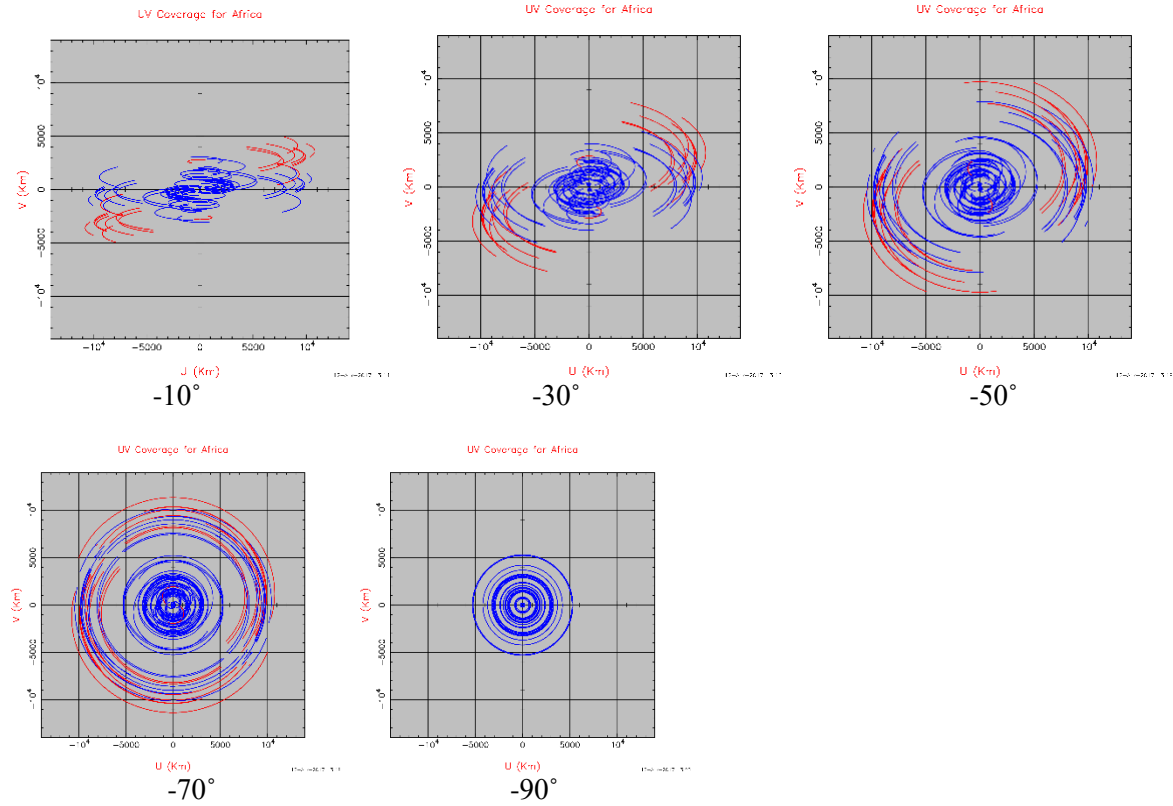


Table 4.11: Percentages of U-V Coverage at short baselines for LBA + AVN antennas at K-Band

Networks	U-V Coverage % Short Baselines				
	-10°	-30°	-50°	-70°	-90°
LBA	1.97 ± 0.29	2.71 ± 0.29	3.61 ± 0.28	4.80 ± 0.28	0.35 ± 0.29
LBA+ AVN	16.42 ± 0.86	22.26 ± 1.24	28.67 ± 1.53	34.42 ± 1.74	17.73 ± 0.77
LBA +AVN1	7.93 ± 0.56	12.82 ± 0.85	19.48 ± 1.15	29.10 ± 1.52	17.73 ± 0.77
LBA + Kenya	2.25 ± 0.30	3.45 ± 0.33	4.43 ± 0.33	5.95 ± 0.35	2.35 ± 0.29
LBA+ Ghana	2.23 ± 0.30	3.05 ± 0.31	3.98 ± 0.30	5.18 ± 0.30	2.35 ± 0.29
LBA + Zambia	1.97 ± 0.29	3.20 ± 0.32	4.76 ± 0.37	7.23 ± 0.43	4.42 ± 0.37
LBA + Mauritius	3.35 ± 0.37	5.18 ± 0.44	7.85 ± 0.53	13.33 ± 0.79	8.53 ± 0.49
LBA + Madagascar	2.84 ± 0.34	4.50 ± 0.40	6.82 ± 0.48	10.80 ± 0.63	7.04 ± 0.45
LBA + Namibia	2.06 ± 0.29	3.06 ± 0.31	4.85 ± 0.37	7.66 ± 0.48	3.68 ± 0.33
LBA + Ethiopia	2.29 ± 0.30	3.37 ± 0.33	4.25 ± 0.32	5.53 ± 0.33	2.35 ± 0.29
LBA + Egypt	2.12 ± 0.29	2.90 ± 0.30	3.81 ± 0.30	4.80 ± 0.28	2.35 ± 0.29
LBA + Nigeria	2.18 ± 0.29	3.02 ± 0.30	3.91 ± 0.30	5.10 ± 0.30	2.35 ± 0.29
LBA + Senegal	2.27 ± 0.30	10.98 ± 0.29	4.05 ± 0.31	5.11 ± 0.30	2.35 ± 0.29
LBA + Morocco	2.22 ± 0.30	5.18 ± 0.44	3.77 ± 0.29	4.80 ± 0.28	2.35 ± 0.29

Table 4.12: Percentages of U-V Coverage at long baselines for LBA + AVN antennas at K-Band

Networks Declinations	U-V Coverage % Long Baselines				
	-10°	-30°	-50°	-70°	-90°
LBA	3.16 ± 0.23	3.78 ± 0.23	4.46 ± 0.23	5.84 ± 0.23	3.08 ± 0.23
LBA+ AVN	10.74 ± 0.55	15.49 ± 0.82	21.59 ± 1.11	30.19 ± 0.14	16.67 ± 0.59
LBA +AVN1	6.57 ± 0.40	10.11 ± 0.59	15.04 ± 0.82	24.84 ± 1.15	16.67 ± 0.59
LBA + Kenya	3.56 ± 0.25	4.59 ± 0.28	5.80 ± 0.31	7.94 ± 0.36	3.08 ± 0.23
LBA+ Ghana	3.37 ± 0.24	4.30 ± 0.26	5.50 ± 0.29	7.77 ± 0.34	3.08 ± 0.23
LBA + Zambia	3.44 ± 0.25	4.53 ± 0.28	5.91 ± 0.33	9.26 ± 0.42	6.89 ± 0.36
LBA + Mauritius	3.76 ± 0.27	4.92 ± 0.30	6.40 ± 0.34	9.80 ± 0.45	6.16 ± 0.32
LBA + Madagascar	3.66 ± 0.26	4.78 ± 0.30	6.16 ± 0.34	9.39 ± 0.43	6.44 ± 0.33
LBA + Namibia	3.39 ± 0.25	4.50 ± 0.28	6.03 ± 0.34	10.46 ± 0.51	6.43 ± 0.32
LBA + Ethiopia	3.55 ± 0.25	4.56 ± 0.28	5.67 ± 0.30	7.38 ± 0.32	3.08 ± 0.23
LBA + Egypt	3.44 ± 0.25	4.36 ± 0.27	5.32 ± 0.28	5.84 ± 0.15	3.08 ± 0.23
LBA + Nigeria	3.39 ± 0.24	4.35 ± 0.27	5.15 ± 0.29	7.65 ± 0.33	3.08 ± 0.23
LBA + Senegal	3.30 ± 0.24	7.95 ± 0.26	5.13 ± 0.28	6.78 ± 0.29	3.08 ± 0.23
LBA + Morocco	3.30 ± 0.24	4.02 ± 0.25	4.67 ± 0.25	5.84 ± 0.23	3.08 ± 0.23

For the k-band, Ghana (see Table 4.8 (a), Appendix I) improves the u-v coverage at long baselines in the North-South direction at a declination of -70° . It adds absolutely no u-v coverage at -90° . Kenya adds the u-v coverage in the North-south direction but on top of the existing u-v coverage. Madagascar improves u-v coverage at a declination -70° at shorter baselines both in the East-West and North-South west direction and medium to long baselines at -90° . Mauritius improves the u-v coverage for -70° and -90° as well. Namibia and Zambia improves the u-v coverage at -70° and -90° at the longer baselines both in the East-West and North-South directions.

The AVN1 nicely fills in the u-v coverage from short, medium to long baselines at -70° and fills in u-v coverage at long baselines at -90° in all directions. The AVN2 antennas do not add much to the LBA k-band apart from Nigeria which slightly improves the u-v coverage for long baselines in the North-South direction at a declination of -90 degrees. AVN generally improves the u-v coverage at -70° and -90° for all baselines in all directions.

At a declination of -10° , the AVN1 and AVN2 reduce background and add to the u-v coverage along the long baselines. Individual antennas do not add much to the u-v coverage. At short to medium baselines, Mauritius contributes the most to the u-v coverage. At -30° , Madagascar adds u-v coverage along the long baselines, Mauritius and Madagascar reduce the background and add to the u-v coverage on the short-medium baselines. The case is similar at -50° . At -70° , on long baselines Namibia and Madagascar add to

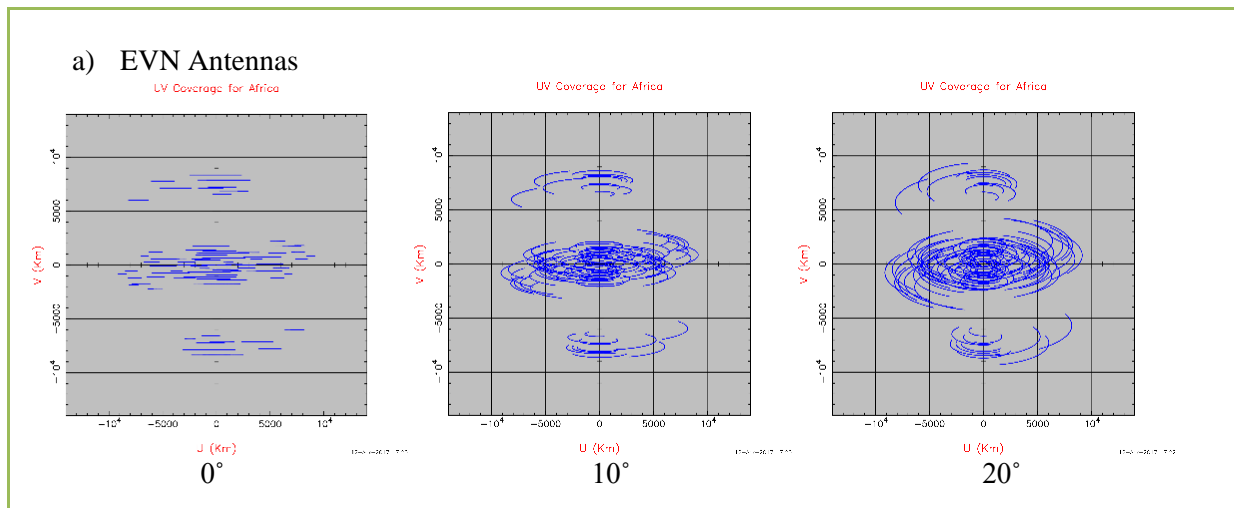
the u-v coverage and reduces the background significantly. At -90° Madagascar improves the u-v coverage at the long baselines but at shorter baselines, the AVN1 and AVN in general do not add much to the u-v coverage at -90° . This is because sources at -90° are way down beyond the visibility of these antennas.

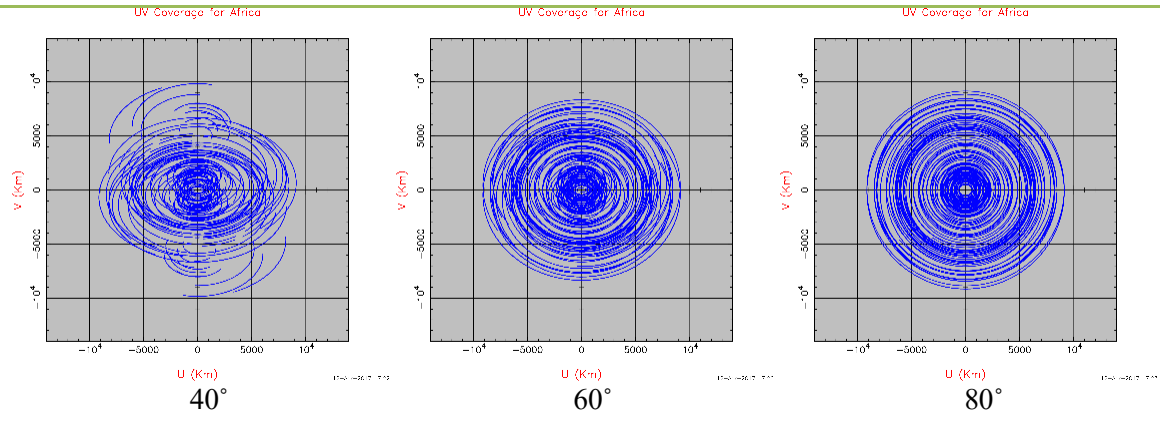
4.3.3 U-V Coverage for EVN + AVN Antennas

Table 4.13 below shows the u-v coverage plots for the EVN antennas only, and the LBA antennas + the Kenyan antenna at x-band at different declinations, all the other plots for the AVN antennas are found in Table 4.13 (continued) Appendix I with their accompanying histograms. All the EVN antennas used are listed in section 3.4.

Tables 4.14 and 4.15 show the percentages of the u-v coverage for the EVN plus AVN antennas at x-band at both the long and short baselines respectively at different declinations. Generally, the AVN improves the u-v coverage by more than a factor of three at all declinations. The AVN1 also more than doubles the u-v coverage of the EVN. Once again, the Kenyan antenna singularly stands out by improving the u-v coverage of the EVN at declinations of 0, 10, 20, and 40 while the Ghanaian antenna stands out at the declinations of 60 and 80 at all baselines. The Namibia antenna adds the least to the u-v coverage of the EVN at all declinations at all baselines. Meanwhile, the AVN2 antennas do not stand out as much and contribute as much as the AVN1 antennas.

Table 4.13: U-V Coverage for EVN + AVN antennas at X-Band.





a) EVN + Kenyan Antenna

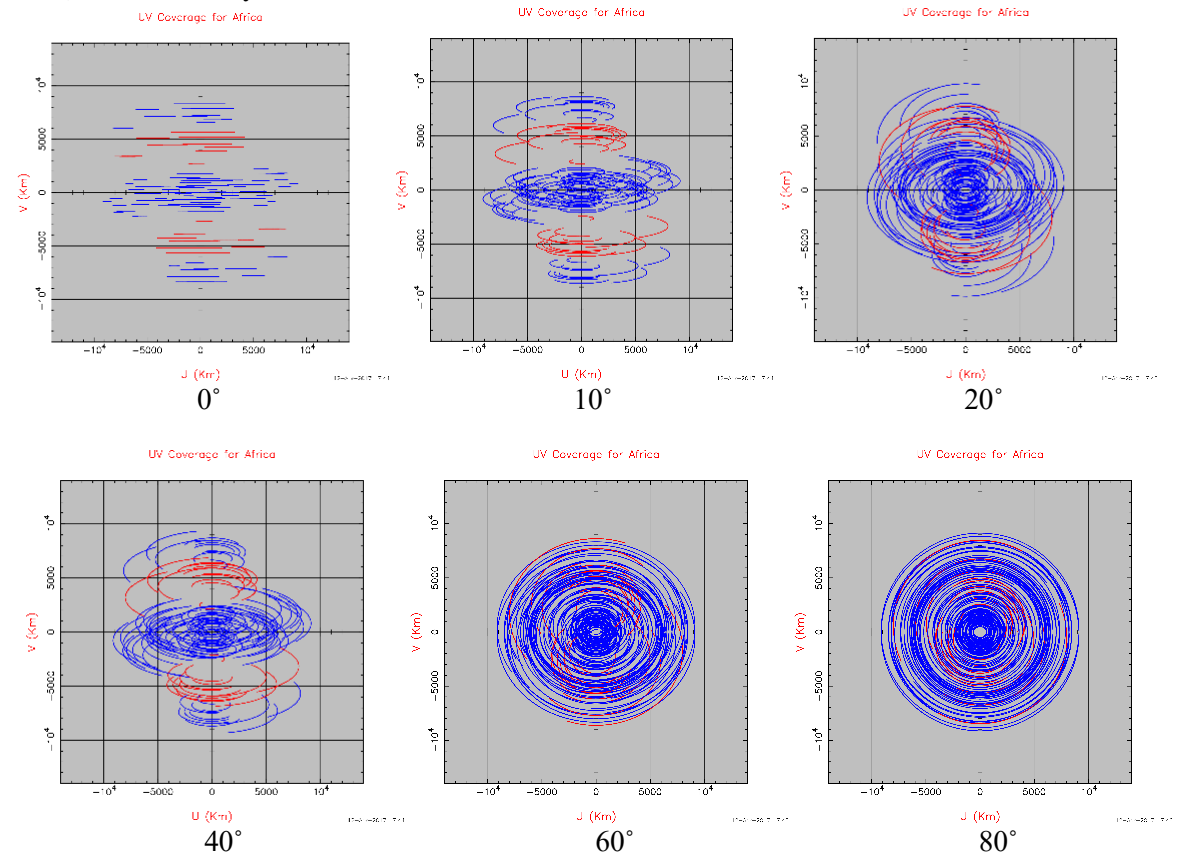


Table 4.14: Percentages of U-V Coverage at short baselines for EVN + AVN antennas at X-Band

Networks Declinations	Short Baselines U-V Coverage %					
	0°	10°	20°	40°	60°	80°
EVN	6.47 ± 0.26	11.93 ± 0.25	15.96 ± 0.25	29.29 ± 0.21	42.36 ± 0.17	47.23 ± 0.16
EVN+ AVN	28.76 ± 0.84	43.27 ± 1.43	48.87 ± 1.61	60.47 ± 1.85	70.07 ± 2.04	73.29 ± 1.91
EVN +AVN1	18.14 ± 0.62	28.53 ± 0.39	33.24 ± 1.07	45.68 ± 1.16	54.45 ± 1.19	53.46 ± 0.80
EVN + Kenya	8.76 ± 0.33	15.57 ± 0.41	20.09 ± 0.46	33.17 ± 0.48	44.97 ± 0.47	49.60 ± 0.45
EVN+ Ghana	8.34 ± 0.29	14.77 ± 0.38	19.12 ± 0.40	32.49 ± 0.43	45.31 ± 0.46	51.36 ± 0.55
EVN + Zambia	8.16 ± 0.31	14.73 ± 0.39	19.03 ± 0.41	32.03 ± 0.38	44.07 ± 0.33	47.23 ± 0.16
EVN + Mauritius	8.18 ± 0.35	14.77 ± 0.40	18.91 ± 0.42	32.52 ± 0.41	44.58 ± 0.36	47.23 ± 0.16
EVN + Madagascar	8.46 ± 0.32	14.98 ± 0.40	18.69 ± 0.42	32.43 ± 0.41	44.42 ± 0.34	47.23 ± 0.16
EVN + Namibia	7.69 ± 0.30	13.75 ± 0.34	17.83 ± .33	31.24 ± 0.33	43.17 ± 0.25	47.23 ± 0.16
EVN + Ethiopia	8.73 ± 0.33	15.56 ± 0.41	20.01 ± 0.43	33.26 ± 0.51	46.44 ± 0.54	52.61 ± 0.69
EVN + Egypt	8.16 ± 0.30	14.89 ± 0.39	19.19 ± 0.44	32.64 ± 0.49	46.40 ± 0.55	52.68 ± 0.68
EVN + Nigeria	8.33 ± 0.29	14.59 ± 0.35	19.23 ± 0.41	32.46 ± 0.44	45.31 ± 0.45	50.92 ± 0.55
EVN + Senegal	8.14 ± 0.31	14.86 ± 0.38	19.53 ± 0.44	32.99 ± 0.50	45.91 ± 0.53	53.18 ± 0.78
EVN + Morocco	7.57 ± 0.29	13.83 ± 0.35	18.15 ± 0.40	31.73 ± 0.47	47.76 ± 0.68	53.67 ± 0.68

Table 4.15: Percentages of U-V Coverage at long baselines for EVN + AVN antennas at X-Band

Networks Declinations	Long Baselines U-V Coverage %					
	0°	10°	20°	40°	60°	80°
EVN	4.96 ± 0.22	7.68 ± 0.22	9.52 ± 0.22	15.02 ± 0.20	20.62 ± 0.18	23.21 ± 0.18
EVN+ AVN	14.43 ± 0.47	21.38 ± 0.75	24.41 ± 0.86	30.41 ± 1.02	36.03 ± 1.18	39.19 ± 1.25
EVN +AVN1	10.14 ± 0.37	14.99 ± 0.53	17.50 ± 0.61	23.43 ± 0.68	27.44 ± 0.72	26.91 ± 0.53
EVN + Kenya	5.91 ± 0.25	9.19 ± 0.28	11.23 ± 0.30	16.63 ± 0.31	21.87 ± 0.32	24.27 ± 0.31
EVN+ Ghana	5.77 ± 0.24	8.95 ± 0.28	10.98 ± 0.29	16.69 ± 0.31	22.72 ± 0.36	25.96 ± 0.42
EVN + Zambia	5.67 ± 0.24	8.87 ± 0.28	10.85 ± 0.29	16.54 ± 0.30	21.73 ± 0.27	23.21 ± 0.18
EVN + Mauritius	5.66 ± 0.26	8.92 ± 0.28	10.99 ± 0.30	16.81 ± 0.31	21.59 ± 0.26	23.21 ± 0.18
EVN + Madagascar	5.78 ± 0.25	8.96 ± 0.28	10.82 ± 0.30	16.61 ± 0.30	21.55 ± 0.26	23.21 ± 0.18
EVN + Namibia	5.57 ± 0.24	8.66 ± 0.27	10.58 ± 0.27	16.31 ± 0.28	21.34 ± 0.24	23.21 ± 0.18
EVN + Ethiopia	5.90 ± 0.25	9.18 ± 0.28	11.19 ± 0.29	16.66 ± 0.32	22.31 ± 0.34	25.48 ± 0.40
EVN + Egypt	5.66 ± 0.24	8.91 ± 0.28	10.86 ± 0.29	16.42 ± 0.32	22.31 ± 0.34	25.53 ± 0.40
EVN + Nigeria	5.76 ± 0.23	8.88 ± 0.27	11.00 ± 0.29	16.61 ± 0.31	22.45 ± 0.34	25.56 ± 0.40
EVN + Senegal	5.70 ± 0.24	9.03 ± 0.28	11.23 ± 0.31	17.01 ± 0.34	23.49 ± 0.43	28.10 ± 0.60
EVN + Morocco	5.44 ± 0.24	8.53 ± 0.26	10.53 ± 0.29	16.23 ± 0.32	23.48 ± 0.43	26.78 ± 0.45

The EVN u-v coverage at declinations of 0, 10 and 20 degrees has huge gaps in the medium to long baselines. Ghana adds a small improvement in the u-v coverage at medium baselines in the North-South direction at 0, 10 and 20. Kenyan improves the u-v coverage at medium baselines at 0, 10, 20 and 40 in the North-South direction. Antennas in Madagascar, Mauritius, Namibia and Zambia add no improvement to the u-v coverage of the EVN antennas. AVN1 antennas improve the u-v coverage at medium baselines in the North-South direction at 0, 10, 20, 40 and 60.

Ethiopia improves the u-v coverage at medium baselines in the North-South directions at 0, 10 and 20. Nigeria and Senegal improves the u-v coverage at -90 on the longer baselines in all directions. AVN fills up the medium baselines u-v coverage in the North-South direction 0, 10 and 20 and provides a whole u-v coverage at 90 especially at longer baselines.

At 0° declination, the AVN nicely fills in the background and improves the u-v coverage of the EVN at longer baselines (see table 4.13 (continued), Appendix 1 u-v coverage plots and histograms). At short to medium baselines, the EVN u-v coverage is almost zero, Kenya and Ghana slightly provide u-v coverage at this declination for the EVN. At 10°, Kenya, Ghana and Ethiopia add u-v coverage on the long baselines and reduce the background, so does the AVN1 and AVN which adds new u-v coverage whereas the AVN1 in general adds u-v coverage to the existing EVN u-v coverage and therefore does not reduce the background by much. At the medium to short baselines, an antenna in Kenya will significantly improve the u-v coverage and reduce the background at the same time. So does Ethiopia. The AVN as a whole reduces the background by almost a half.

At 20°, Kenya, Ghana, Ethiopia, AVN1 and AVN slightly reduce the background and slightly add to the u-v coverage on the long baselines. Kenya stands out at the short baselines and Ethiopia as well. Both reduce the background and greatly improve the u-v coverage. The AVN reduces the background by a half. At 40°, Kenya, Ghana, Ethiopia, Senegal and Mauritius contribute to u-v coverage on the long baselines. At medium to short baselines, again Kenya adds a lot to the u-v coverage and reduces the u-v coverage. At 60°, Morocco and Senegal reduce the background and add to the u-v coverage on the longer baselines. Morocco adds the most. At 80°, Senegal, Ghana and Morocco contribute a lot along the long baselines and Senegal improves the u-v coverage at the short to medium baselines.

4.4 Geodetic Products

The geodetic products obtained from VieVS as discussed in section 3.5 are presented in this section. The EOPs results and baseline length repeatabilities plots are presented.

4.4.1 Earth Orientation Parameters

Table 4.16 presents the EOP results for the R1675 + AVN antennas as discussed in section 3.5. It shows the average formal errors in EOPs: polar motion, x and y coordinates, x_err and y_err ; earth's rotation angle, ut_err and earth's nutation motion in the x and y coordinates, dx_err and dy_err . The stations included in the R1675 session are given in section 3.5.

The formal errors of EOPs is a very good indicator that can be used to assess the importance of a specific VLBI station (Hase, 2010). Adding the AVN antennas to the R1675 session, almost halves the errors in polar motion y coordinate (y_err), the earth's rotation angle and the nutation. Adding the AVN1 antennas to the R1675, R1675+AVN1 similarly reduces the average formal errors in the EOPs and especially the y_err . Removing the Kenyan antenna from AVN-Kenya increases the error in x pol by a value more than a 100. Similarly, removing Kenya, AVN1-Kenya almost doubles the error in the polar motion.

Table 4.16: Earth Orientation Parameters (EOPs).

STATIONS	x_err (μ as)	y_err (μ as)	ut_err (μ s)	dx_err (μ as)	dy_err (μ as)
R1675 real	22.842	46.336	2.64	18.033	16.44
R1675 Simulated	27.25 \pm 0.66	51.35 \pm 1.24	3.26 \pm 0.08	24.01 \pm 0.58	22.92 \pm 0.56
R1675+AVN	18.31 \pm 0.30	24.81 \pm 0.41	1.98 \pm 0.03	13.13 \pm 0.22	12.61 \pm 0.21
AVN	121.49 \pm 2.73	46.47 \pm 1.05	8.01 \pm 0.18	25.23 \pm 0.57	25.66 \pm 0.58
AVN-Kenya	133.38 \pm 2.42	51.22 \pm 0.93	8.86 \pm 0.16	27.48 \pm 0.50	28.00 \pm 0.51
R1675+AVN1	19.18 \pm 0.37	33.36 \pm 0.64	2.47 \pm 0.05	15.64 \pm 0.30	15.40 \pm 0.29
R1675+AVN1-Kenya	19.51 \pm 0.37	34.75 \pm 0.66	2.54 \pm 0.05	16.64 \pm 0.32	16.04 \pm 0.31
AVN1	280.74 \pm 9.01	168.85 \pm 5.42	15.84 \pm 0.51	54.43 \pm 1.75	55.40 \pm 1.78
AVN1-Kenya	429.27 \pm 16.30	247.66 \pm 9.40	19.79 \pm 0.75	61.74 \pm 2.34	64.33 \pm 2.44
R1675+AVN2	22.57 \pm 0.54	35.36 \pm 0.85	2.23 \pm 0.05	18.51 \pm 0.44	18.05 \pm 0.43
R1675+AVN2+Kenya	21.71 \pm 0.37	34.00 \pm 0.58	2.23 \pm 0.04	17.61 \pm 0.30	17.02 \pm 0.29
AVN2	231.36 \pm 7.41	66.84 \pm 2.14	14.95 \pm 0.47	48.92 \pm 1.57	46.22 \pm 1.48
R1675+Kenya	23.42 \pm 0.55	49.44 \pm 1.16	3.016 \pm 0.07	22.41 \pm 0.52	21.23 \pm 0.50

Table 4.17 shows the number of scans, the total number of observations made and the number of sources observed using a given network configuration. Adding the AVN antennas to the R1675 triples the number of observations made and increases the number of sources observed by adding 28 more sources. The number of scans is also increased. Adding the AVN1 alone to the R1675 session also more than doubles the number of observations, increases the number of scans and adds 21 new sources to the R1675 session. Adding the Kenyan antenna only to the R1675 session increases the total number of observations made by more than 1,000 and adds 10 new sources to the R1675 session.

Table 4.17: The number of scans, total observations and number of sources observed per network.

Session	No. of Stations	No. of Scans	Total Observations	No. of Sources
R1675	7	1,129	9,665	203
R1675+AVN	18	1,696	35,207	231
AVN	11	683	15,909	227
AVN- Kenya	10	671	12,999	211
R1675+AVN1	13	1,453	20,779	224
R1675+AVN1-Kenya	12	1,415	18,125	218
AVN1	6	518	6,865	202
AVN1-Kenya	5	479	5,345	180
R1675+AVN2	12	1,483	19,111	218
R1675+AVN2+Kenya	13	1,526	20,746	226
AVN2	5	519	4,710	194
R1675+Kenya	8	1,200	10,786	213

4.4.2 Baseline Length Repeatabilities

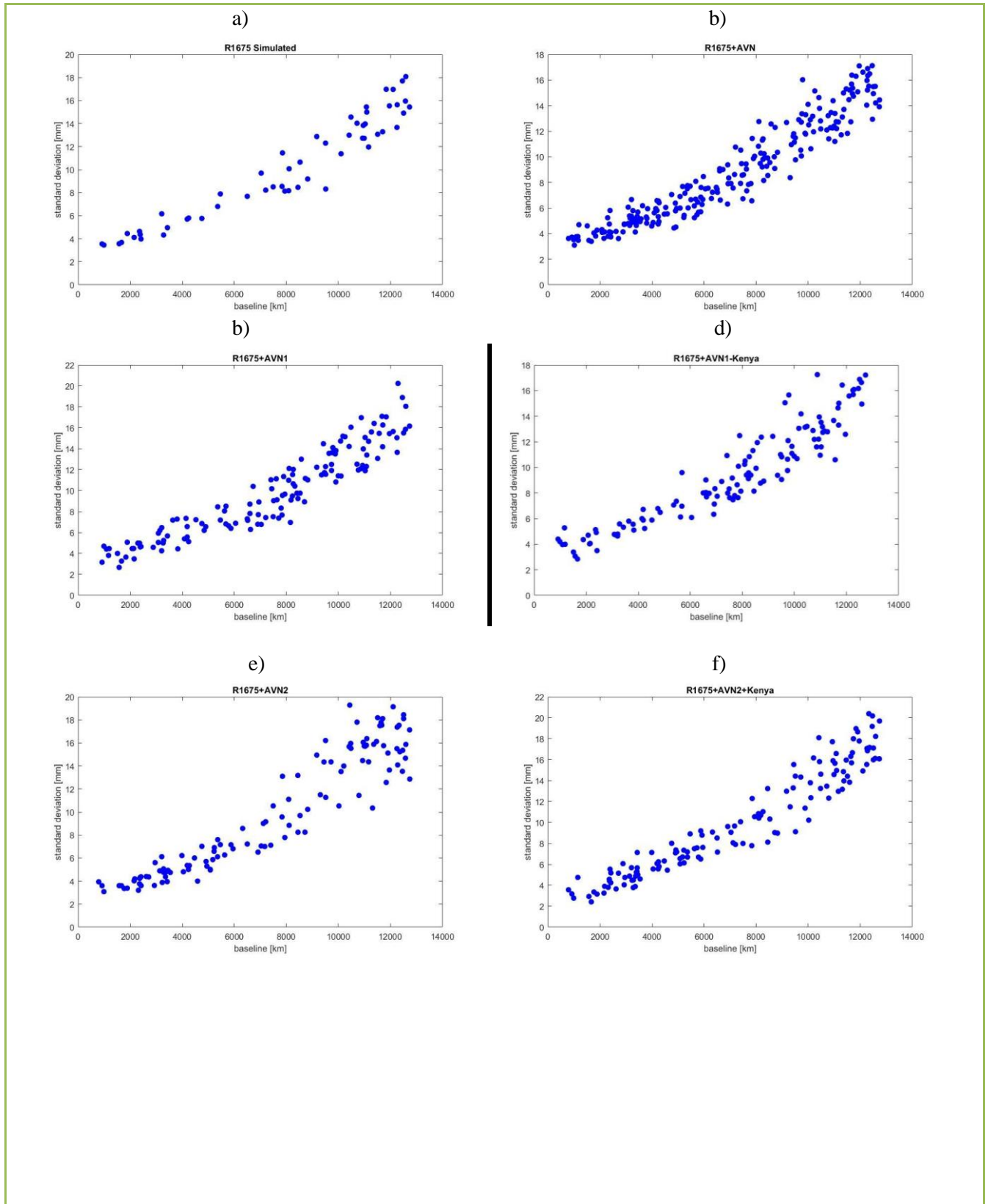
The tables below show the results from Baseline length analysis as done by VieVS. Table 4.18 shows the baselines length between all the AVN antennas as generated by VieVS whereas Table 4.19 the plots of the baseline length repeatabilities for the R1675 + AVN antennas as simulated and analyzed using VieVS.

Table 4.18: Baselines Length (km).

STATION	HartR AO	Ghana	Kenya	Zambia	Madag	Maurit	Namib	Nig	Eth	Mor	Sen	Egy
HartRAO		4,524	2,885	1,167	2,132	3,081	1,192	4,470	3,987	7,114	6,320	5,950
Ghana	4,524		4,085	3,830	5,674	6,601	3,635	1,016	4,241	3,157	2,081	4,180
Kenya	2,885	4,085		1,835	2,294	3,084	3,265	3,396	1,148	5,725	5,919	3,430
Zambia	1,167	3,830	1,835		2,076	3,141	1,512	3,574	2,930	6,282	5,753	4,894
Madag	2,132	5,674	2,294	2,076		1,088	3,208	5,262	3,214	7,325	7,462	5,494
Maurit	3,081	6,601	3,084	3,141	1,088		4,189	6,154	3,780	8,307	8,290	5,972
Namib	1,192	3,635	3,265	1,512	3,265	4,189		3,793	4,266	6,470	5,385	5,881
Nigeria	4,470	1,016	3,396	3,574	5,262	6,154	3,793		3,372	2,956	2,710	3,232
Ethiopia	3,987	4,241	1,148	2,930	3,214	3,780	4,266	3,372		5,222	5,873	2,418
Morocco	7,114	3,157	5,725	6,282	7,325	8,307	6,470	2,956	5,222		2,366	3,541
Senegal	6,320	2,081	5,919	5,753	7,462	8,290	5,385	2,710	5,873	2,366		5,074
Egypt	5,950	4,180	3,430	4,894	5,494	5,972	5,881	3,232	2,418	3,541	5,076	

Ghana provides the longest baseline lengths in the AVN1 as shown in the above table 4.18. The longest baseline length in the AVN1 is the Ghana-Mauritius baseline at 6,601, followed by Ghana-Madagascar at 5,674 km and Ghana-HartRAO at 4,524 km. Overall, the longest baseline lengths in the AVN will be Mauritius-Morocco at 8,307 km and Mauritius-Senegal at 8,290 km. Morocco will provide the longest baseline length to HartRAO at 7,114 km.

Table 4.19: Plots of baseline length repeatabilities for R1675 + AVN antennas.



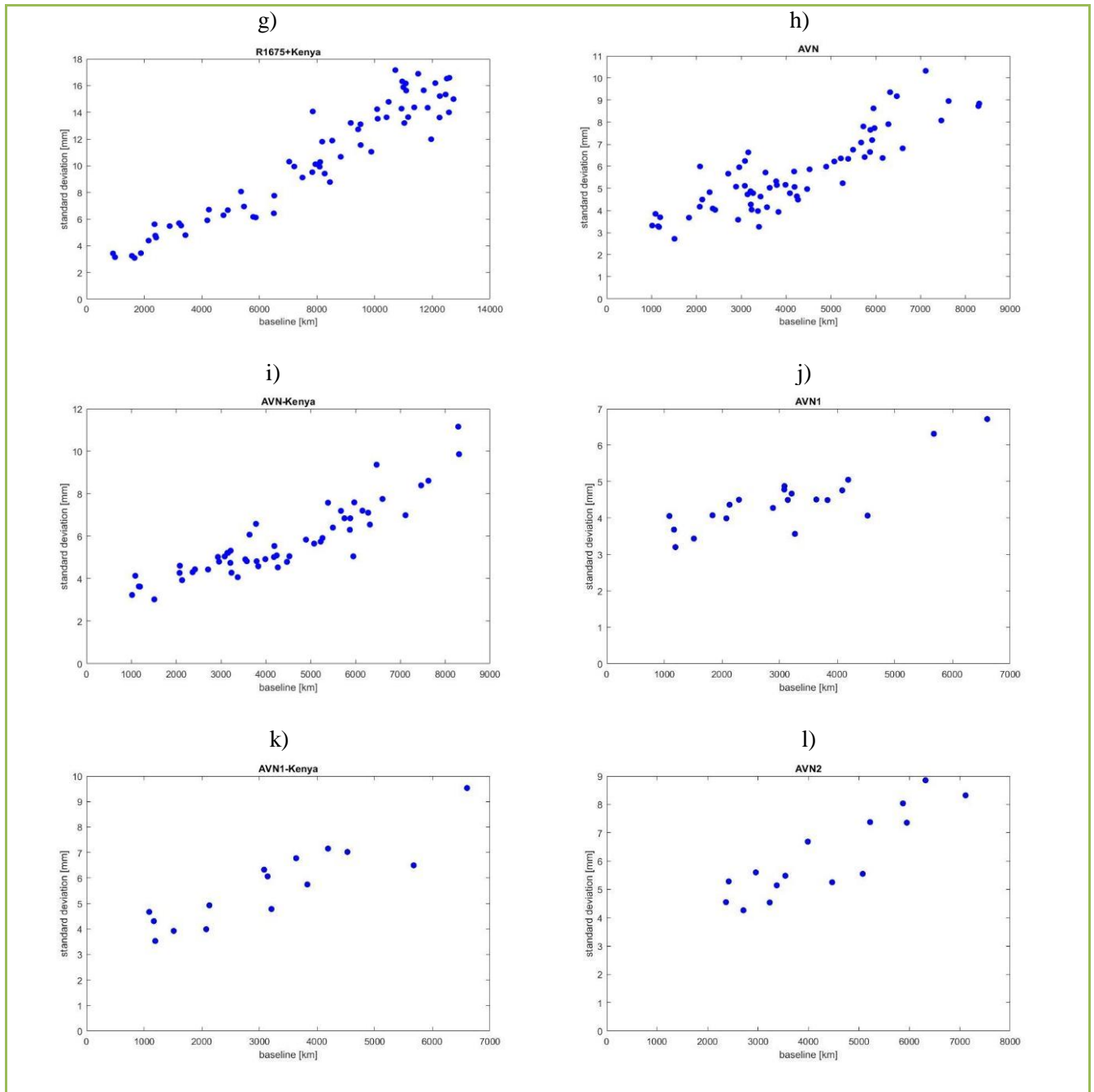


Table 4.19 shows the scatter plots of the baseline length repeatabilities against their standard deviation. Comparing the scatter plots of different networks configuration can be used to quantify the importance of a particular station in a geodetic VLBI experiment.

For example, comparing the first scatter plot (a) of the R1675 against the second scatter plot (b) of R1675 + AVN antennas, the second scatter plot has more points almost uniformly along all baselines and with a smaller standard deviation as compared to the R1675 only plot. The AVN1 antennas add points on the

scatter plots along the medium baseline lengths. Removing the Kenyan antenna, R1675+AVN1-Kenya, reduces the points on the scatter plot especially on the shorter baseline lengths. Adding the AVN2 antennas, R1675+AVN2 adds points on the longer baseline lengths on the scatter plot. Adding Kenya, R1675+AVN2+Kenya, adds points uniformly along all baseline lengths. Adding Kenya, R1675+Kenya, adds the points on the scatter plot especially on the medium baselines. This is probably so because Kenya is located almost halfway between HartRAO and the EVN antennas. Removing Kenya from the AVN 1, AVN1-Kenya, reduces the points on the scatter plot, especially along the medium baseline lengths. The baseline length repeatabilities for AVN1 or AVN2 antennas alone are terrible due to the same number of observations.

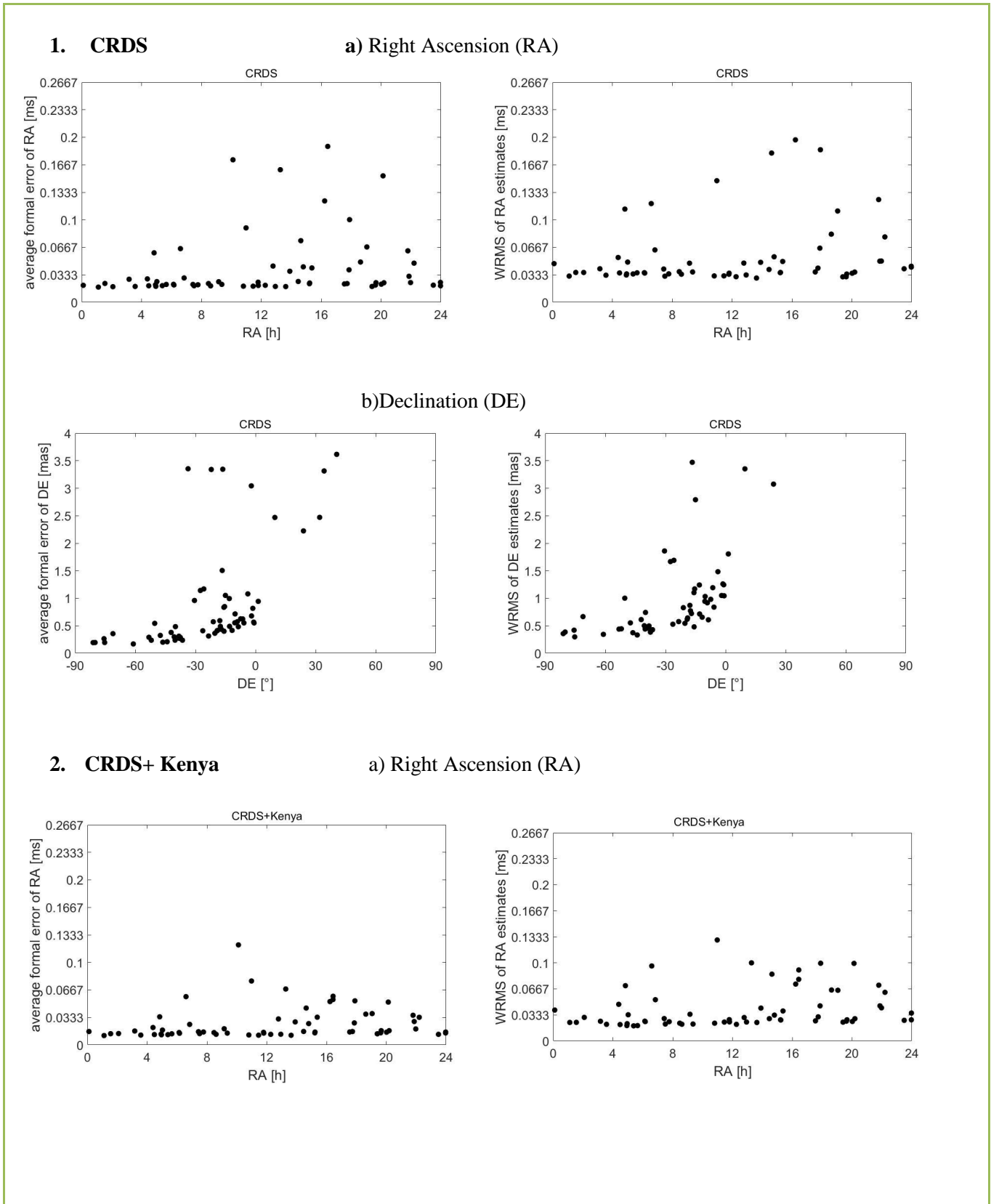
4.5 Source Position Estimates

In this section, results from the simulated source positions using the VieVS software as discussed in section 3.6 are presented. Table 4.20 presents the mean average errors in the RA and DE of source position estimates using the IVS-CRDS + the AVN1 antennas. Table 4.21 shows the plots of the RA and DE against the average formal error in position of these sources. Table 4.21 (continued), Appendix I shows all the plots of the RA and DE against their average formal errors and Weighted Root Mean Standard (WRMS) for CRDS + all the AVN1 stations.

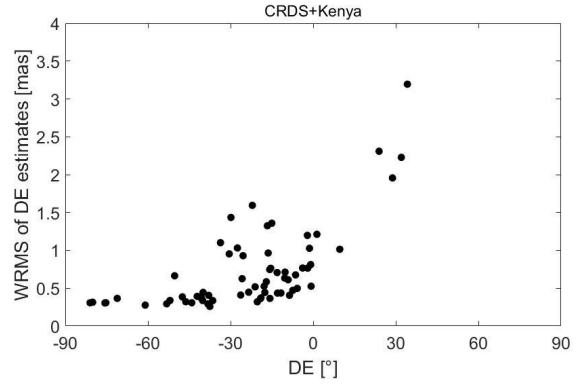
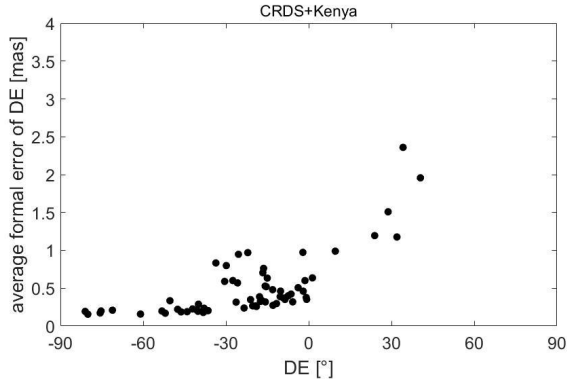
Table 4.20: Mean average values for the Right Ascension, RA (hour) and Declination, DE (degree).

Stations	Mean Average RA (ms)	WRMS RA (ms)	Mean Average DE (mas)	WRMS DE (mas)
CRDS	0.345	0.6	0.557	0.870
CRDS+Kenya	0.240	0.435	0.351	0.525
CRDS+Madagascar	0.240	0.450	0.423	0.679
CRDS+Mauritius	0.240	0.435	0.415	0.658
CRDS+Namibia	0.255	0.510	0.478	0.780
CRDS+Zambia	0.255	0.480	0.431	0.687
CRDS+AVN1	0.135	0.33	0.242	0.457
CRDS+AVN1-Kenya	0.165	0.375	0.308	0.594
CRDS+AVN1-Madagascar	0.150	0.315	0.261	0.461
CRDS+AVN1-Mauritius	0.150	0.345	0.262	0.463
CRDS+AVN1-Namibia	0.165	0.330	0.266	0.476
CRDS+AVN1-Zambia	0.150	0.315	0.256	0.462
AVN1	0.735	1.050	0.609	0.860

Table 4.21: Plots of Right Ascension (RA) and Declination (DE).

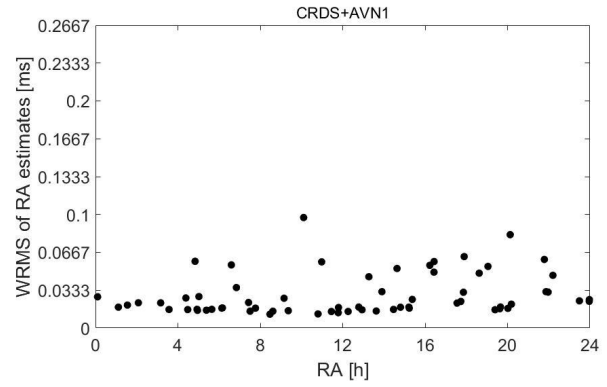
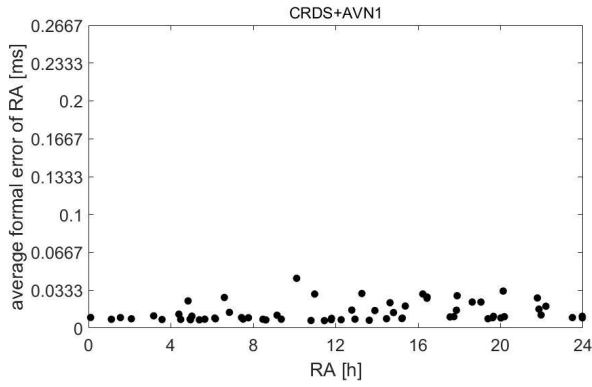


b) Declination (DE)

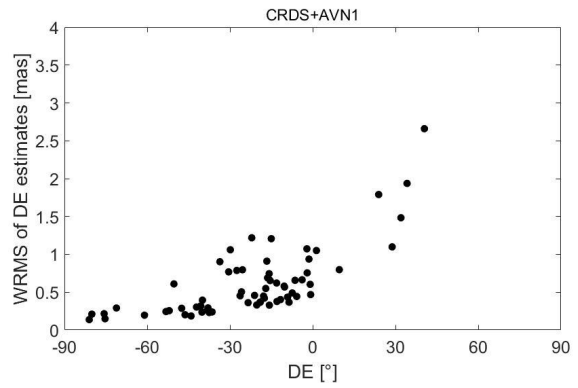
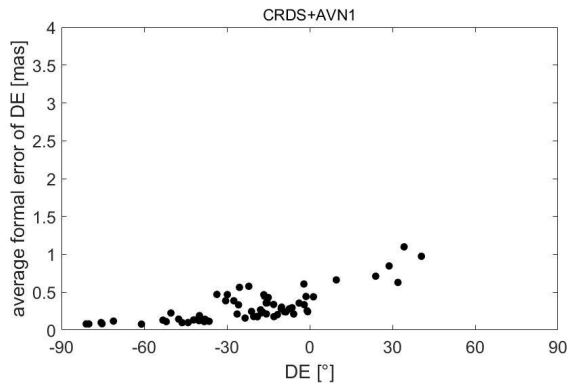


3. CRDS+AVN1

a) Right Ascension (RA)

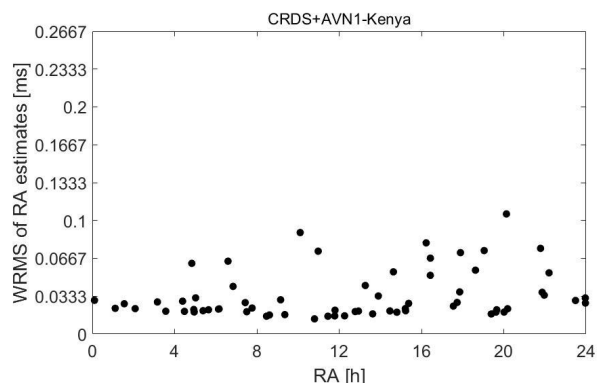
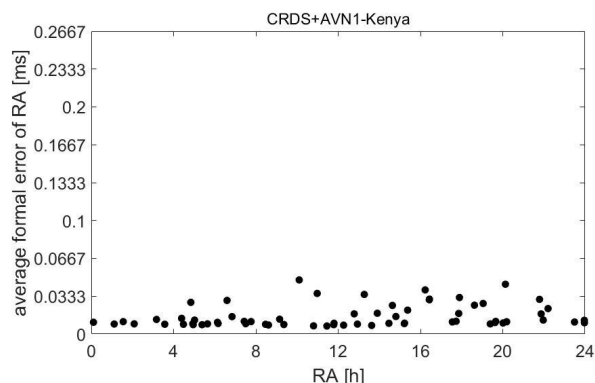


b) Declination (DE)

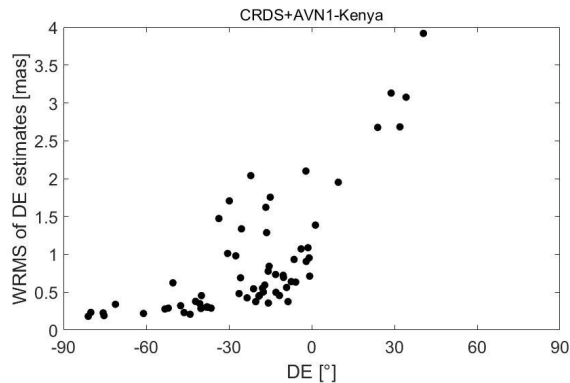
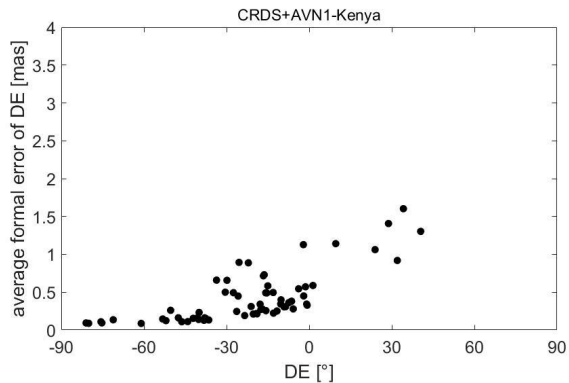


4. CRDS+AVN1-Kenya

a) Right Ascension (RA)



b) Declination (DE)



The AVN1 antennas south of the equator (southern hemisphere) were added to the IVS-CRDS session. The mean average in RA and DE, and the weighted root mean standard for the RA and DE are shown in Table 4:20. The results indicate that adding the AVN antennas to the CRDS will largely decrease the errors in the RA and DE of sources in the southern hemisphere. Adding the CRDS+AVN1, the error in RA is reduced by almost 200 and DE is reduced by about 300. Removing the Kenyan antenna, CRDS+AVN1-Kenya increases the error in both RA and DE. Removing the Kenyan antenna from the session increases the errors in both RAA and DE more than when any other station is removed. This is so because the Kenyan antenna is far up north compared to the other AVN1 antennas at -1.02° and 36.50° . Similarly, adding the Kenyan antenna, CRDS+ Kenya, greatly reduces the error in DE by a factor almost a 100 more than any other single antenna in the AVN1.

Looking at the scatter plots for RA and DE, Table 4:21 and also in appendix I, the average formal error of RA for sources observed ranges from 0.2 to 0.0333 ms. Adding the Kenya antenna, CRDS+Kenya, reduces the formal average error in RA of the sources observed to less than 0.1 ms. All the AVN1 antennas, CRDS+AVN1 reduce the error in RA to less than 0.0333 ms. Removing the Kenyan antenna, CRDS+AVN1-Kenya, raises the error in RA slightly to 0.05ms.

Majority of the sources observed by the IVS-CRDS session lie between -30° to 0° with an error of up to 3.5 mas. Adding the Kenyan antenna, CRDS+ Kenya increases the observations of sources between -60° and 0° and adds a few sources upto 45° . Adding the Kenyan antenna also reduces the formal average error of the DE to below 2.5 mas. Adding all the AVN1 antennas, CRDS+AVN1, brings the formal average error in DE to below 1.0 mas and the sources observed are concentrated between -60° and 0° . Removing the Kenyan antenna, CRDS+AVN1-Kenya, slightly raises the formal average error to 1.5 mas.

In this chapter, all the results of all the objectives of this thesis have been presented and discussed in detail. Conclusions from this work and recommendations for immediate and future consideration are given in the next chapter.

CHAPTER FIVE

CONCLUSION AND RECOMMENDATION

5.1 Conclusion

In this thesis, the evaluation of the AVN and the impact that it could have on global VLBI networks has been shown. RFI and the atmospheric opacity has been assessed and the u-v coverage, EOPs and source positions estimated using simulations.

The assessment of the RFI using population and geographical locations has been presented. RFI affects observations in the lower frequencies such as at x-band while on the other hand, atmospheric opacity affects VLBI observations at high frequencies. Based on these results, all AVN sites are ideal for observations at 43 GHz. The conclusion about each site based on RFI and weather assessment is summarized below:

1. HartRAO (South Africa): This first component of the AVN was used as the reference station since it's the only functional radio astronomy observatory in the African continent. The site is far away from major towns and is well shielded from RFI by mountains. The site is very dry throughout the year and thus is conducive for VLBI observations at very high frequencies with little atmospheric interference.
2. Kuntunse (Ghana): This is the second component in the AVN as conversion has already been completed. However, the site has very high RFI from the large number of people living nearby, is on a very flat land and not naturally shielded by mountains from RFI. It's also very near the ocean meaning that the opacity values are very high. Station is not conducive for very high frequency VLBI observations.
3. Longonot (Kenya): The site has little RFI since it has a small human population density around it and is naturally shielded by a mountain and hill. The atmospheric opacity values are low implying that the site is suitable for high frequency VLBI observations.
4. Gemsberg (Namibia): This proposed AVN site has the least RFI and is well located very far away from any settlements. It's the ideal site for radio astronomical observations at low frequencies. It's the driest site in the AVN and thus ideal for high frequency VLBI observations.
5. Antananarivo (Madagascar): The site also has little RFI and has a physical RFI barrier on one side. The site is fine for high frequency VLBI observations.
6. Mwembeshi (Zambia): The site has a considerable amount of RFI from human activities and is not shielded by any physical barriers. The site is also suitable for high frequency observations since it generally has small opacity values throughout the year.

7. Cassis (Mauritius): So far this is the worst AVN site in terms of RFI due to the fact that the site is located right in the middle of Port Luis city and thus has very high population of people surrounding it. It's also on a flat land and lacks any form of natural physical barriers. The current site is not ideal for high frequency observations because the site is close to the ocean and thus very high atmospheric opacity.
8. AVN2: Apart from the Nigerian site, all the other sites would have the worst RFI due to the high population and lack of any form of natural physical barrier against the RFI. The AVN2 are surprisingly ideal for high frequency observations reason being that they are located in relatively dry sites.

The Kenyan antenna alone does not add much to the u-v coverage of the LBA in the x-band. Mauritius and Madagascar greatly improves the LBA u-v coverage especially at -70 and -90. Namibia and Zambia also improve the u-v coverage for long baseline lengths at -90. Generally, all the AVN1 antennas combined greatly improve the u-v coverage for the LBA at all declinations. The AVN2 antennas do not add anything to the LBA, this is because they are too far north to observe much in the Southern hemisphere. All the AVN antennas improve the u-v coverage of the LBA antennas, mainly the AVN1 antennas.

Adding the AVN1 and all the AVN antennas to a typical EOP session such as the R1675, reduces all the errors in the observed EOPs almost by half and more than doubles the number of observations made, adds to the number of sources observed and increases the number of scans and this means better results. The AVN on its own is also able to provide very long baselines just like all the other global VLBI networks. Also, adding the AVN antennas to the R1675 session increases the baseline length repeatabilities implying that more and more antennas are used in each scan for any particular observation. The AVN1 antennas also increase the precision in source position estimates of sources in the southern hemisphere. Adding the AVN1 antennas to a typical astrometry VLBI session like the CRDS, more than halves the errors in the RA and Declination of sources in the southern hemisphere.

Finally, it's clear from our results and discussions that not only is the Kenyan site favourable for radio astronomical VLBI due to the site's little RFI and physical location, but it will also improve the u-v coverage of the EVN in the northern hemisphere. It will also contribute to precise measurements of the EOPs as it helps reduce the errors in the EOPs and especially in the polar and nutation motions of the earth. It also increases the number of sources that can be observed in the typical EOP session and increases the baseline length repeatabilities to the geodetic session especially on the longer baselines. The Kenyan station also clearly stands out in source position estimate for the southern hemisphere as compared to all other AVN1 stations. It significantly improves the declination and Right Ascension

precisions of sources observed in the southern hemisphere. Therefore, an antenna in Kenya will have a great impact in astronomical, geodetic and astrometric VLBI experiments.

5.2 Recommendations

1. Effort should be put in place to convert the Kenyan antenna next as it contributes the most in terms of u-v coverage in the southern hemisphere and significantly reduces the errors in the source position estimates for the southern hemisphere as it provides long baselines for the LBA.
2. The AVN antennas already exist and thus RFI cannot be avoided. RFI mitigation measures must be taken into consideration so as to achieve the AVN science goals and the improved sensitivity for the other global VLBI networks. This can be done by regulation so as to minimize the already existing RFI and also by constructing receivers during conversions which will be able to filter out the RFI as required during radio astronomy observations.
3. Mauritius site will contribute significantly to the AVN and global VLBI networks, thus a new site location has to be considered instead of conversion of the dish at Cassis due to RFI and bad weather.
4. The AVN2 sites are favorable for radio astronomical and geodetic VLBI experiments though new builds instead of conversion might have to be located to new sites due to the RFI at lower frequency observations.

REFERENCES

- Ambrosini, R., Bolli, P., Bortolotti, C., Gaudiomonte, F., Messina, F., and Roma, M. (2010). Radio frequency self-interference from a data processing centre at a radio telescope site. *Experimental Astronomy*, 27(3), 121-130.
- Booth, R. S., de Blok, W. J. G., Jonas, J. L. and Fanaroff, B. (2009). An Open Invitation to the Astronomical Community to propose Key Project Science with the South African Square Kilometre Array Precursor: MeerKAT. Astro-ph.IM
- Cambridge University Press 978-0-521-87808-1 - An Introduction to Radio Astronomy, Third Edition
Bernard F. Burke and F. Graham-Smith
- Charlot, P., Campbell, R., Alef, W., Borkowski, K., Conway, J., Foley, A., Garrington, S., Kraus, A., Nothnagel, A., Sovers, O., TRigilio, C., Venturi, T. and Xinyong, H. 2000. ITRF2000 Positions of Non-Geodetic Telescopes in the European VLBI Network. Proceedings of the 15th Working Meeting on European VLBI for Geodesy and Astrometry, Barcelona, Spain 2001.
- Dale, D., Combrinck, L. and de Witt A. (2014). A Strategic Independent Geodetic VLBI Network for Europe. IVS General Meeting Proceedings.
- De Witt, A., Mayer, D., Macleod, G., Combrinck, L., Petrov, L. and Nickola, M. (2016). Optimising the African VLBI Network for Astronomy and Geodesy. IVS General Meeting Proceedings, Johannesburg, South Africa, March 2016.
- De Witt, A., Combrinck, L. and Dale, D. (2016). A Strategic Independent VLBI Network for Europe to Accurately Determine Earth Orientation Parameters Needed for Precision Positioning and Navigation on Earth and in Space. *South African Journal of Geology*, 2016. Vol. 119.1, Pg 109-116.
- Edwards, P. G. and Phillips, C. (2015). The Long Baseline Array. *The Korean Astronomical Society*, 2015. Vol. 30, Pg 659-661.
- Emmerson, D. (2002). Single-Dish Radio Astronomy: Techniques and Applications. ASP Conference Proceedings, Astronomical Society of the Pacific, Vol. 278, p. 27-43.
- Ellingson, W. S. (2004). RFI Mitigation and the SKA. *Experimental Astronomy*, 2004. Vol. 17, 261-267.
- Gaylard, M.J., Bietenholz, M. F., Combrinck, L., Booth, R. S., Buchner, S. J., Macleod, G. C., Nicolson, G. D., Venkatasubramani, T. L., and Stronkhorst, P. (2014). An African VLBI network of Radio Telescopes. Astro-ph. IM.
- Gilloire, A., and Sizun, H. (2009). RFI Mitigation of GNSS Signals for Radio Astronomy: Problems and Current techniques. *Annals of Telecommunications*, 64(9), 625-638.
- Girolletti, M., Paragi, Z., Bignall, H., Doi, A., Foschini, L., Gabanyi, E., Reynolds, J., Blanchard, R., Campbell, M., Colomer, F., Hong, X., Kadler, M., Kino, M., van Langevelde, H. J., Nagai, H., Phillips, C., Sekido, M., Szomoru, A. and Tzioumis, A. K. (2011). Global e-VLBI Observations of the Gamma-ray Narrow Line Seyfert 1 PMN J0948+0022. *A&A*, 2011. Vol. 528, L11.

- Gulyaev, S., Natusch, T. and Wilson, D. (2010). Characterization and Calibration of the 12-m Antenna in Warkworth, New Zealand. IVS 2010 General Meeting Proceedings, pg. 113-117.
- Hase, H., Behrend, D., Ma, c., Petrancheko, W., Schuh, H. and Whitney, A. (2010). The Future Global VLBI2010 Network of the IVS. <http://www.evga.org/files/2011Bonn/hase.pdf>
- Jin, C. J., Nan, R. D. and Gan, H. Q (2008). The FAST Telescope and its Possible Contribution to High Precision Astrometry. International Astronomical Union doi:10.1017/S1743921308018978
- Kruithof N.,(2014). e-VLBI Using a Software Correlator. Grid Enabled Remote Instrumentation, Springer Science+Business Media, LLC pp 537-544 ISBN 978-0-387-09663-6. Joint Institute for VLBI in Europe (JIVE).
- Kraus, J.D. (1966). Radio Astronomy (1996). McGraw-Hill.
- Kucuk, I., Uler, I., Oz, S., Onay, S., and Sarikaya, M. (2012). Site selection for radio astronomy observatory in Turkey: atmospherical, meteorological and radio frequency analyses. Springer Science+Business Media B.V 2011.33:1-26).
- Lee, S., Byun, D., Oh, C.S., Han, S., Je, D., and Kim, K. (2011). Single-Dish Performance of KVN 21 m Radio Telescopes: Simultaneously Observations at 22 and 43 GHz. Publications of the Astronomical Society of the Pacific, Vol. 123, No. 910.
- Lena, P., (2012). Space-Time Reference Frames. Observational Astrophysics, Astronomy and Astrophysics Library, pp. 127-129. Springer Verlag Berlin Heidelberg 2012.
- Lindqvist M., (2016). Science with the EVN. 5th International VLBI Technology Workshop, MIT Haystack Observatory, October 12-14 2016.
- Lovell, J.E.J., McCallum, J.N., Reid, P.B. et al. J Geod (2013). The AuScope geodetic VLBI array Vol 87: pp 527. doi:10.1007/s00190-013-0626-3.
- Ma, C., MacMillan, D., Le Bail,K., and Gordon, D. (2016). Aspects of ICRF-3, IVS 2016 General Meeting Proceedings.
- Mayer, D., Bohm, J., Combrinck, L., Botai, J. and Bohm, S. (2014). Importance of the Hartebeesthoek Radio Astronomy Observatory for the VLBI Network. Acta Geod Geophys. DOI 10.1007/s40328-014-0063-7.
- Middelberg, E. and Bach, U. (2008). High Resolution Radio Astronomy using Very Long Baseline Interferometry. Reports on Progress in Physics, Vol. 71, p.32.
- Molod, A., Takacs, L., Suarez, M., Bacmeister, J., Song, I. and Eichmann, A. (2012). The GEOS-5 Atmospheric General Circulation Model: Mean Climate and Development from MERRA to Fortuna. NASA/TM–2012-104606/Vol 28

- Munghemezulu, C., Combrink, L., Mayer, D., and Botai, O.J. (2014) Comparison of Site Velocities Derived from Collocated GPS, VLBI and SLR Techniques at the Hartebeesthoek Radio Astronomy Observatory. *J. Geod. Sci.* 2014; 4:1-7.
- Ojha, R., Fey, A. L., Charlot, P., Jauncey, D. L., Johnsto, K. J., Reynolds, J. E., Tzioumis, A. K., Quick, J. F., Nicolson, G. D., Ellingsen, S. P. and McCulloch, P. M. (2005). VLBI Observations of Southern Hemisphere ICRF Source II. Astrometric Suitability Based on Intrinsic Structure. *The Astronomical Journal*, 130:2529-2540, 2005 December.
- Paragi, Z., Godfrey, L., Reynolds, C., Rioja, M., Deller, A., Zhang, B., Gurvits, L., Bietenholz, B., and Gaylard, M., (2014). Very Long Baseline Interferometry with the SKA. *Proceedings of Science. Advancing Astrophysics with the Square Kilometre Array*, June 8-13, 2014 Giardini, Naxos, Italy.
- Pearson, T. J. and Readhead, A.C.S (1984). *Annu Rev Astron Astrophys*, 22, 97
- Perryman, M. (2012). The History of Astrometry. *The European Physical Journal*, Vol. 37.5, pp 745-792.
- Petrov, L., Phillips, C., Beertarinic, A., Deller, A., Pogrebenko, S., and Mujunen, A. (2009). Use of the Long Baseline Array in Australia for Precise Geodesy and Absolute Astrometry. *Publications of the Astronomical Society of Australia*, 26, 75-84.
- Petrov, L., Phillips, C., Tzioumis, T., Stansby, B., Reynolds, C., Bignall, H. E., Guyaev, S., Natusch, T., Palmer, N. and Collet, D. (2011). First Geodetic Observations Using New VLBI Stations ASKAP-29 and WARK12M. *Publications of the Astronomical Society of Australia*, 2011, Vol. 28, pp107–116.
- Porko, J.G. (2011). *Radio Frequency Interference in Radio Astronomy*.
- Preuss, E. (2002). The Beginnings of VLBI at the 100-m Radio Telescope. *Proceedings of the 6th European VLBI Symposium*, June 25th -28th 2002, Bonn, Germany.
- Schliiter, W. and Behrend, D. (2006). The International VLBI Service for Geodesy and Astrometry (IVS): Current Capabilities and future prospects. *JGeod* (2007) SI: 379-388.
- Schuh, H. and Behrend, D. (2012). VLBI: A Fascinating Technique for Geodesy and Astrometry. *Journal of Geodynamics* 61, pg 68-80.
- Stierwalt, S., Peck, A., Braatz, J. and Bemis, A. (2017). *Introduction to Radio Interferometry*. science.nrao.edu.
- Umar R., Abidin, Z.Z., Ibrahim Z.A., Rosli, Z. and Noorazlan, N. (2014). Selection of Radio Astronomical Observation Sites and its Dependence on Human Generated RFI. *Research in Astronomy and Astrophysics*, Vol. 14, No. 2.
- Verschuur, G.L. (2007). *The Invisible Universe*. Springer.
- Wakker, B.P. (2004). Recent Developments Concerning High-Velocity Clouds. *Astrophysics and Space Science*, Vol. 289(3), pg. 381-390.

Wright, A. (2004). Single-dish Radio Astronomy. Originally Submitted for the Astronomy online course at Swinburne University of Technology, 2004.

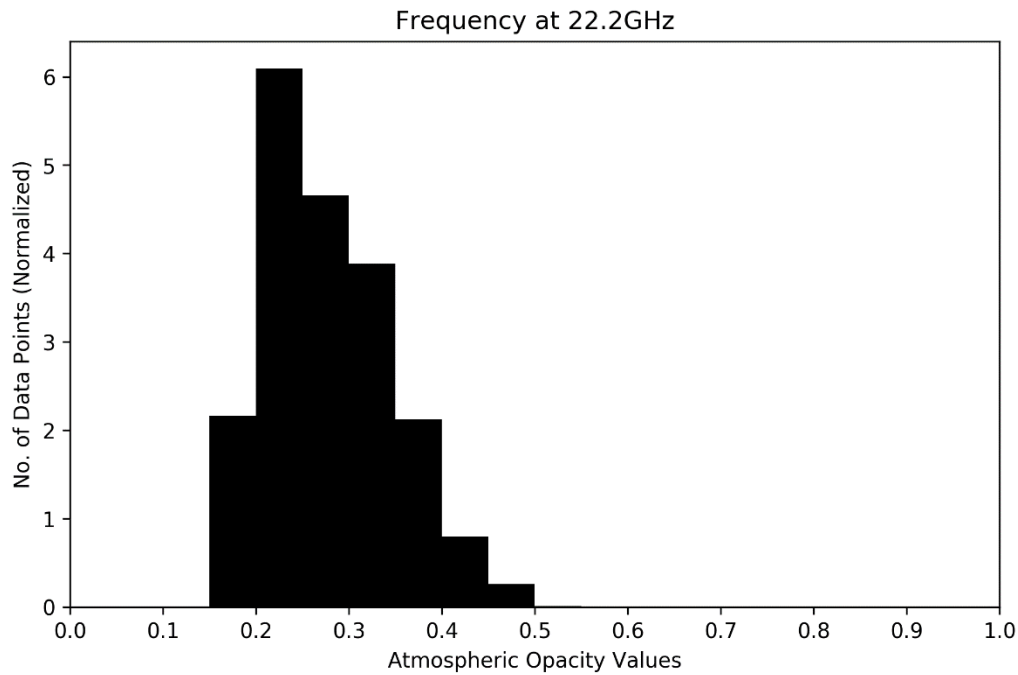
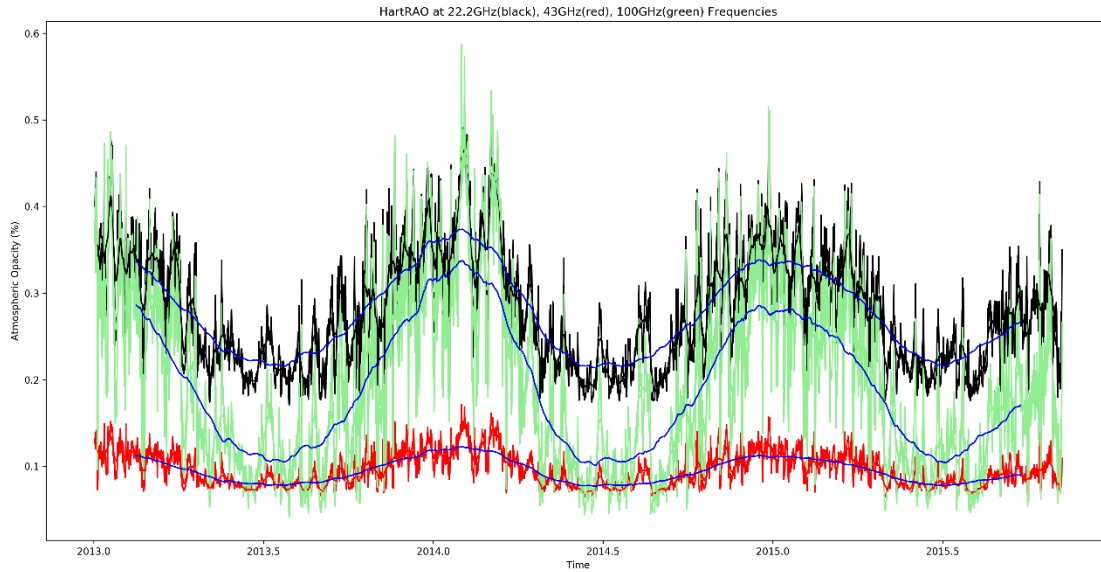
Sedac.ciesin.columbia.edu/mapping/popest/gpw-v4/

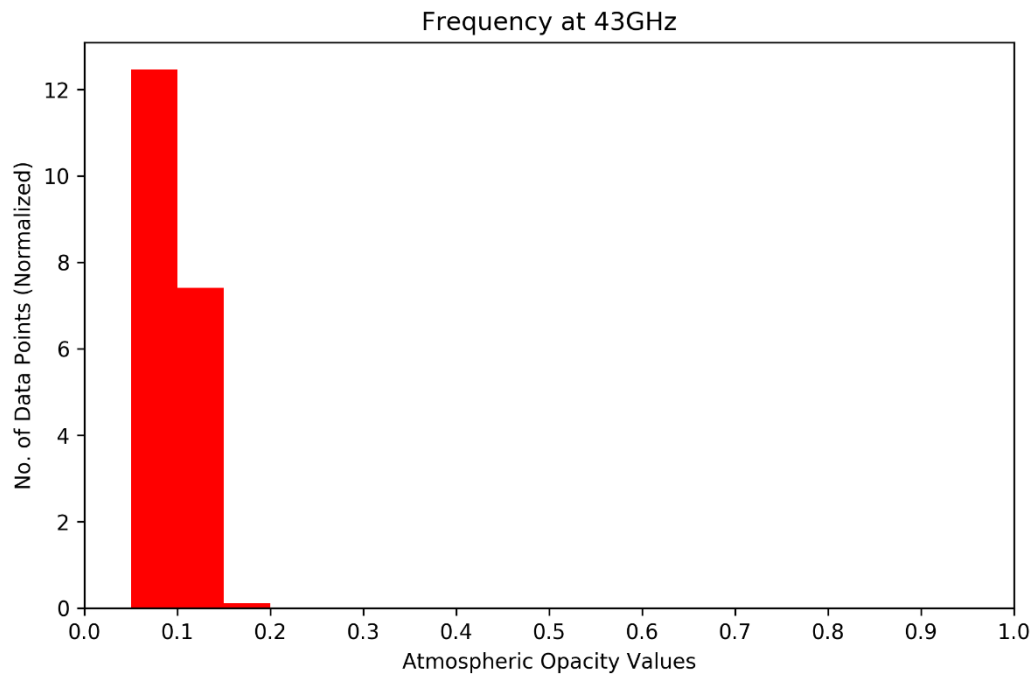
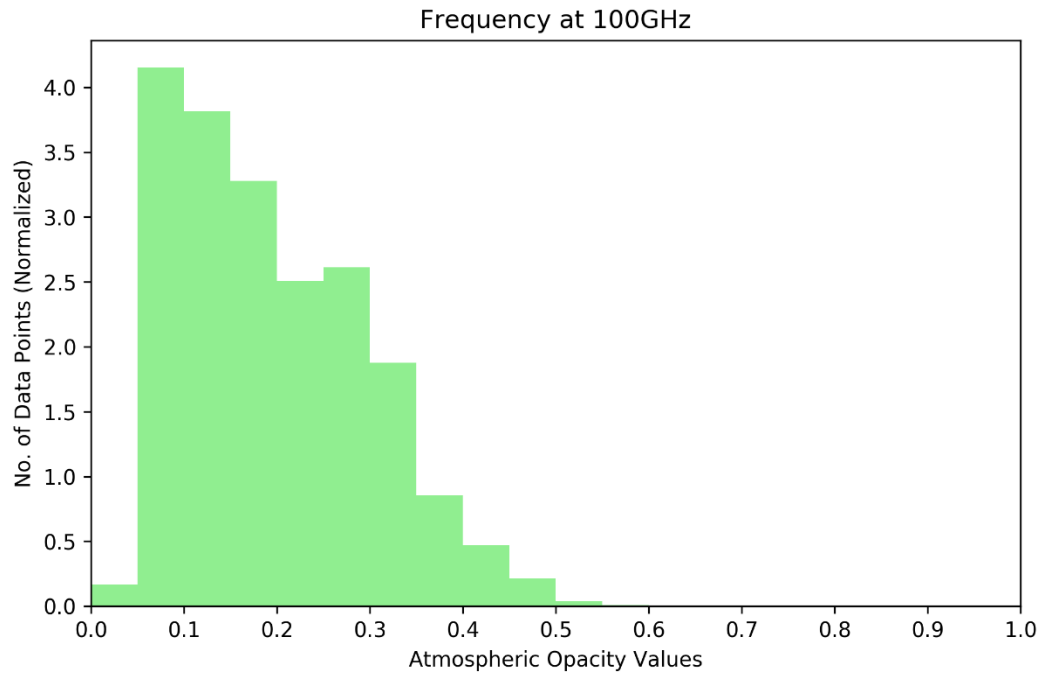
APPENDIX

This appendix presents all of the results and plots generated in this research.

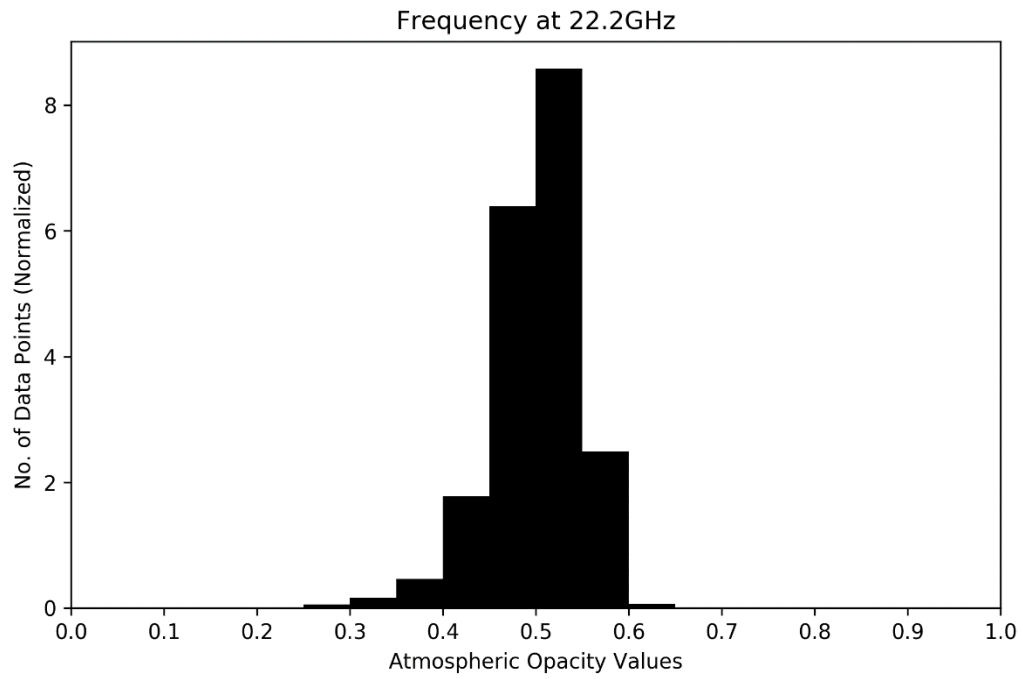
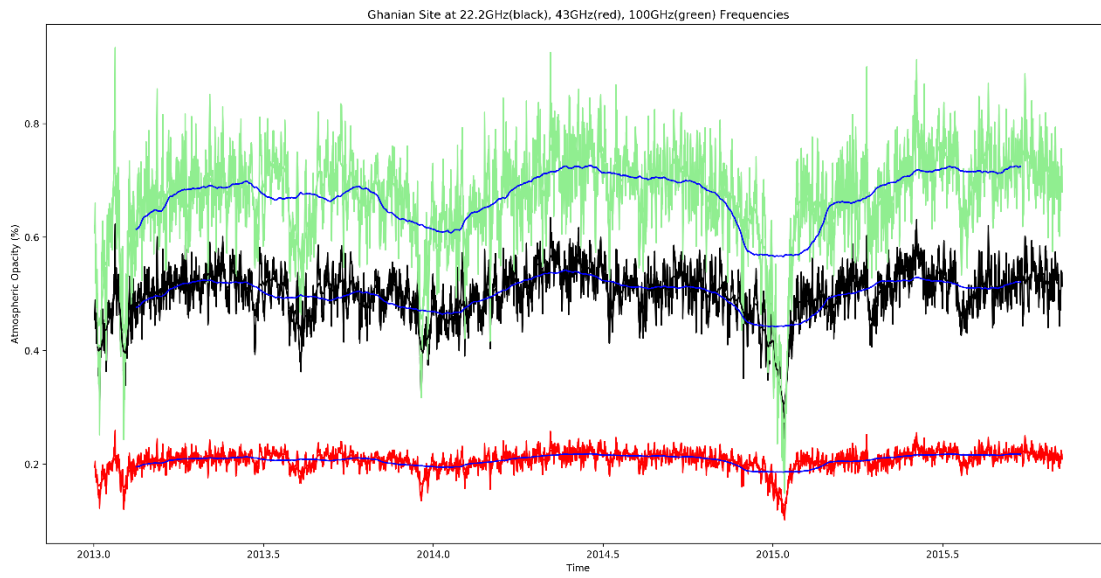
Table 4.6: (b) Plots of atmospheric opacity for continuous mean at 22.2, 43 and 100 GHz for each AVN site accompanied by their histograms.

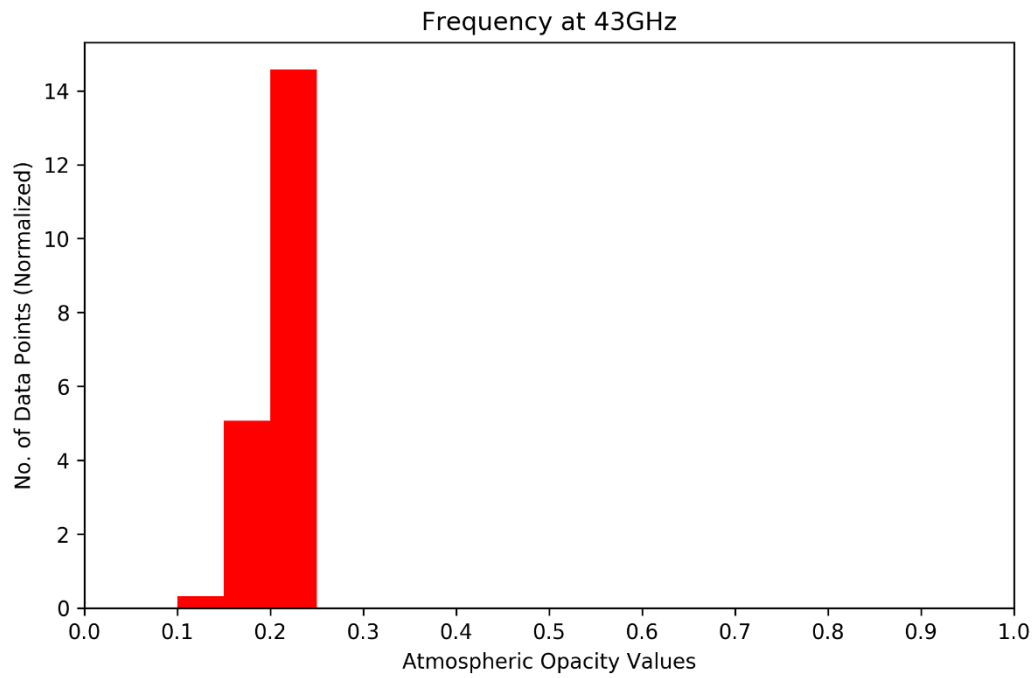
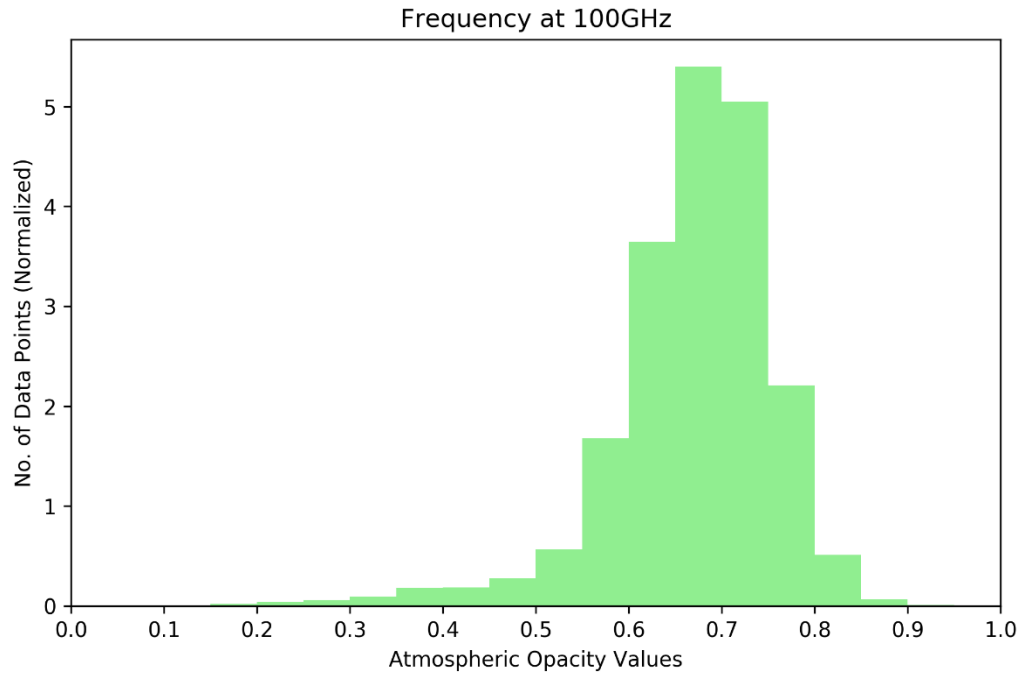
1. HartRAO



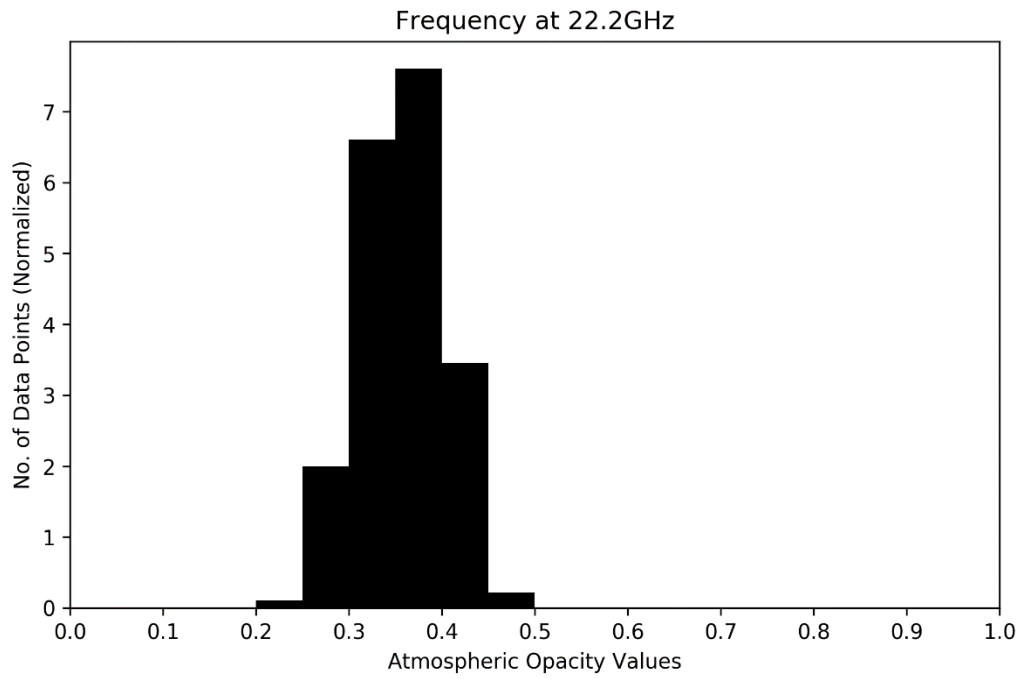
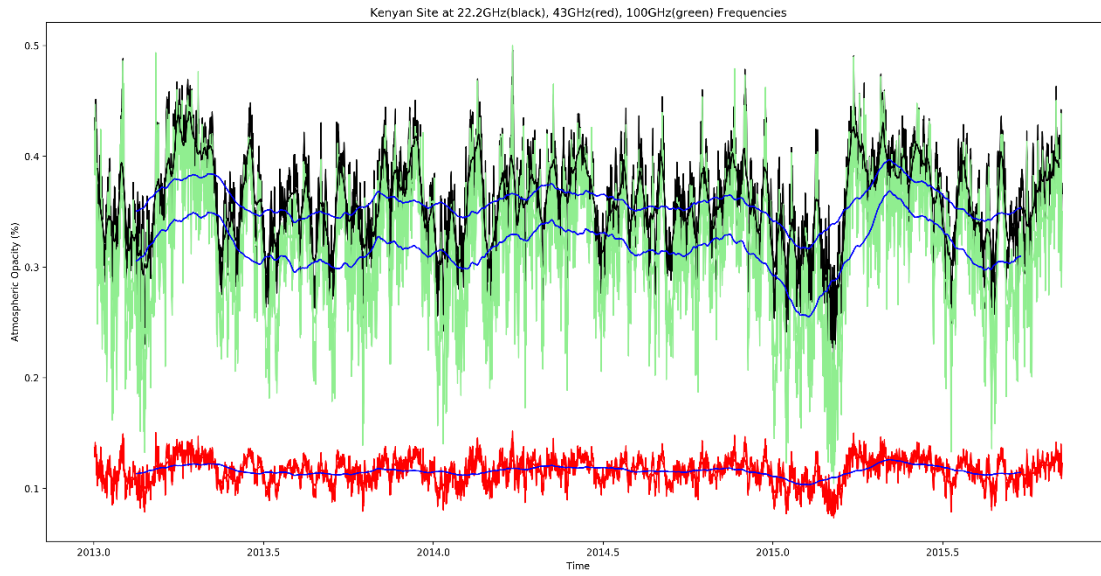


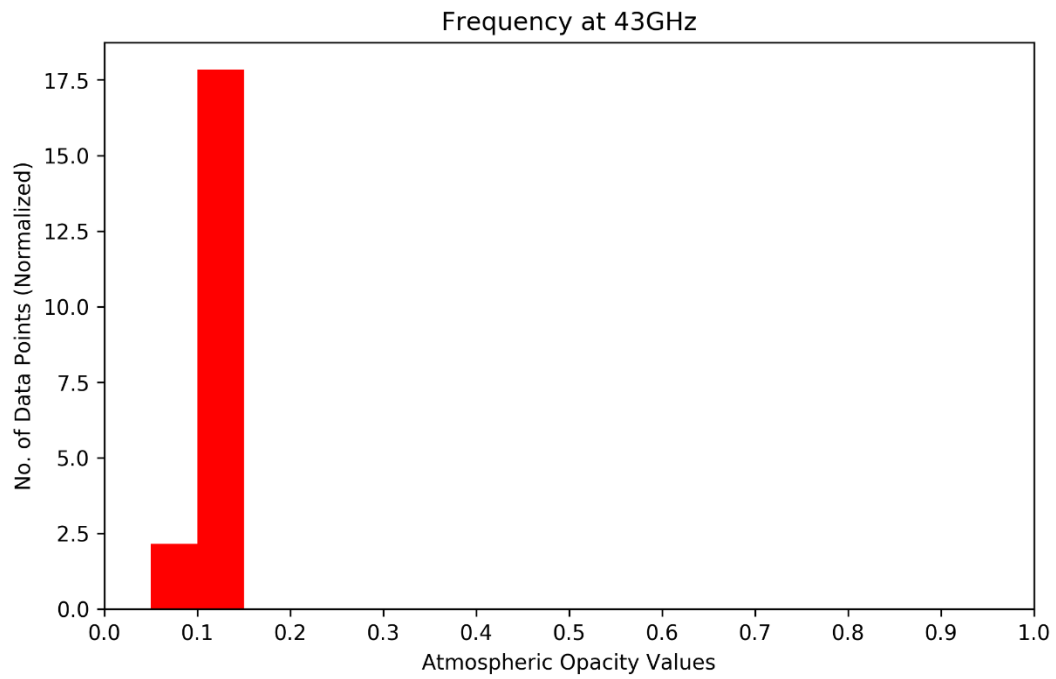
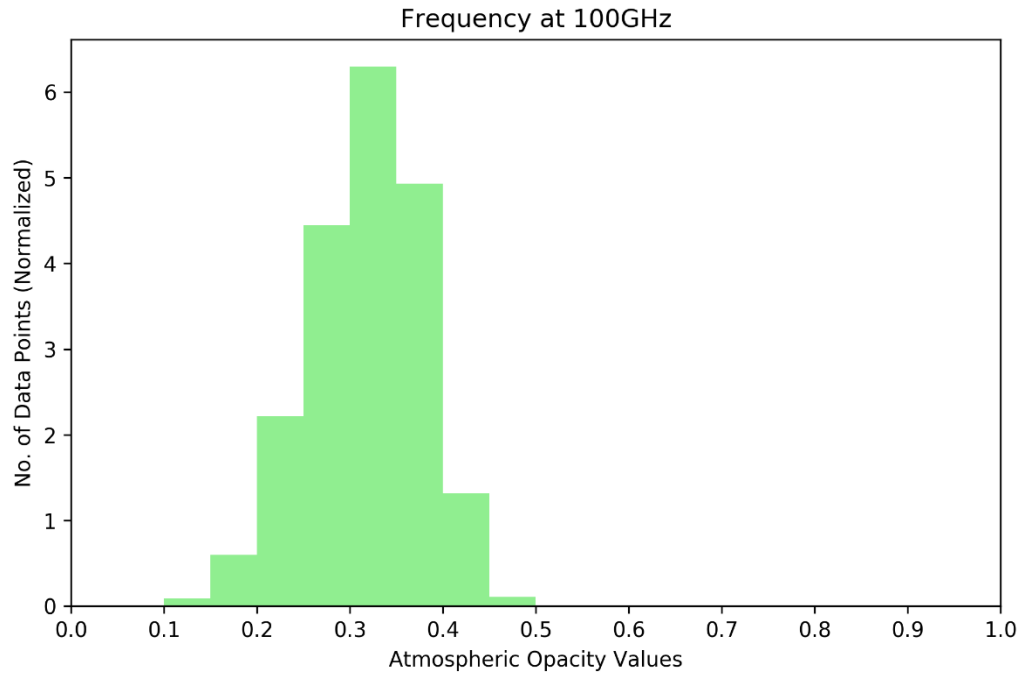
2. Ghana



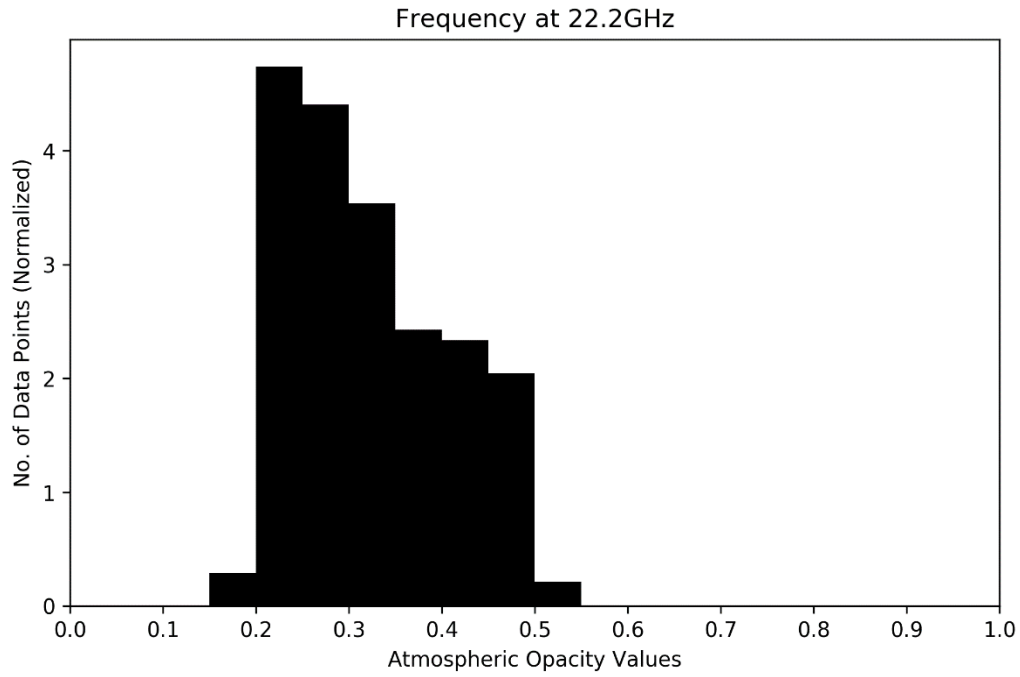
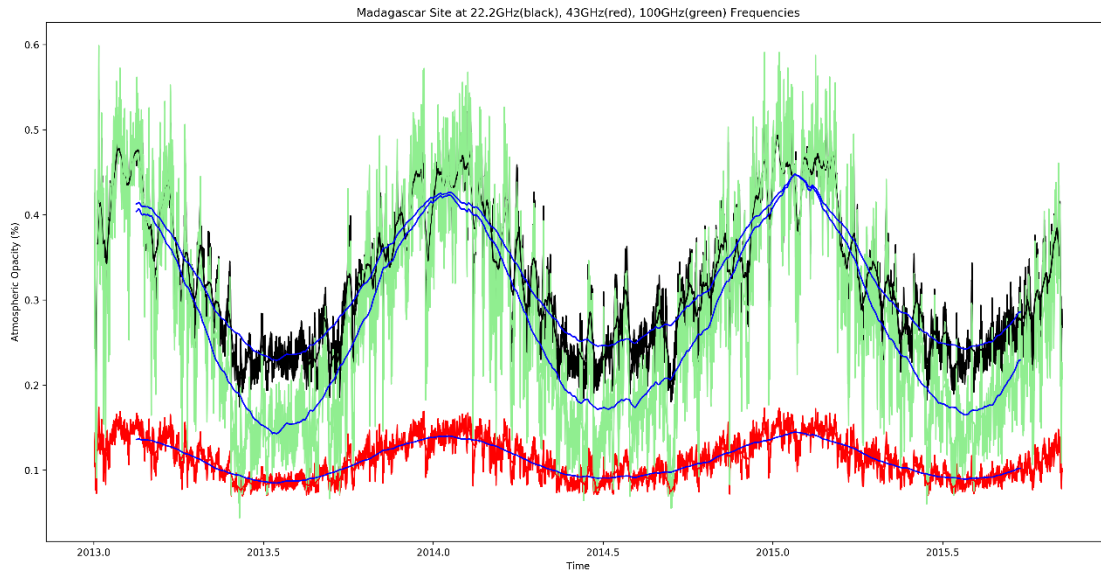


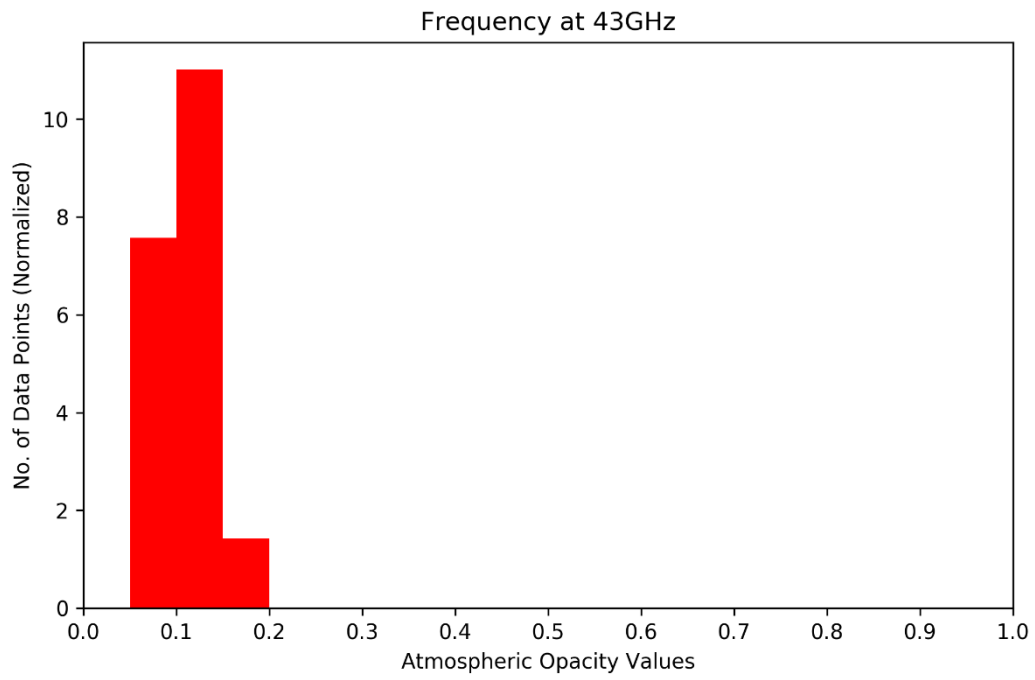
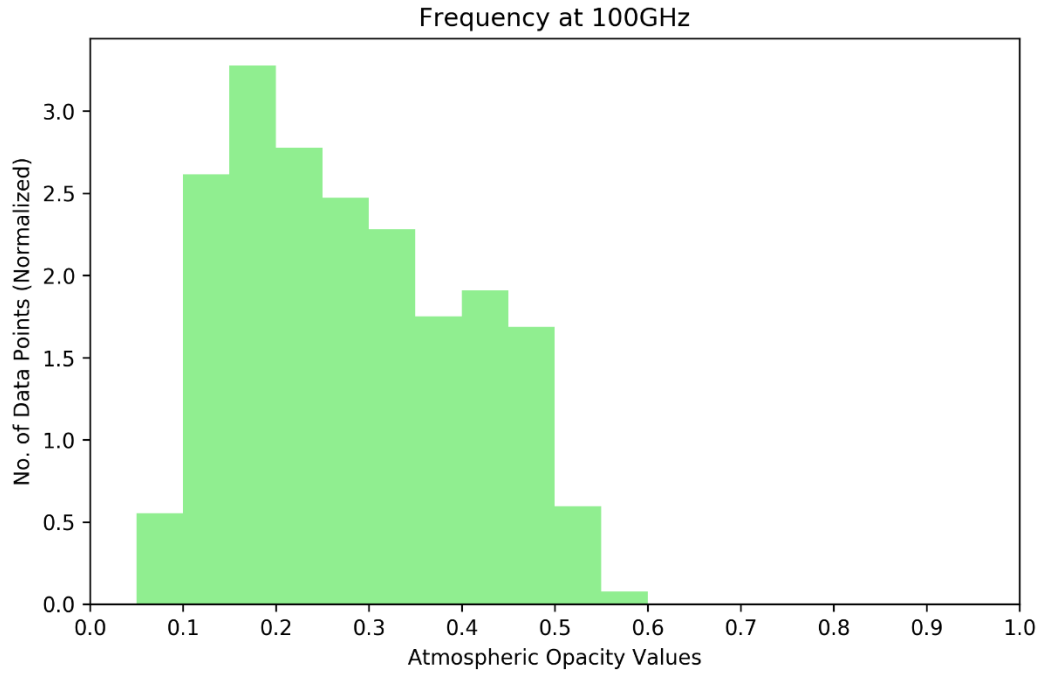
3. Kenya



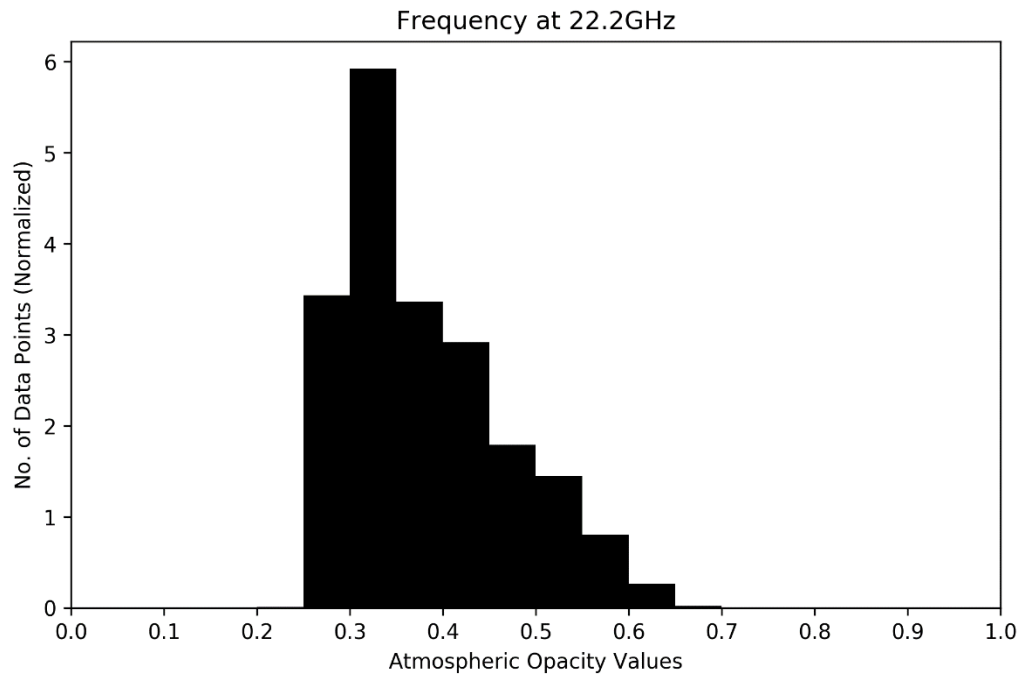
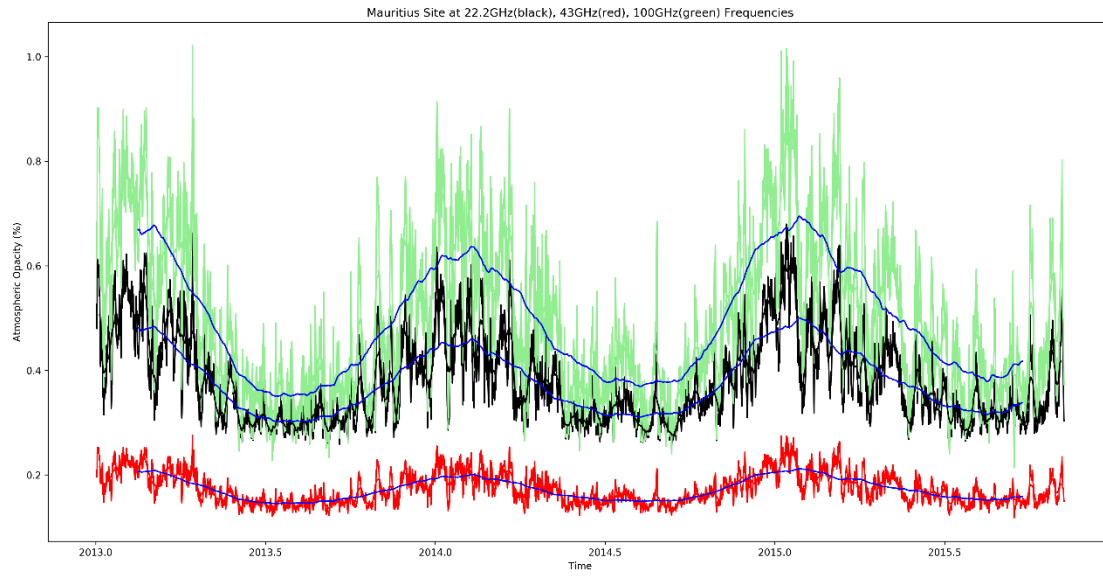


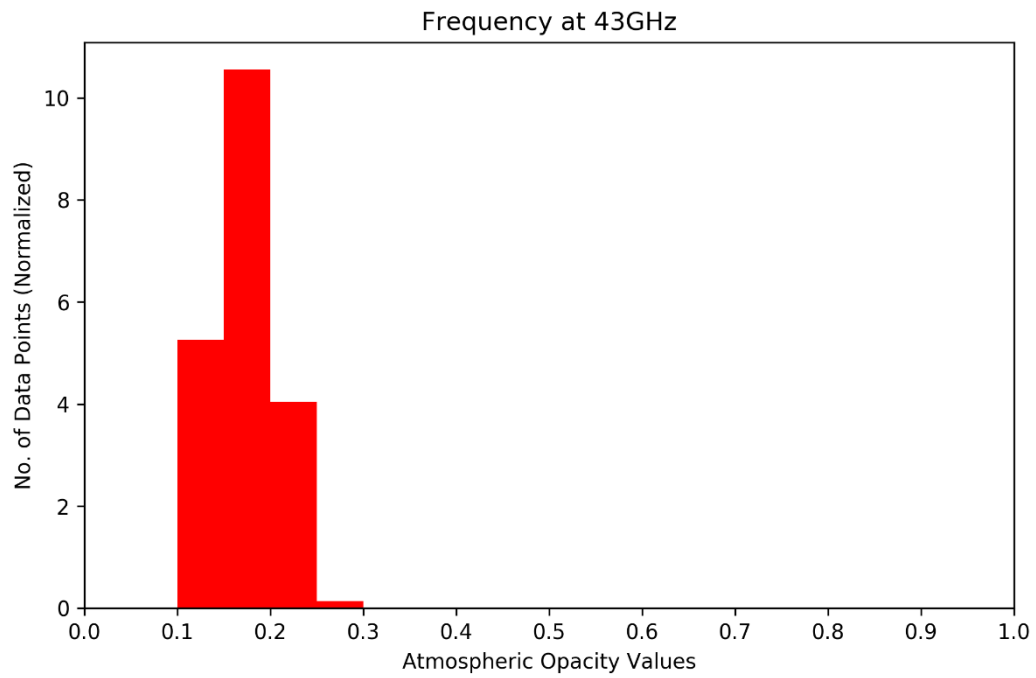
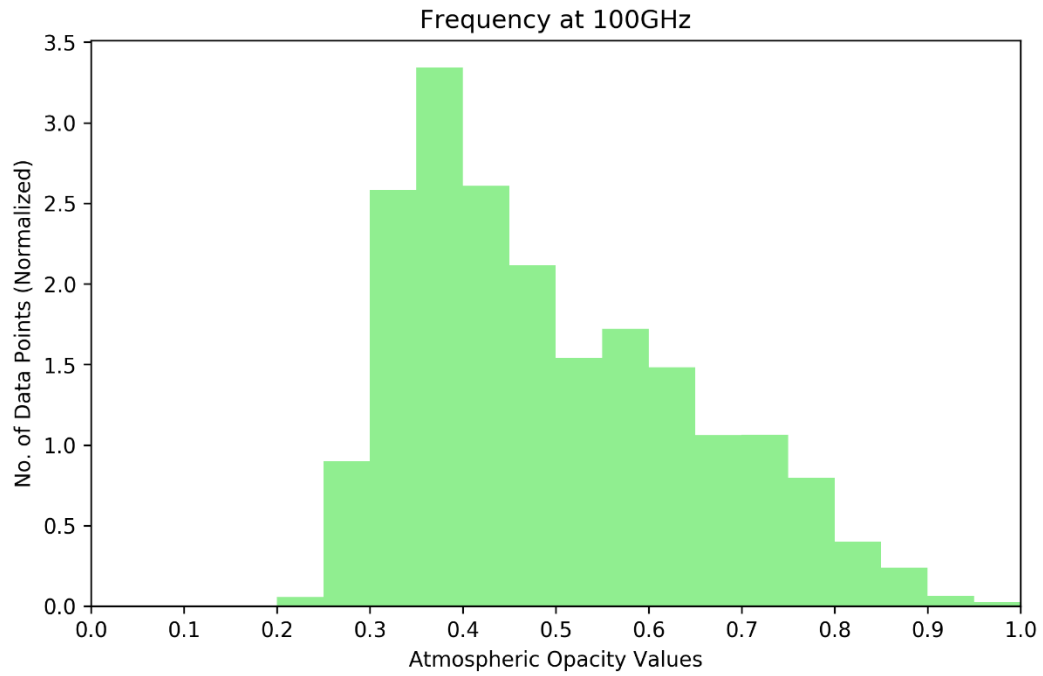
4. Madagascar



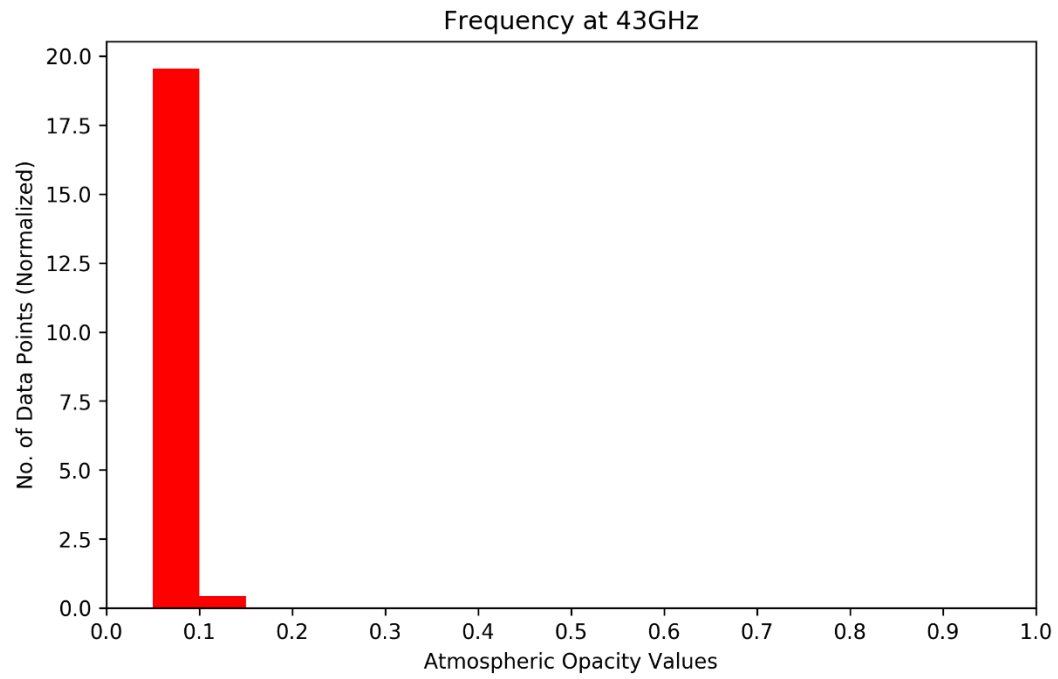
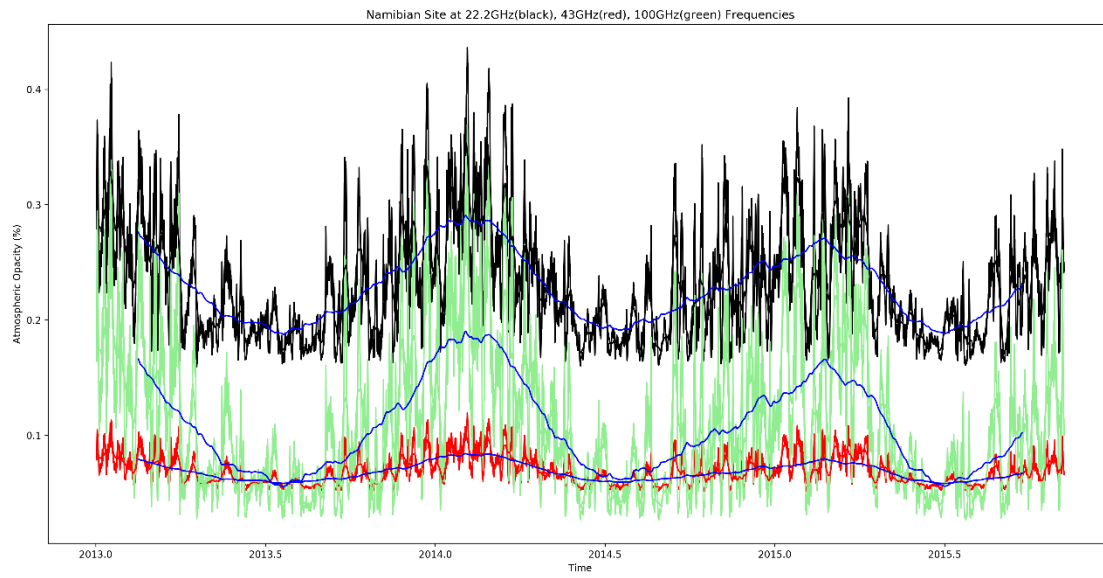


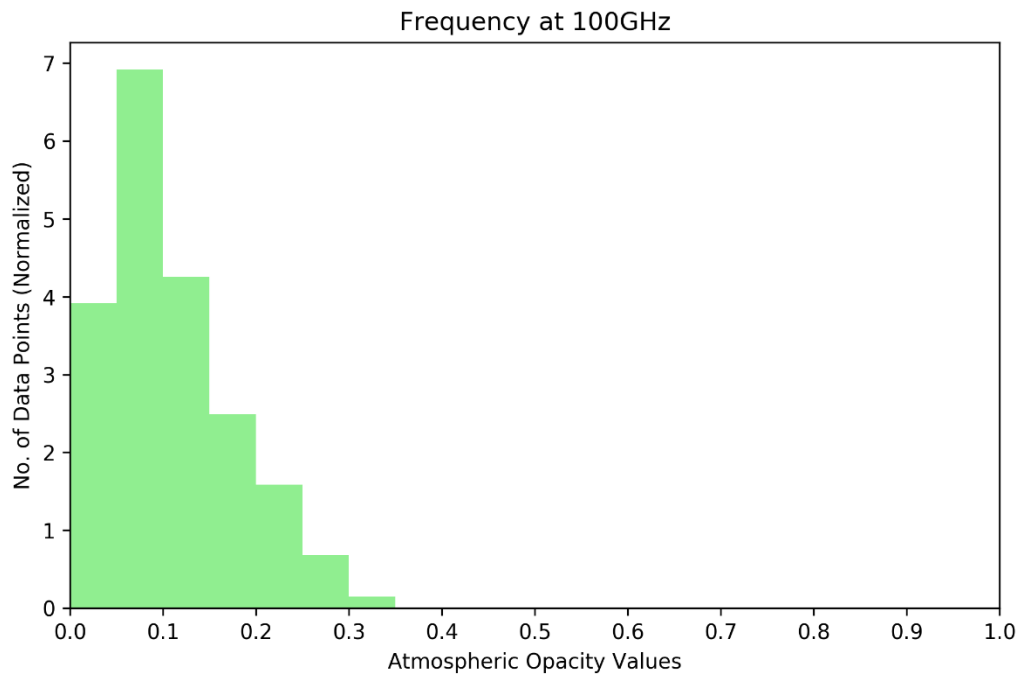
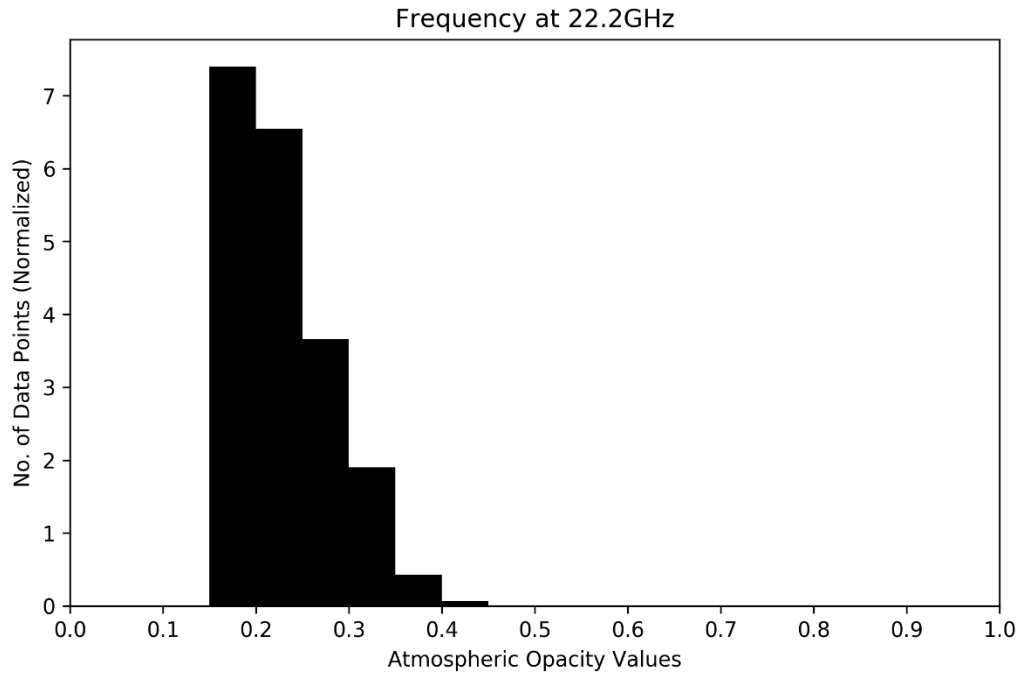
5. Mauritius



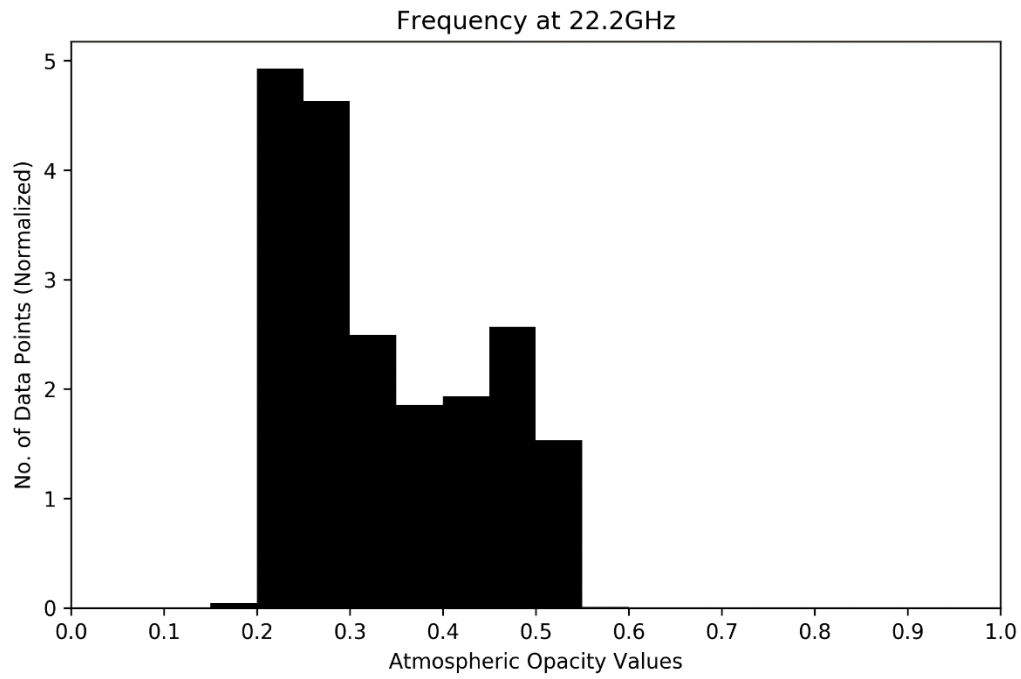
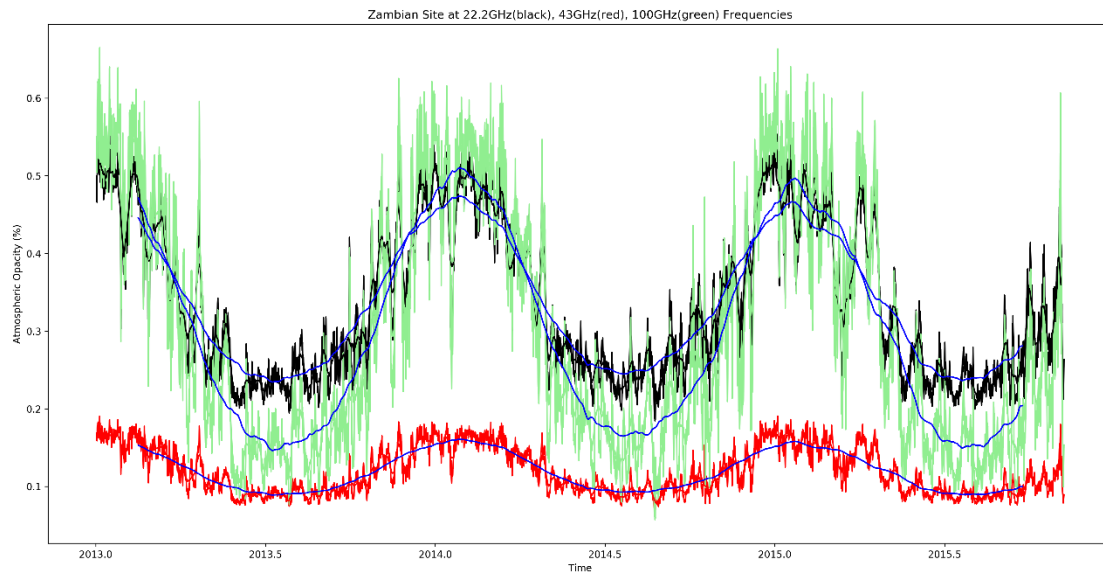


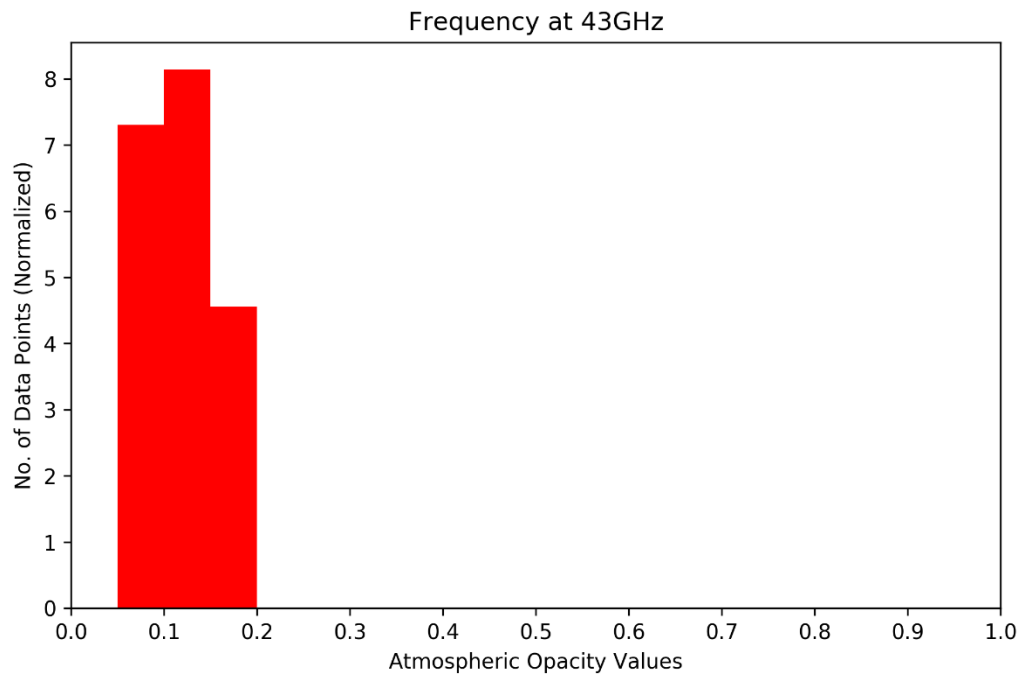
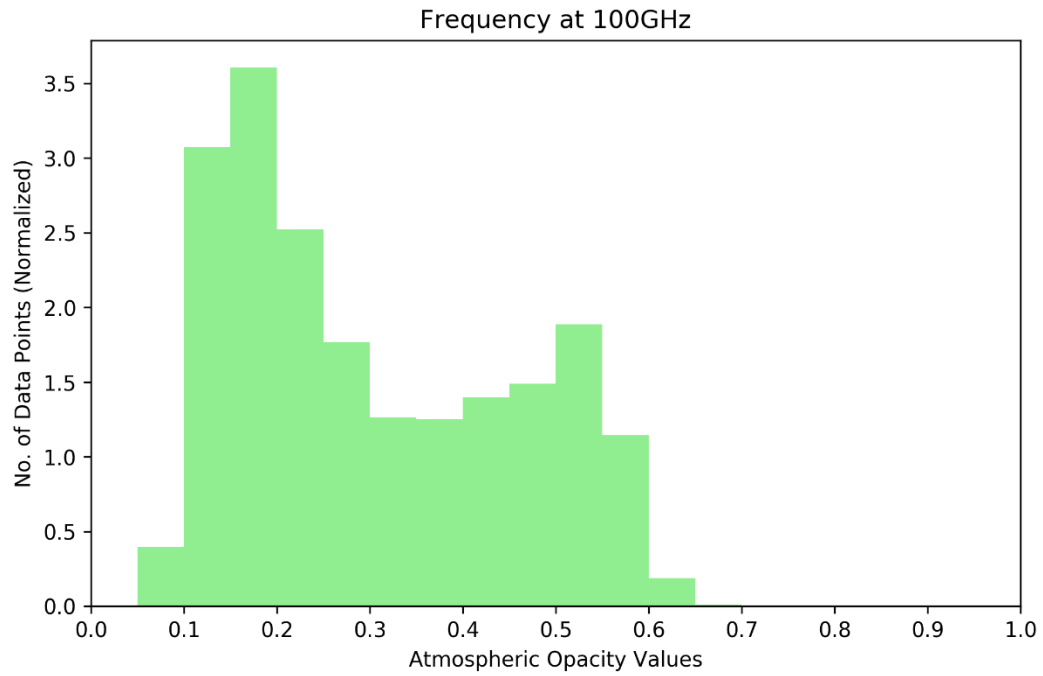
6. Namibia



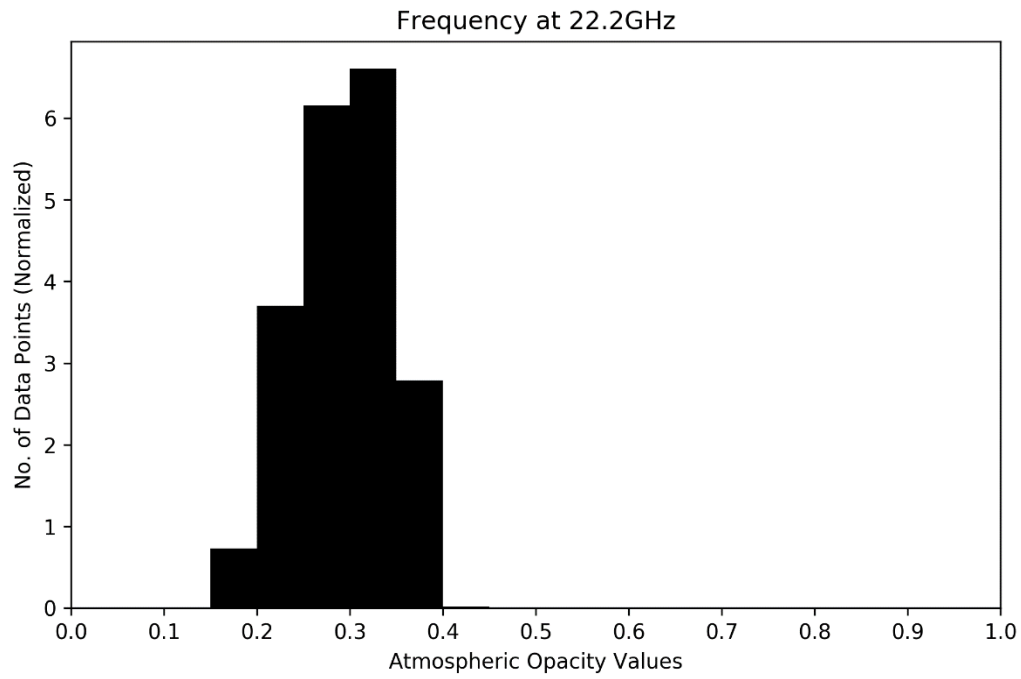
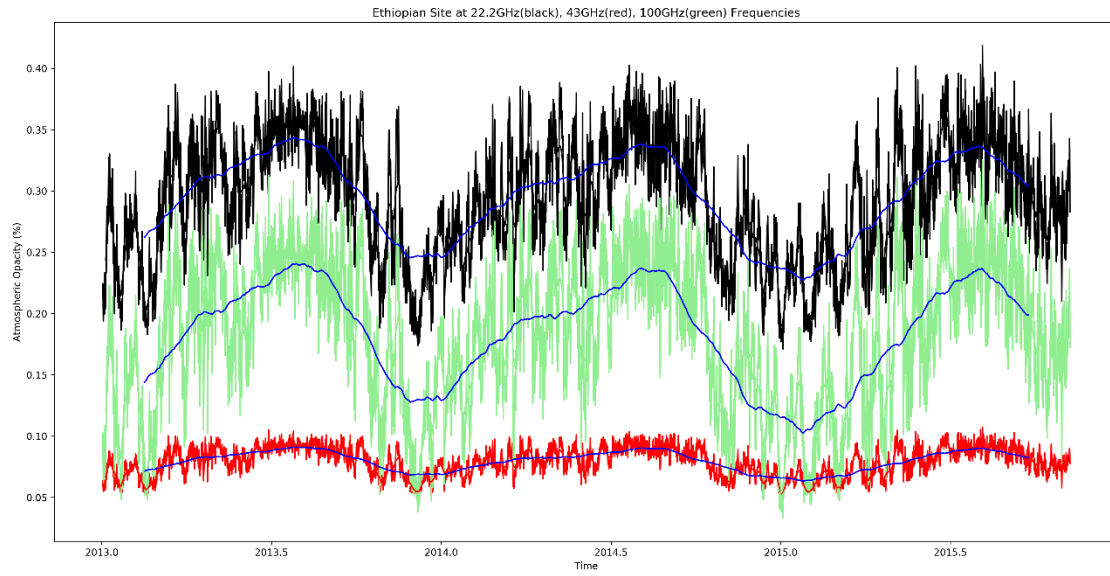


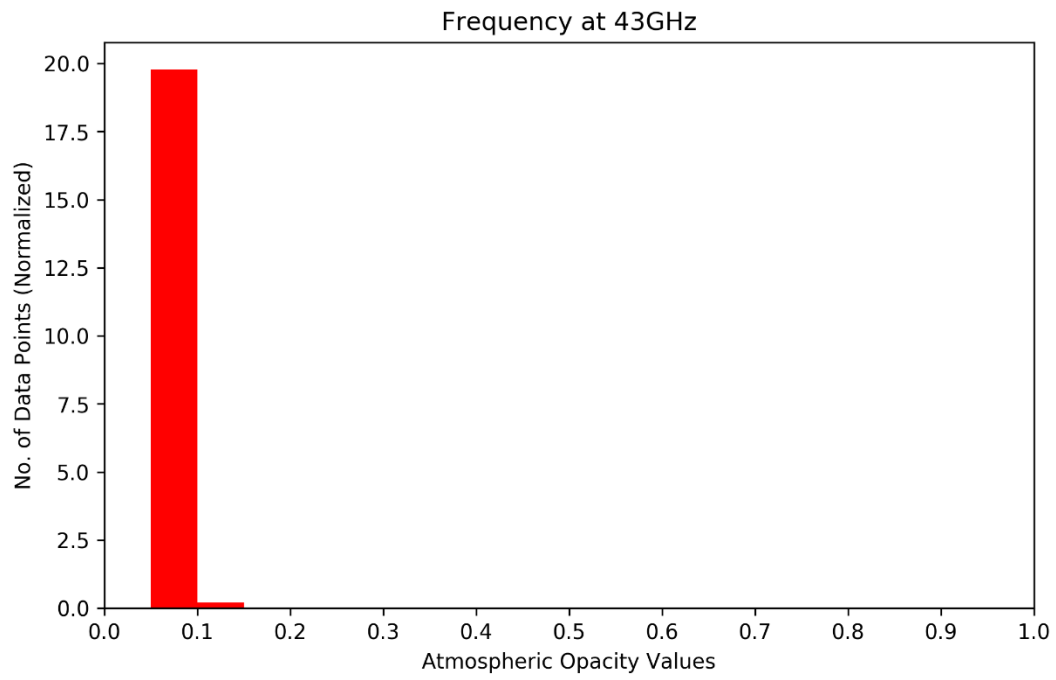
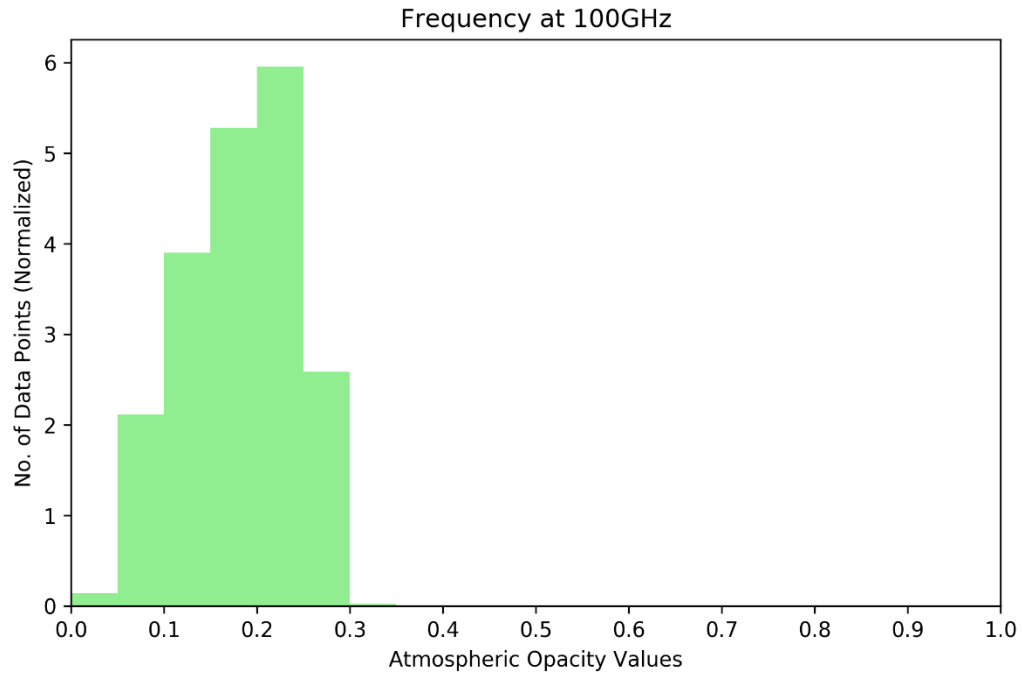
7. Zambia



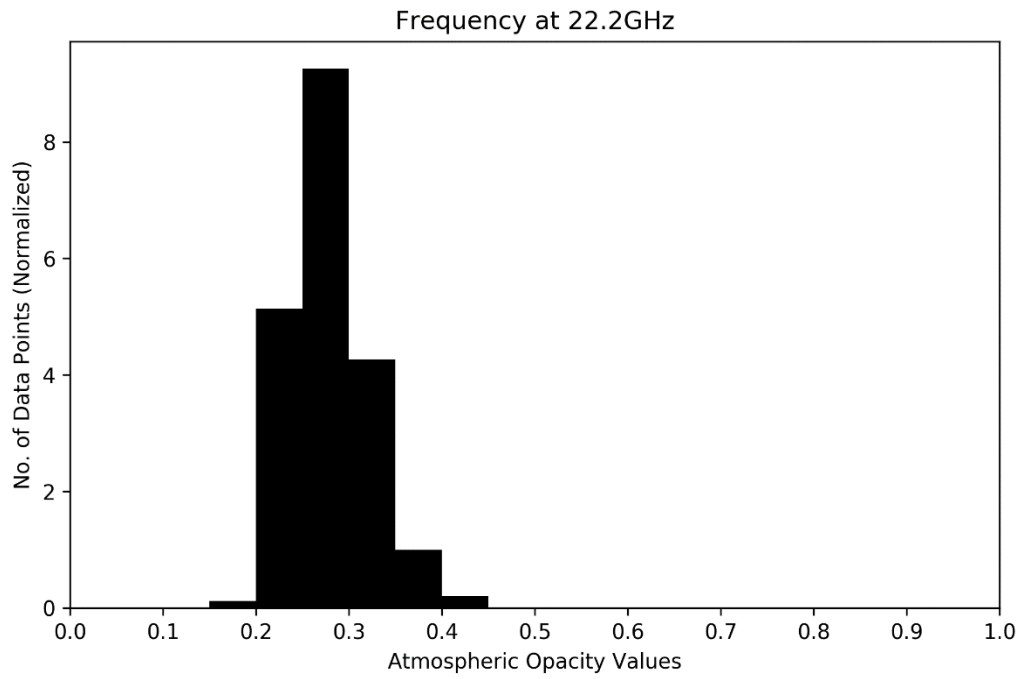
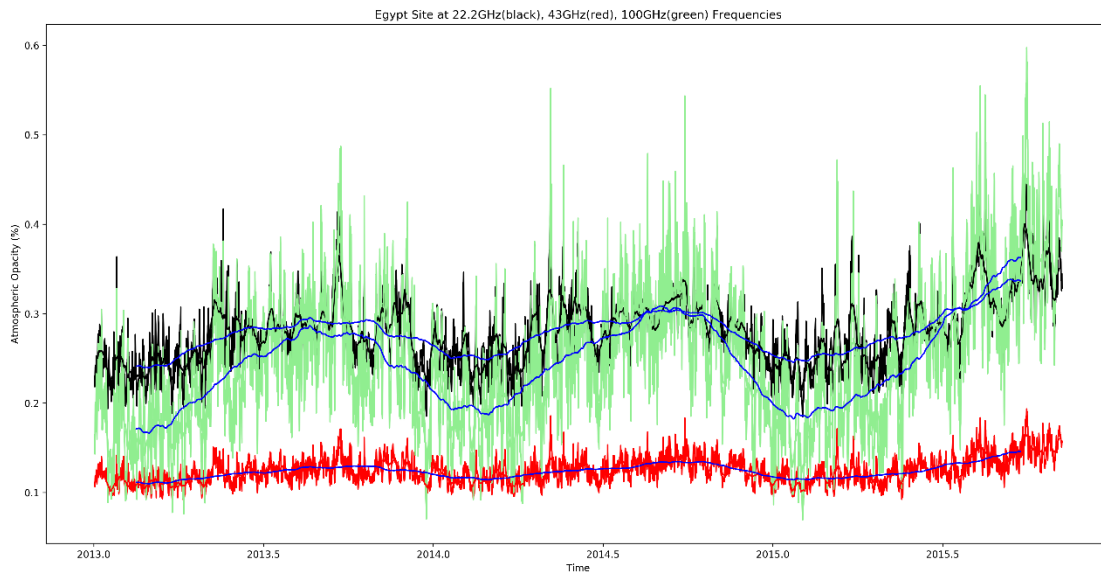


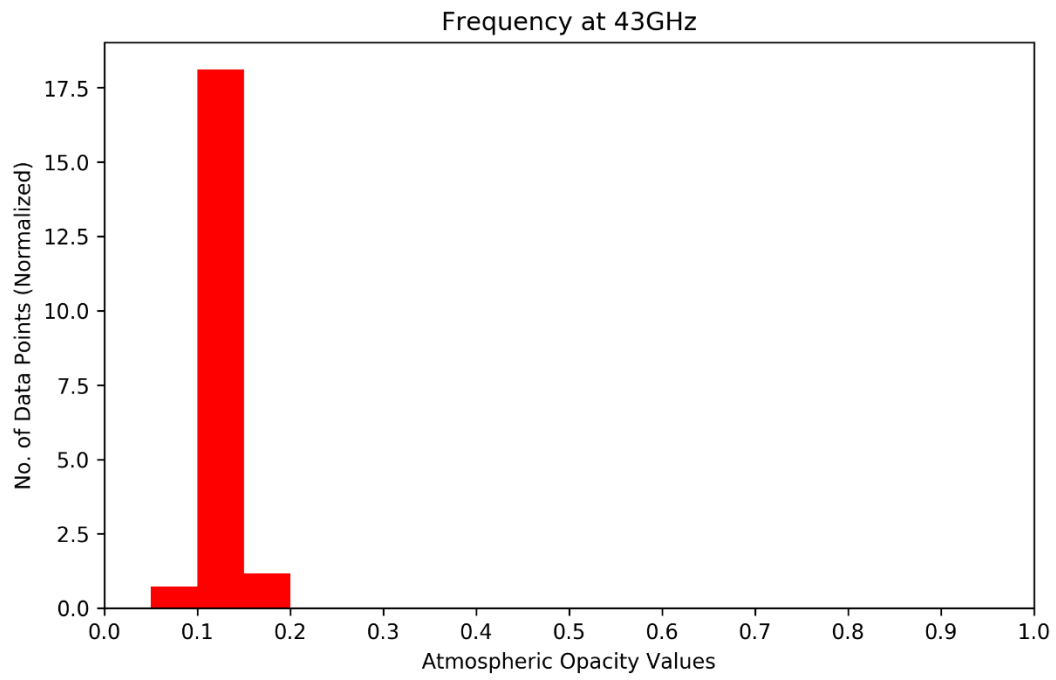
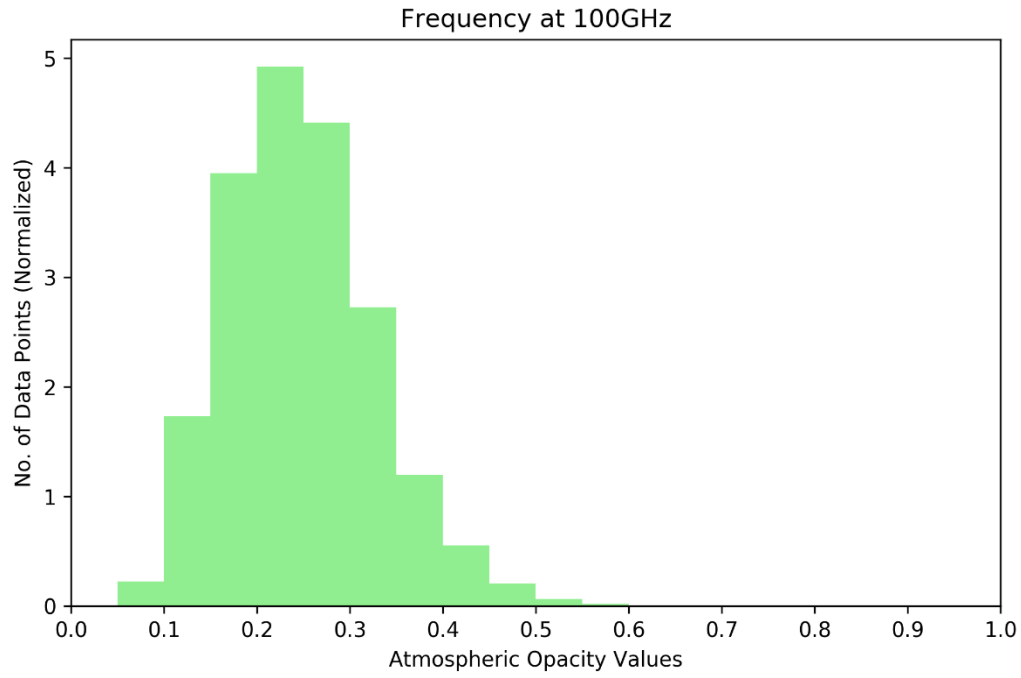
8. Ethiopia



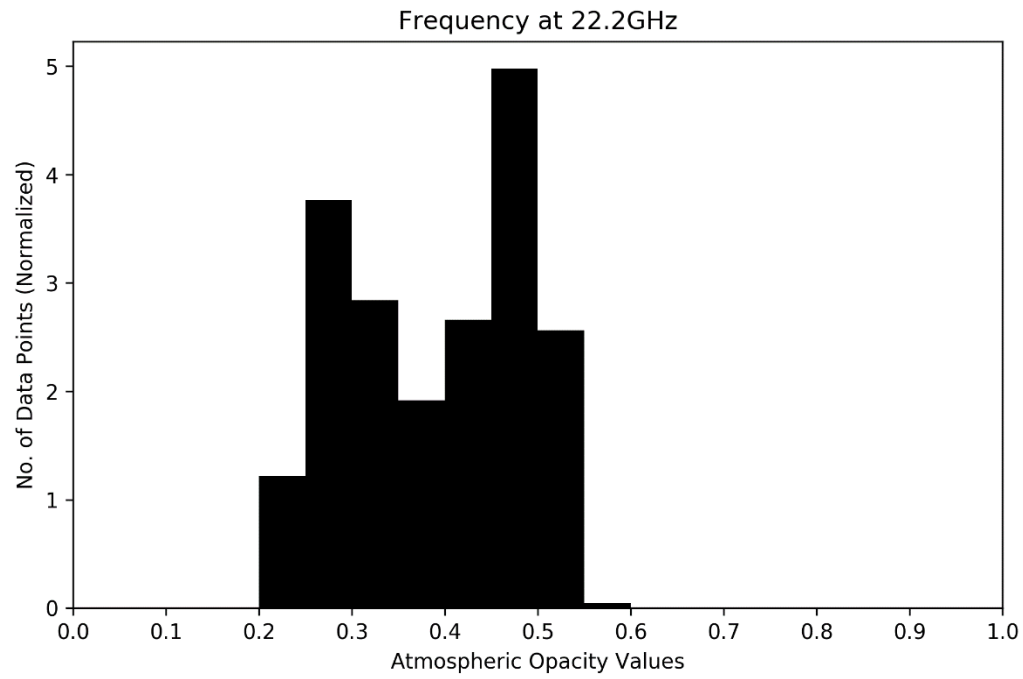
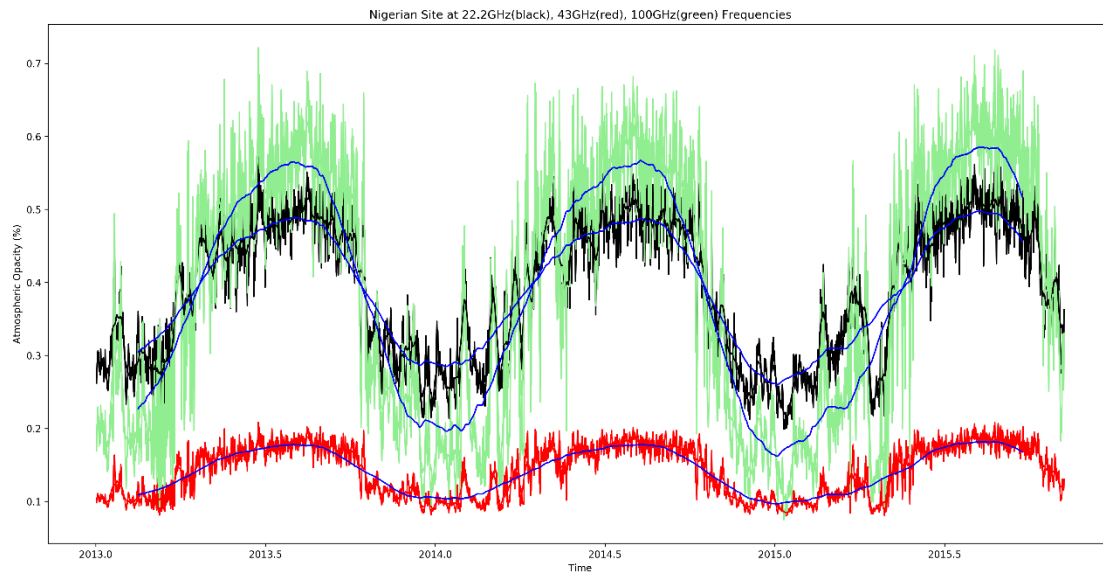


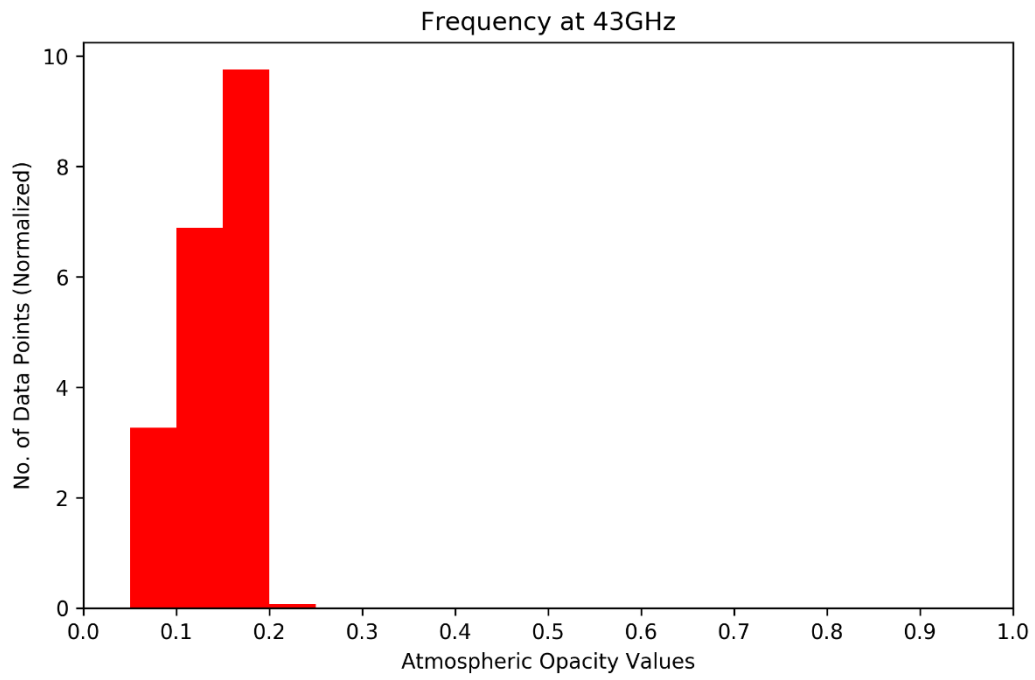
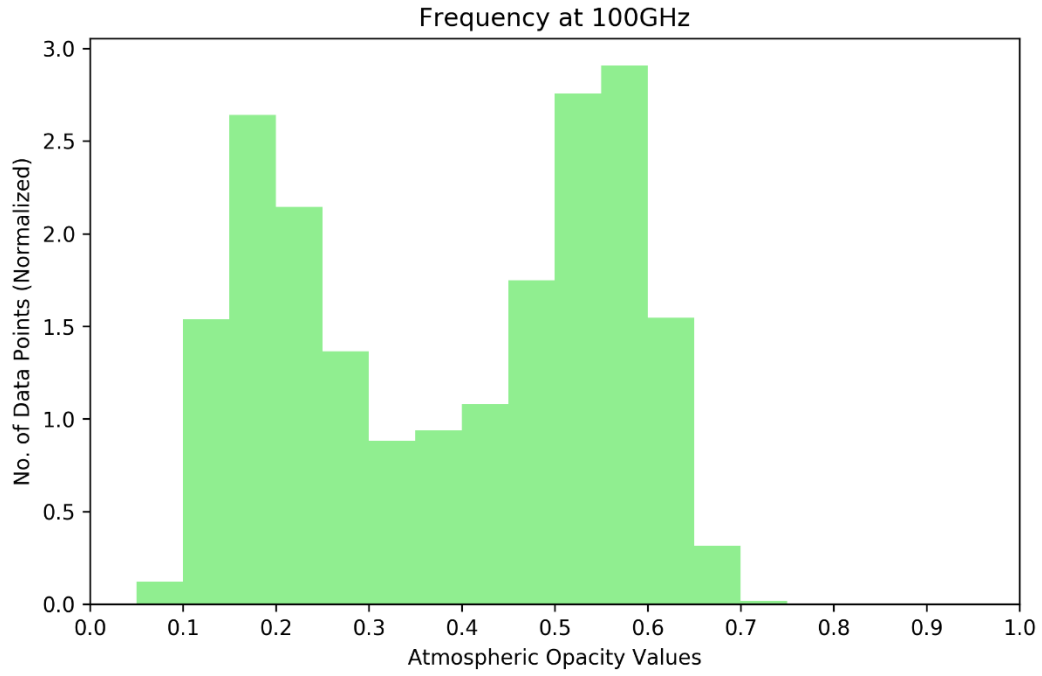
9. Egypt



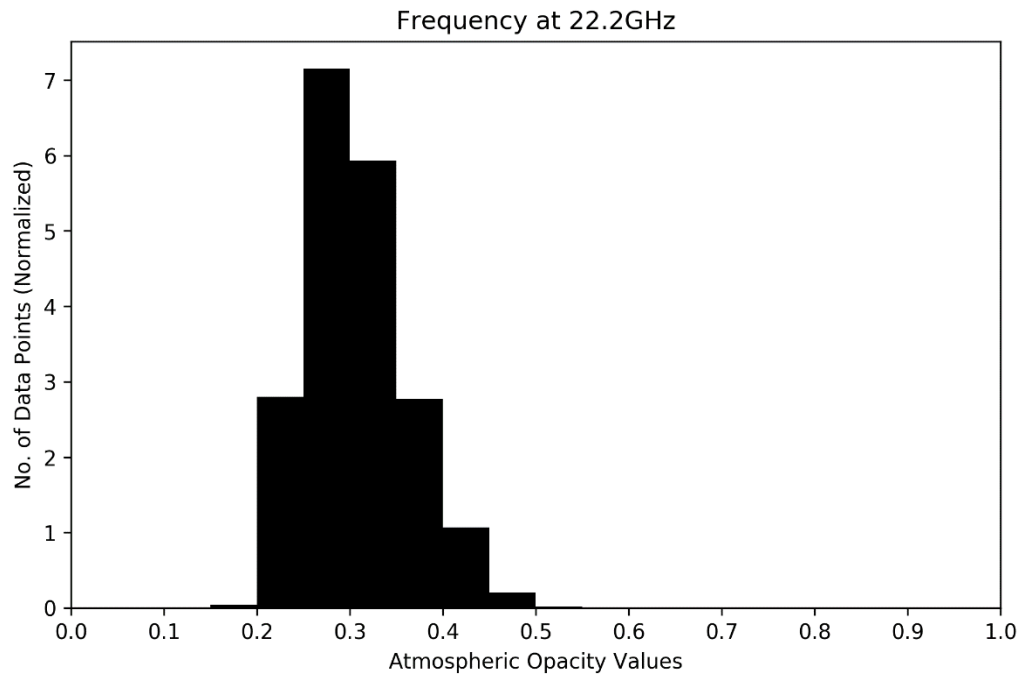
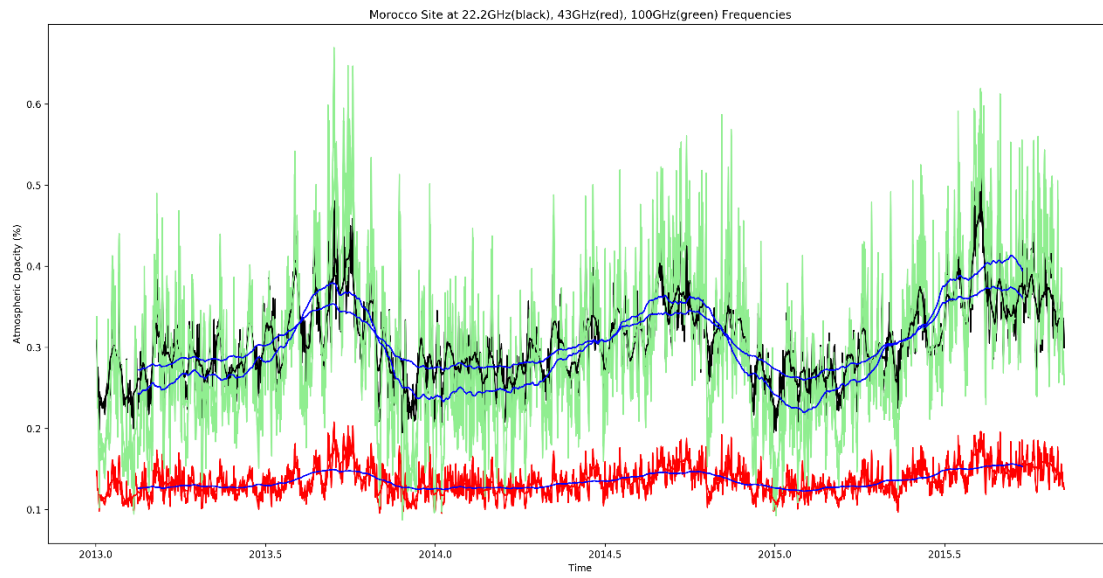


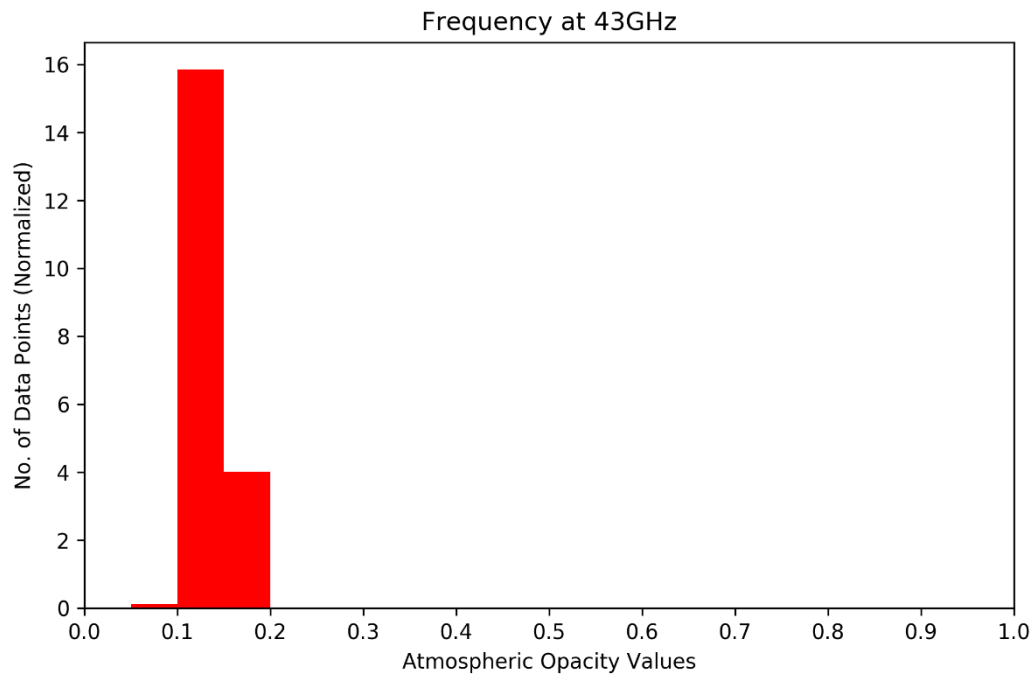
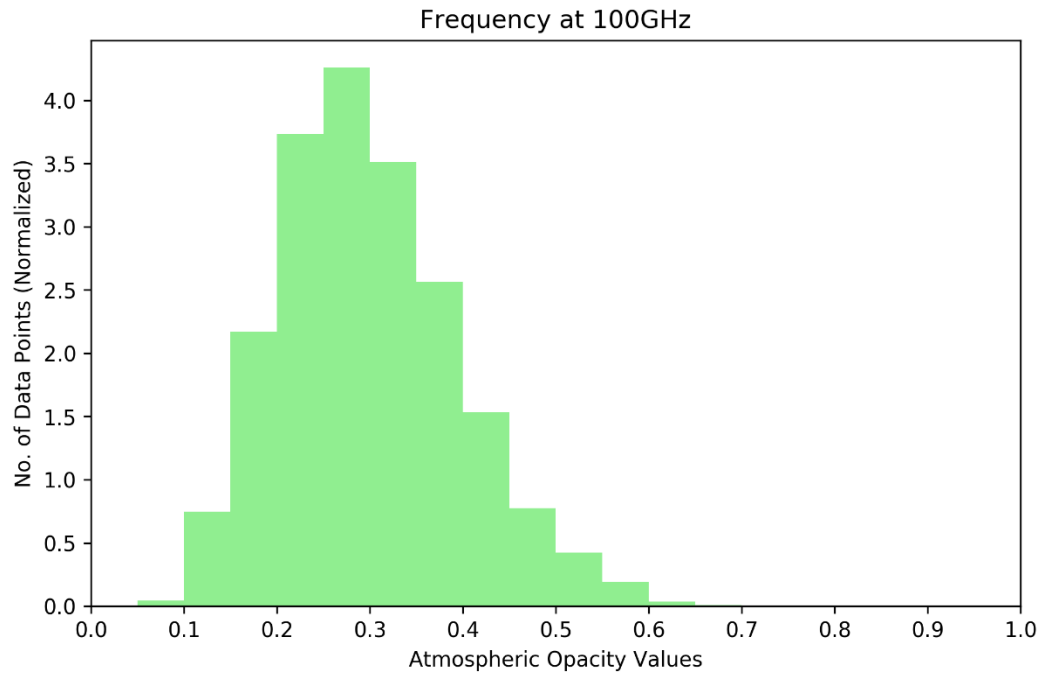
10. Nigeria



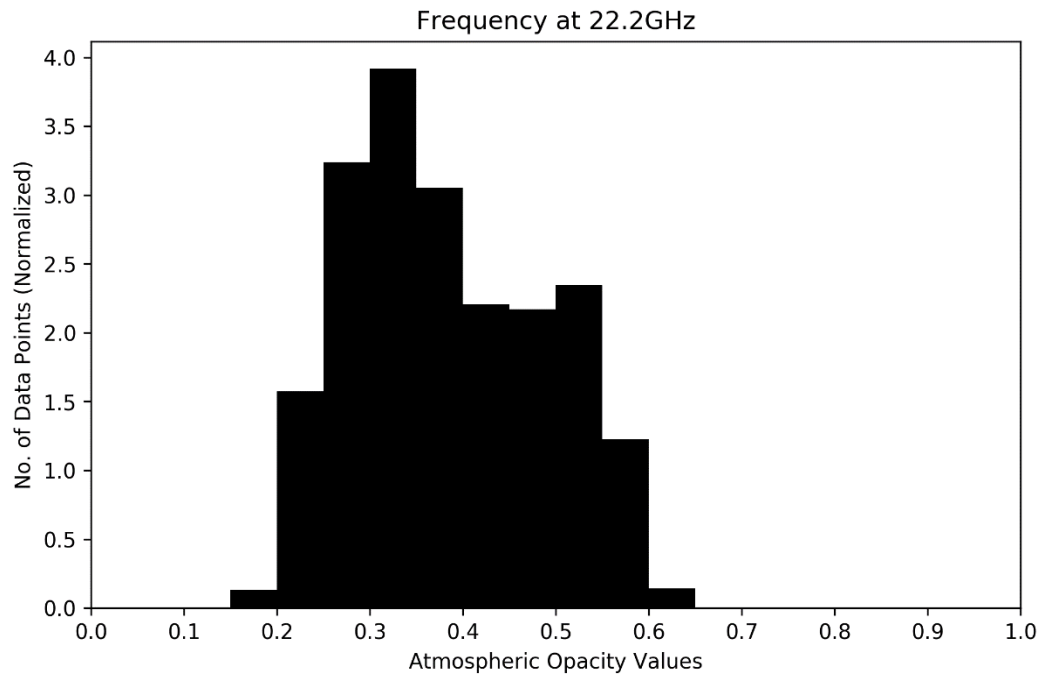
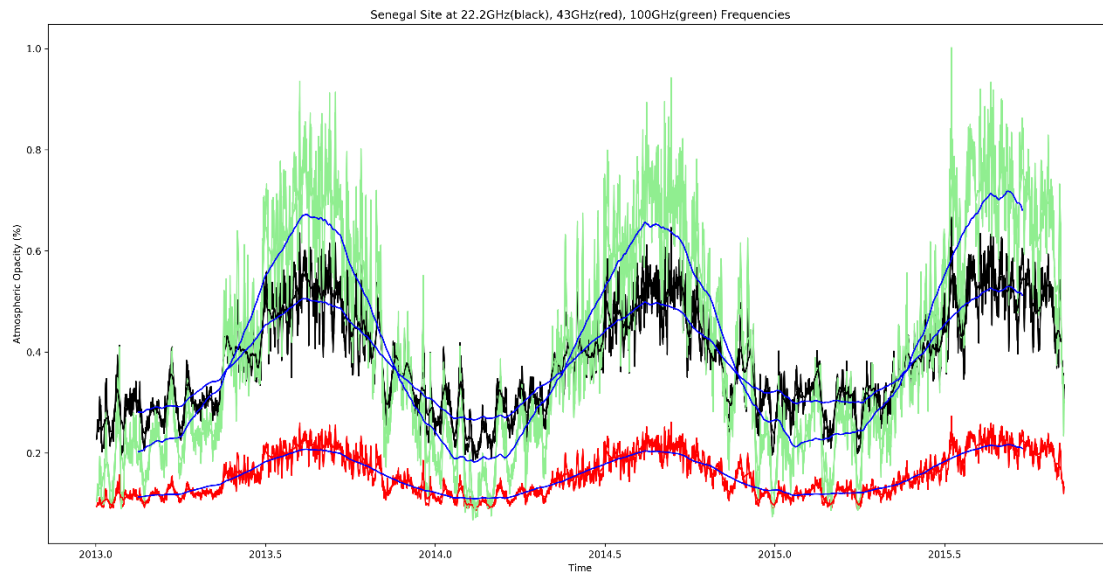


11. Morocco





12. Senegal



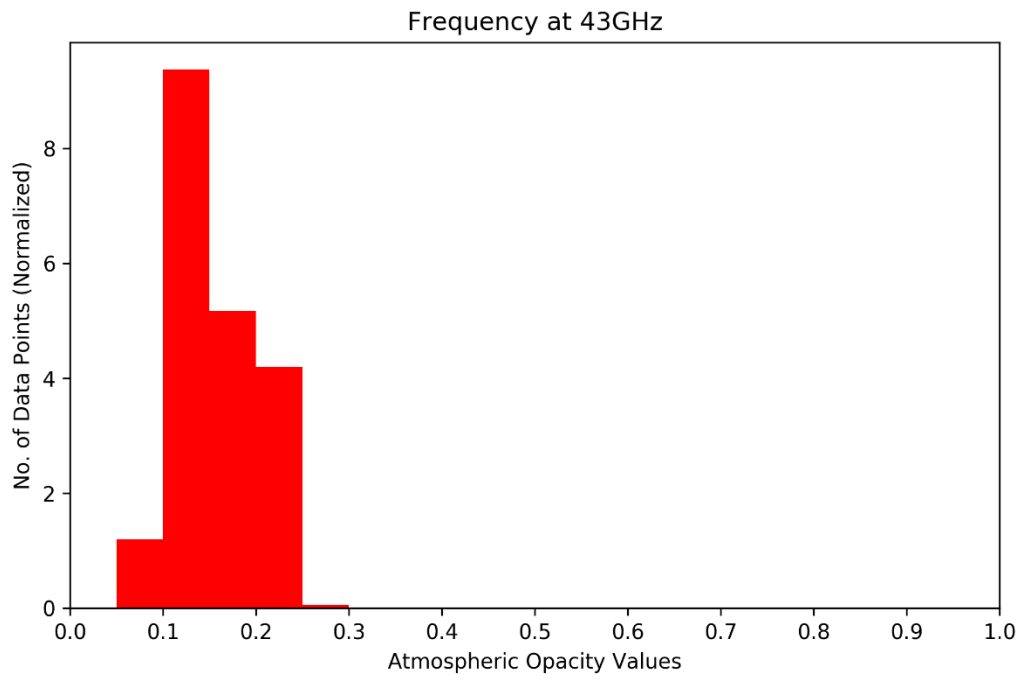
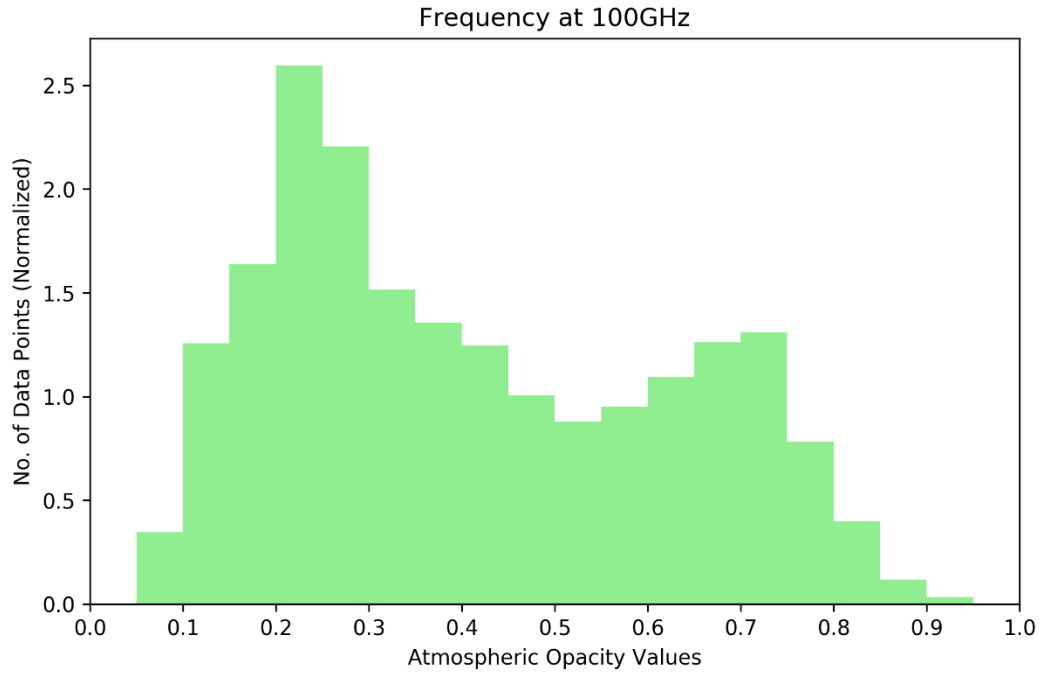
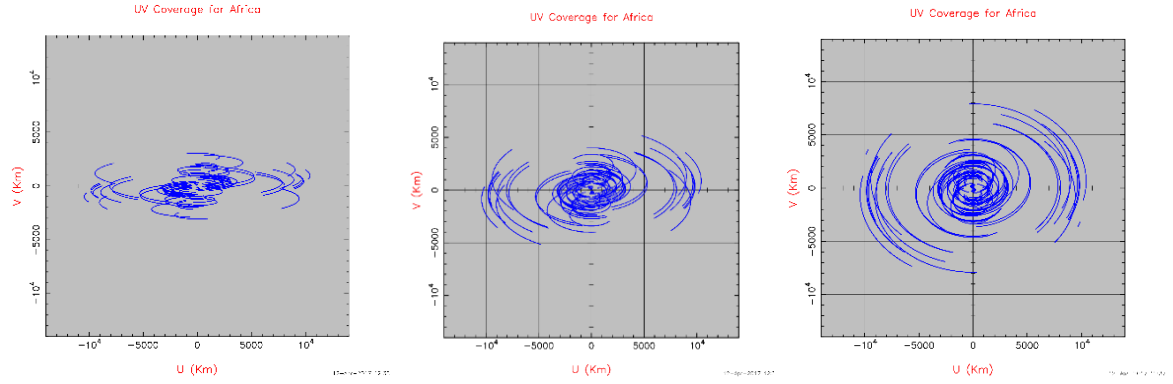


Table 4.7 (continued): U-V Coverage Plots for LBA + AVN Antennas at X-Band

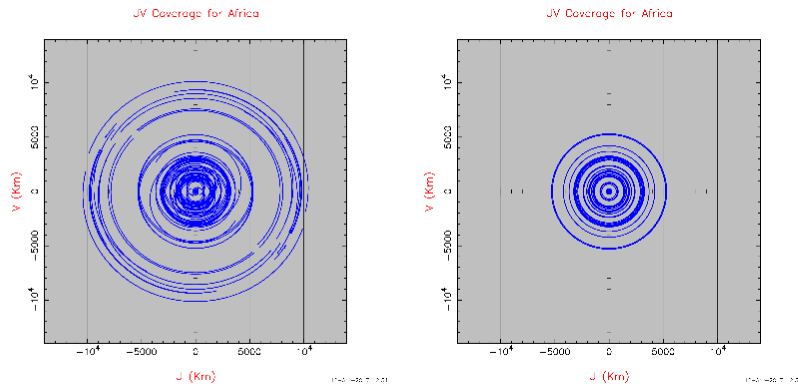
a) LBA Antennas



-10°

-30°

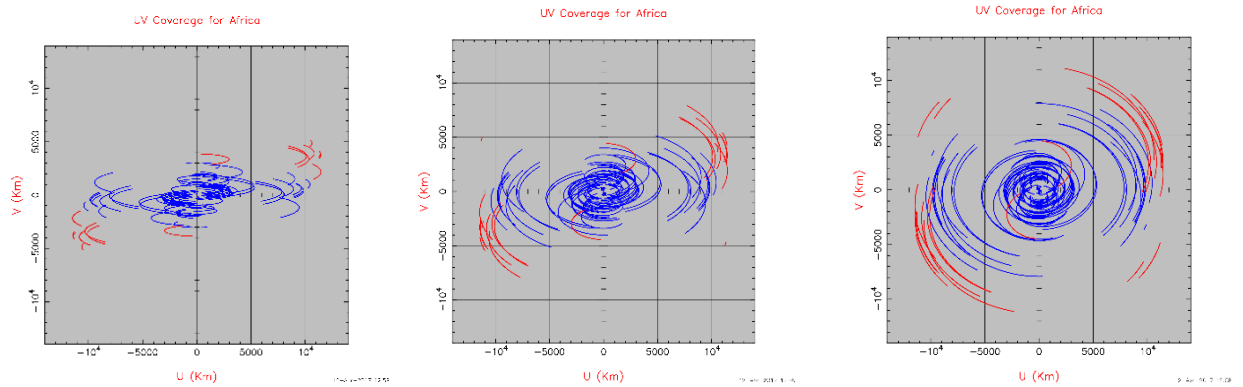
-50°



-70°

-90°

b) LBA + Ghana antenna

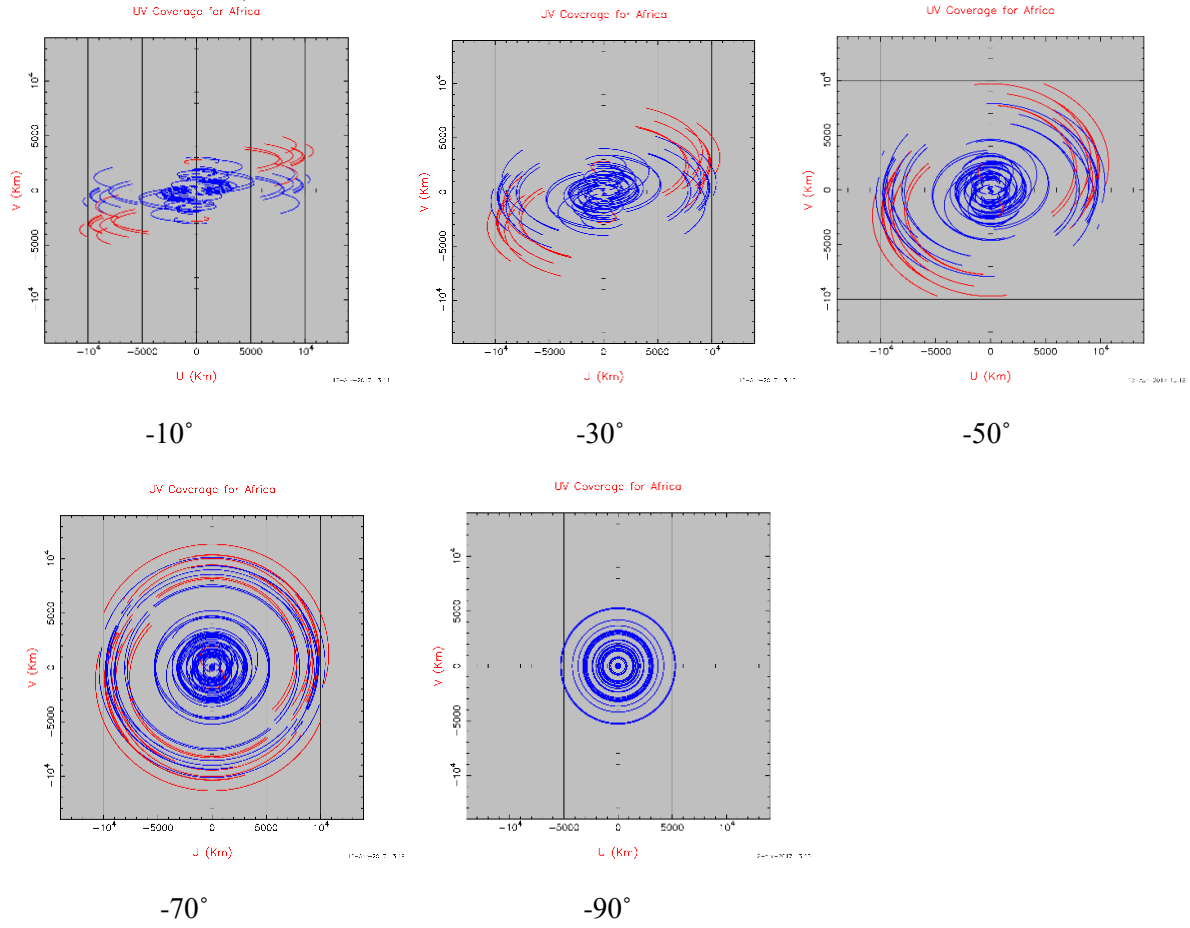


-10°

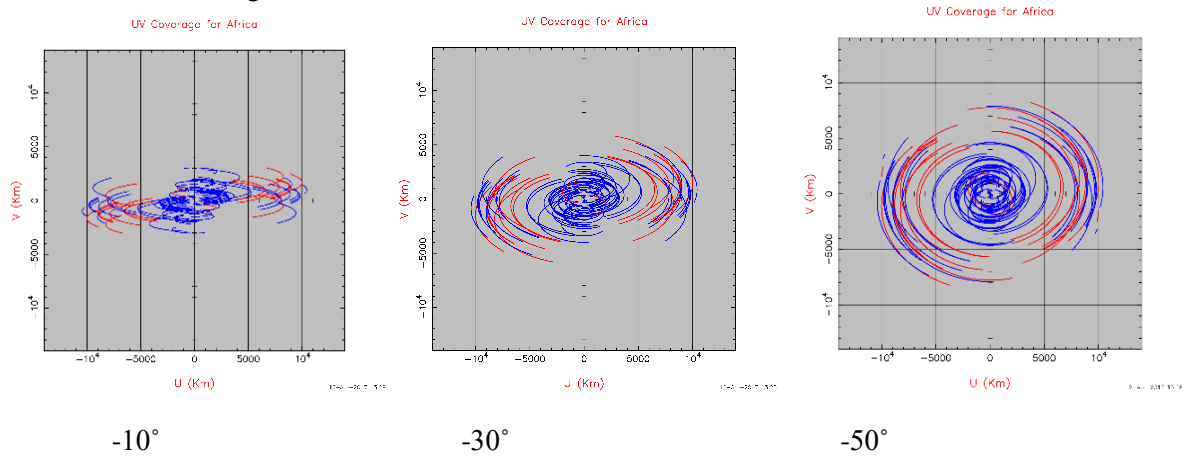
-30°

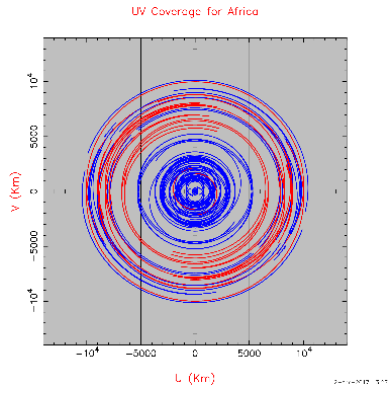
-50°

c) LBA + Kenya antenna

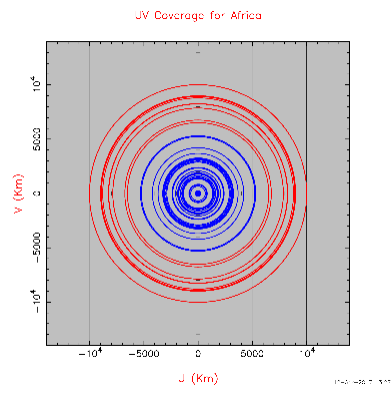


d) LBA + Madagascar Antenna



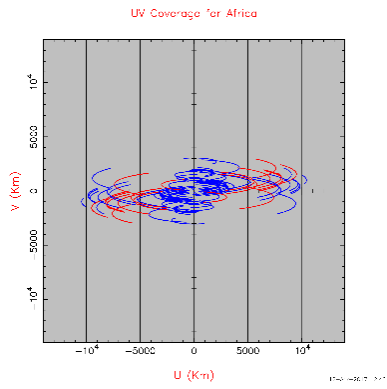


-70°

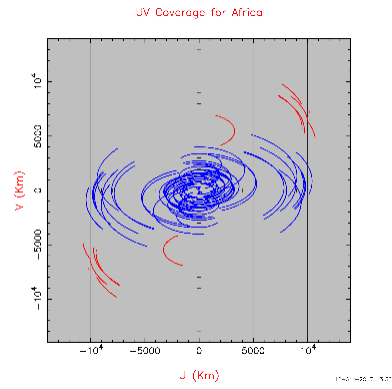


-90°

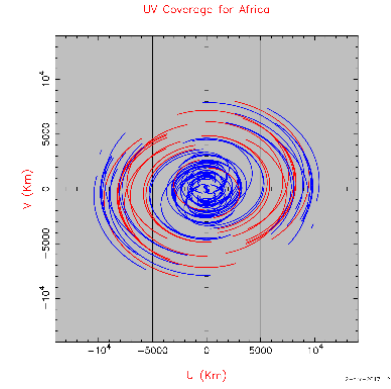
e) LBA + Mauritius Antenna



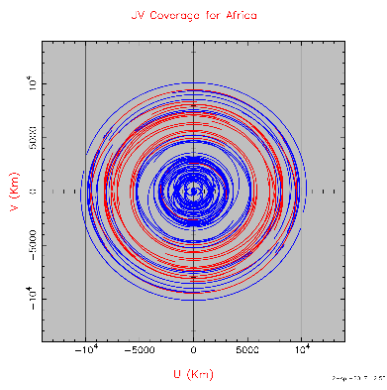
-10°



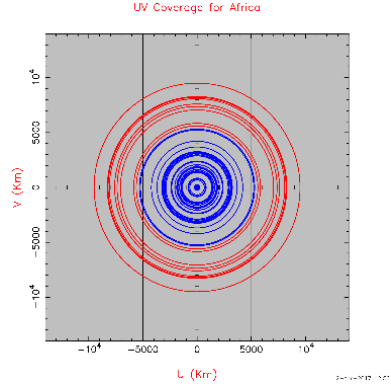
-30°



-50°

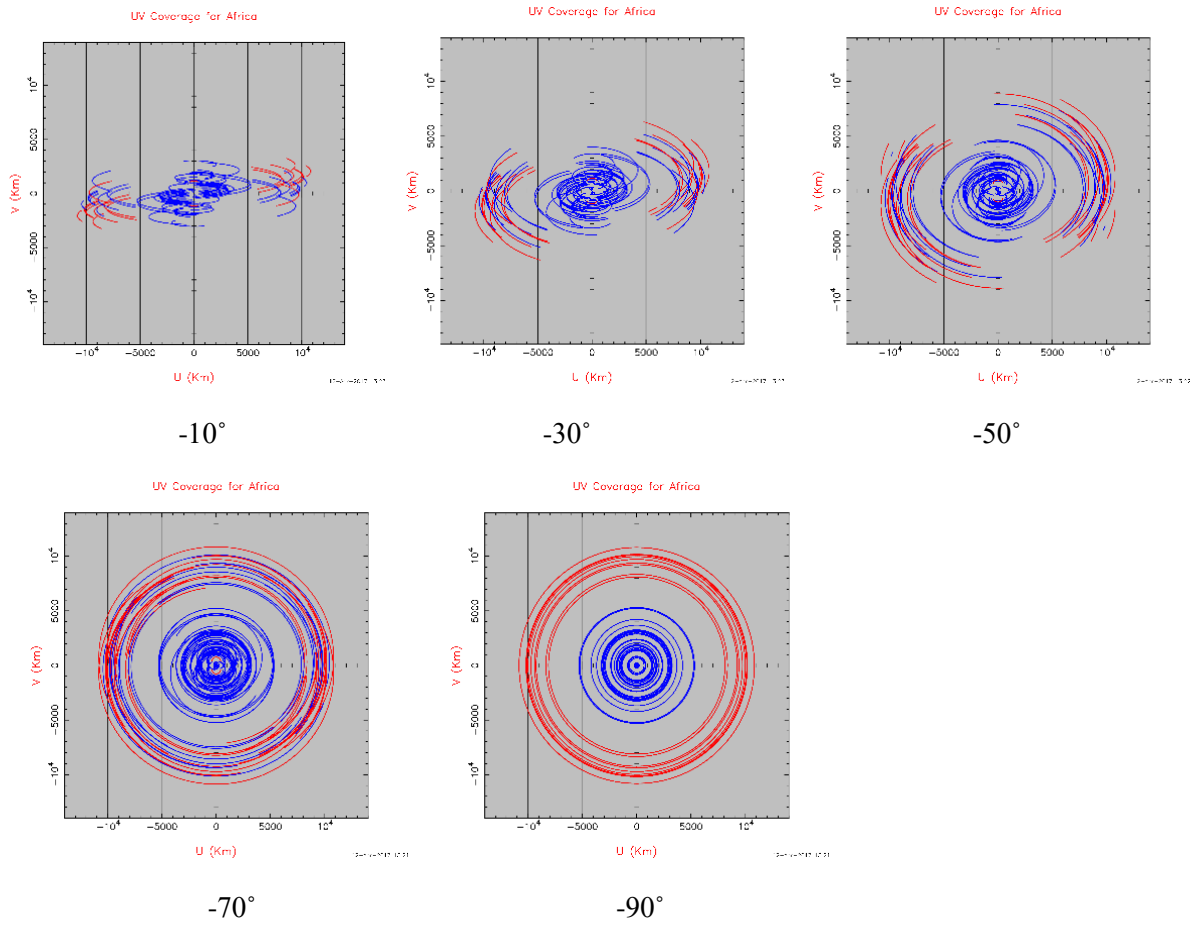


-70°

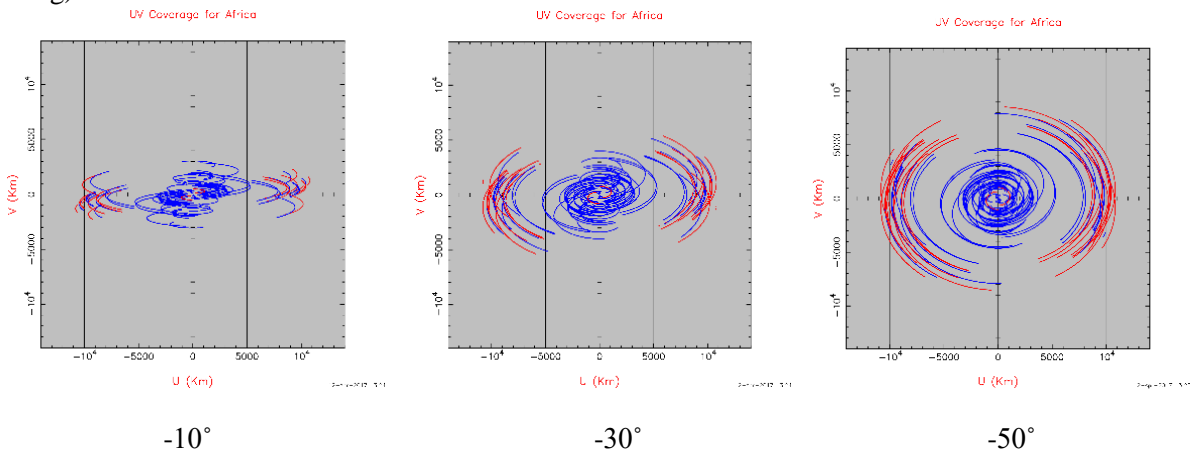


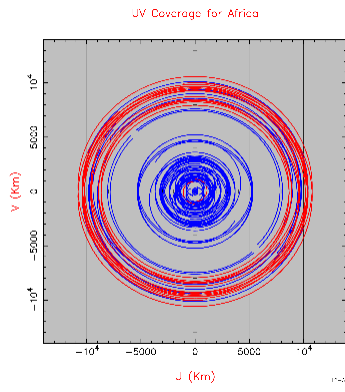
-90°

f) LBA + Zambia antenna

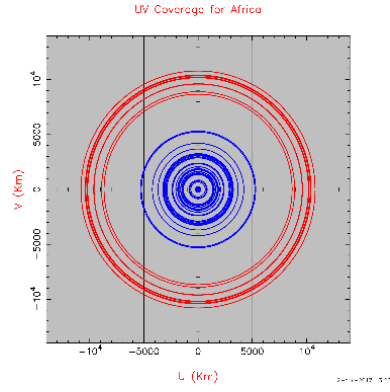


g) LBA + Namibia antenna



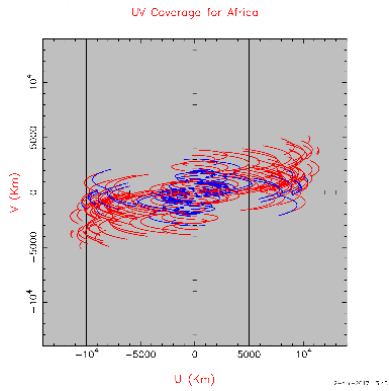


-70°

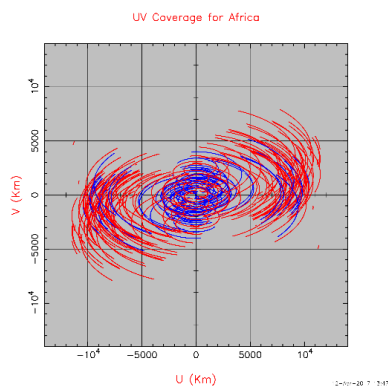


-90°

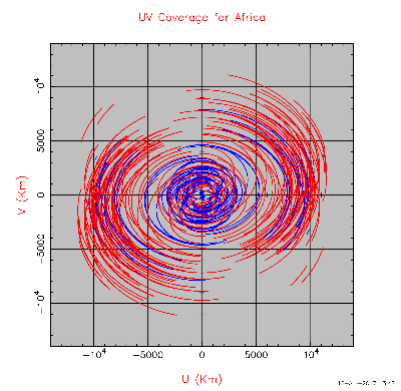
h) LBA + AVN1 antennas



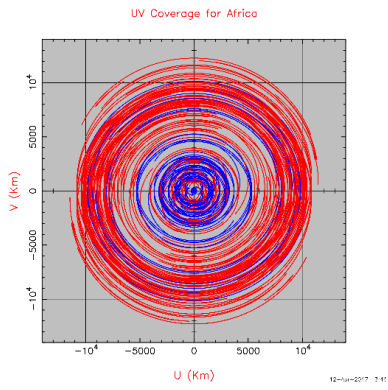
-10°



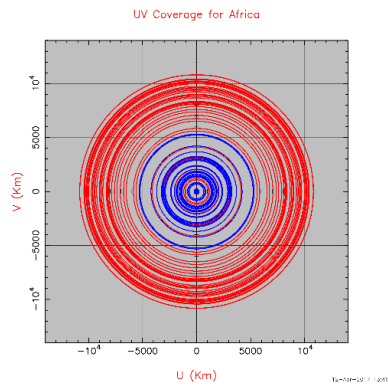
-30°



-50°

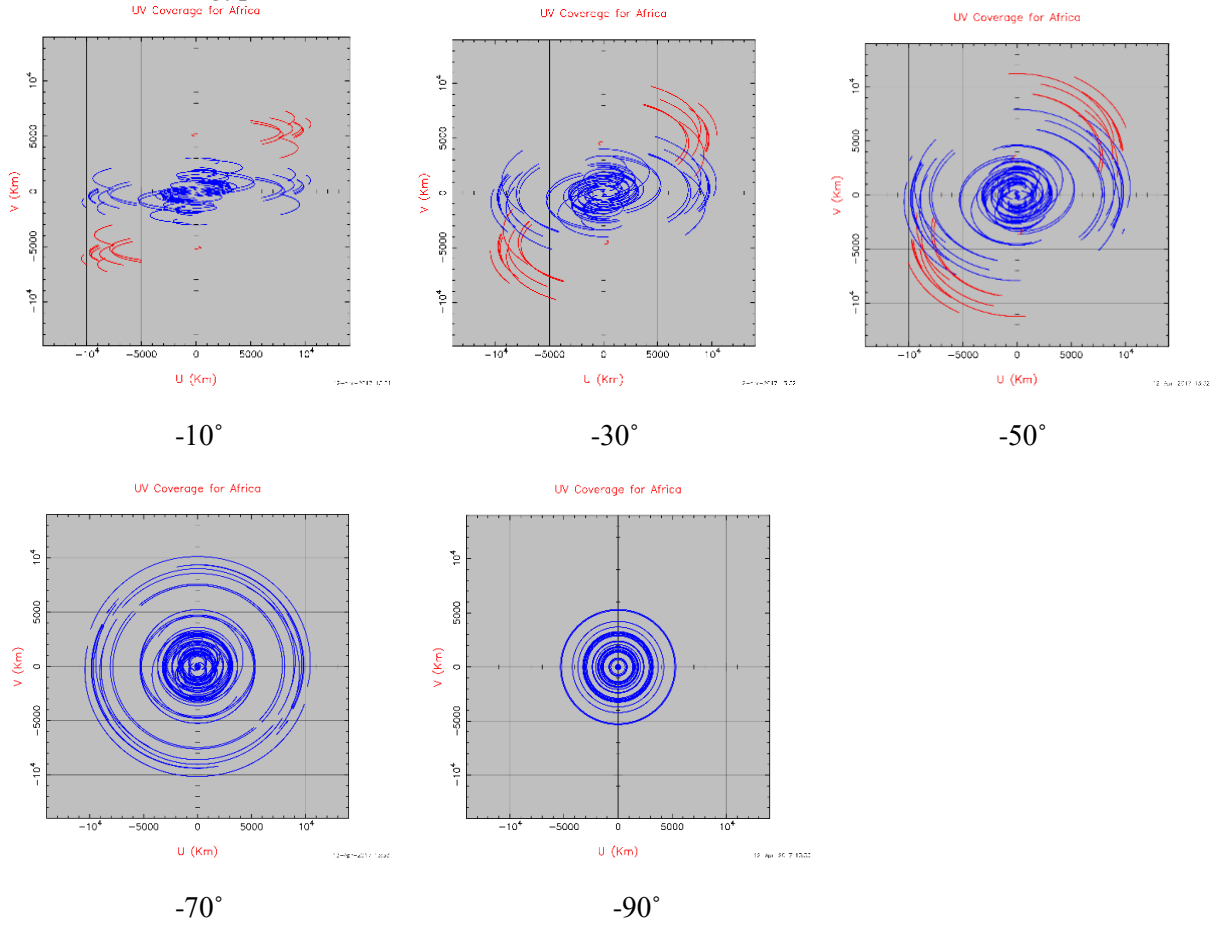


-70°

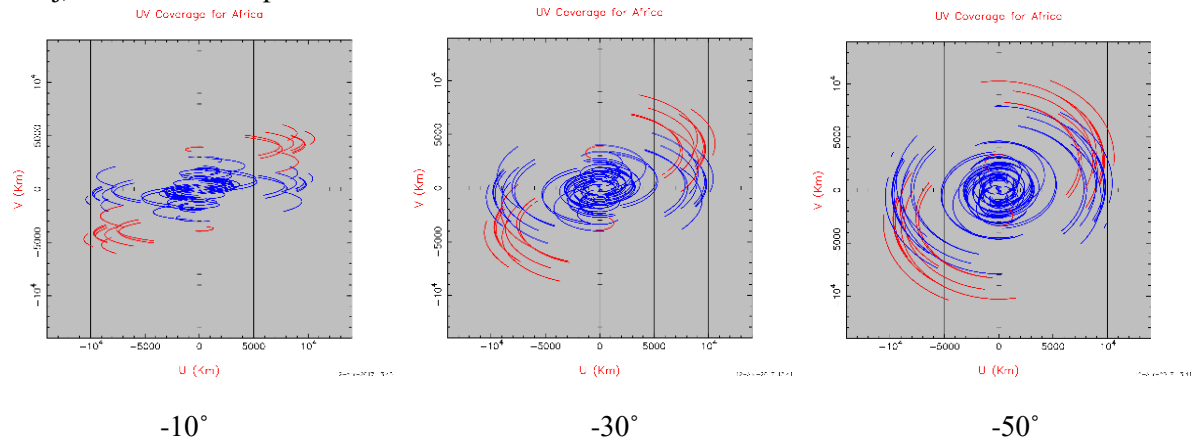


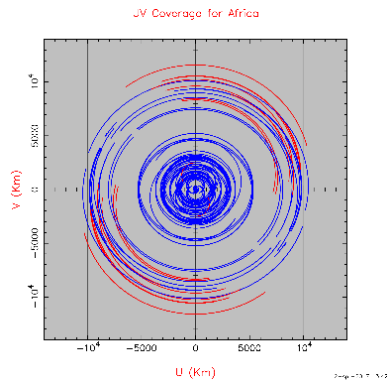
-90°

i) LBA + Egypt Antenna

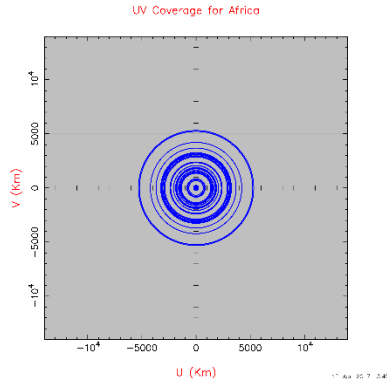


j) LBA + Ethiopia antenna



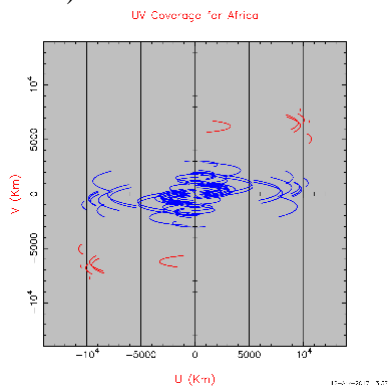


-70°

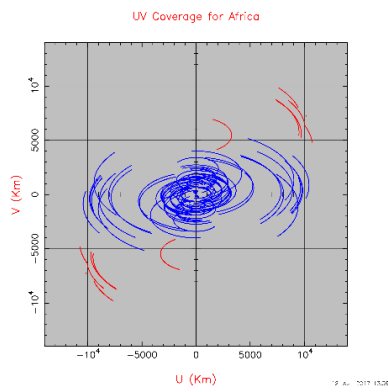


-90°

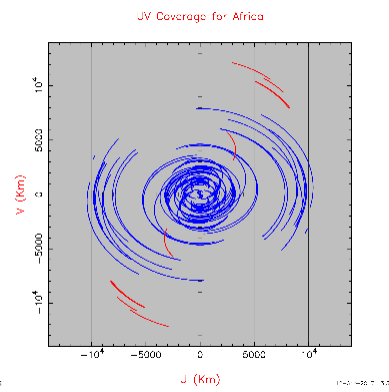
k) LBA + Morocco antenna



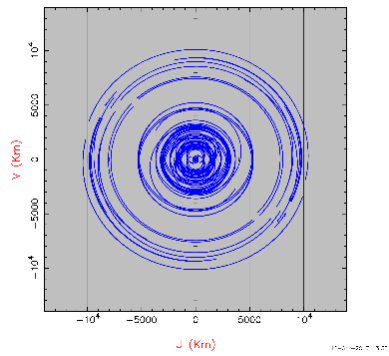
-10°



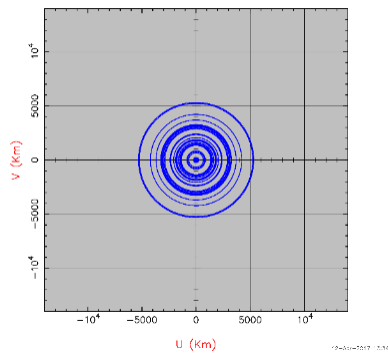
-30°



-50°

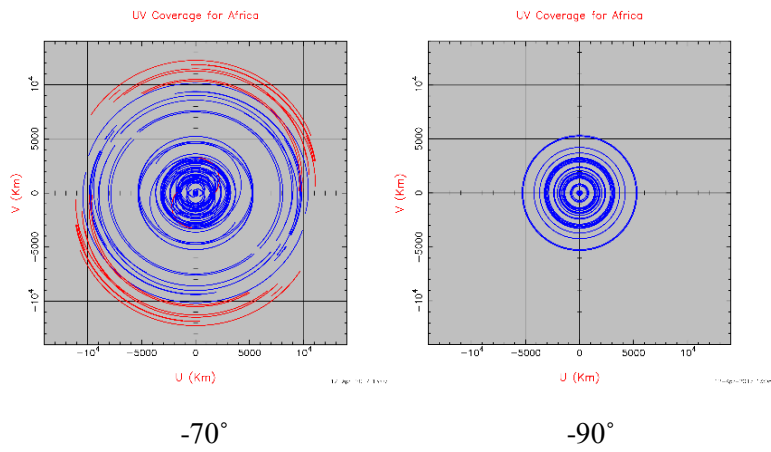
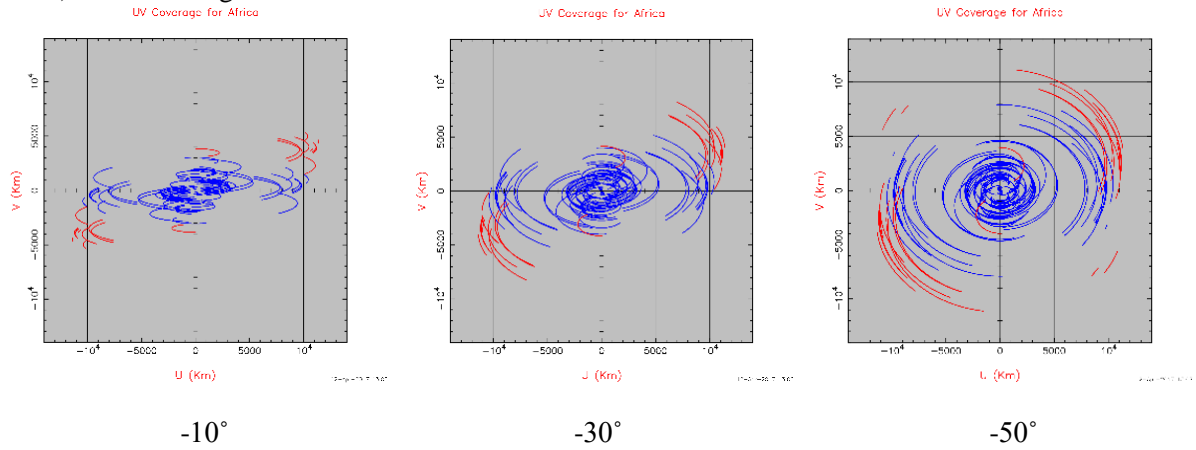


-70°

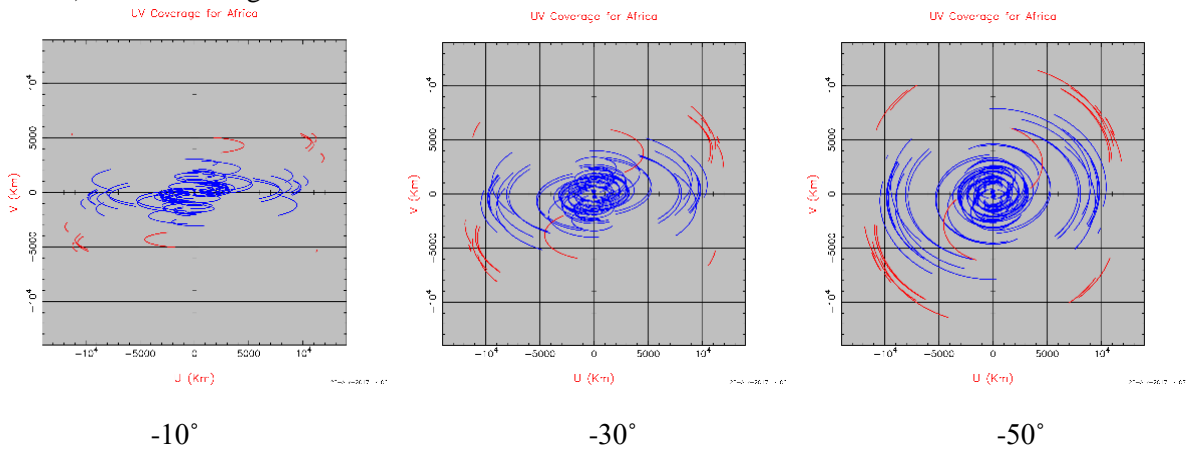


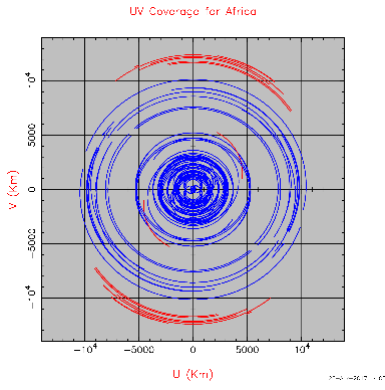
-90°

l) LBA + Nigeria antenna

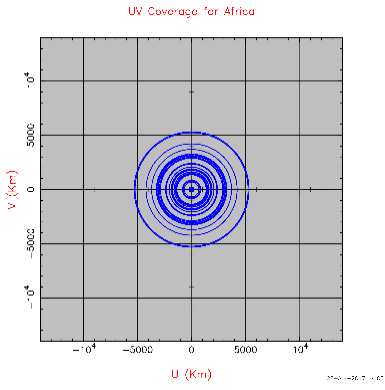


m) LBA + Senegal antenna



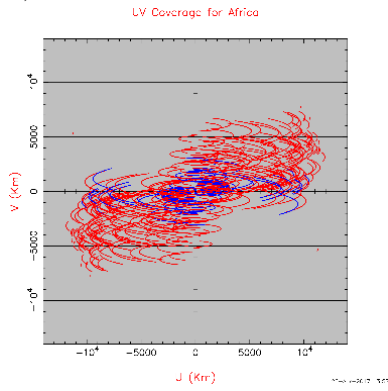


-70°

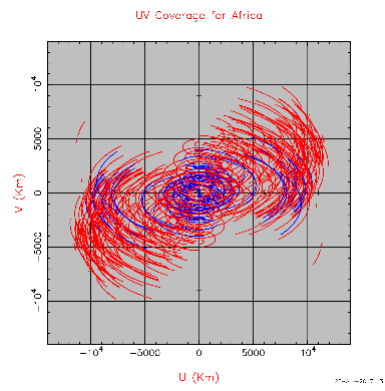


-90°

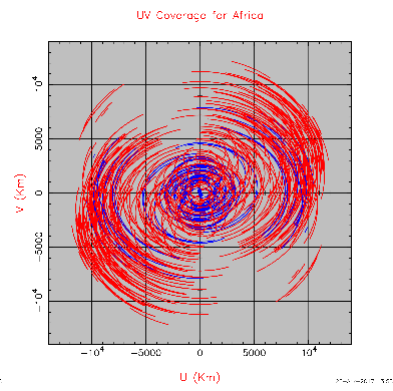
n) LBA + AVN antennas



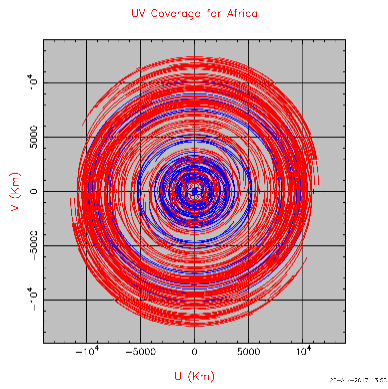
-10°



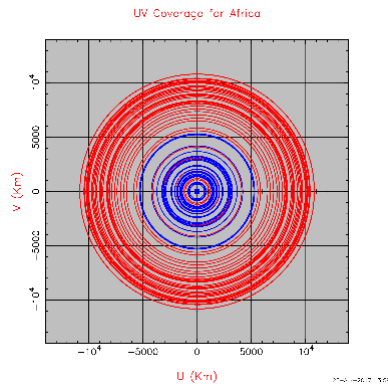
-30°



-50°



-70°



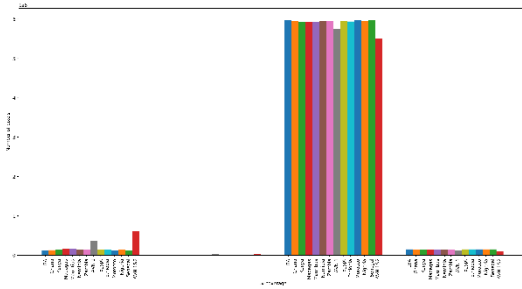
-90°

2) U-V Coverage Histograms for LBA + AVN antennas at x-band

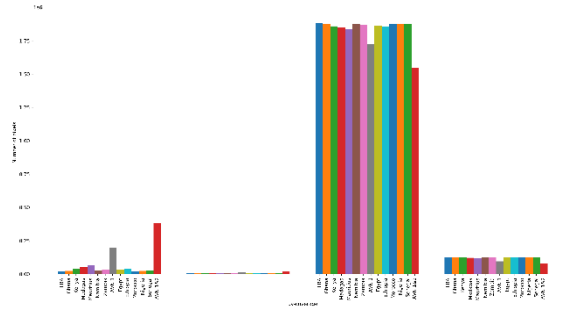
The first portion of the histogram represents the red tracks on the U-V Coverage plots above. The red tracks show what the AVN antennas add to the LBA U-V Coverage. The second portion of the histogram shows how much of the background (grey colour) in the U-V Coverage plots is reduced by adding the AVN antennas. The third and last portion of the histogram shows the initial U-V Coverage of the LBA antennas only (in blue colour): if the new AVN antenna adds new U-V Coverage area, the.....; if the new AVN antenna only adds U-V Coverage on the area already covered by the LBA antennas only, the bars remain the same as the original blue tracks since the new antenna in reality adds no new U-V Coverage. First histogram a) shows the U-V Coverage on longer baselines while the second histogram b) shows the U-V Coverage at medium to shorter baselines.

i) At a declination of 10 degrees

a)

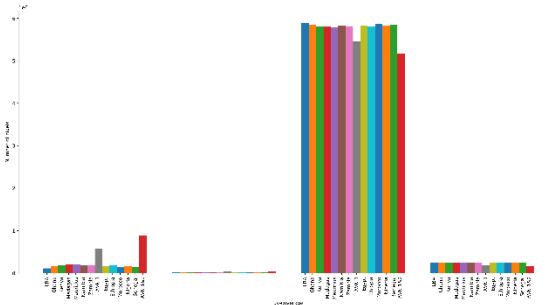


b)

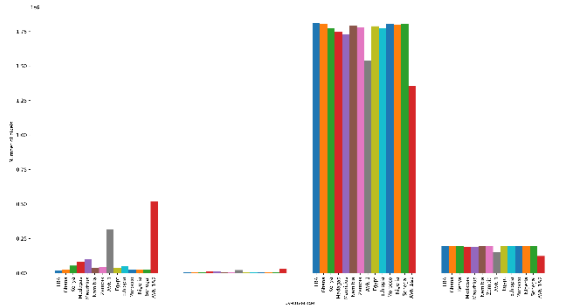


ii) At a declination of 30 degrees

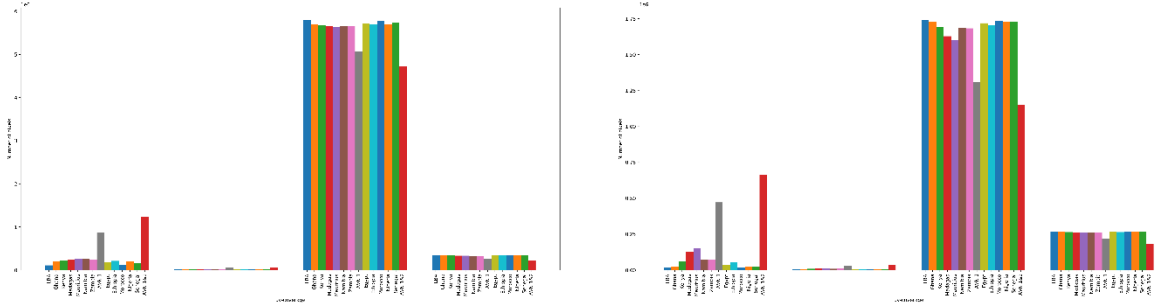
a)



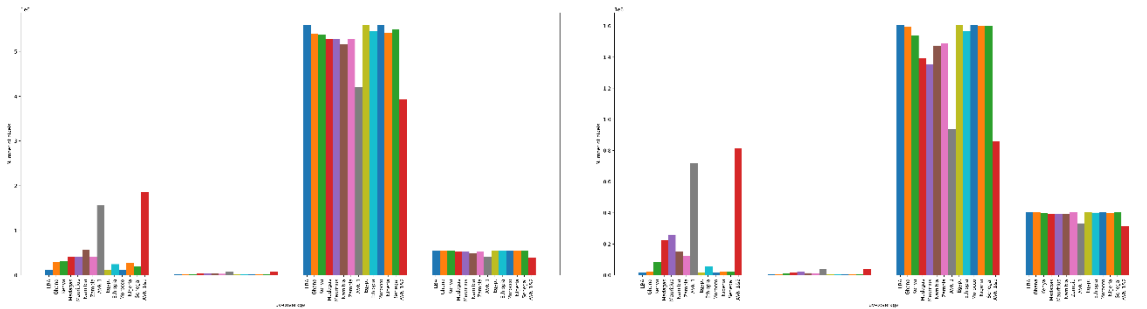
b)



iii) At a declination of 50 degrees



iv) At a declination of 70 degrees



v) At a declination of minus 90 degrees

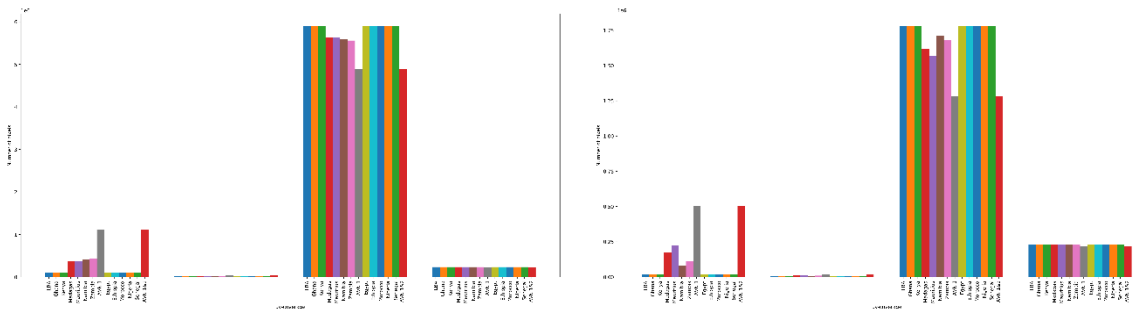
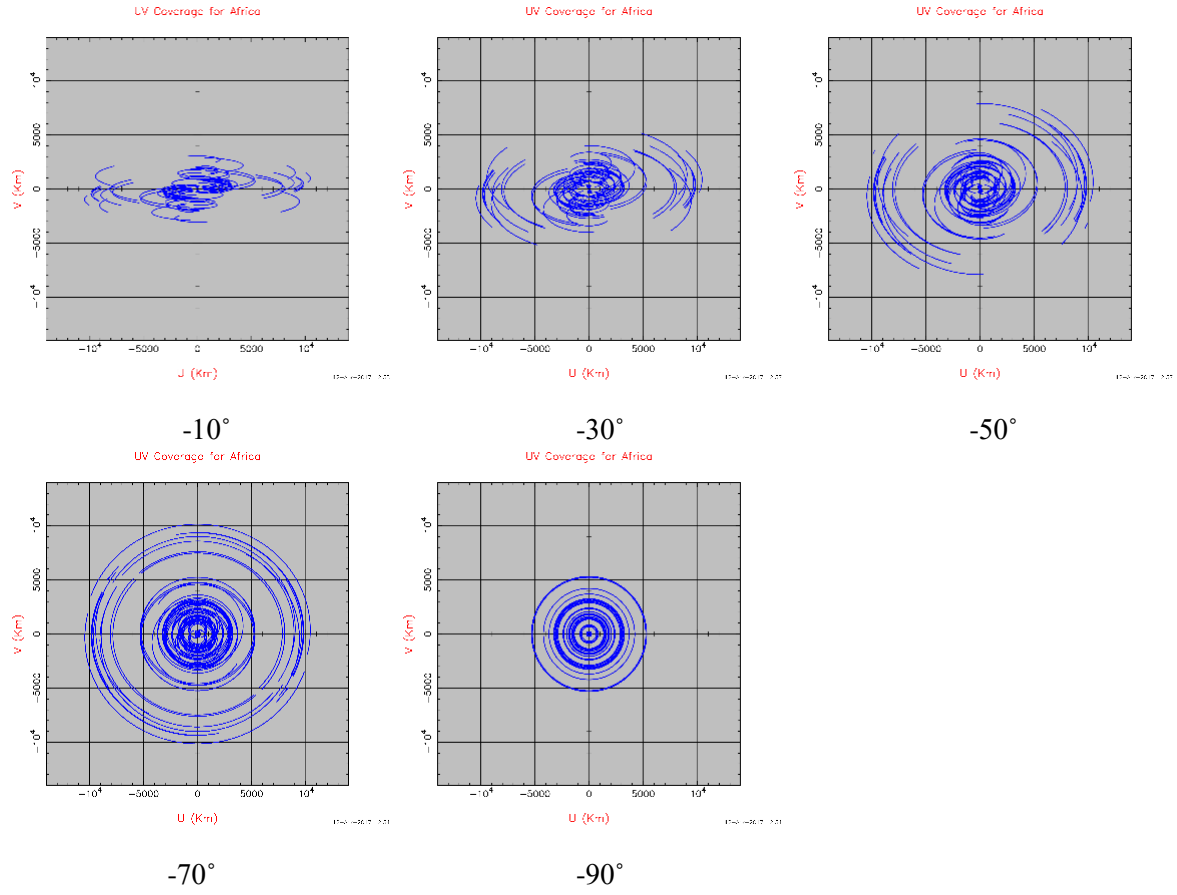
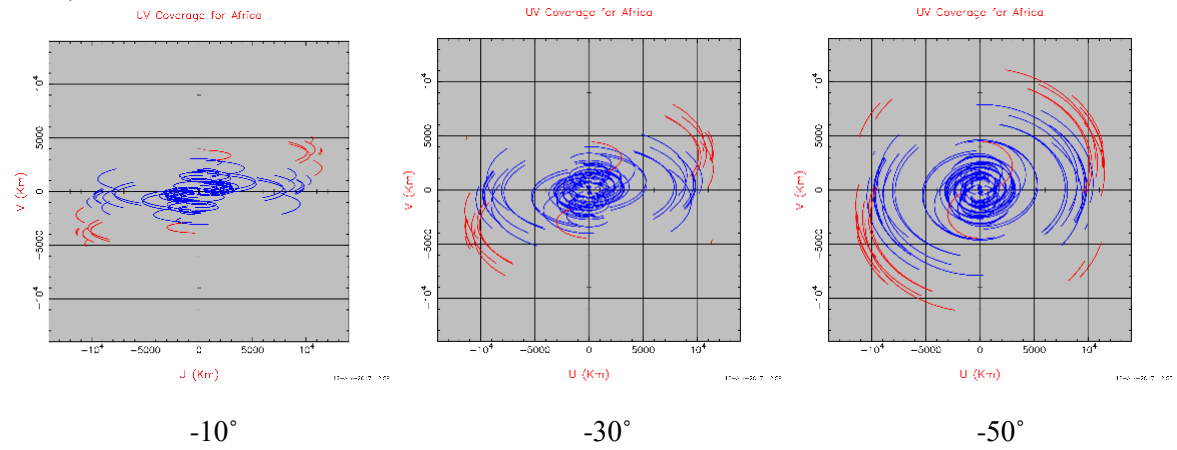


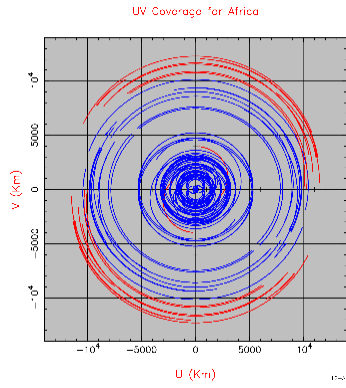
Table 4.10 (continued): U-V Coverage Plots for LBA + AVN Antennas at K-Band

a) LBA antennas

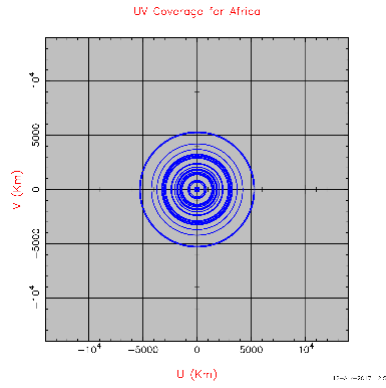


b) LBA + Ghana antenna



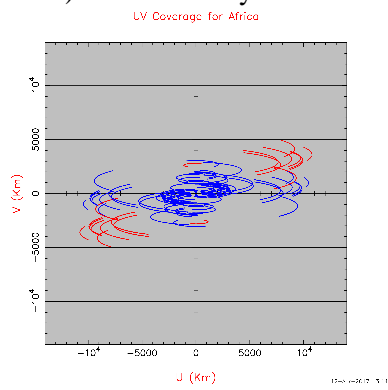


-70°

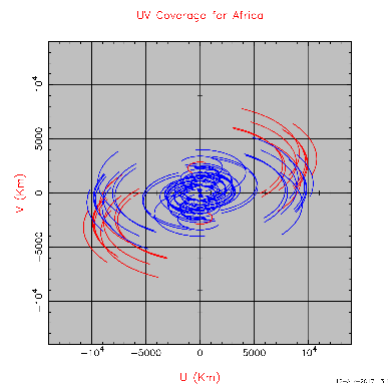


-90°

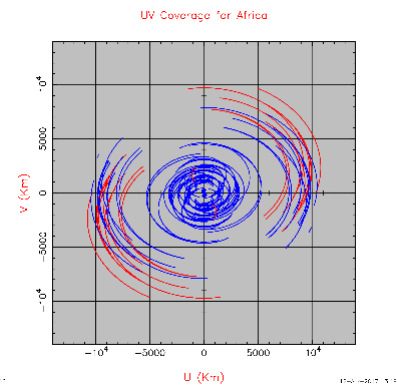
c) LBA + Kenya antenna



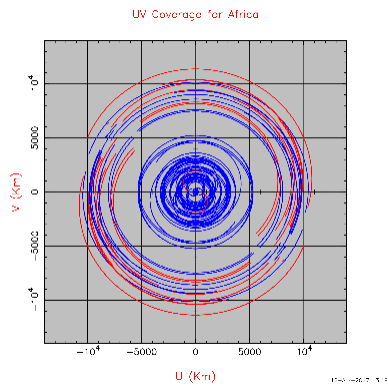
-10°



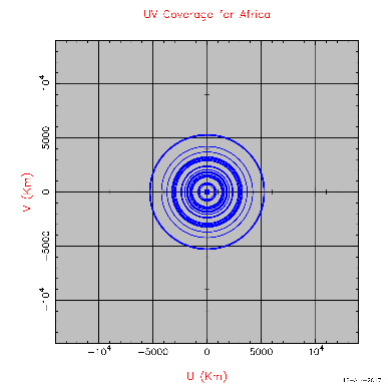
-30°



-50°

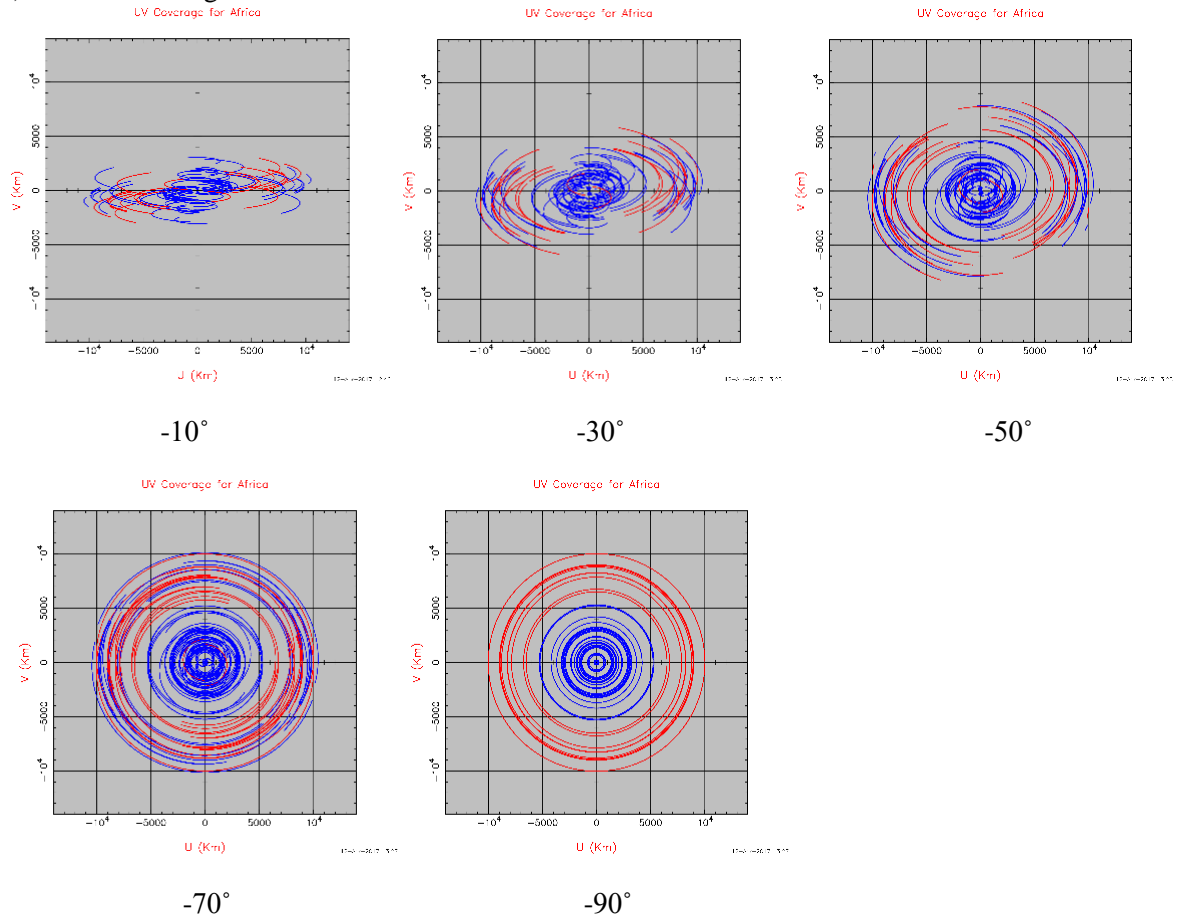


-70°

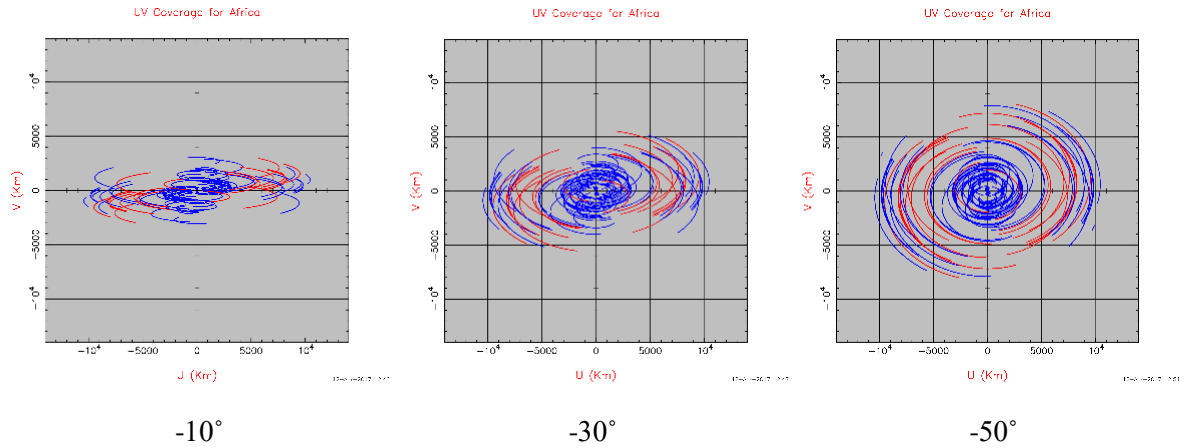


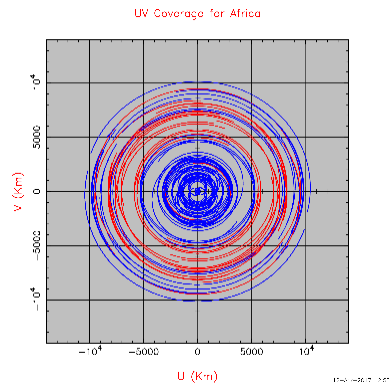
-90°

d) LBA + Madagascar antenna

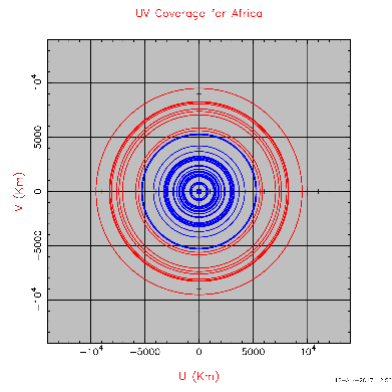


e) LBA + Mauritius antenna



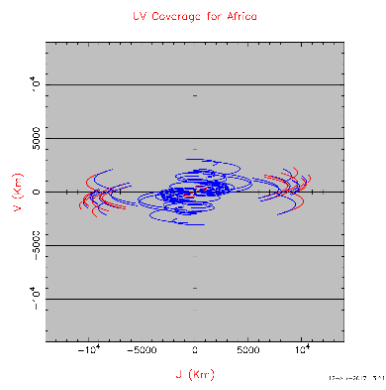


-70°

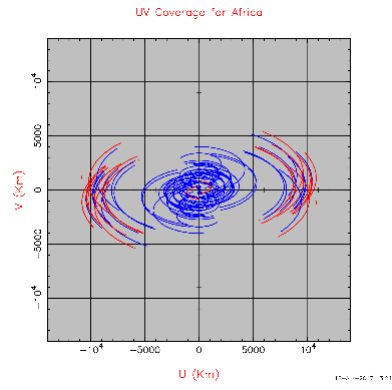


-90°

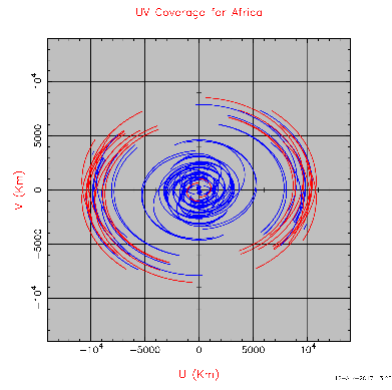
f) LBA + Namibia antennas



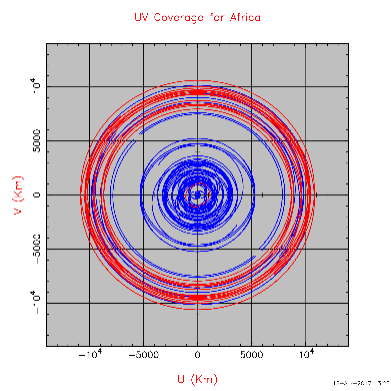
-10°



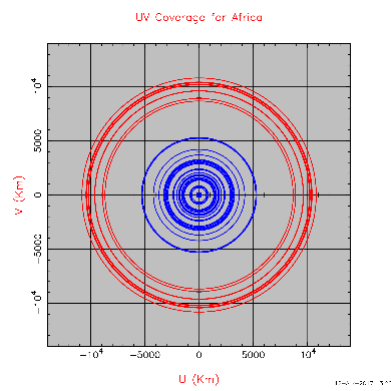
-30°



-50°

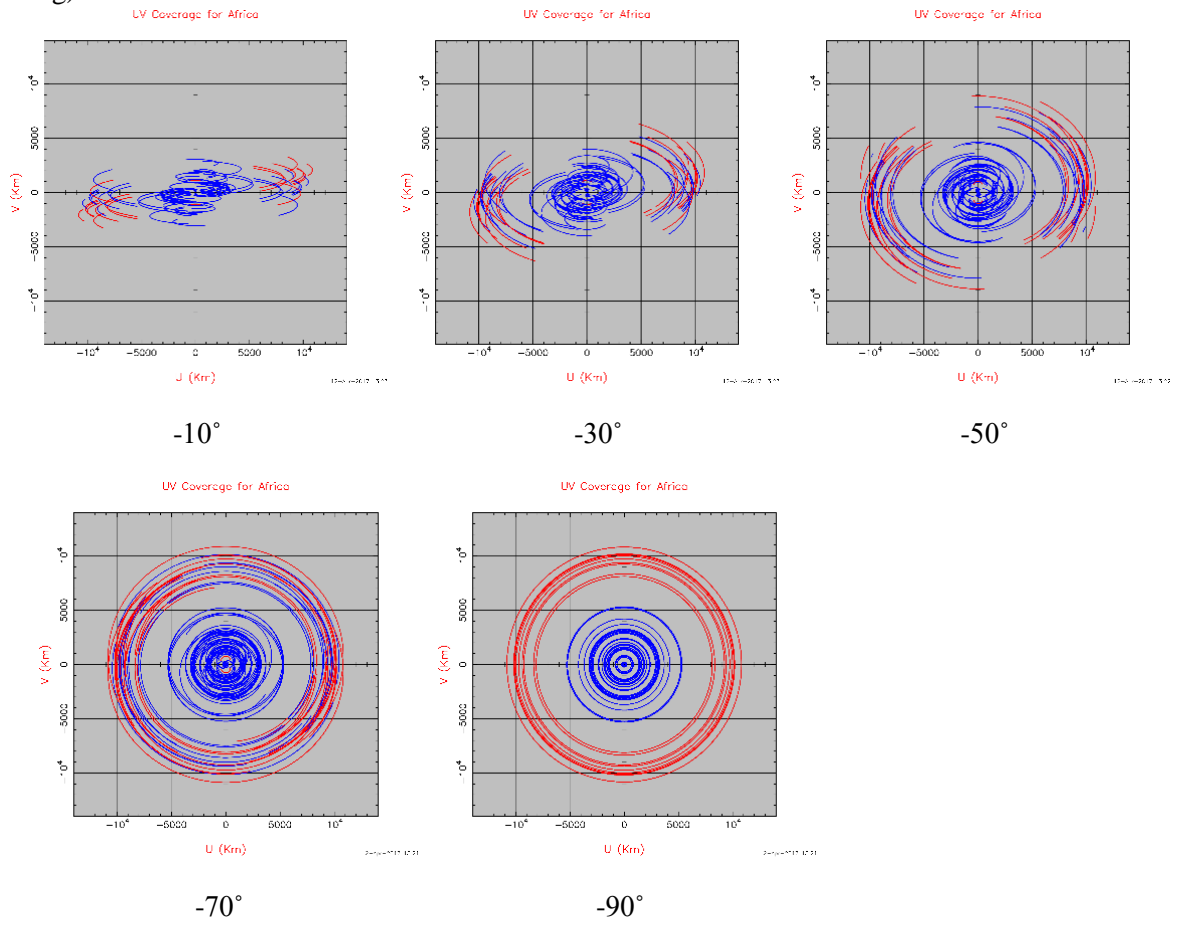


-70°

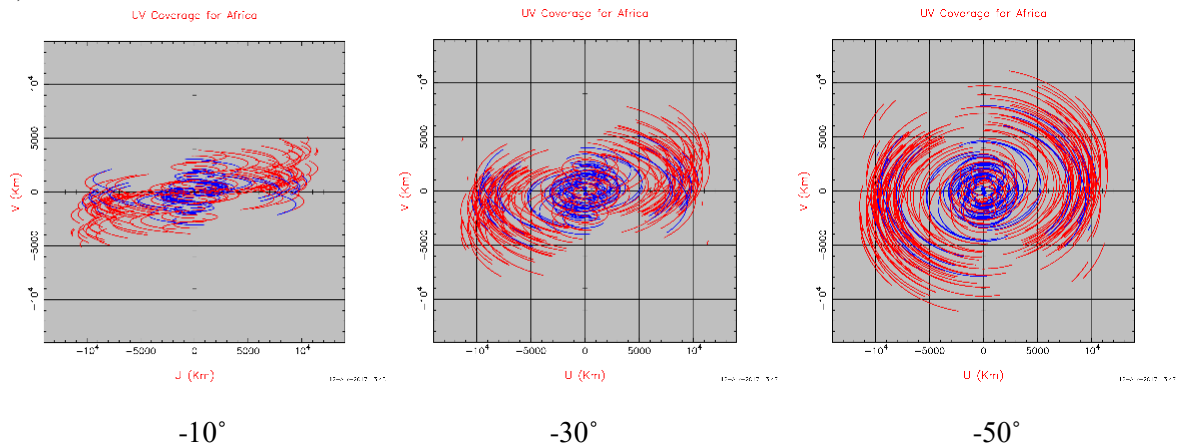


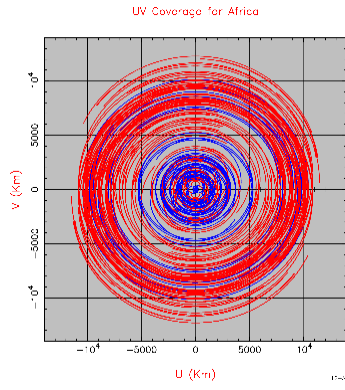
-90°

g) LBA + Zambia antenna

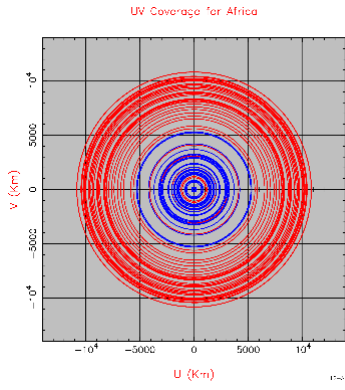


h) LBA + AVN1 antennas



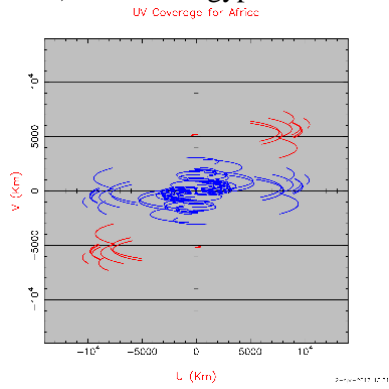


-70°

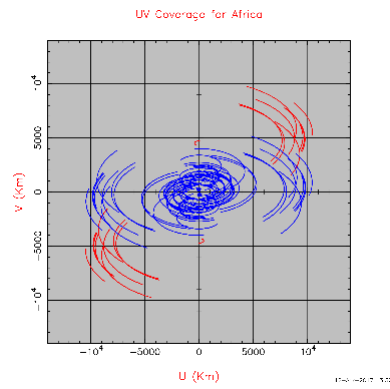


-90°

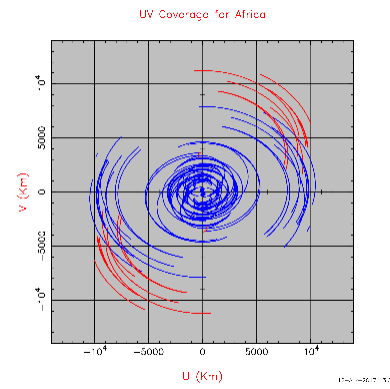
i) LBA + Egypt antenna



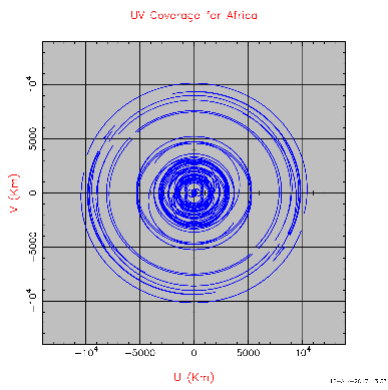
-10°



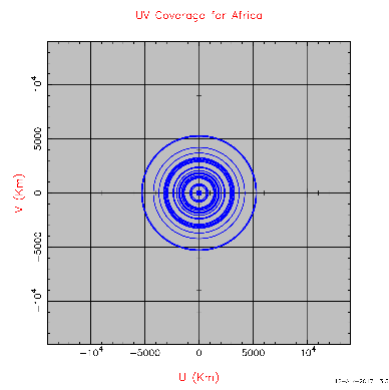
-30°



-50°

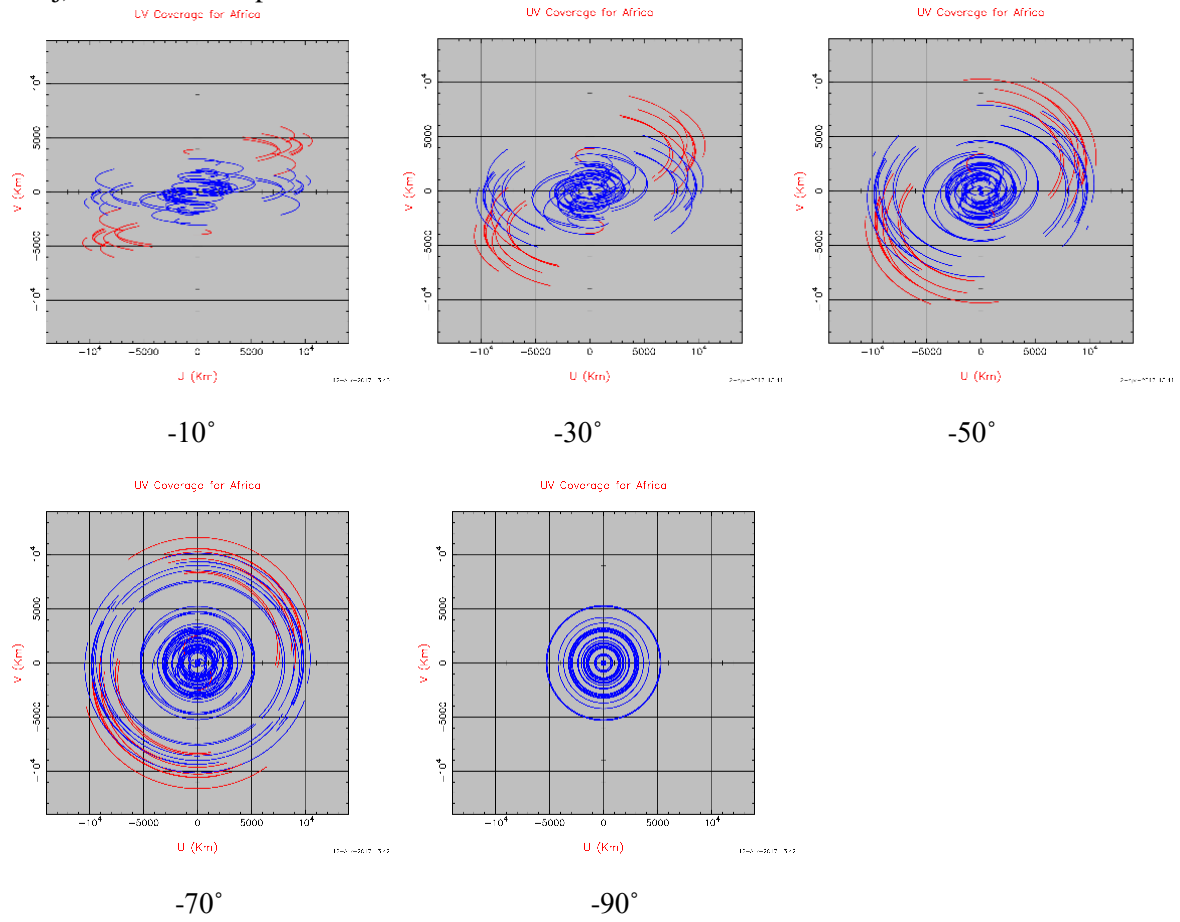


-70°

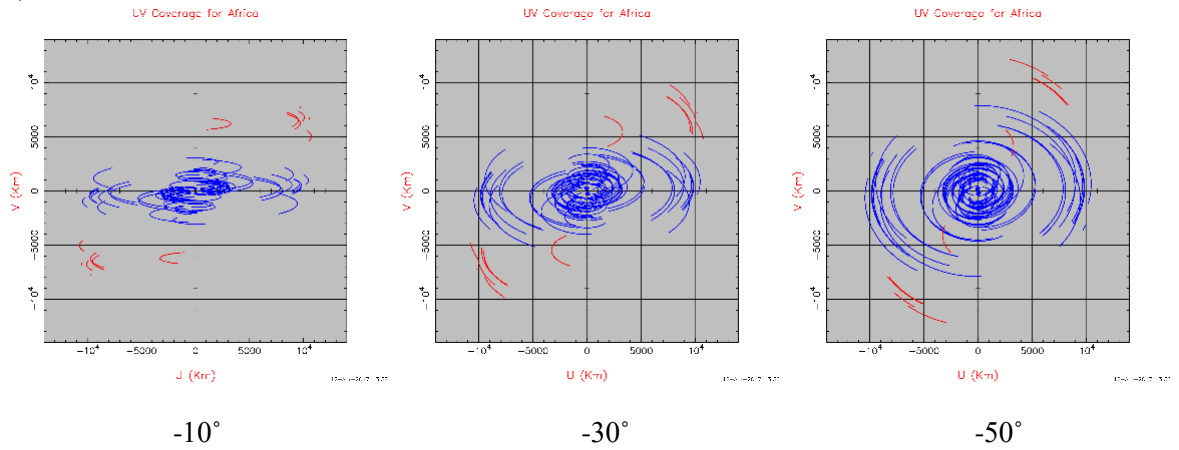


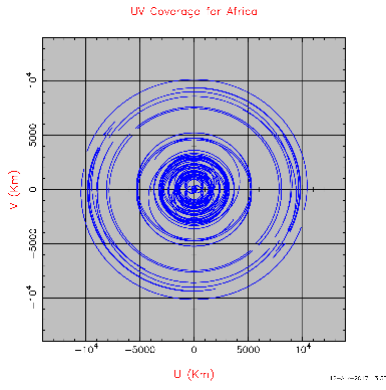
-90°

j) LBA + Ethiopia antenna

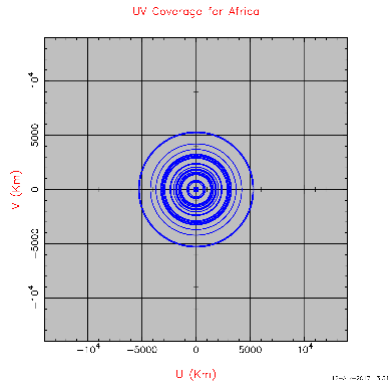


k) LBA + Morocco antenna



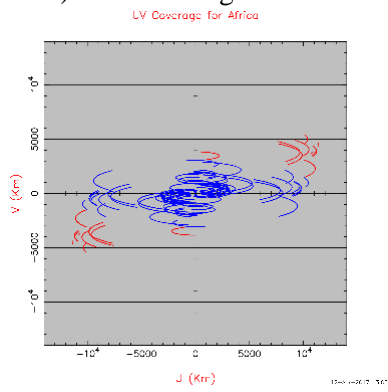


-70°

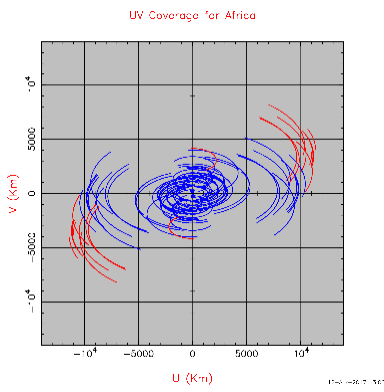


-90°

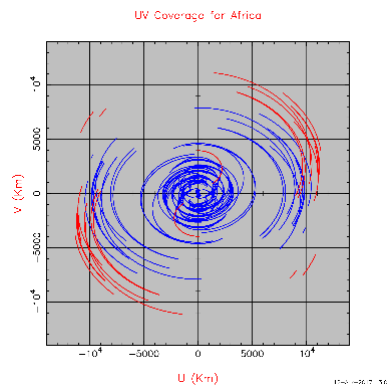
1) LBA + Nigeria antenna



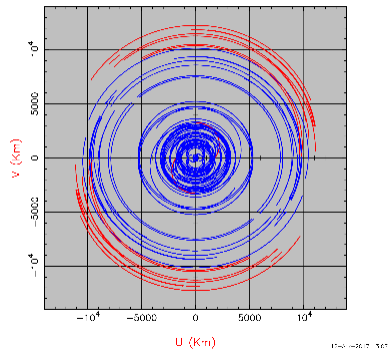
-10°



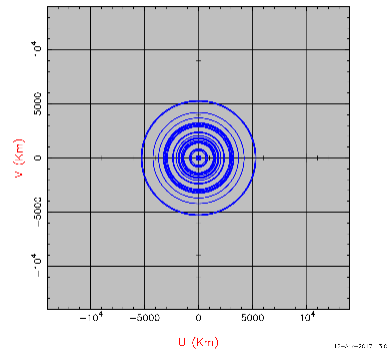
-30°



-50°

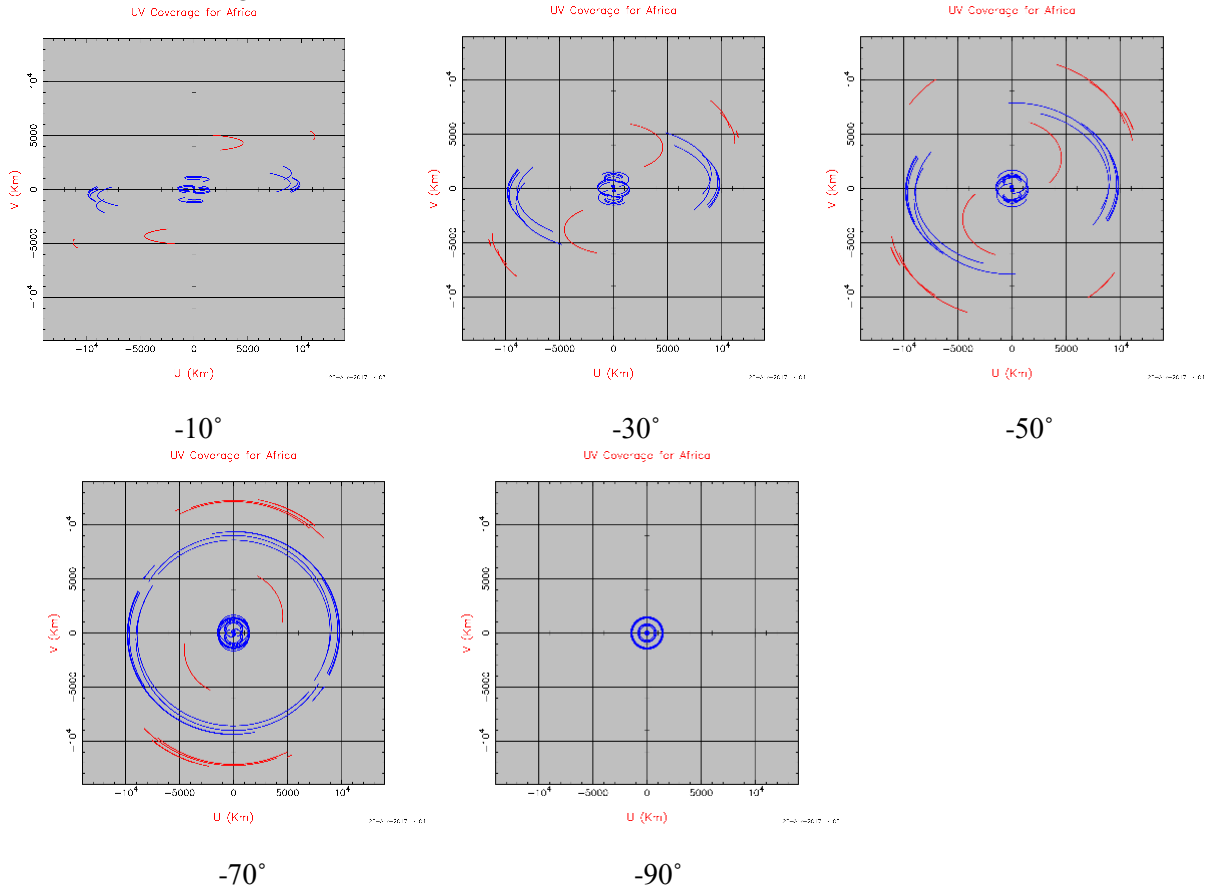


-70°

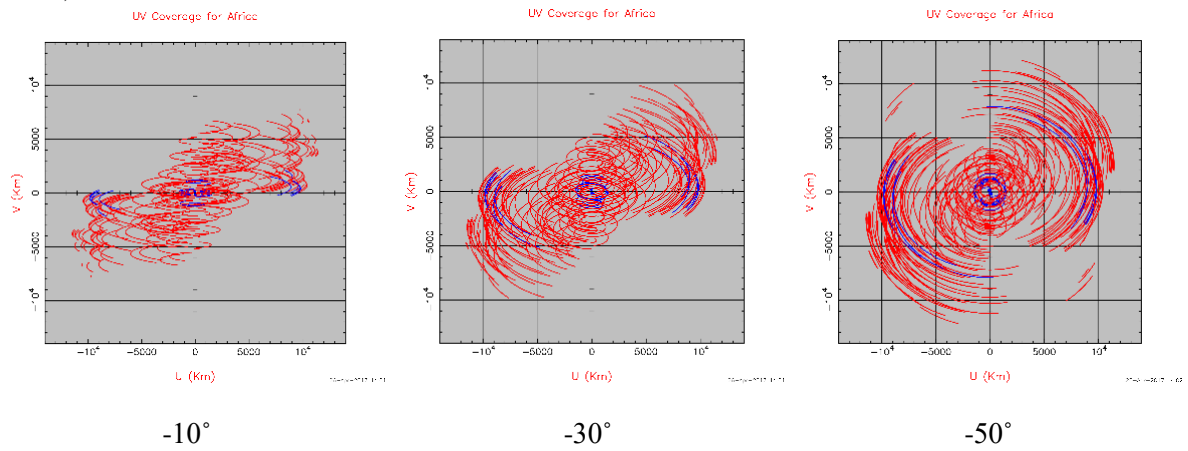


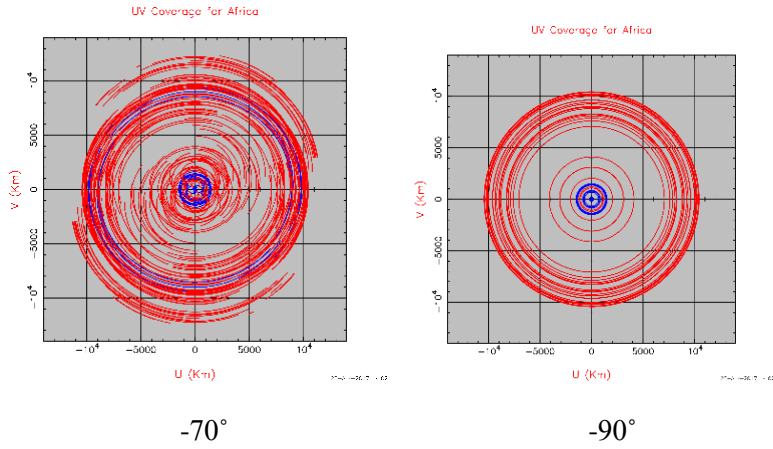
-90°

m) LBA + Senegal antennas



n) LBA + AVN Antennas

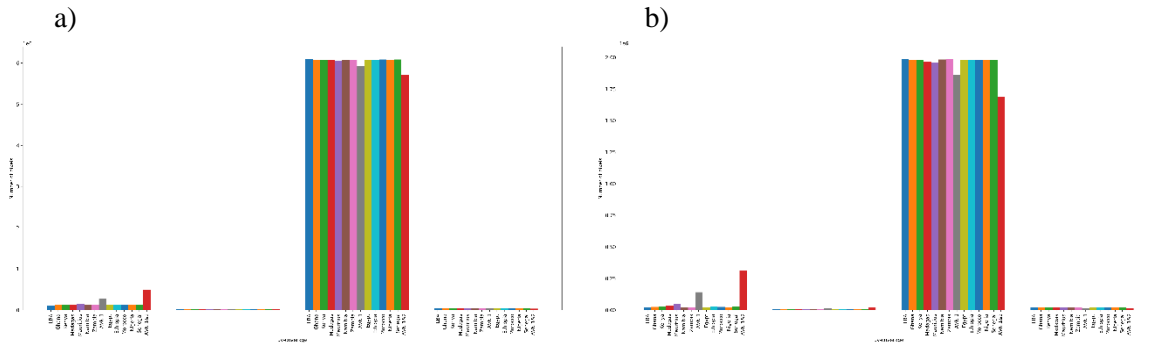




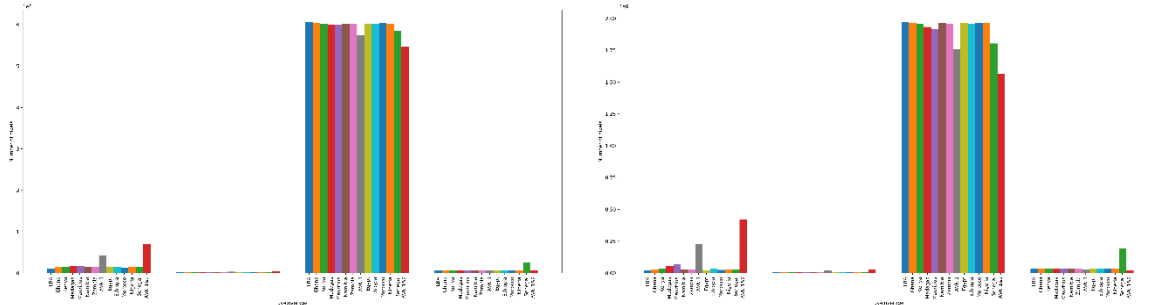
2. U-V Coverage Histogram for LBA + AVN antennas at K-band

The description of the histograms is given in the previous section.

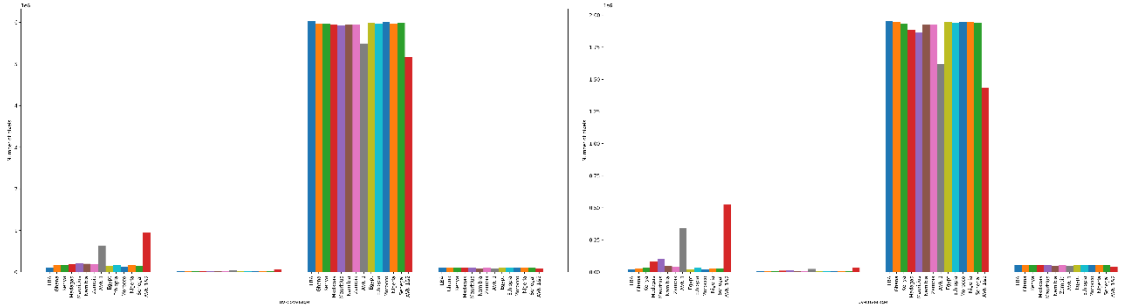
i) At a declination of minus 10 degrees



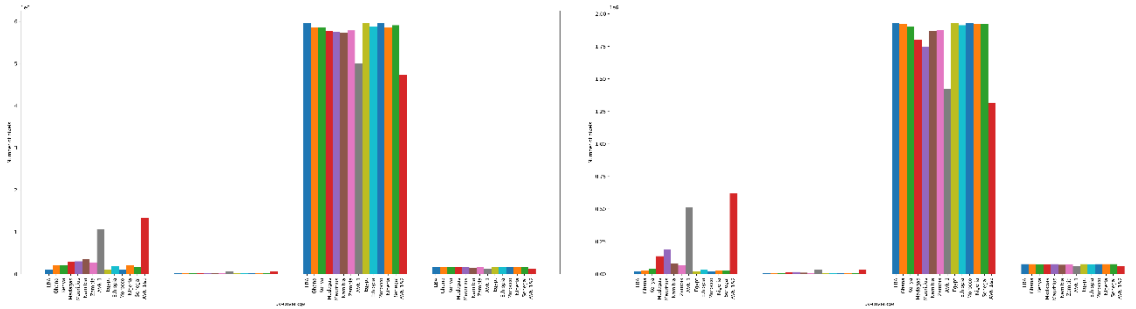
ii) At a declination of minus 30 degrees



iii) At a declination of minus 50 degrees



iv) At a declination of minus 70 degrees



v) At a declination of minus 90 degrees

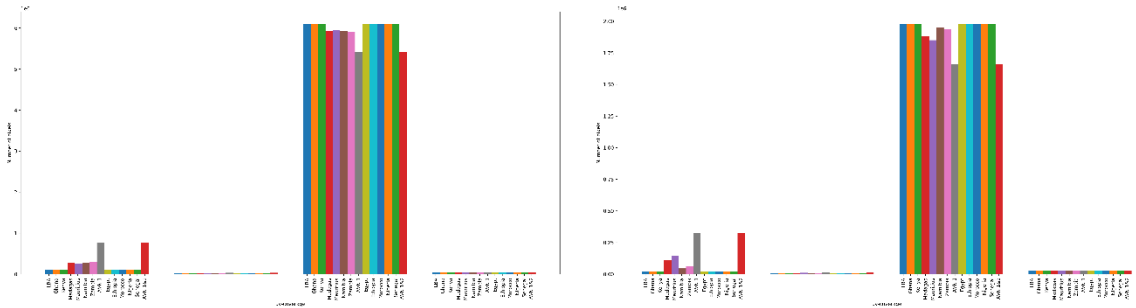
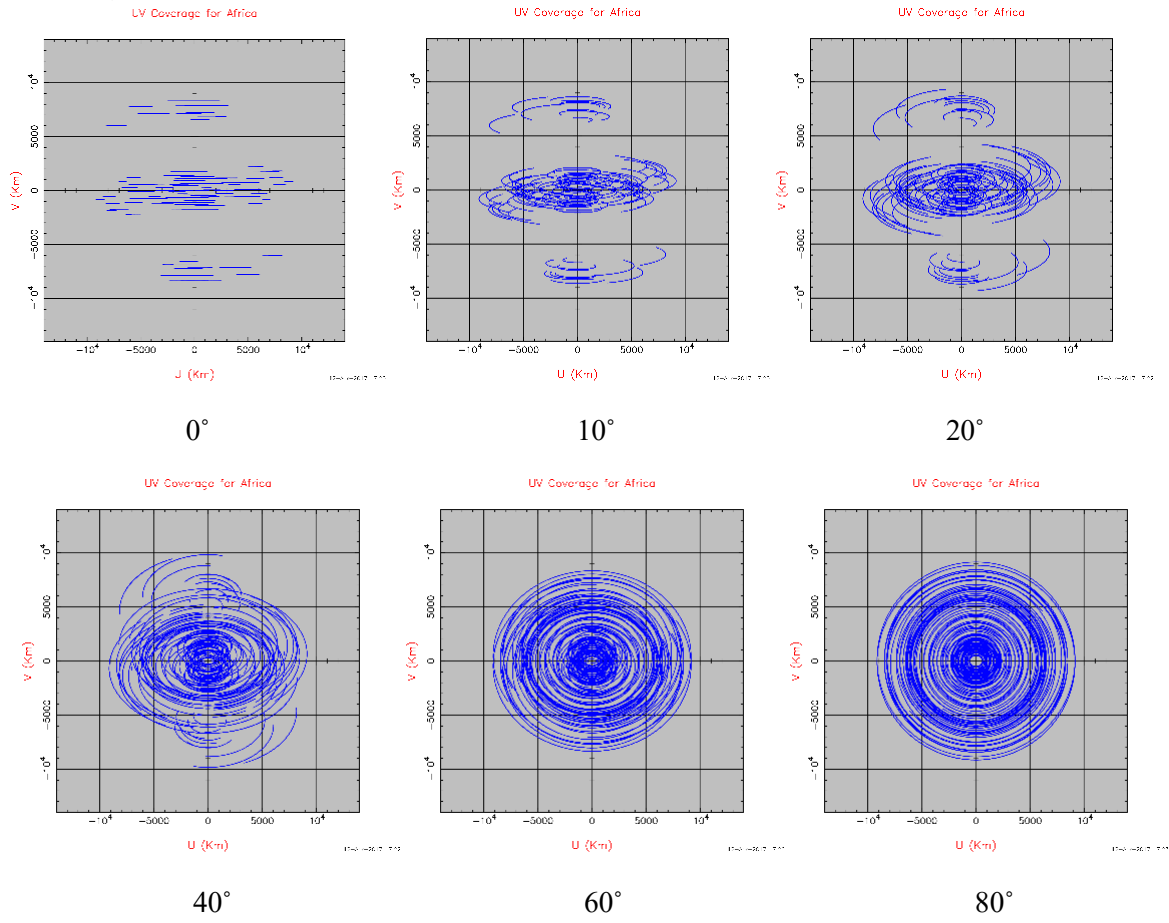
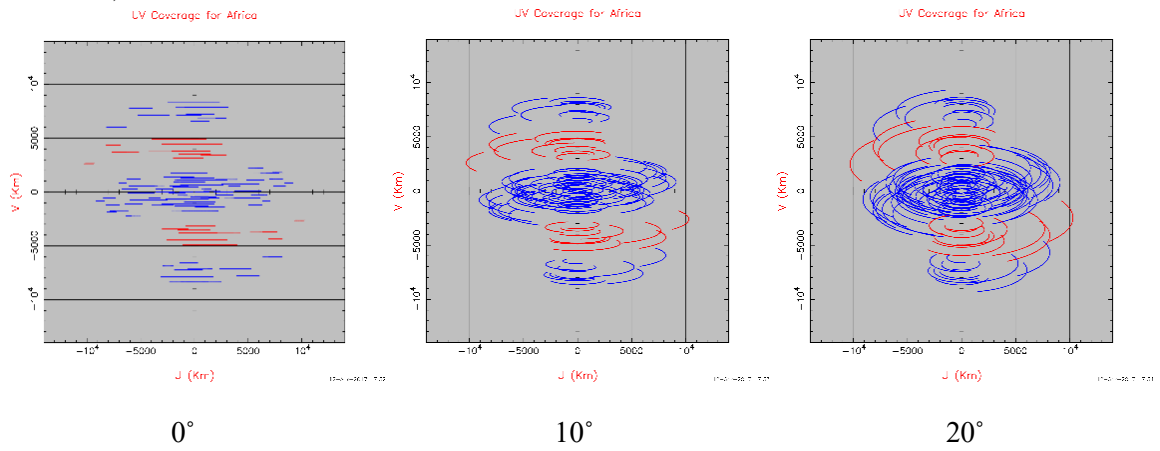


Table 4.13 (continued): U-V Coverage Plots for EVN + AVN antennas at X-Band

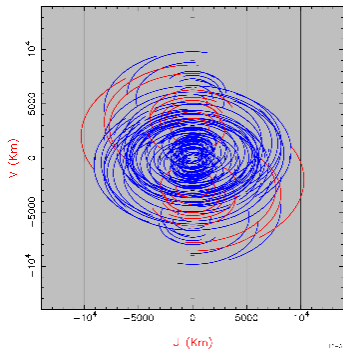
a) EVN Antennas



b) EVN + Ghana antenna

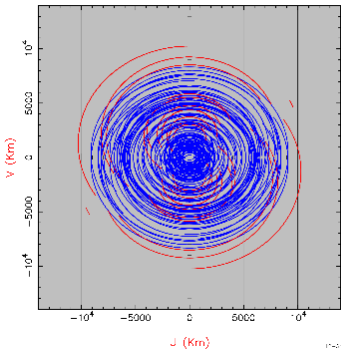


JV Coverage for Africa



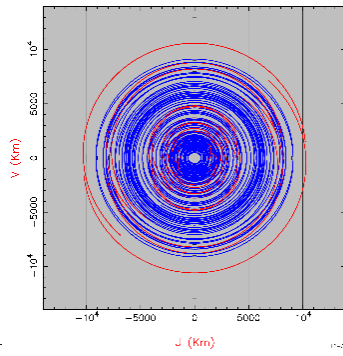
40°

JV Coverage for Africa



60°

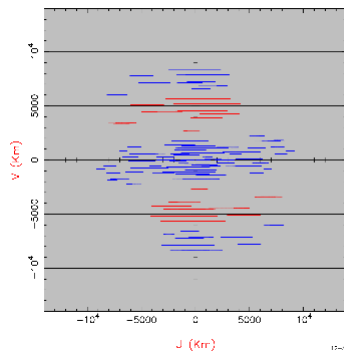
JV Coverage for Africa



80°

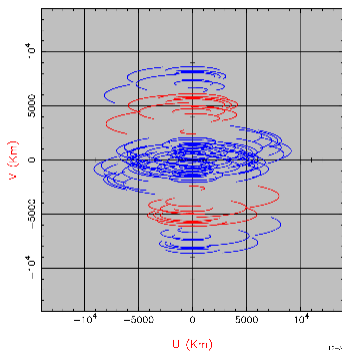
c) EVN + Kenya antenna

LV Coverage for Africa



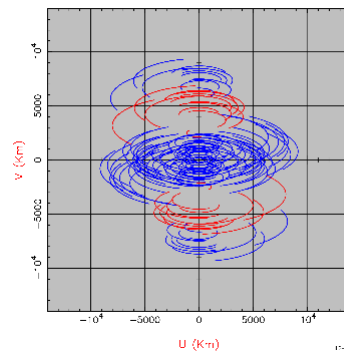
0°

UV Coverage for Africa



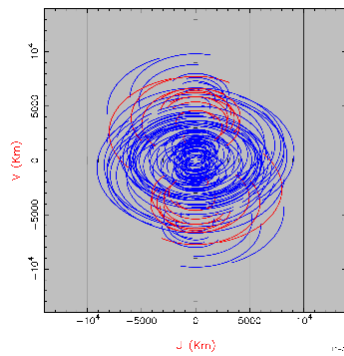
10°

UV Coverage for Africa



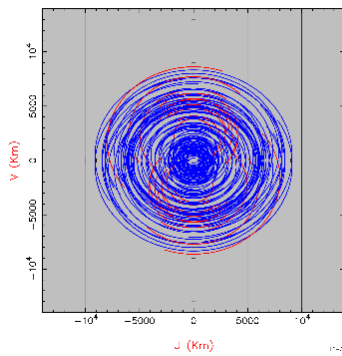
20°

JV Coverage for Africa



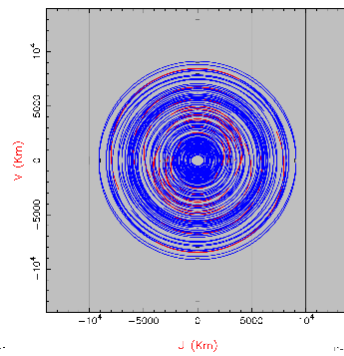
40°

JV Coverage for Africa



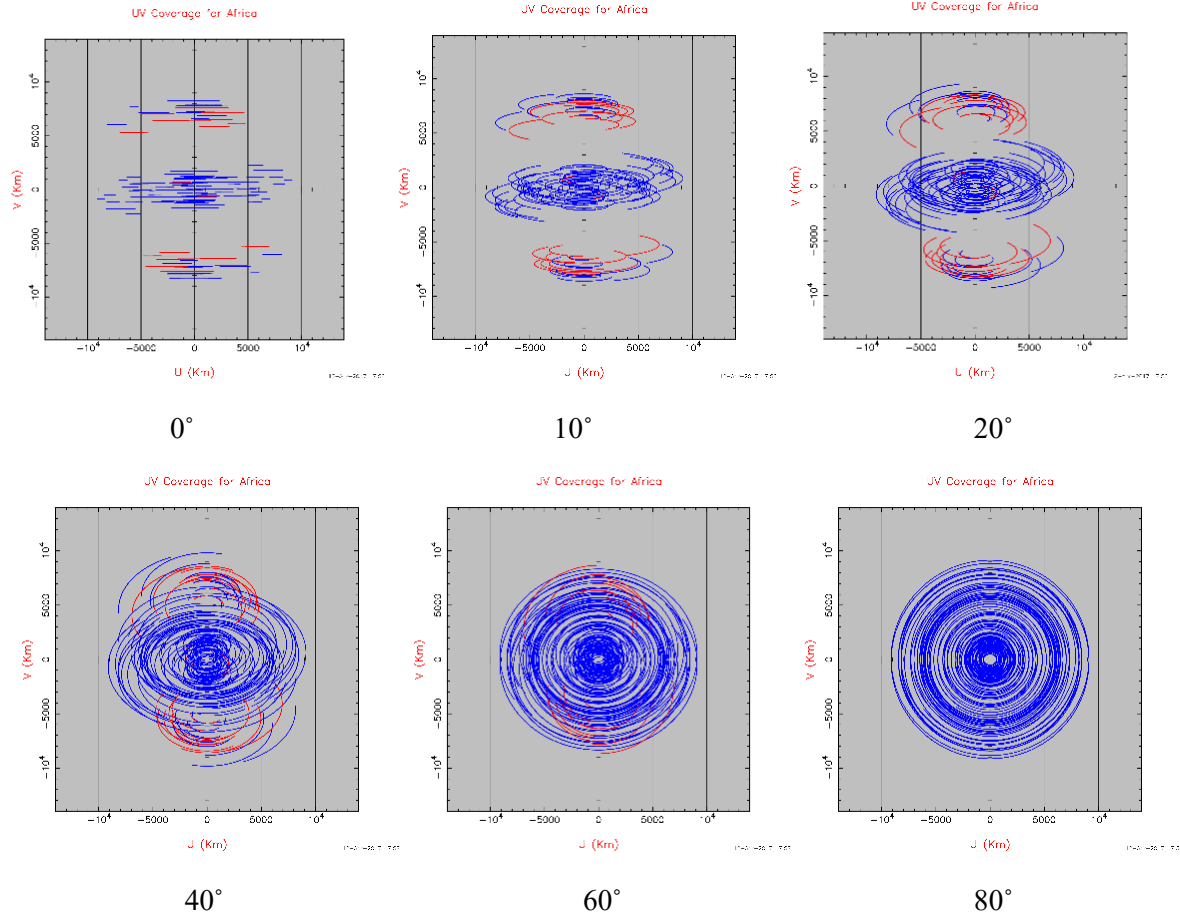
60°

JV Coverage for Africa

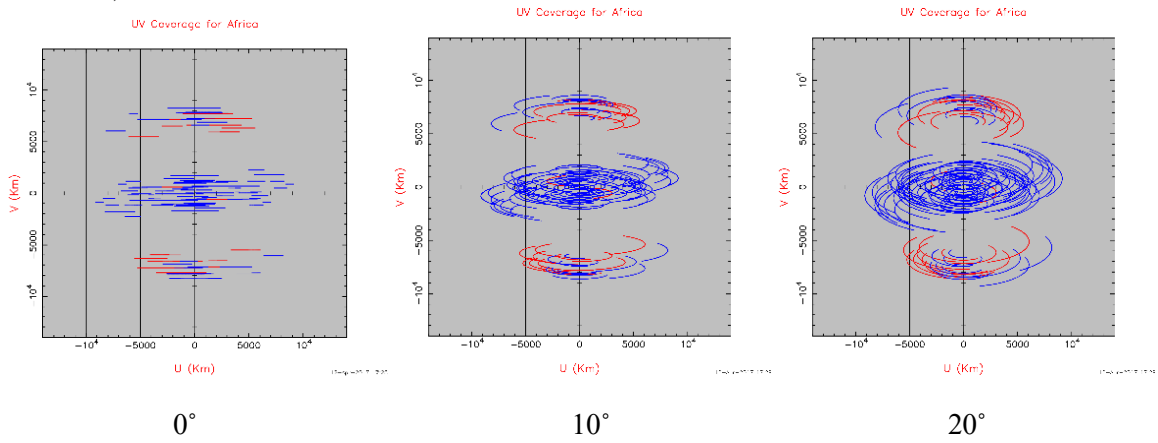


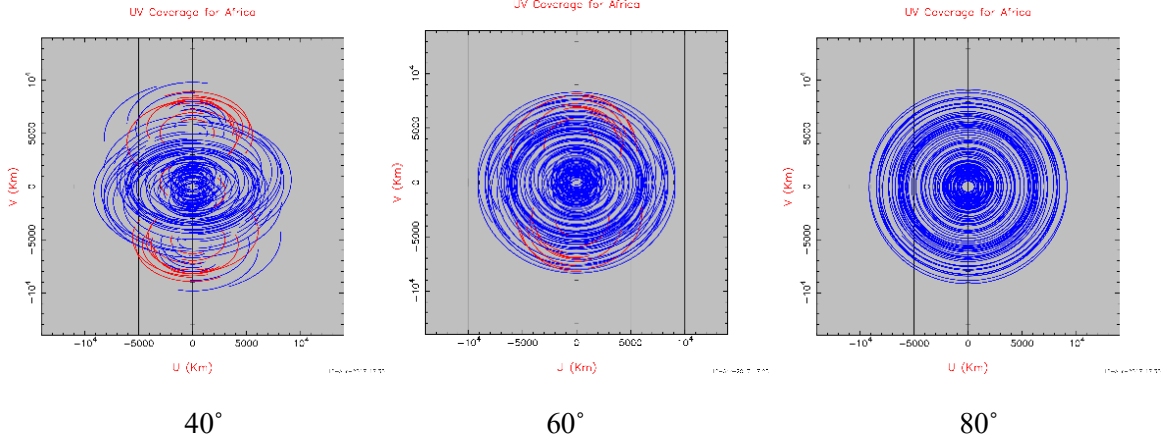
80°

d) EVN + Madagascar Antenna

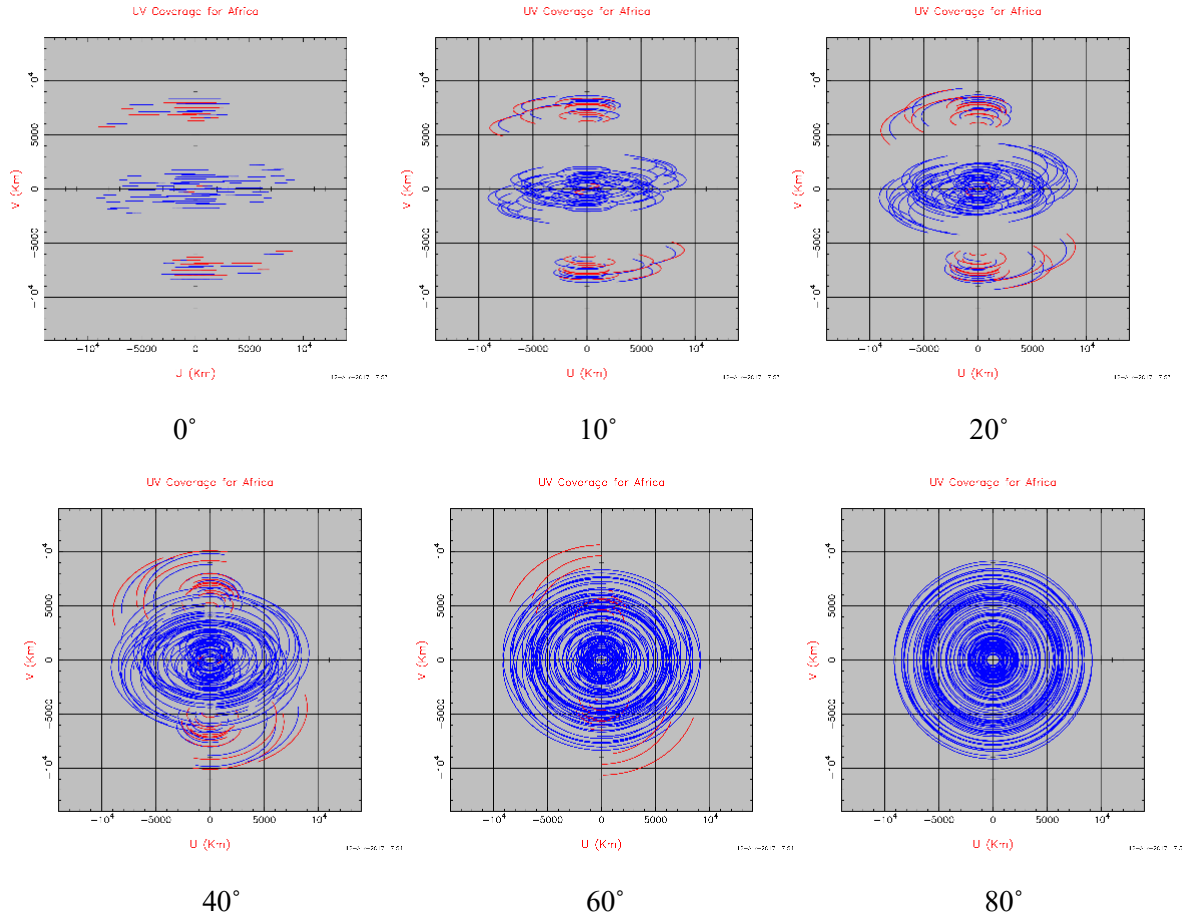


e) EVN + Mauritius antennas

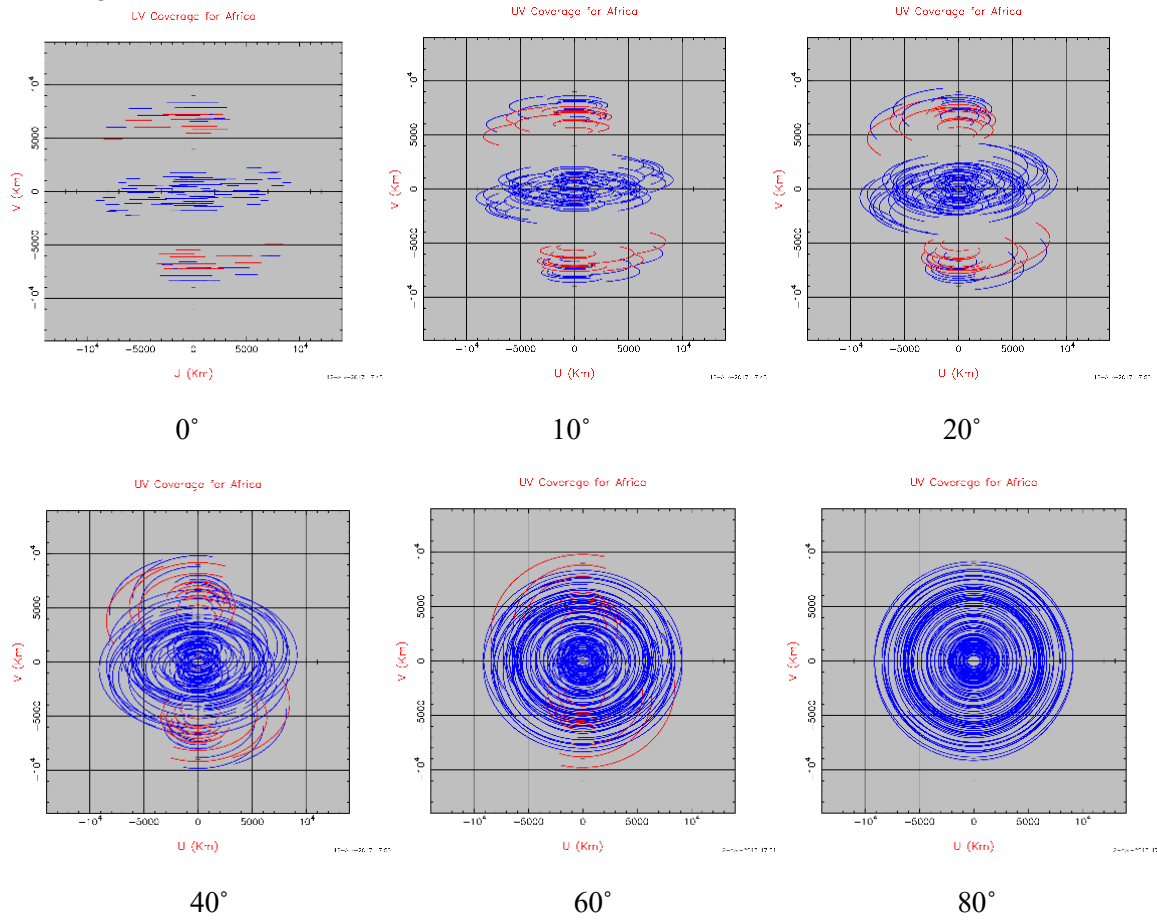




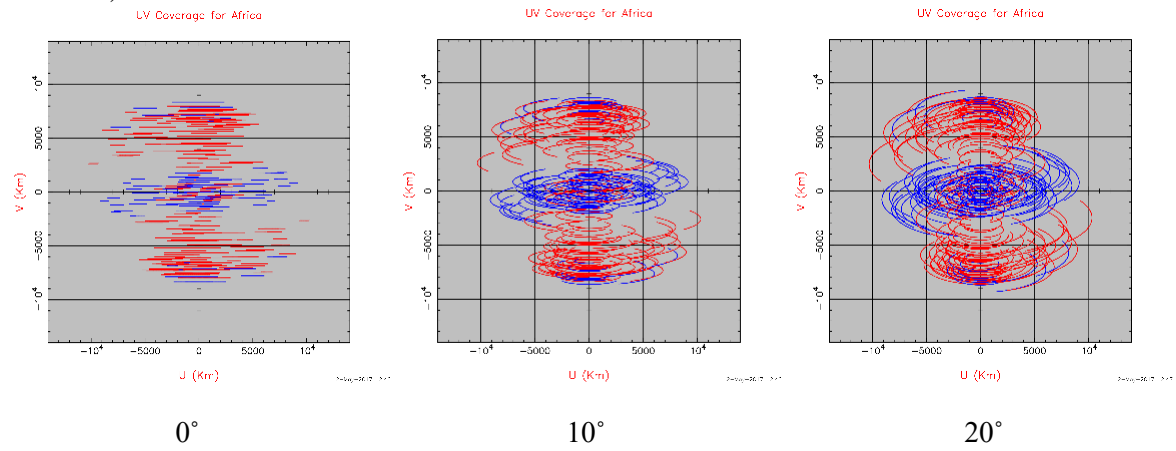
f) EVN + Namibia antenna

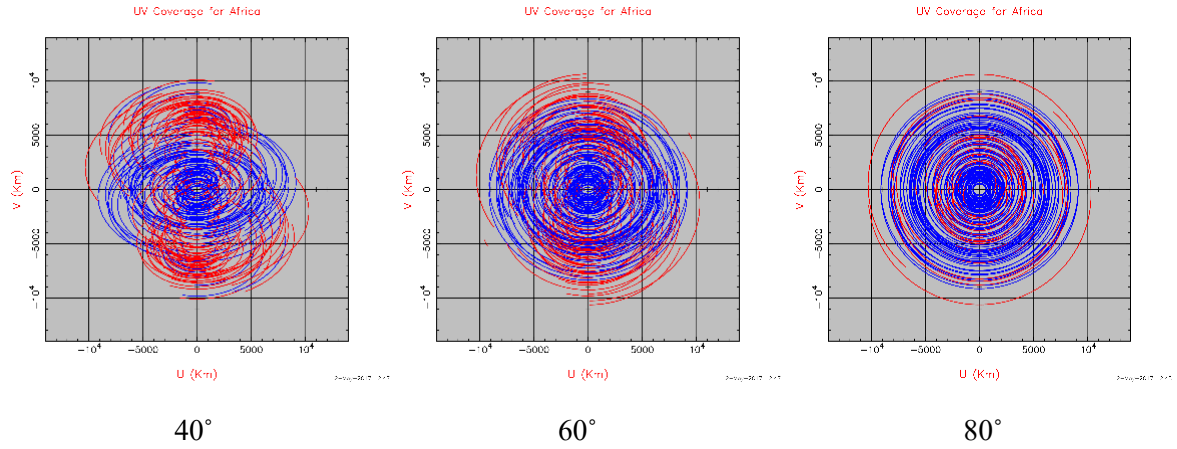


g) EVN + Zambia antenna

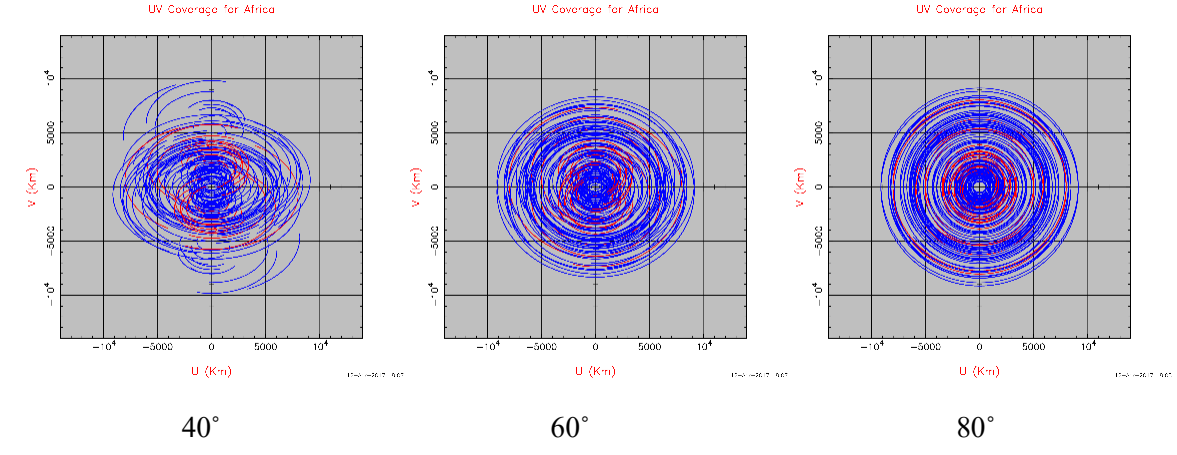
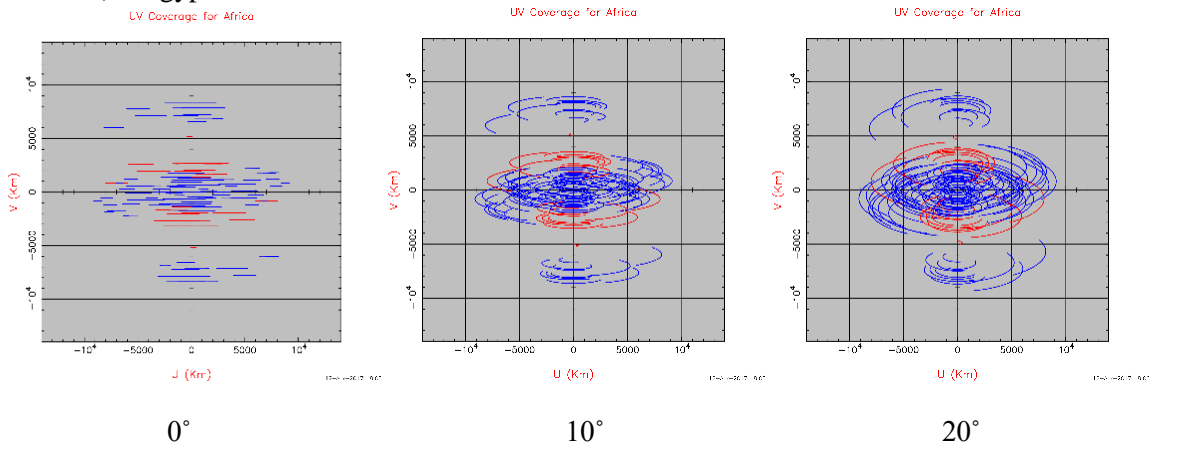


h) EVN + AVN1 antennas

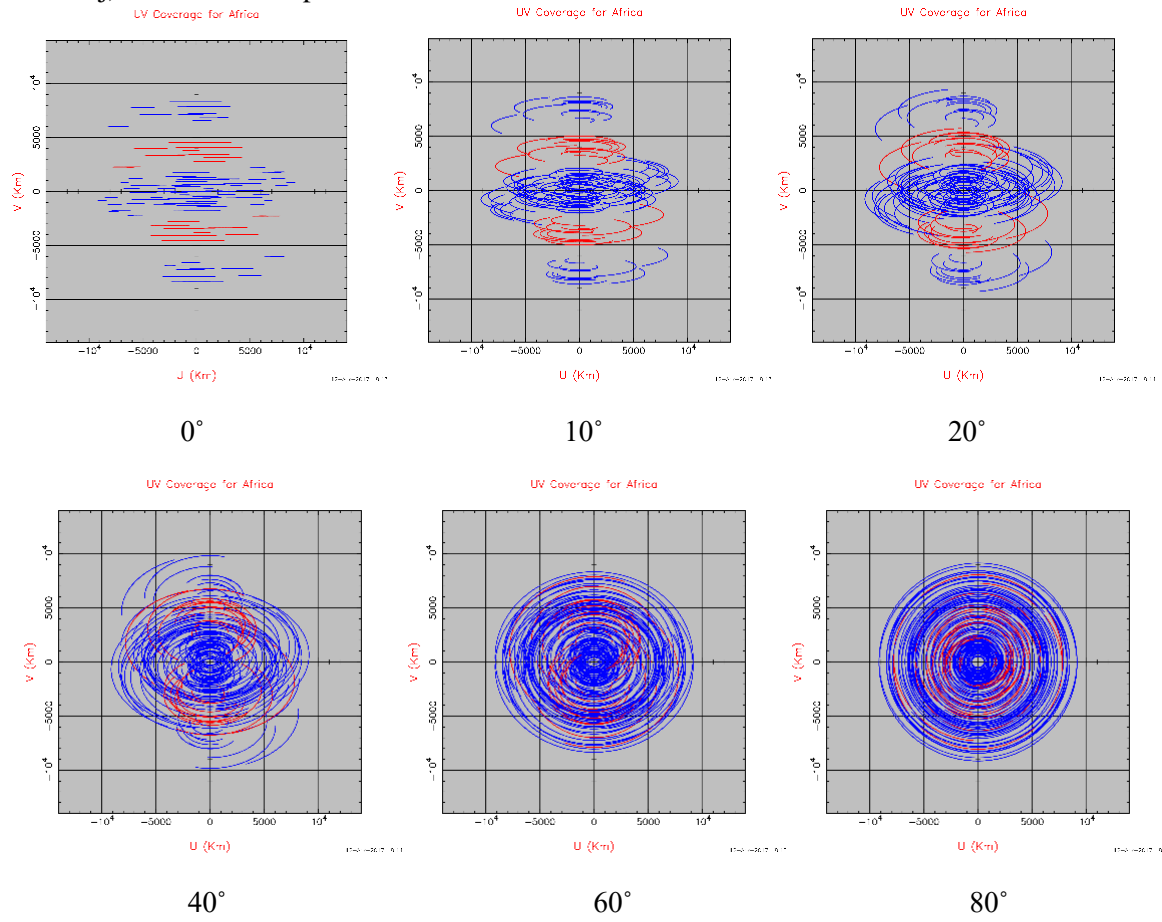




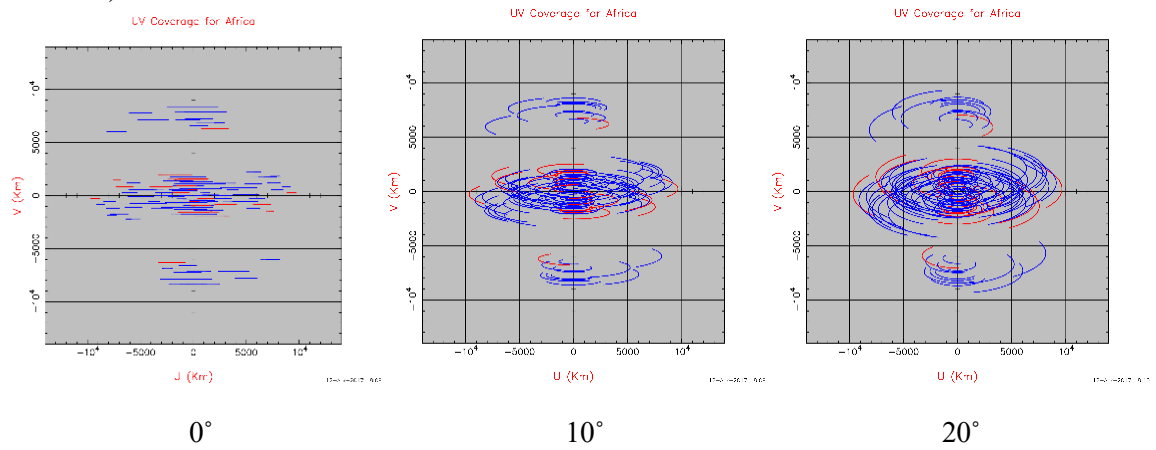
i) Egypt

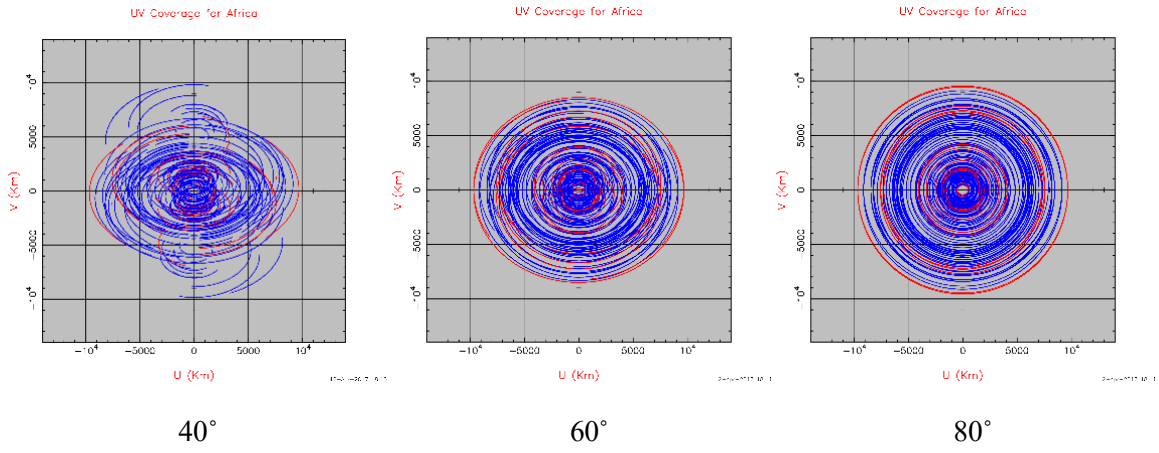


j) EVN + Ethiopia antenna

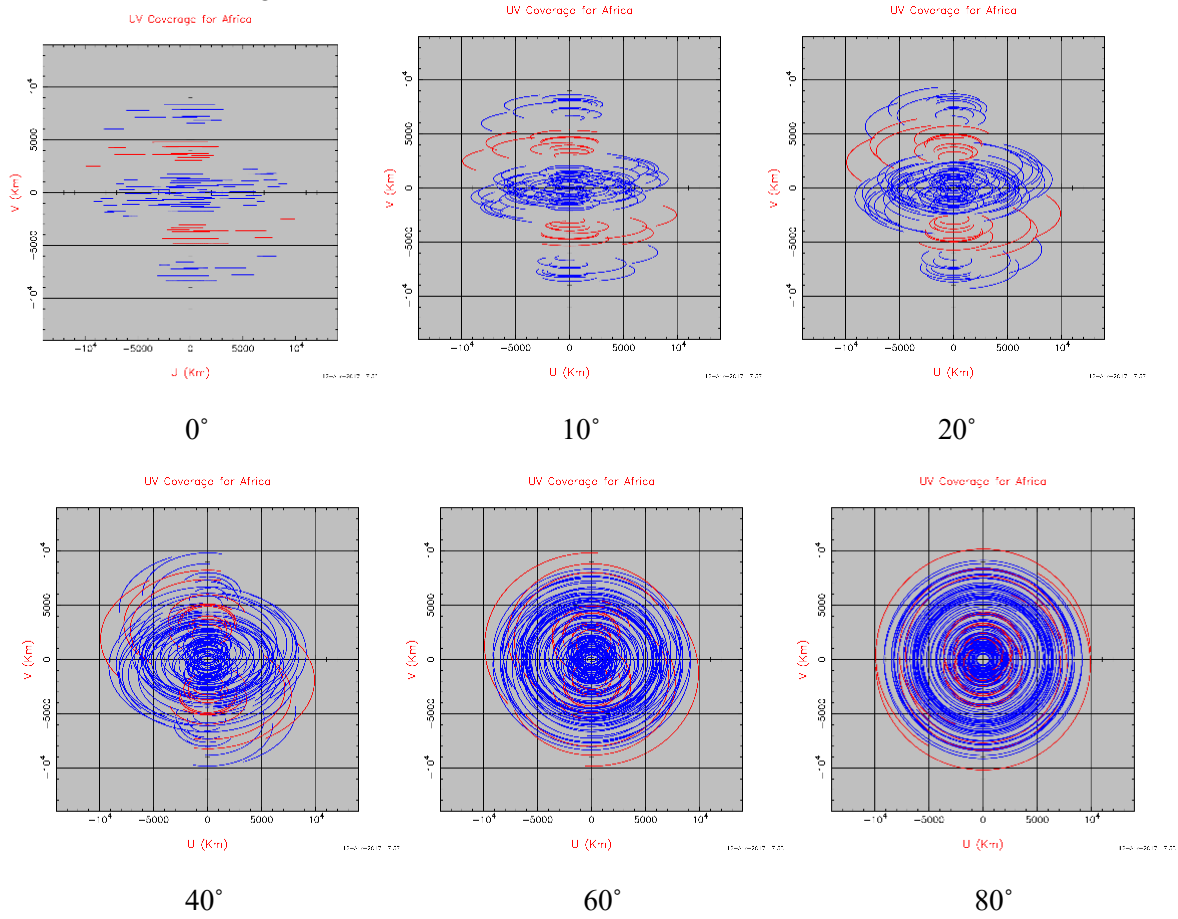


k) EVN + Morocco antenna

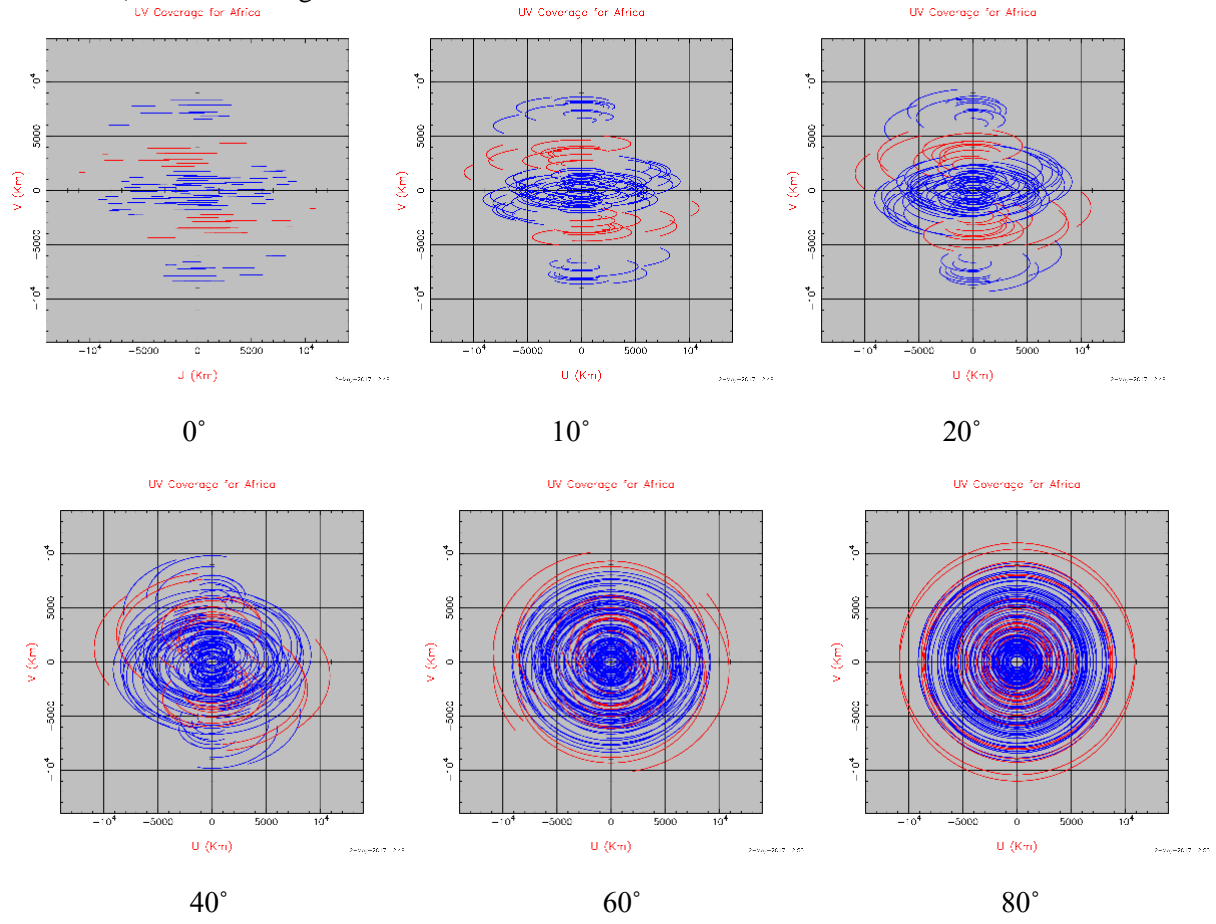




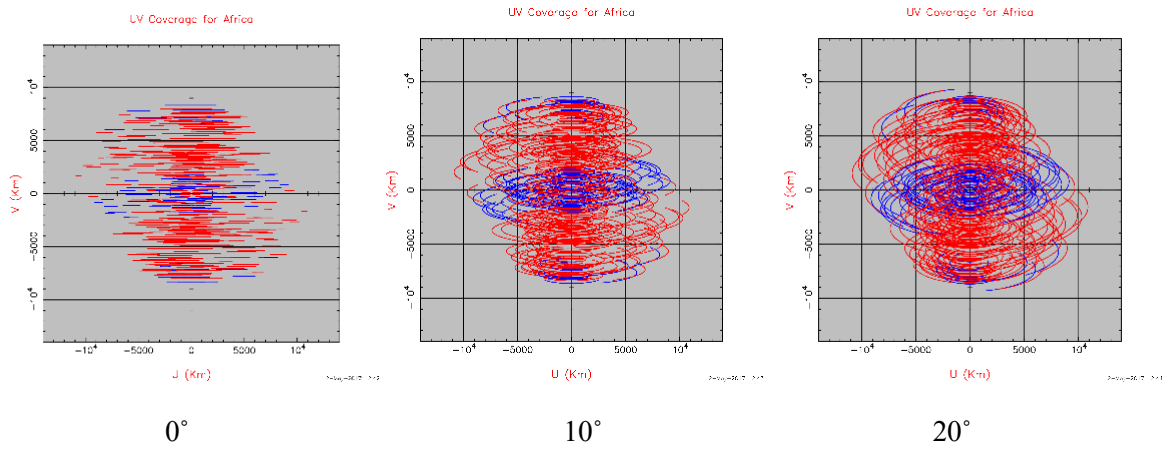
1) EVN + Nigeria antenna

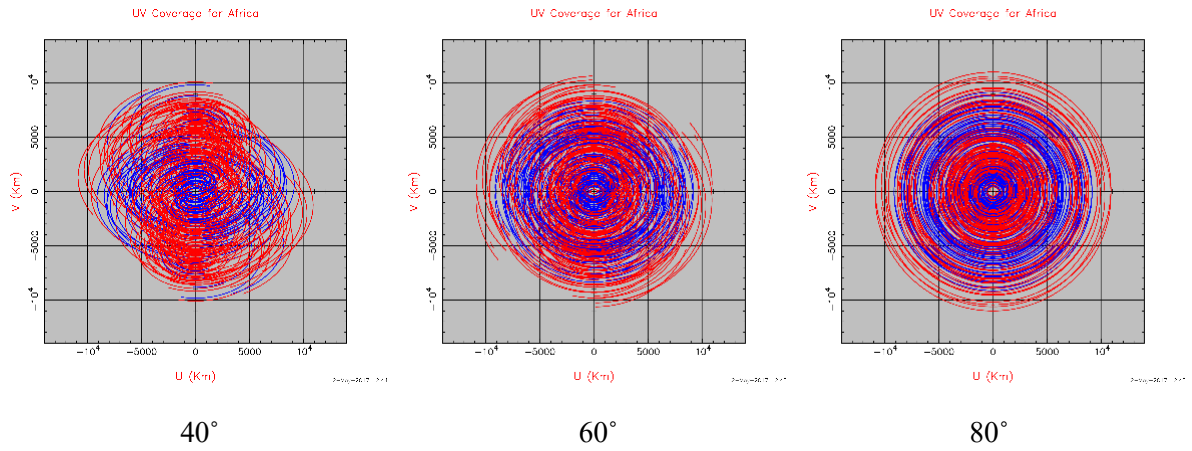


m) EVN + Senegal antennas



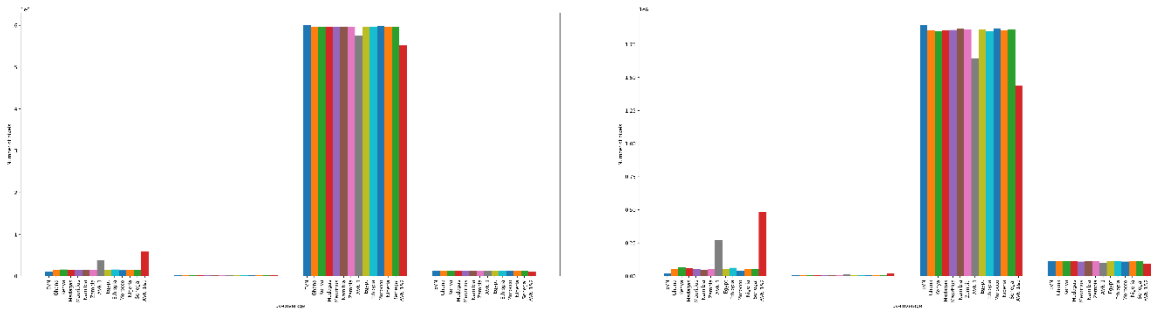
n) EVN + AVN antennas



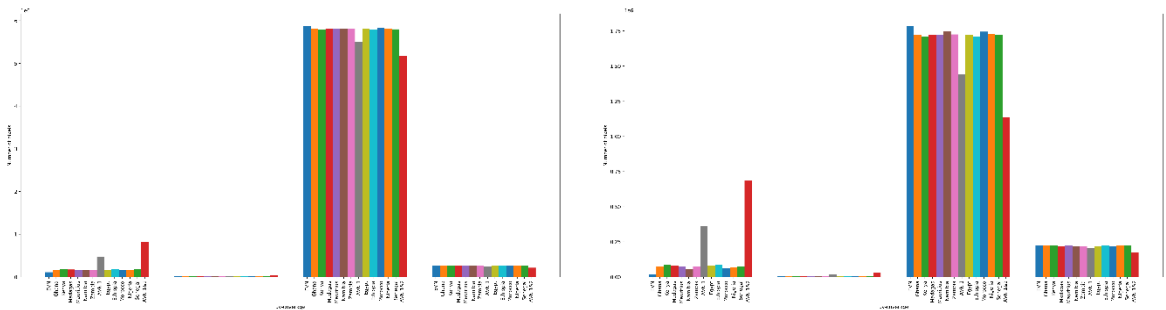


2. U-V Coverage Histograms for the EVN + AVN antennas
 The description of the histograms similar to histograms in 4.8 (a) and 4.9 (a).

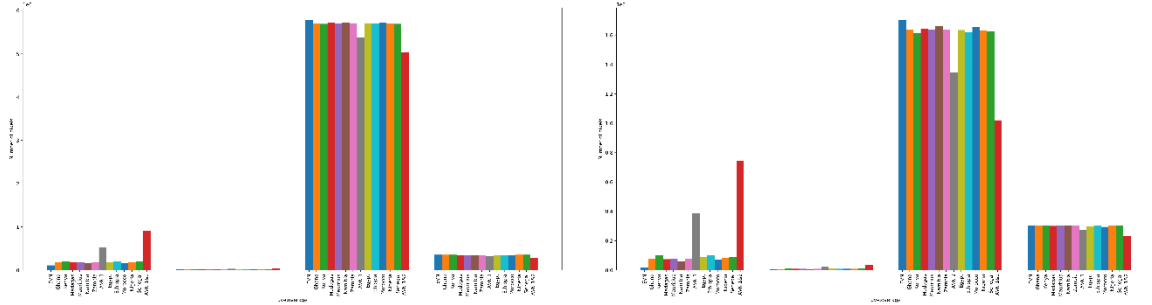
i) At a declination of 0 degrees



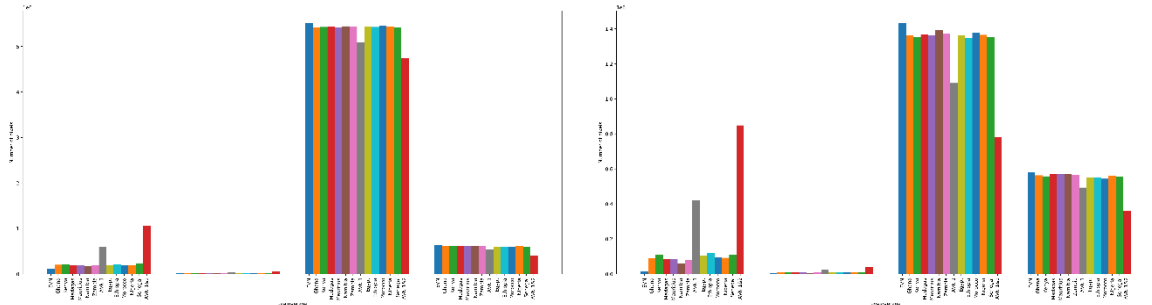
ii) At a declination of 10



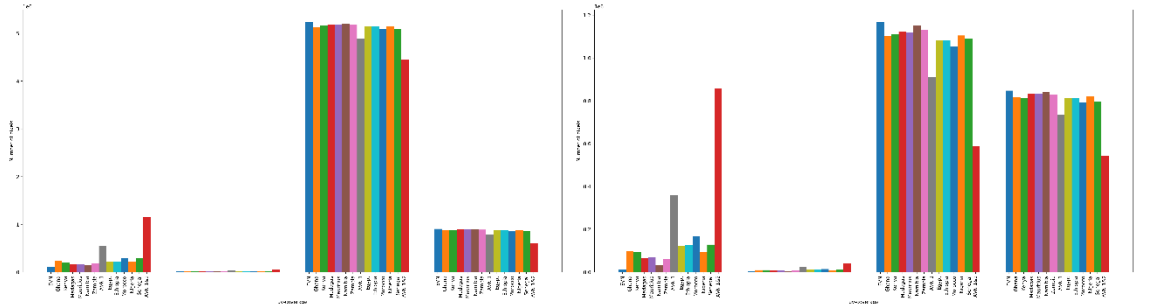
iii) At a declination of 20



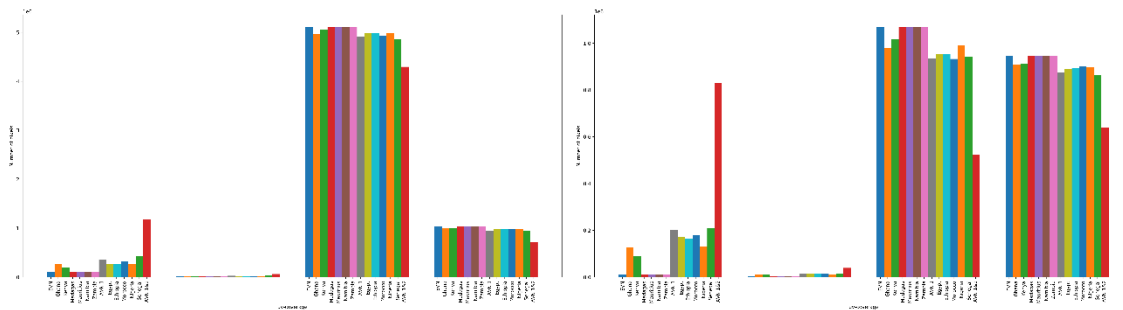
iv) At a declination of 40



v) At a declination of 60



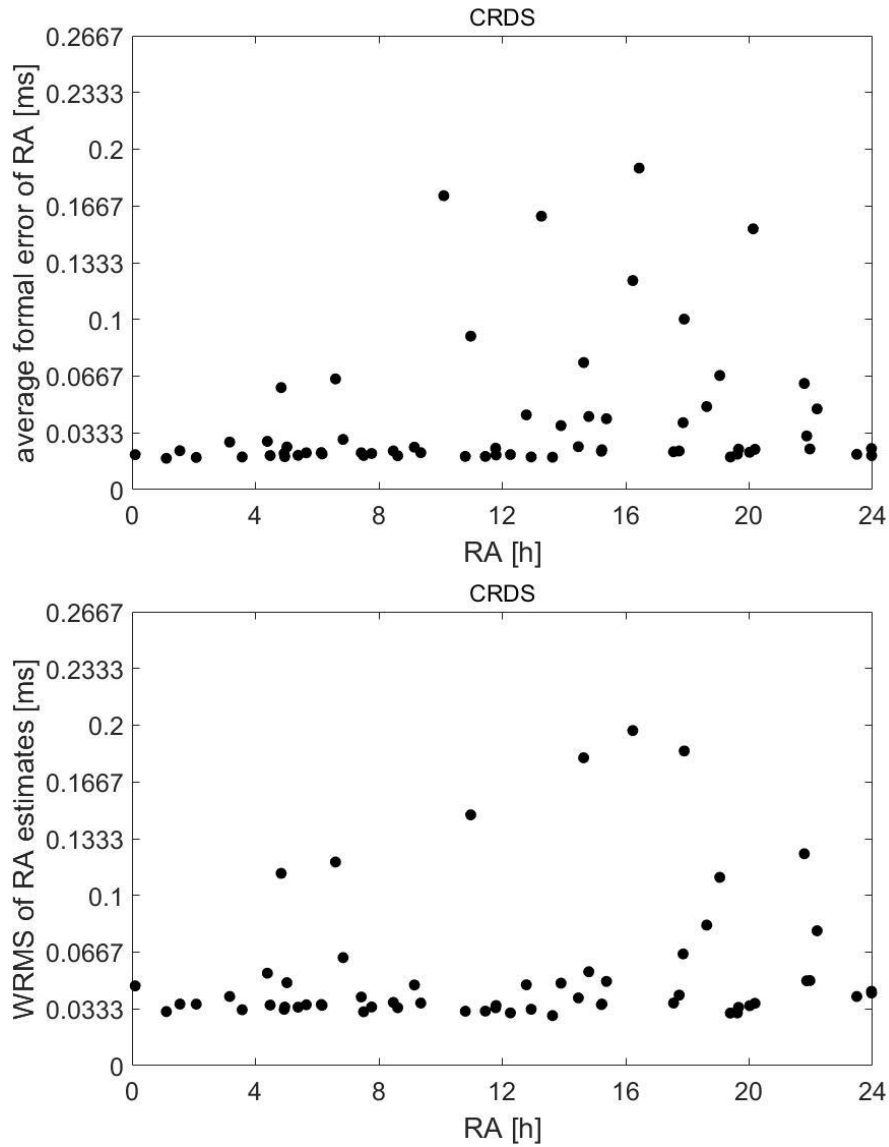
vi) At a declination of 80

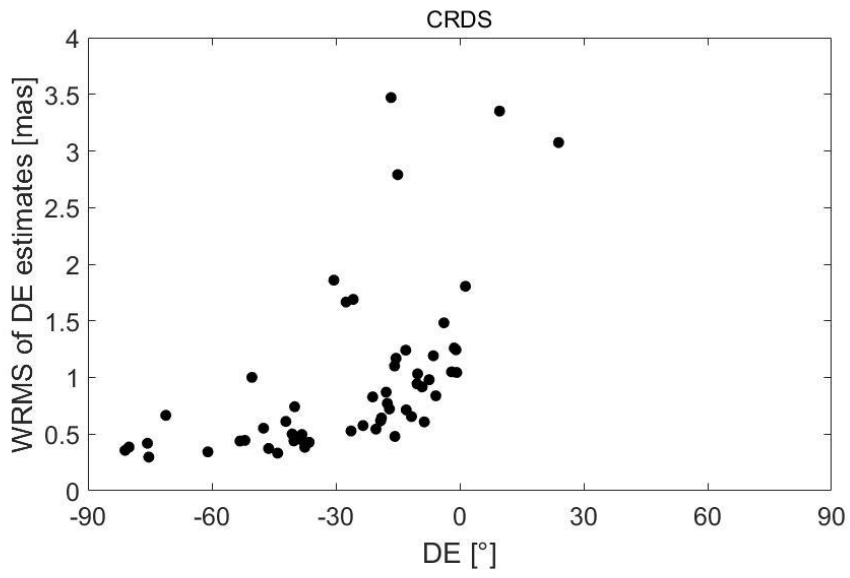
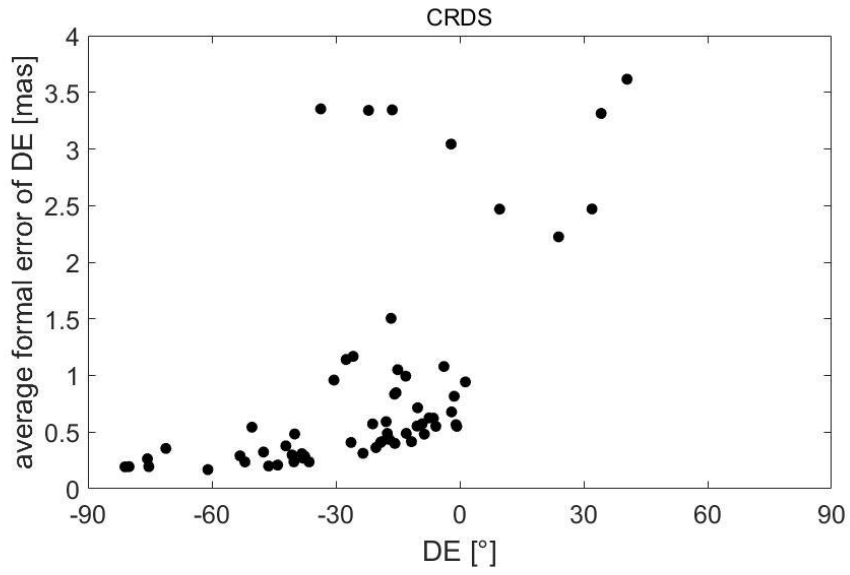


ASTROMETRIC RESULTS: Plots of RA and DE

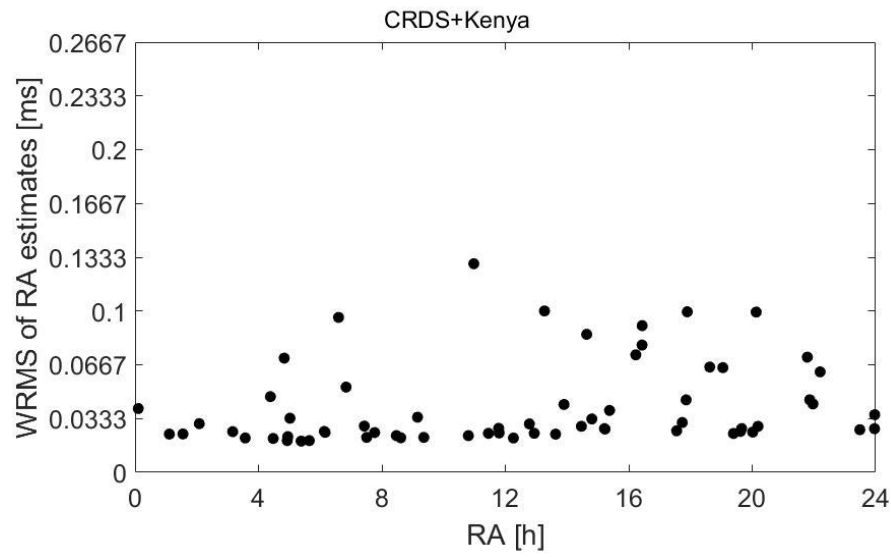
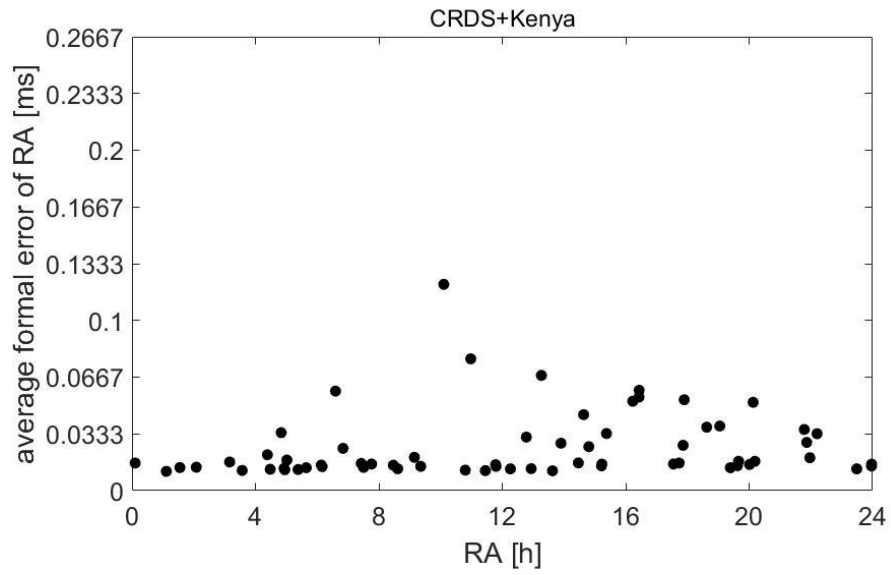
Table 4.21 (continued): Plots of Right Ascension (RA) and Declination (DE).

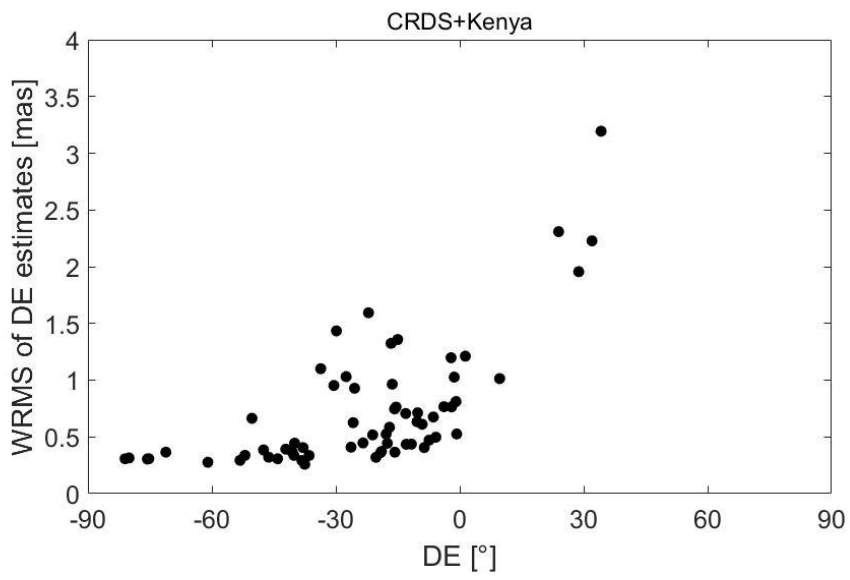
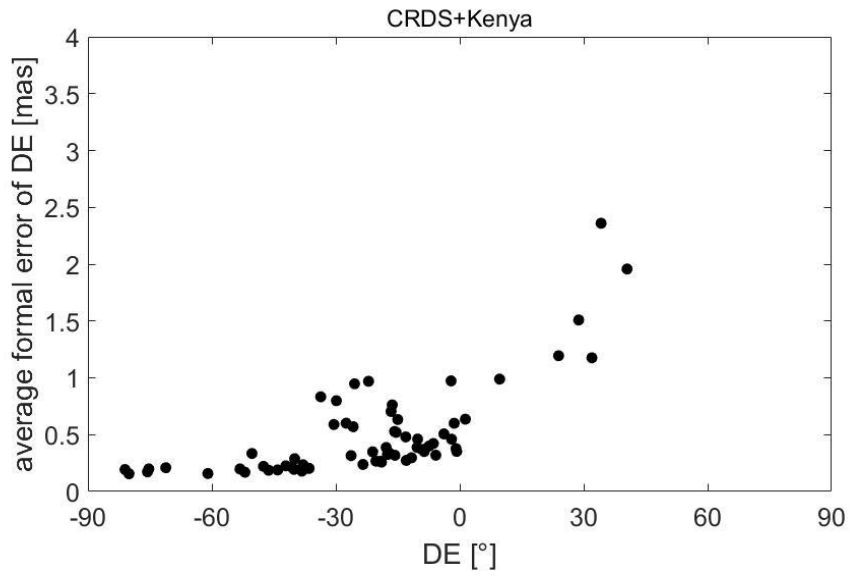
1. CRDS



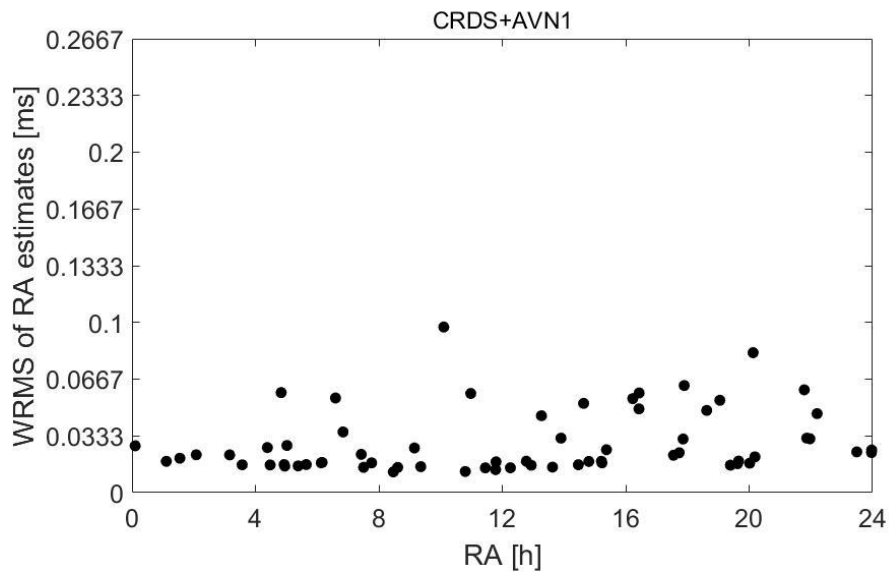
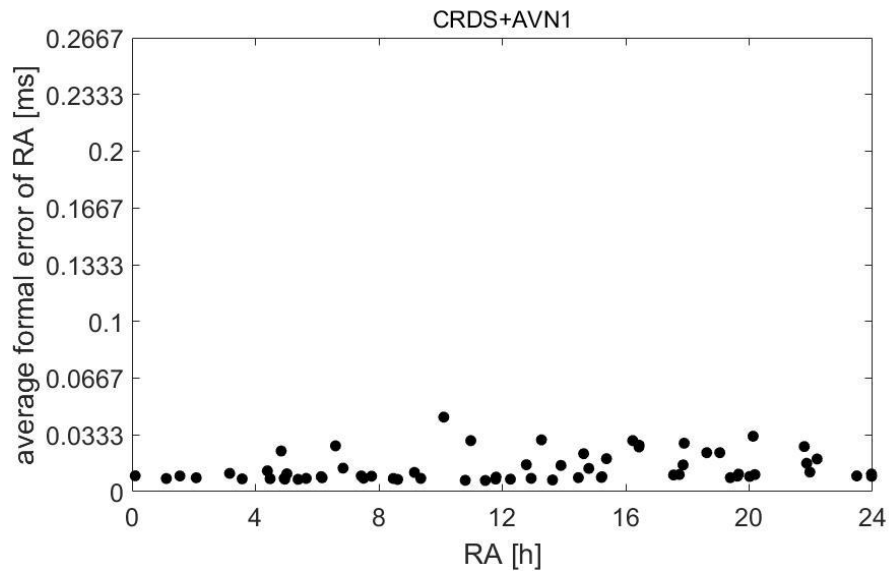


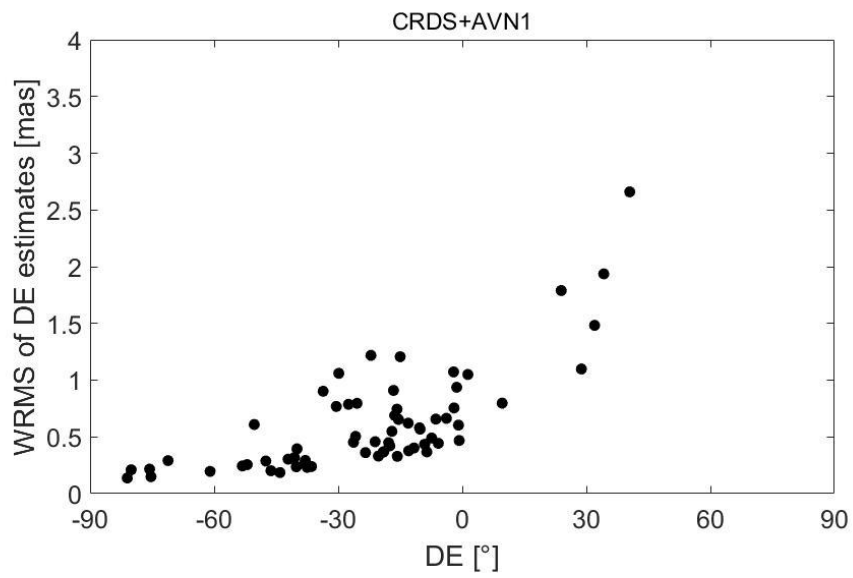
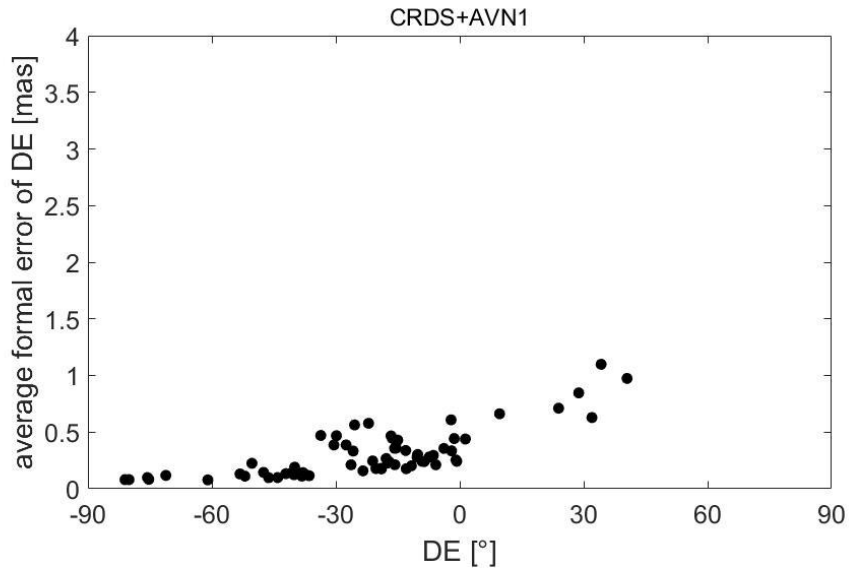
1 CRDS+KENYA



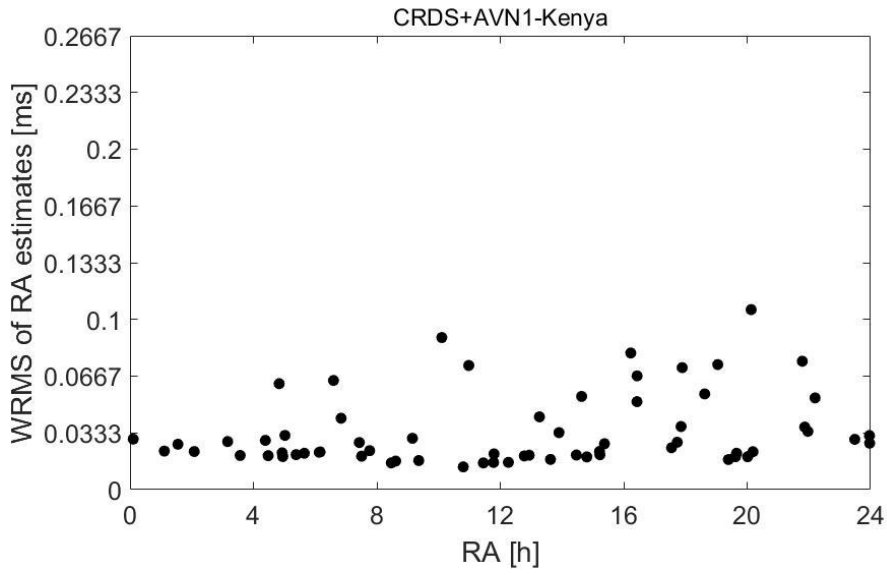
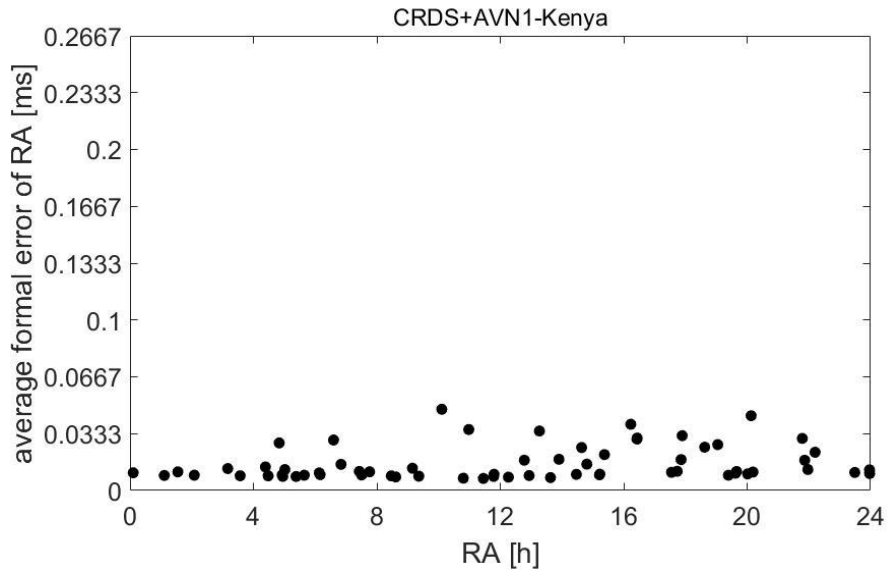


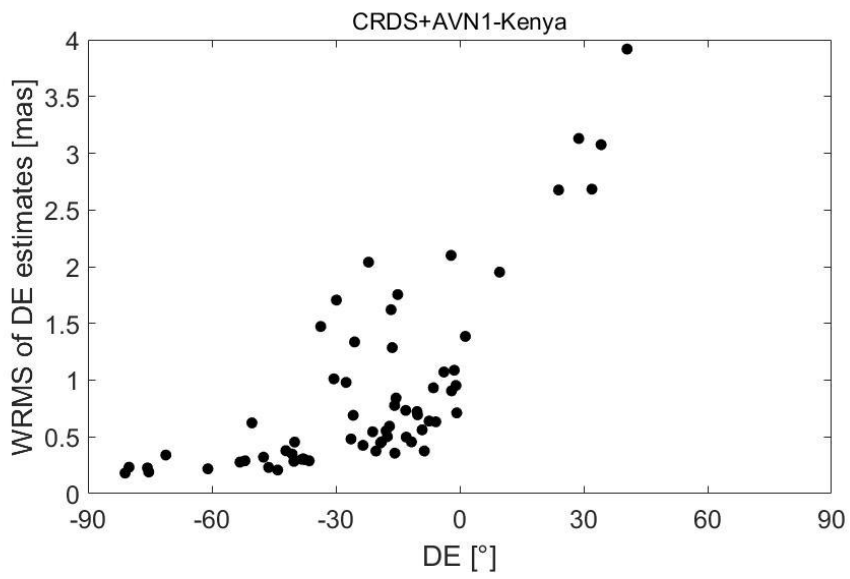
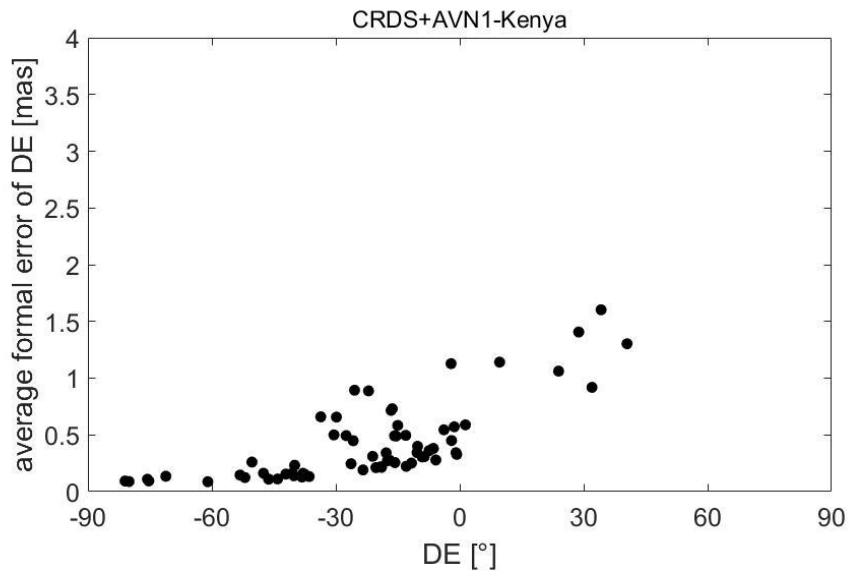
2. CRDS + AVN1



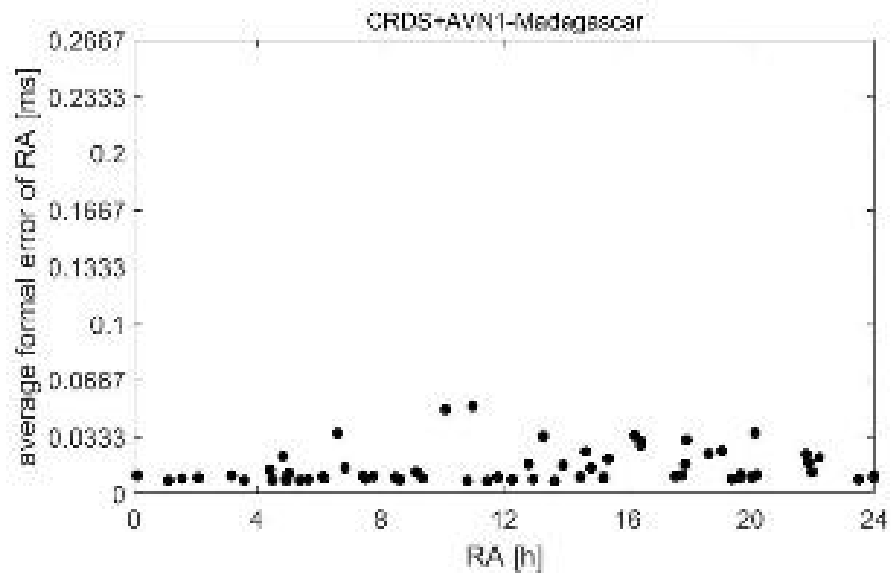


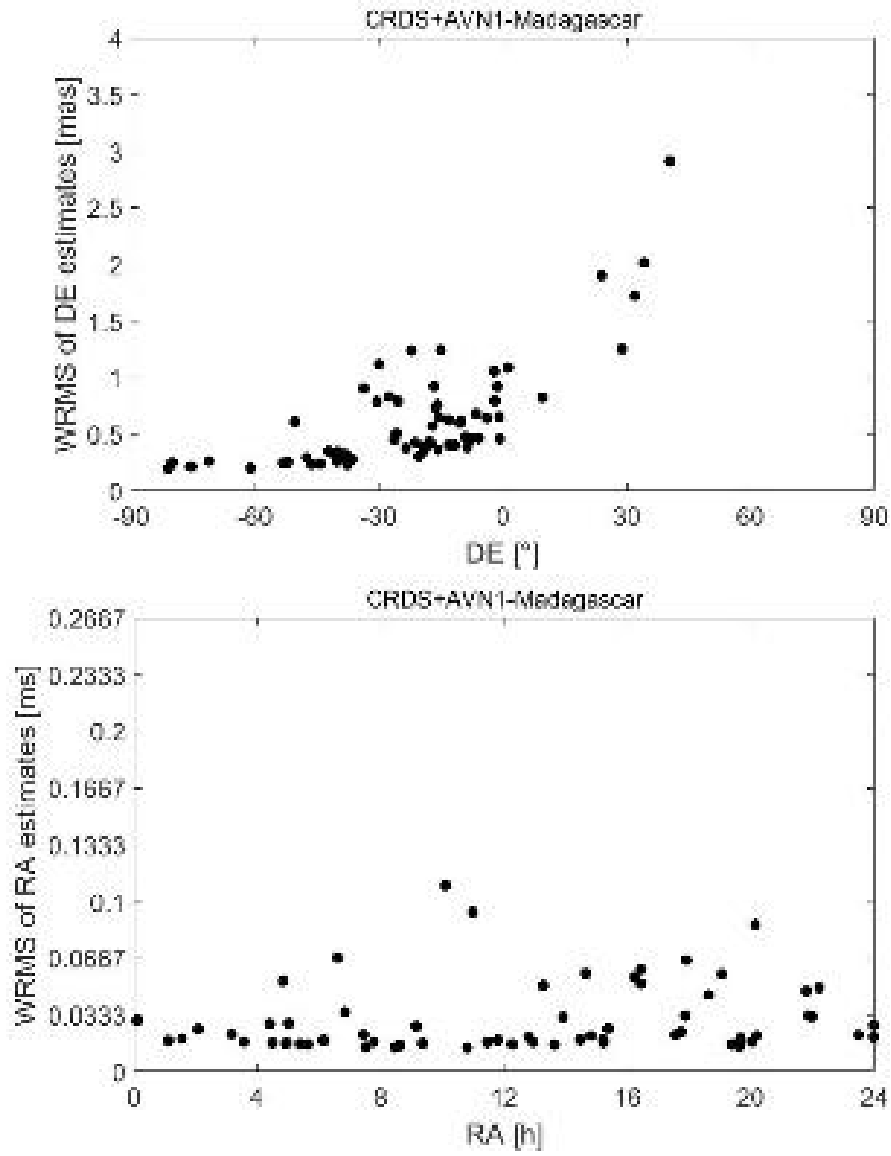
3. CRDS + AVN1 – Kenya

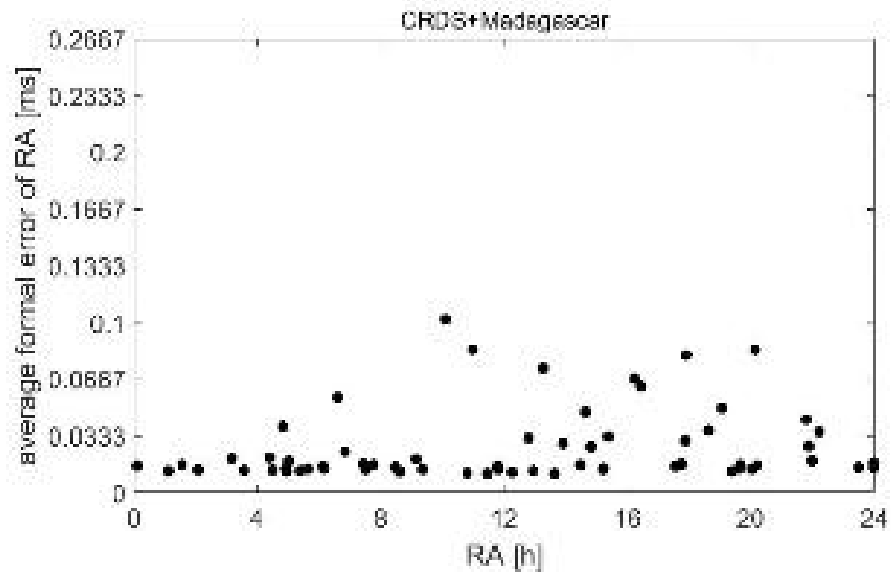
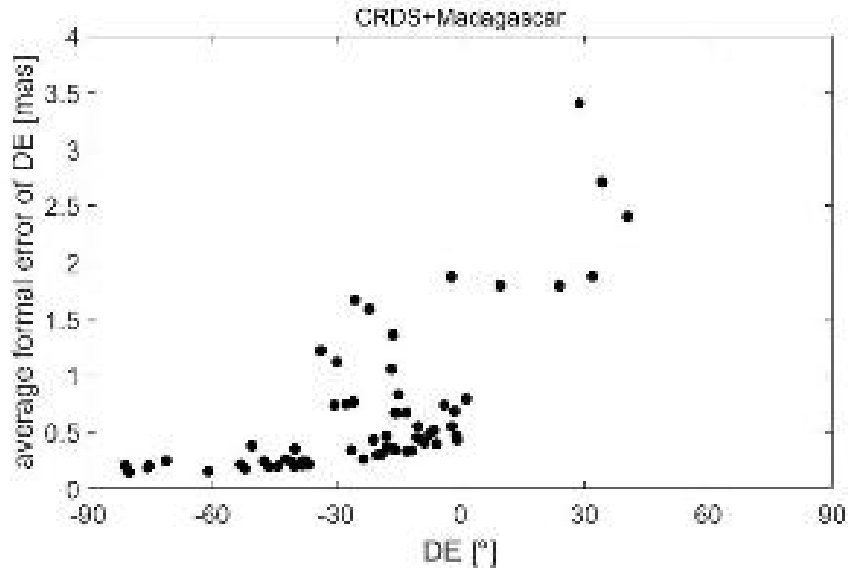


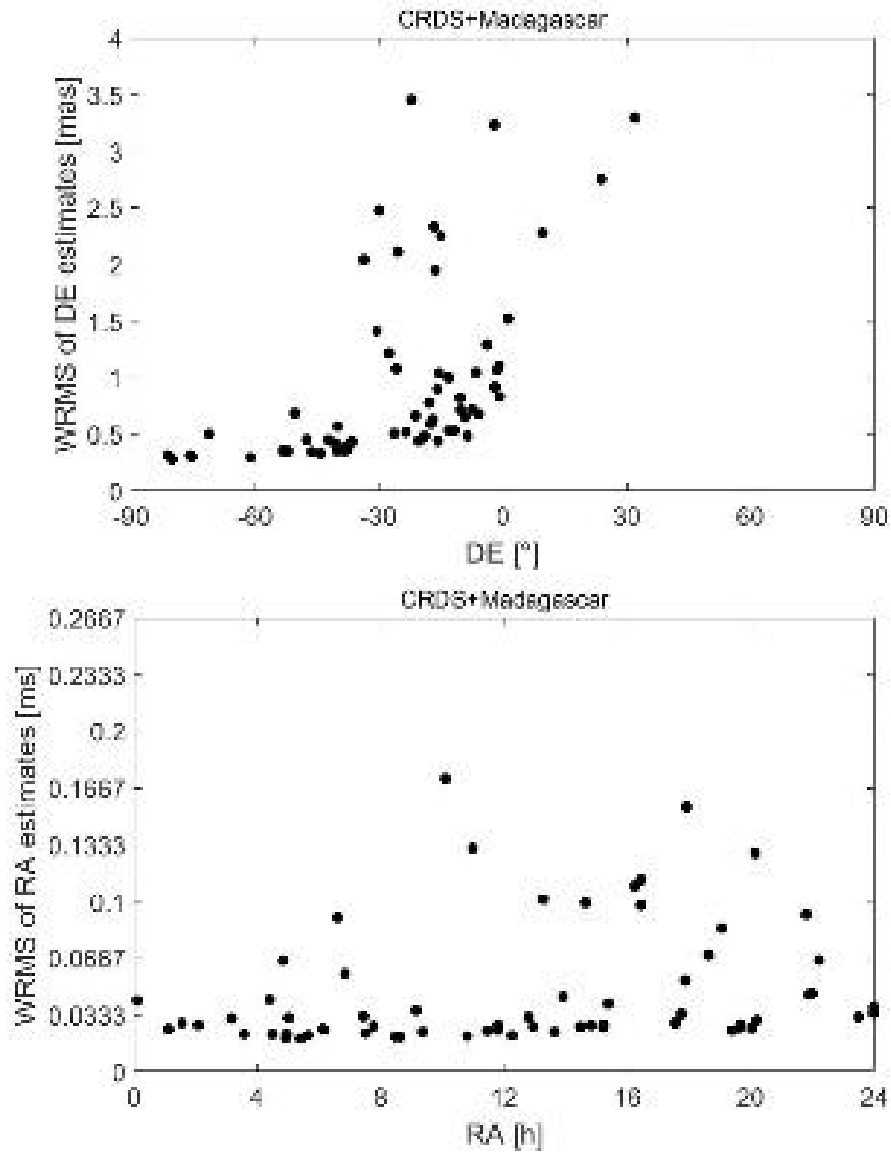


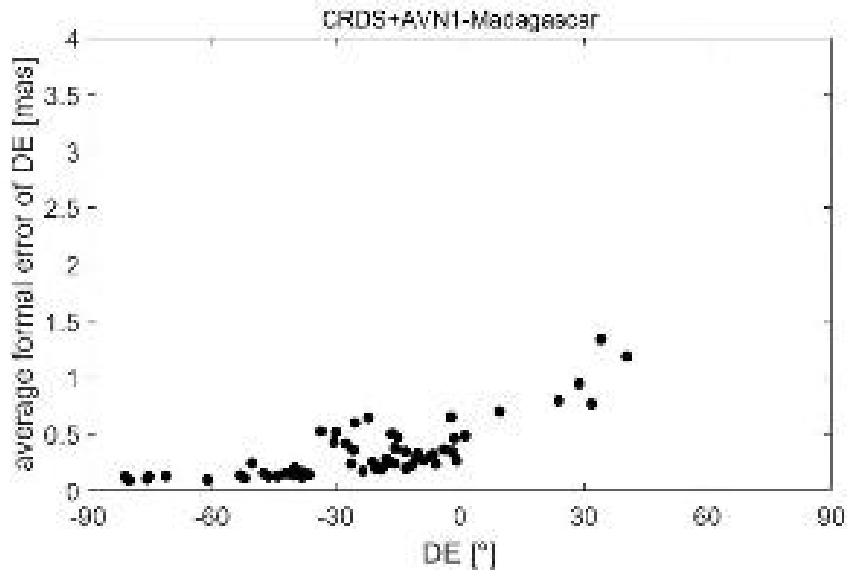
4. CRDS + MADAGASCAR



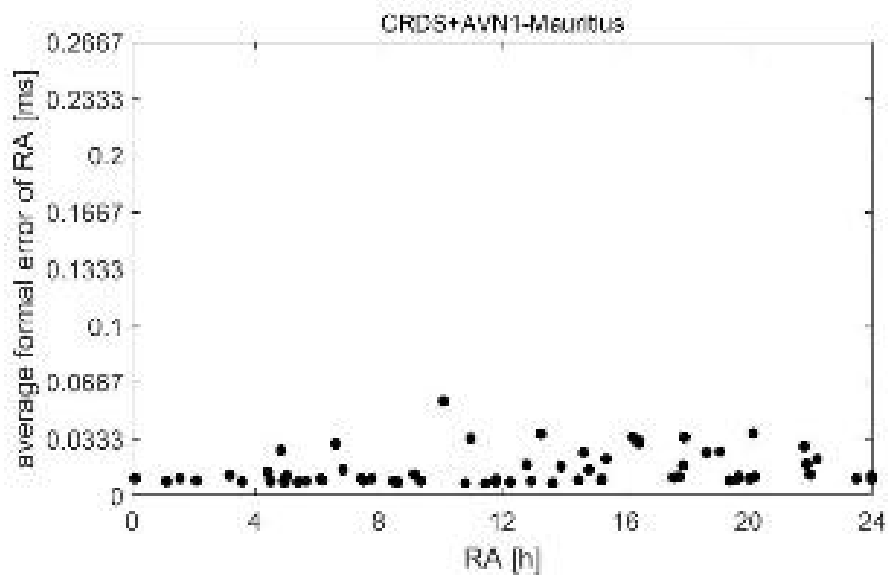


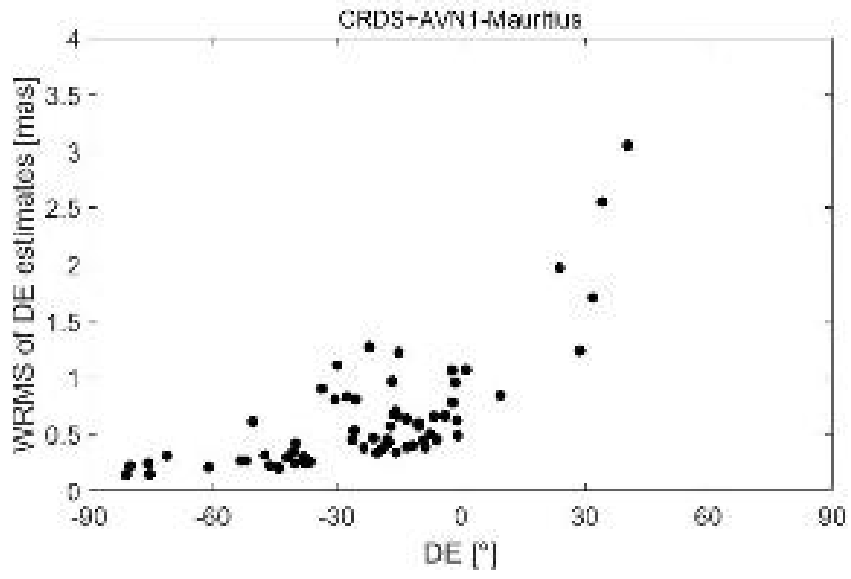


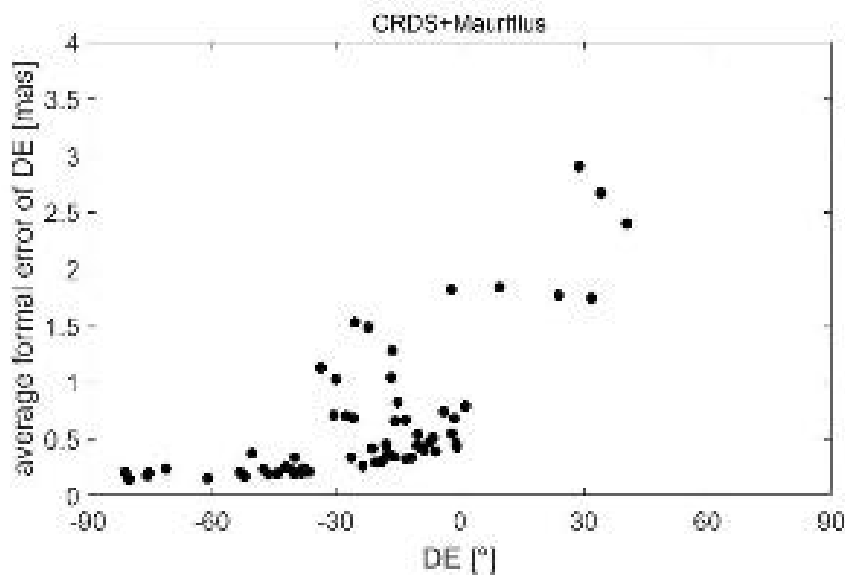
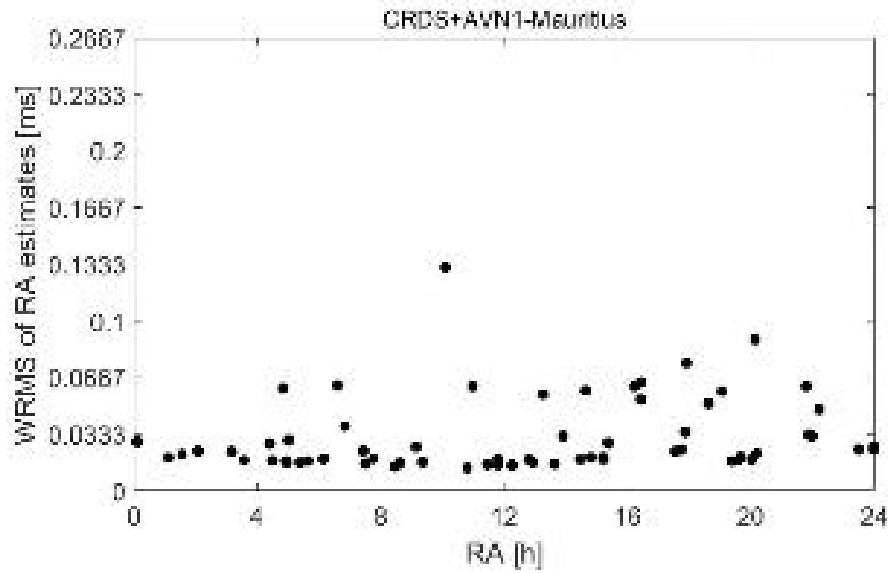


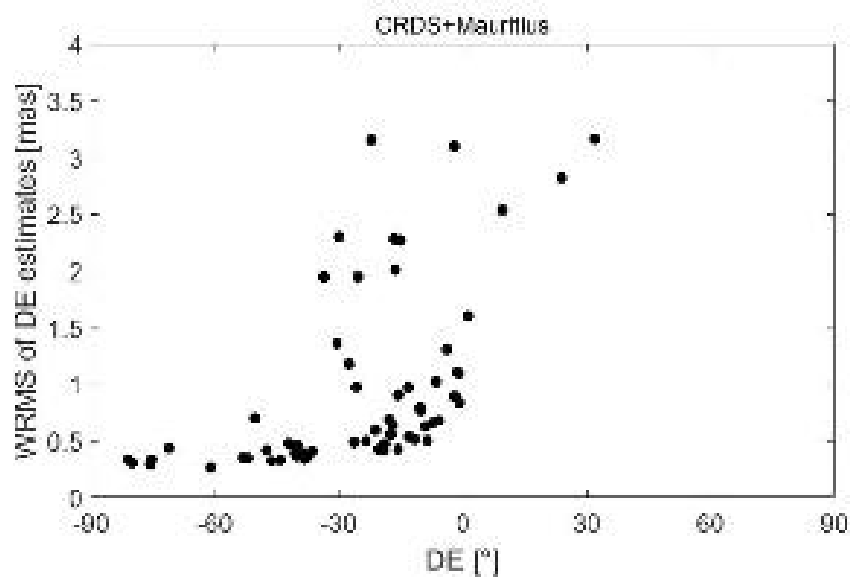
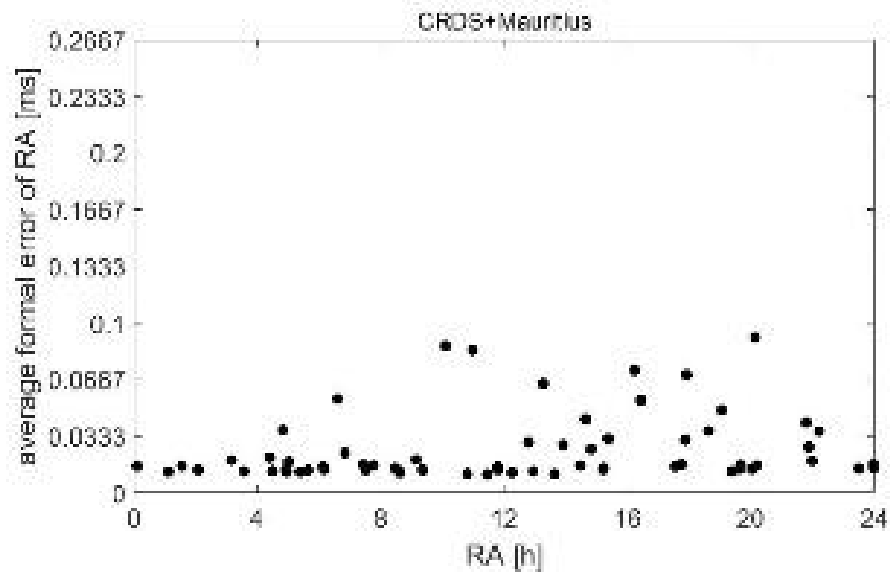


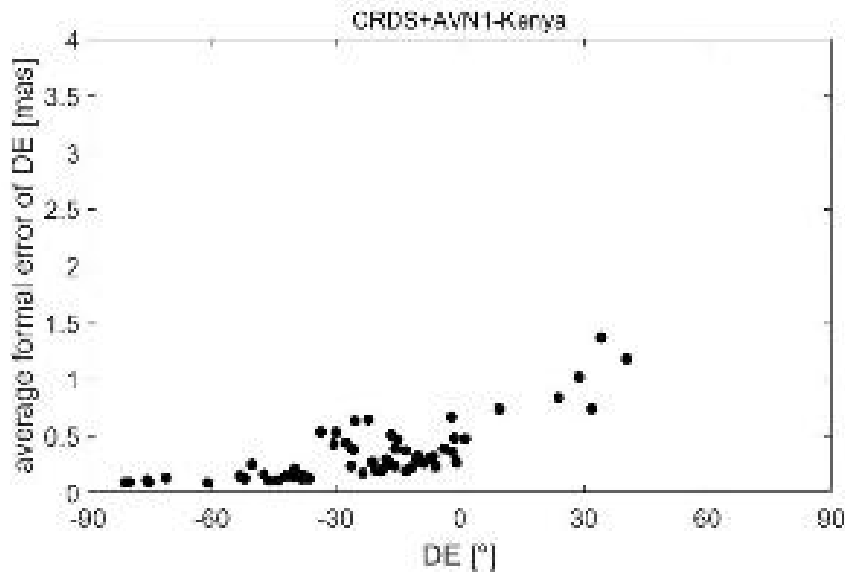
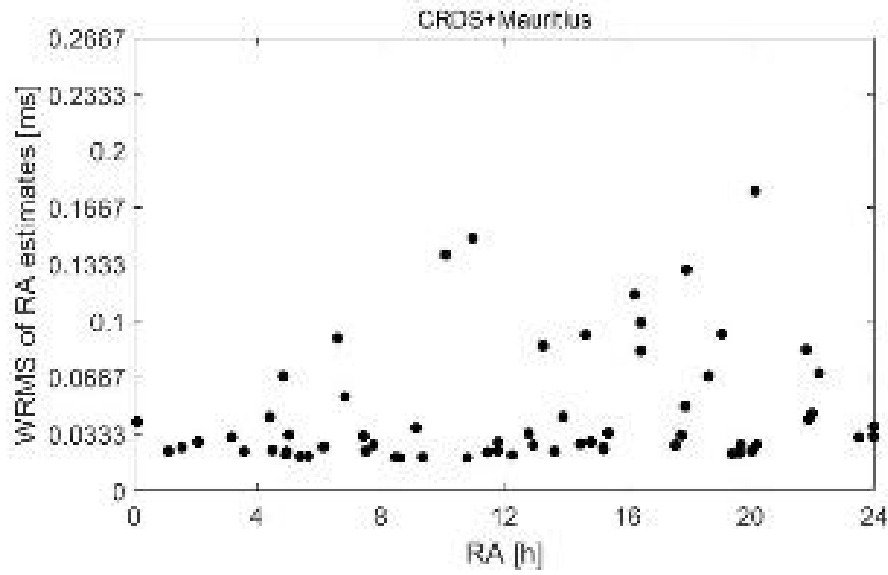
5. CRDS+Mauritius



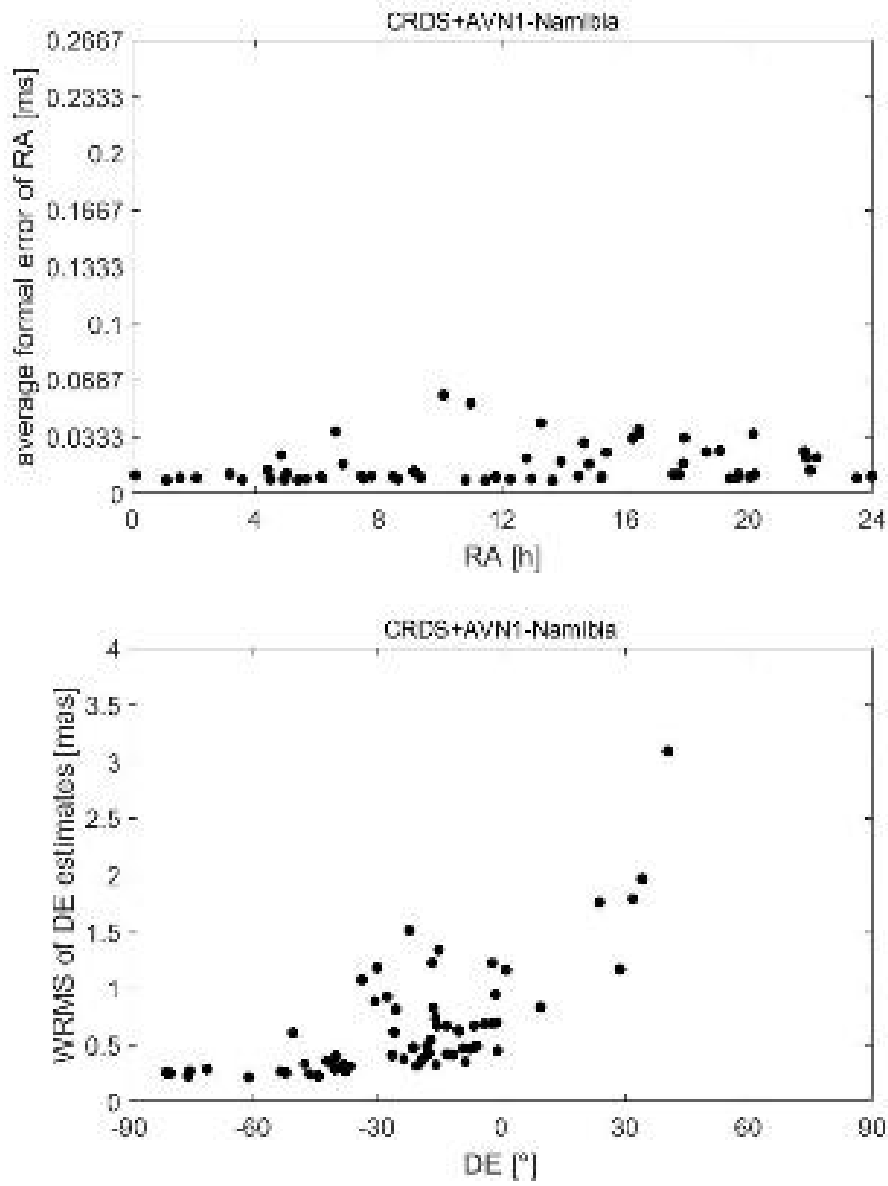


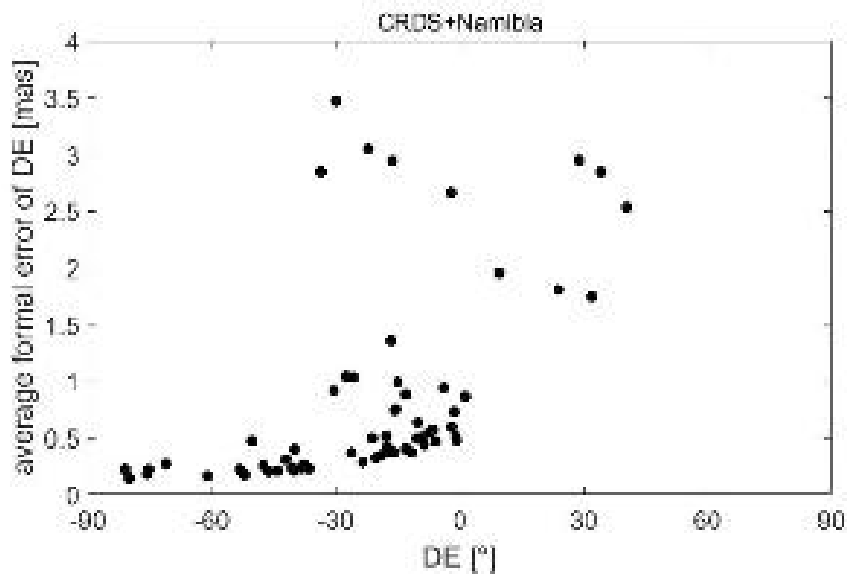
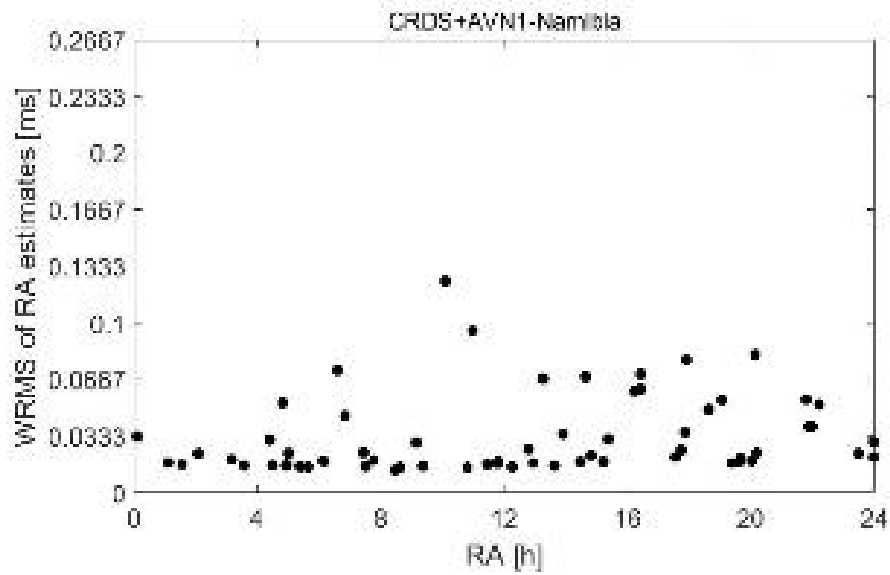


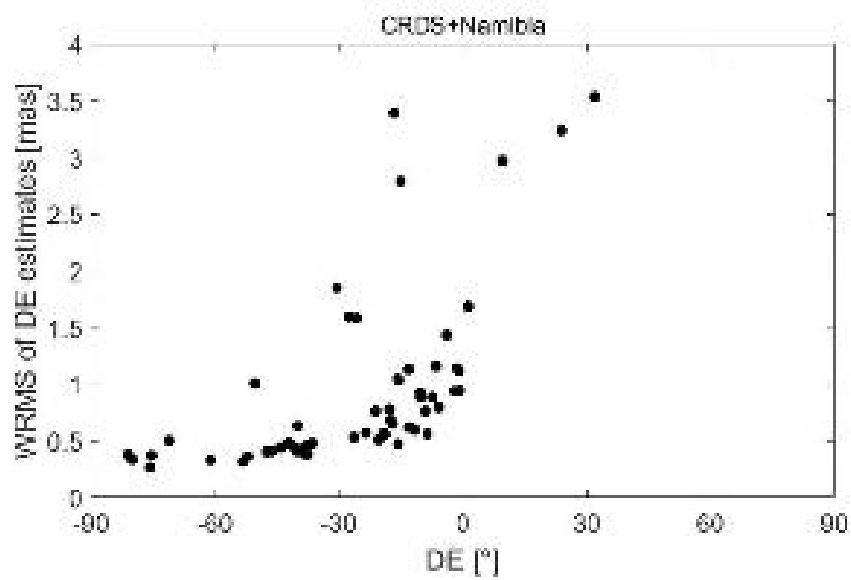
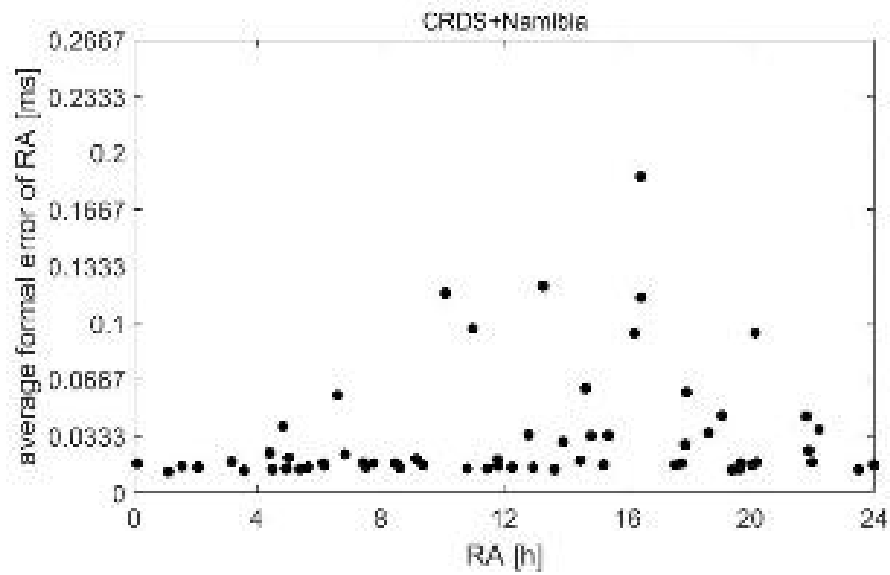


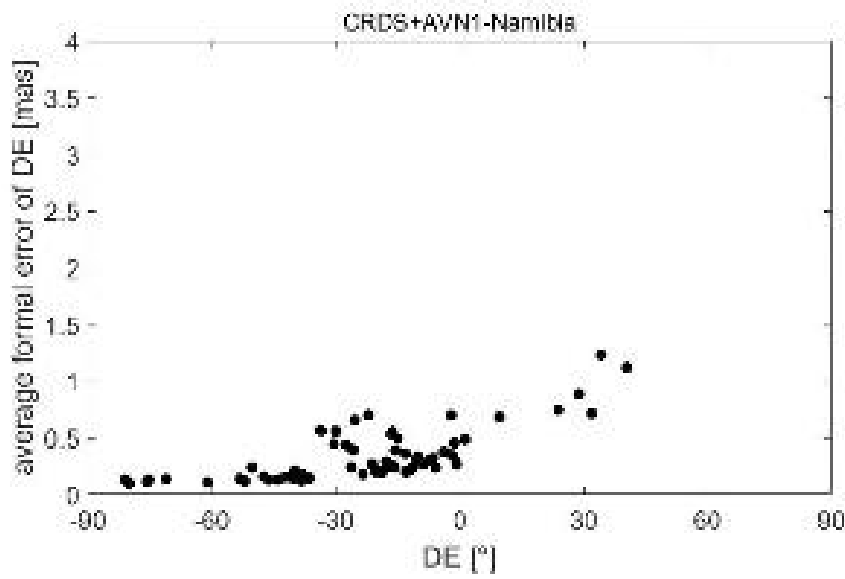
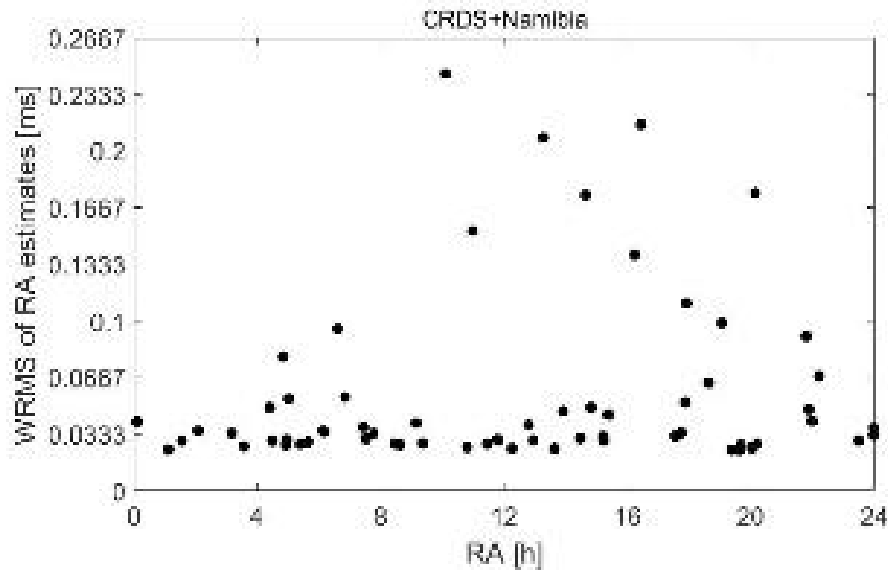


6. CRDS + NAMIBIA









7. CRDS + ZAMBIA

